UiT

THE ARCTIC UNIVERSITY OF NORWAY

Faculty of Science and Technology

Exploring Quorum Sensing Dynamics and Biofilm Formation in the Fish Pathogen *Aliivibrio salmonicida*

Gene inactivation, functional analysis and transcriptomics

—

Miriam Khider

A dissertation for the degree of Philosophiae Doctor – June 2019

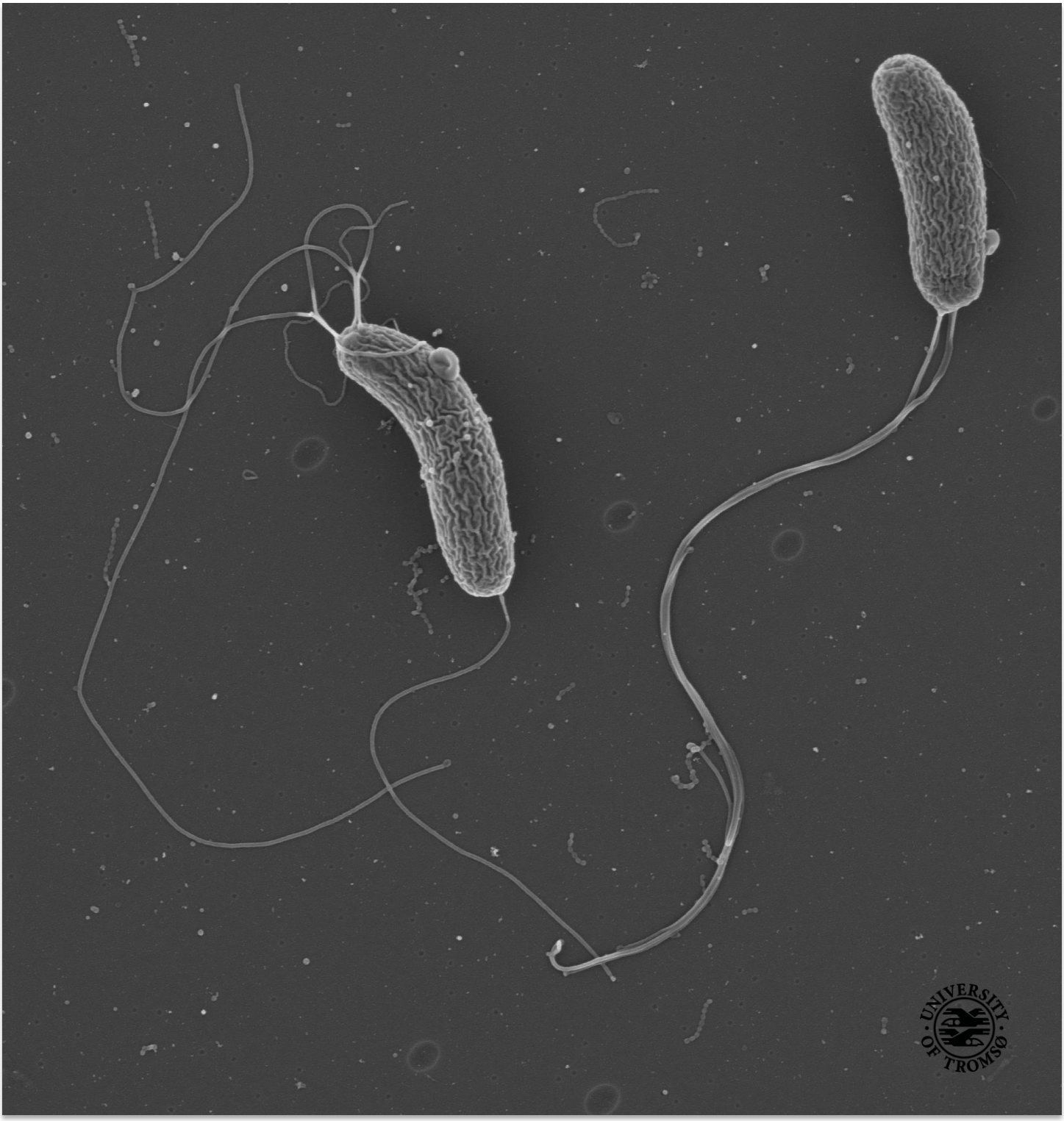

Exploring Quorum Sensing Dynamics and Biofilm Formation in the Fish Pathogen *Aliivibrio salmonicida*

Gene inactivation, functional analysis and transcriptomics

Miriam Khider

A dissertation for the degree of Philosophiae Doctor

Department of Chemistry

Faculty of Science and Technology

June 2019

Evaluating Committee:

Prof. Bjarnheidur Kristin Gudmundsdöttir
Faculty of Medicine, University of Iceland
Reykjavík, Iceland
E-mail: bjarngud@hi.is

Prof. Ingrid Bakke
Department of Biotechnology and Food Science
Norwegian University of Science and Technology-NTNU,
Trondheim, Norway
E-mail: ingrid.bakke@ntnu.no

Prof. Hanne-Kirsti Schrøder Leiros
Department of Chemistry
The Arctic University of Norway-UiT
Tromsø, Norway
E-mail: hanna-kirsti.leiros@uit.no

Contents

ACKNOWLEDGMENTS

The work presented in this thesis was carried out at the Molecular Biosystems Research Group, Norstruct, Department of Chemistry - The Arctic University of Norway-UiT.

First of all, I would like to express my deepest appreciation to my wonderful supervisors: Prof. Nils Peder Willassen, Prof. Peik Haugen, and Senior researcher Hilde Hansen for their support and guidance throughout the PhD studies. They have always provided me advice and generous support. Thank you, Nils Peder for giving me a chance and for the best five years of my career so far.

Thank you, Hilde for mentoring me during my lab work and continuing to advise me through my experiments and manuscript writing. Thank you, Peik, for helping me throughout my thesis.

I am especially grateful to Sunniva Katharina Thode for helping me understand the RNA sequencing and the transcriptomics. I would like to express my sincere gratitude to Eric Hjerde for the excellent work on transcriptomics data analysis. I am also grateful to Dr. Simen Foyn Nørstebø from the Norwegian University of Life Sciences for providing constructed mutants used in some of my experiments.

I would like to especially mention Tim Kahlke, May-Laura Kilano Khider, William K. Paintsil and Peik Haugen for their generosity in donating time to proofread and give valuable feedback on my thesis.

Finally, I would like to extend my sincerest thanks to my family: my husband, my children and my parents for believing in me and for making my life a brighter one. Without them, I would not be who and where, I am today. Without their unconditional support and love, this work over the past five years would not have been possible.

I appreciate the past five years spent in this beautiful city, Tromsø, with wonderful friends and colleagues at Norstruct, this will be engraved in my memory forever.

Miriam Khider

June 2019, Tromsø, Norway

SUMMARY

The marine pathogen *Aliivibrio salmonicida* is the causative agent of cold-water vibriosis, affecting mainly farmed salmonid fish when water temperatures are below 10°C. Even though cold-water vibriosis is no longer threatening Norwegian aquaculture, the reemergence of the disease is still a possibility. Therefore, it is crucial to gain knowledge and understanding of the pathogenicity of *A. salmonicida*. Quorum sensing (QS) is one of the communication systems used by bacteria to regulate gene expression in a synchronized way in response to cell density by secreting and sensing extracellular signals called autoinducers (AIs). QS system controls various physiological processes, particularly virulence system and biofilm formation in many pathogenic bacteria. With the increased emergence of antibiotic-resistant in recent years, understanding and targeting QS system is expected to bring potential new breakthroughs for the prevention and treatment of *Vibrio* infections. The present work was initiated to increase the knowledge on the QS system and its regulation on phenotypic traits that may be important for survival and host-pathogen interaction in *A. salmonicida*.

Alternative sigma factors such as RpoS provide the main line of responses to changes in the environment by altering gene transcription. In several vibrios, RpoS has been shown to be connected to QS system. The obtained results in this thesis, clearly indicate that an RpoS-like sigma factor, RpoQ (*VSAL_II0319*) is a component of the QS system and involved in regulating colony rugosity, biofilm formation, and motility in a cell density dependent manner. The transcriptomics analysis further revealed that RpoQ is involved in influencing expression of a large panel of genes including the *syp* operon involved in polysaccharide production. This suggests that the downregulation of biofilm development and wrinkled colony phenotype were due to RpoQ-dependent repression on polysaccharide biosynthesis genes (*syp* genes) at high cell density. In addition to cell density dependent control on biofilm formation and colony rugosity through QS, temperature was shown to influence the regulation of RpoQ on these phenotypes, linking this environmental factor to the development of cold-water vibriosis in seawater at low temperatures.

Previous reports have shown that *A. salmonicida* possesses two functional autoinducer synthases, the LuxI and AinS, which are responsible for the production of eight acyl homoserine lactones (AHLs). In this thesis, the inactivation of *luxI*, but not *ainS*, led to the formation of wrinkled colonies similar to those formed by the *ΔrpoQ* mutant. The transcriptome analysis showed that LuxI is required for repression of *syp* expression, where repression of *syp* is likely operated through the RpoQ sigma factor. When both systems were inactivated simultaneously, strains

(*ΔainSluxI*$^{-}$) with wrinkled colonies and mushroom structured biofilm were formed. Furthermore, the exogenous addition of either LuxI, N-3-oxo-hexanoyl-L-homoserine lactone (3OC6-HSL) or AinS, N-3-hydroxy-decanoyl-L-homoserine lactone (3OHC10-HSL), to the *ΔainSluxI*$^{-}$ double mutant, inhibited biofilm development. This suggested that the downregulation of biofilm formation is operated through a common pathway when the AHL concentrations are high.

The results presented in this work, add new knowledge about the nature of the QS mechanism of *A. salmonicida* and elucidate some aspects of the complex mechanism of biofilm formation, contributing to advancement of research in this field.

LIST OF PAPERS

Paper I

Miriam Khider, Nils Peder Willassen and Hilde Hansen (2018). The alternative sigma factor RpoQ regulates colony morphology, biofilm formation and motility in the fish pathogen *Aliivibrio salmonicida*. Published in BMC Microbiology. **18**:16. https://doi.org/10.1186/s12866-018-1258-9

Paper II

Miriam Khider, Erik Hjerde, Hilde Hansen and Nils Peder Willassen (2019). Differential expression profiling of *ΔlitR* and *ΔrpoQ* mutants reveals insight into QS regulation of motility, adhesion and biofilm formation in *Aliivibrio salmonicida*. Published in BMC Genomics. **20**:220. https://doi.org/10.1186/s12864-019-5594-4

Paper III

Miriam Khider, Hilde Hansen, Jostein A. Johansen, Erik Hjerde and Nils Peder Willassen (2019). Exploring the transcriptome of *luxI*$^{-}$ and *ΔainS* mutants and the impact of N-3-oxo-hexanoyl-L- and N-3-hydroxy-decanoyl-L-homoserine lactones on biofilm formation in *Aliivibrio salmonicida*. Published in PeerJ. 7: e6845. https://doi.org/10.7717/peerj.6845

ABBREVIATIONS

AHL	Acyl homoserine lactone
AI	Autoinducer
CPS	Capsular polysaccharides
EPS	Extracellular polymeric substance
VPS	Vibrio polysaccharides
SYP	Symbiotic polysaccharides
In vivo	In the living organism
In vitro	In an artificial environment outside the living organism
spp.	Species
OD	Optical density
QS	Quorum sensing
RNA-seq	RNA sequencing
RNA	Ribonucleic acid
rRNA	Ribosomal RNA
DEGs	Differentially expressed genes
HCD	High cell density
LCD	Low cell density
Bp	Base pair
Mb	Megabases / Million base pairs
e.g.	For example
i.e.	That is

1 BACKGROUND

1.1 The *Vibrionaceae* family

The name *Vibrionaceae* was originally defined by Véron in 1965 for a group of fermentative bacteria with polar flagella and a positive oxidase reaction [1]. Currently the *Vibrionaceae* family is divided into the genera *Aliivibrio, Allomonas, Candidatus Photodesmus, Catenococcus, Echinimonas, Enterovibrio, Grimontia, Paraphotobacterium, Photobacterium, Photococcus, Salinivibrio, Thaumasiovibrio* and *Vibrio* [2]. *Vibrionaceae* species (spp.) are Gram-negative gammaproteobacterial of curved or straight rod-shaped form. The members are also facultative anaerobes capable of fermentation and motile by one or several polar flagella [3].

The genus *Vibrio* is among the most abundant *Vibrionaceae* genera. Members of this genus are found in aquatic habitats and in association with a wide range of living organisms [3]. Vibrios commonly possess two circular chromosomes: chromosome I harbors most of the essential housekeeping genes and is of similar size throughout the group (average size 3.0 to 4.2 Mb); chromosome II varies in size (average size 0.8 to 2.4 Mb) and harbors species specific genes that play an important role in environmental adaptation [4-6]. The presence of two chromosomes is thought to give the bacteria advantages under specific environmental conditions and to facilitate rapid cell replication [4, 6, 7]. In 2007 the genus *Vibrio* was spilt into two genera; the *Vibrio* genus and the *Aliivibrio* genus. Several species originally classified within *Vibrio* such as *Vibrio fischeri*, *Vibrio wodanis*, *Vibrio salmonicida* and *Vibrio logei* were reclassified and renamed to *Aliivibrio fischeri, Aliivibirio wodanis*, *Aliivibrio salmonicida* and *Aliivibrio logei* [8]. Studies have shown that these four species are closely related and were phylogenetically and phenotypically distinct from other species in the *Vibrio* genus [8]. Later other species were included to this genus such as *Aliivibrio finisterrensis* [9], *Aliivibrio sifiae* [10] and *Aliivibrio thorii* [11].

Most of the *Vibrionaceae* family members are able to degrade chitin and require at least 0.5 to 3% salt concentration for growth [3, 12]. Sodium ions are required for Na^+ antiporters to transduce energy into the cytoplasm, to maintain cell wall integrity. Therefor the occurrence of vibrios in fresh water is limited with exception of *Vibrio cholerae* and *Vibrio mimicus* that are non-halophilic and have shown a great tolerance of freshwater [13, 14]. Additionally, most of the *Vibrionaceae* spp. require certain temperatures for growth. The preferred range of growth temperature varies

between *Vibrio* and *Aliivibrio* spp. Some species like *A. salmonicida*, *A. wodanis* and *A. logei* are psychrophiles. These species are cold adapted and do not grow at temperatures above room temperature [15, 16]. However, others like *V. cholerae* are able to grow at temperatures above or equal to 37°C [7].

Most members of *Vibrionaceae* family are flexible to adapt to new environments. Some may exist in a free-swimming planktonic state as well as in association with aquatic organisms. Vibrios are often found in high densities in and /or on marine organisms such as corals [17], shrimps, fish, molluscs, sponges and zooplanktons [3, 18]. Some vibrios are the causative agents for severe diseases in humans and animals, such as cholera disease [3], while others live in symbiotic relation with fish or squid such as the bioluminescent bacteria *A. fischeri.* This bacterium colonizes the external light organs of the squid (*Euprymna scolopes*) and the bioluminescence produced during this interaction provides an anti-predatory benefit to *E. scolopes* during nocturnal activities [19, 20].

1.2 *Vibrionaceae* pathogens

Various members of the *Vibrionaceae* family are pathogenic to both vertebrates and invertebrates, although they are mostly known for their role as causative agents for severe diseases in humans. Infections caused by vibrios termed as vibriosis, which is mostly associated with skin or blood infections. Several virulence-related factors have been found in numerous pathogenic *Vibrio* spp. such as cytotoxins, siderophores, capsular polysaccharides, adhesive factors, proteases, haemolysins, lipopolysaccharides and flagella, although the pathogenicity of vibrios still need to be elucidated.

1.2.1 Vibrios as human pathogens

Vibrio infections in humans are mainly transmitted through consumption of raw or undercooked contaminated seafood, contaminated water or even through wounds [21, 22]. Among the most common human *Vibrio* pathogens, is *V. cholerae*, the etiological agent of the cholera disease, which occurs mainly in developing countries and areas of natural disasters and war [23, 24]. The main cause of cholera is consumption of contaminated water and food which results in severe diarrhea and can be quickly fatal if untreated [24]. The cholera toxin and toxin coregulated pilus (TCP) are among the most important virulence agents associated with the *V. cholerae* pathogenicity [25]. Other serious human pathogens are *Vibrio parahaemolyticus* and *Vibrio vulnificus*. *V. parahaemolyticus* is the most common cause of seafood-borne gastroenteritis in the United States which is typically associated with consumption of raw oysters. The bacteria can also cause a variety of other disease including wound, ear infections and septicaemia that may be life-

threatening to individuals [26, 27]. The pathogenicity of *V. parahaemolyticus* is usually associated with the presence of two virulence genes; the thermostable direct hemolysin (*tdh*) and a thermostable TDH-related homolysing (*trh*) in combination with a type III secretion system (TTSS) [26, 28-30]. Pathogenic *V. vulnificus* are distinguished into three biotypes that are known to cause human disease. Biotype I is pathogenic to humans causing septicaemia and self-limiting gastroenteritis. Biotype 2 and 3, however are only responsible for direct wound infections. Pathogenicity in *V. vulnificus* is associated with multiple virulence factors such as the capsular polysaccharide, lipopolysaccharide, the hemolysin VvhA, cytotoxin VvRTX, extracellular metalloprotease, pili and flagellum [31, 32]. In addition to the mentioned, other *Vibrio* spp. are also known to infect humans such as *Vibrio alginolyticus, Vibrio fluvialis, V. mimicus, Photobacterium* (*vibrio*) *damsela* and *Grimontia* (*vibrio*) *hollisae* [32].

1.2.2 Vibrios as aquatic animal pathogens

The most common and serious disease in fish and shellfish is vibriosis, leading to substantial economic losses in the aquaculture industry worldwide. Major *Vibrio* spp. *Vibrio harveyi, V. alginolyticus*, *Vibrio anguillarum, V. parahaemolyticus, V. vulnificus, Vibrio splendidus* are usually associated with shrimp and fish diseases. *V. harveyi* is associated with luminescence vibriosis in cultured shrimps, but it can also cause skin ulcers [32, 33]. *V. parahaemolyticus* which in addition to the effect on human health is also a common pathogen for fish and shellfish, specially shrimps. Infected shrimps exhibit an array of clinical signs including lethargy, soft shells and anorexia [34]. *V. vulnificus* biotype 2 and *V. anguillarum* are among the main bacterial pathogens in several fish species [35]. *V. anguillarum* used to be the first isolated *Vibrio* to which "Red Pest of eels" was attributed, during early 1900s [36]. There are several *V. anguillarum* serotypes although serotype O1 and O2 and to less extend serotype O3 are associated with vibriosis in fish. The other *V. anguillarum* serotypes are environmental strains and are mostly non-pathogenic [37]. *Vibrio ordalii* is a pathogen of wild and cultured salmonids in particular geographic areas. Recently the pathogen was also reported in other fish such as rainbow trout, ayu and rockfish. The vibriosis caused by *V. ordalii* is associated with necrosis and haemorrhagic lesions in the tissue surrounding the site of infection including the ventral fin and anal pore [38, 39].

1.2.3 Aliivibrio salmonicida and The Hitra disease

A. salmonicida, the focus of this thesis is the etiological agent of cold-water vibriosis or Hitra disease in Atlantic salmon (*Salmo salar*), rainbow trout (*Oncorhynchus mykiss*) and captive Atlantic cod (*Gadus morhua*) [40-43]. In 1979 the cold-water vibriosis appeared for the first time at Norwegian salmon farms close to Hitra island, south of Trondheim-Norway. Since then the disease was controlled by vaccination, but reappeared in 2011 at Atlantic salmon farms despite

vaccination [40, 41, 44]. The disease occurs mainly at late autumn, winter and early spring when seawater temperatures are below 10°C. The early stages of the cold-water vibriosis lead to lethargy, swimming disturbances and cessation of feeding. Affected fish turn dark and exophthalmos may be seen. The disease is characterized by hemorrhagic septicaemia and result in anemia [38, 40-42, 45, 46].

A. salmonicida similar to other members of *Vibrionaceae* is motile Gram-negative bacterium of curved rod shape which has up to ten polar flagella and no lateral flagellum (Figure 1). The colonies appear small, grey and smooth on agar plates, where the size of cells after 1 day culture are 0.5µm by 2-3µm microscopically [38, 41]. *A. salmonicida* is halophilic and thrives at salinities ranging between 0.5 and 4%, but optimum growth is at 1.5-2% [41, 42]. The bacterium is psychrophilic, where the growth occurs between 1 and 22°C [41], with optimal growth temperature in liquid cultures and solid surfaces at 10°C and 15°C, respectively [47]. The low growth temperature was linked to the virulence of *A. salmonicida* as outbreaks of cold-water vibriosis above 10°C have not been reported [46, 48].

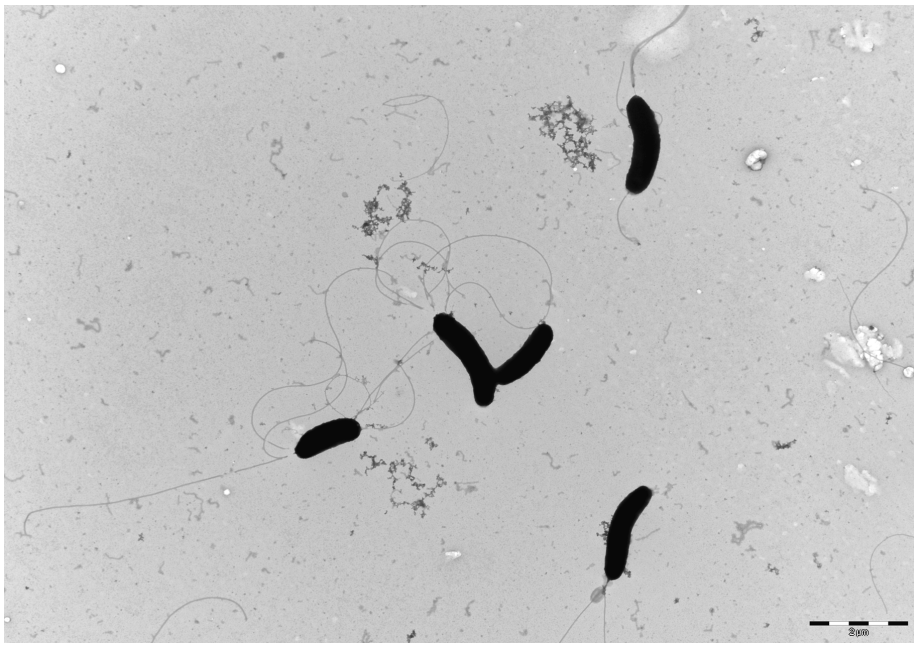

Figure 1 Transmission Electron Microscope (TEM) image of *A. salmonicida* LFI1238. Scale bar = 2µm.

In 2008, the genome of *A. salmonicida* was sequenced and revealed two chromosomes (3.3 Mb and 1.2 Mb) in addition to four plasmids (85.5 Kb, 30.8 Kb, 5.4 Kb and 4.3 Kb) and 4286 predicted protein coding sequences spread over 4.6 Mb of DNA [49]. The genome of *A. salmonicida* has a

high abundance of insertion sequence (IS) elements which are believed to be responsible for the inactivation of at least 156 open reading frames [50].

Despite three decades of research few virulence factors of *A. salmonicida* are known and the pathogenicity of the disease remains poorly understood. Regulation of pathogenicity was proposed to be associated with the *lux* operon (*luxCDABEG*), which encodes the components necessary for bioluminescence production [51]. Deletion of the *luxA* in the *lux* operon of *A. salmonicida* resulted in delay in mortality among the Atlantic salmon [51]. Motility is another important factor that is linked to virulence in several bacteria [52, 53]. Similarly, *A. salmonicida* was shown to depend on its motility to enter the fish, but the motility is inhibited at the late stages of host colonization [54]. However, recently Nørstebø et al. showed that motility is not required for the invasion of Atlantic salmon, although it is involved in the pathogenesis of cold-water vibriosis [55]. Additionally, motility in *A. salmonicida* was affected by salinity and temperatures, correlating these environmental factors to the occurrence of the cold-water vibriosis [56, 57]. Iron sequestration mechanism in *A. salmonicida* was also shown to be temperature dependent, where the production of the major siderophore Bisucaberin related to the pathogenicity was highest at temperatures around 10°C [58, 59]. Moreover, genes for siderophore production such as TonB system and heme uptake system were annotated in the genome of *A. salmonicida* [49, 58]. Recently, the lipopolysaccharides of *A. salmonicida* were shown to be important in virulence [60], where the inactivation of the two gene copies of O-antigen ligase *waaL* resulted in almost avirulent strains [60]. The quorum sensing system described in the next chapter is also suggested to be a possible virulence factor in *A. salmonicida* [57].

1.3 Quorum sensing, bacterial cell-cell communication

1.3.1 Quorum sensing and its chemical language

Quorum sensing (QS) is one of several microbial cell-cell communication systems that allow groups of bacteria to synchronize collective behaviors in response to changes in cell population density. QS occurs both in Gram-negative and Gram-positive bacteria and relies on the production, release and detection of diverse extracellular chemical signals. The chemical signals trigger changes in behavior when population density reaches a critical level. Signal molecules known as autoinducers (AIs) are synthesize by the bacteria intracellularly and then diffuse into the surrounding environment. The released molecules accumulate extracellularly as the bacterial population density increases toward the stationary phase. When a certain threshold level is reached the molecules are recognized by specific receptors which are either membrane bound or presented in the cytoplasm. The receptor then initiates a signal transduction chain resulting in the expression or repression of target genes [61-63]. Many QS systems are autoinduced i.e., the

gene encoding the signal synthase is one of the target genes. This positive feedback loop results in an increase in production of the autoinducer once the threshold of the QS system is reached [63].

Different classes of QS chemical signals have been identified in different bacteria. A typical QS in Gram-negative bacteria uses two types of autoinducers: N-acyl-homoserine lactones (AHLs) also known as AI-1 and furanosyl borate diester (AI-2). The AHLs are considered to be an intra-species communication signal molecule due to its distinct structure in various species, while the AI-2 is considered as an inter-species communication autoinducer [64, 65]. Among *Vibrio* spp. there is a unique AI, 3-hydroxy-tridecan-4-one (CAI-1) which is proposed to be responsible for communication within this group [63]. The AHLs consist of a hydrophobic homoserine lactone ring attached to acyl side chain by an amide bond. The side chain of the acyl group varies in length from 4 to 18 carbon atoms (Figure 2)[66, 67]. Additionally, the saturation of acyl group differs between AHLs: short side chains (C4) are less saturated, which makes them easier to diffuse across the membrane than the long side chains (C14). AHLs are also susceptible to alkaline pH, where short chain molecules are less stable than longer chain at high pH [68].

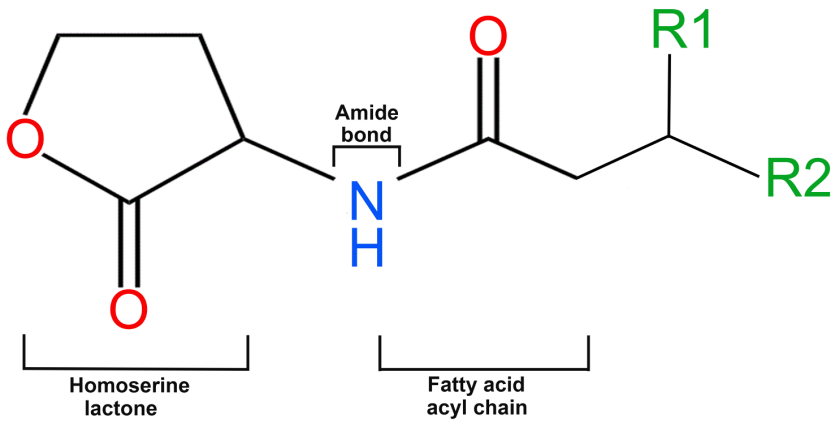

Figure 2 The structure of acylated homoserine lactones. R1 and R2 are acyl groups.

1.3.2 Quorum sensing in Vibrionaceae

The history of QS goes back to the 1970´s when investigators discovered a luminescence in marine bacteria, *V. fischeri* (known later as *A. fischeri*) [69]. In *A. fischeri* the production of light through the luciferase *lux* operon was achieved only at high cell densities in response to accumulation of AI signaling molecules [69]. The marine bacterium *A. fischeri* employs a LuxI-LuxR type QS system

to control bioluminescence and other cellular processes. The LuxI is the AI synthase which synthesizes the N-3-oxo-hexanoyl-L-homoserine lactone (3OC6-HSL), the cognate signal of LuxR cytoplasmic autoinducer receptor (Figure 3). The LuxR of *A. fischeri* is composed of two domains; the first domain the N-terminal ligand binding domain (LBD) that binds AHL and the second domain the C-terminal DNA binding domain (DBD) that regulate target gene expression. When Als concentration is low the N-terminal of LuxR folds back onto HTH domain and thus block DNA binding. As cell density increase the 3OC6-HSL accumulates and binds to LuxR. The ligand binding induces a conformational change that reveals the DBD of LuxR makes it free to bind the promoter. Hence, activating the transcription of the *lux* operon which consists of all bioluminescence producing genes and the autoinducer synthase *luxI* genes resulting in an autoinduction. The subsequent expression of *luxI* leads to the induction of bioluminescence reaction and increase in the production of AHLs [70-73].

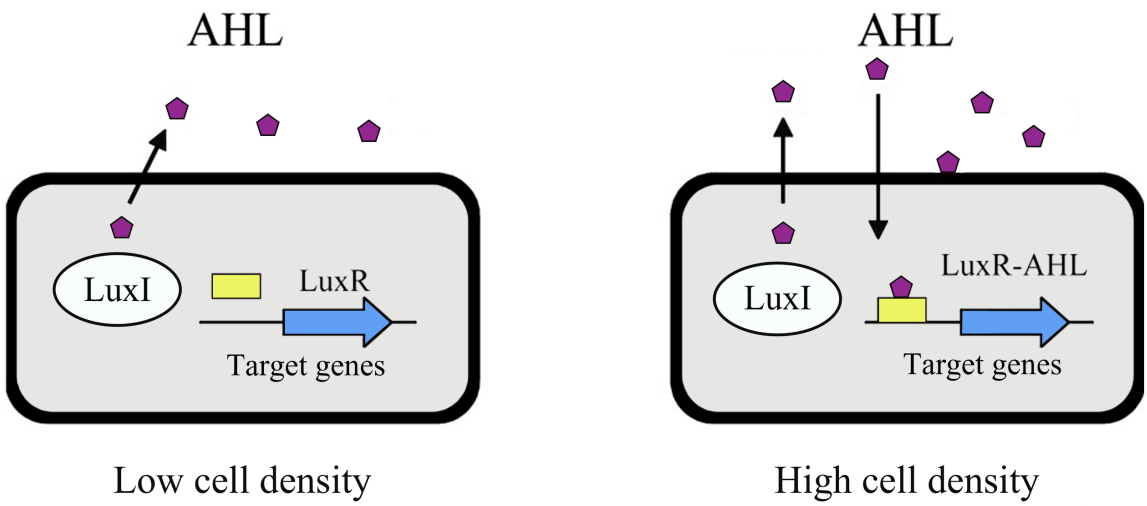

Figure 3 The LuxI-LuxR QS system in Gram-negative bacteria. The LuxI autoinducer synthase is responsible for catalyzing the formation of specific AHL (violet pentagons). The AHLs freely diffuse through the bacterial cell envelope and accumulate at high cell density. The LuxR transcription regulator binds their cognate autoinducers when a sufficient high concentration of the signal has been achieved. The LuxR-AHL complex in turn activates the transcription of the target genes. The figure is modified from Li et al. [74].

In addition to the LuxI-LuxR system described above, which is at the bottom of the QS hierarchy, *A. fischeri* also possesses an additional two systems at the top of the QS cascade. The AinS-AinR and LuxS-LuxPQ that indirectly control luminescence by modulating *luxR* transcription. AinS synthesizes N-octanoyl-L-homoserine lactone (C8-HSL), which is sensed by a histidine kinase AinR. LuxS synthesizes AI-2, which binds to the periplasmic protein LuxP. LuxP form a complex

with a histidine kinase LuxQ. The complex dimerizes within the inner membrane. At low cell density (LCD) the concentration of the AHLs are low. The 3OC6-HSL of LuxI is found at basal level not enough to be sensed by LuxR. The AinR and LuxQ systems autophosphorylate and induce a phophorelay cascade synergistically by transferring a phosphate group to LuxU, a cytoplasmic protein that passes the phosphate to LuxO, a DNA binding response regulator protein. The phosphorylated LuxO cooperates with alternative sigma factor-54 to activate the transcription of small RNAs (sRNAs) known as Qrr. The Qrr interact with an RNA chaperon Hfq and together destabilize the *litR* mRNA of the QS transcription regulator LitR. The LitR is required to activate the transcription of the *lux* operon in order to produce light. Thus, at LCD no light is produced. The production of AHLs in *A. fischeri* occurs at intermediate cell density, where the C8-HLS and AI-2 accumulates and reaches a threshold. The autoinducers bind to the cognate hybrid sensor kinases AinR and LuxPQ, respectively which switch to phosphatase activity. The LuxO is dephosphorylated via LuxU and the expression of the *qrr* sRNAs is not induced. Hence the LitR is expressed. The active LitR regulates early colonization factors, motility, and induces *luxR* transcription linking the AinS-AinR system to the LuxI-LuxR system. LuxR can bind the AinS-HSL (C8-HSL) at low affinity, when the 3OC6-HSL is limited resulting in the transcription of *lux* operon which contains the *luxI* synthases. At high cell density (HCD) the 3OC6-HSL accumulates and binds to LuxR leading to the activation of *lux* operon and light production. Furthermore, the LitR is able to generate a positive feedback loop by activating the *ainS* gene [73, 75-77].

Since then, QS and homologs of LuxI-LuxR in other vibrios has been identified and showed to influence a wide variety of cellular behaviors ranging from virulence to sporulation and motility [61]. Below are some examples of *Vibrio* QS systems.

1.3.2.1 The QS systems of V. cholerae

In *V. cholerae*, the causative agent of the cholera disease in humans, the QS is connected to virulence gene expression, biofilm formation and other cellular processes, all of which are important for survival and adaptation inside and outside of its human host [78, 79]. The canonical QS pathway of *V. cholerae* involves two signaling systems that function through phosphorelay cascade [80, 81]. The LuxS-LuxPQ system, which produces and detects AI-2 and the CqsA-CqsS system, which produces and detects CAI-1 (for cholera autoinducer-1), this system was firstly identified in *V. cholerae* and named cholera quorum sensing [80]. Both systems pass the sensory information in parallel through LuxU to activate LuxO. When the concentration of these two AIs is low or below the detectable threshold level (LCD), LuxQ and CqsS function as kinases to phosphorylate LuxU. The phosphorylated LuxU transfers the phosphate to LuxO, which together with sigma factor-54 activates the expression of four Qrrs sRNA, Qrr1-4. These Qrr sRNAs

reciprocally control the expression of the QS transcription regulators HapR and AphA. At LCD the HapR expression is repressed, while AphA is activated. At HCD the AIs accumulate and bind to their cognate receptors CqsS and LuxPQ, converting them into phosphatases. As a consequence, phosphate flow is reversed, leading to dephosphorylation and deactivation of LuxO and subsequent termination of the Qrr transcription production of HapR and repression of AphA. The reciprocal production of HapR and AphA at LCD and HCD represents a central element in the QS system in *V. cholerae* and *V. harveyi* [79, 80, 82, 83]. In addition, two new receptors, the CqsR and VpsS have been reported to channel information through LuxO, proposing the existence of four sensory signals in *V. cholerae* [84]. Another recently discovered, QS system produces a signaling molecule called DPO (3,5-dimethylpyrazin-2-ol), that is sensed by VqmA, a cytoplasmic LuxR-type transcriptional regulator, which induces the transcription of VqmR sRNA. The VqmR inhibits biofilm formation by repressing the transcription of VpsT and inhibits virulence gene expression by inhibiting the AphA [85].

1.3.2.2 The QS systems of V. harveyi

The QS system of the marine bacterium *V. harveyi* possesses three AIs and three cognate receptors that function in parallel to pass information into a shared regulatory pathway [81]. In *V. harveyi*, QS regulate bioluminescence, siderophore and metalloprotease production as well as production of exopolysaccharide [86-88]. The first AI is N-3-hydroxy-butanoyl-L- homoserine lactone (3OHC4-HSL) also known as HAI-1. It is synthesized by LuxM and binds a membrane bound histidine kinase receptor, LuxN. The second AI of *V. harveyi,* AI-2 is synthesized by LuxS and binds to a periplasmic receptor, LuxP. The LuxP-AI-2 complex interacts with a membrane bound histidine kinase, LuxQ. Both LuxM-LuxN and LuxS-LuxPQ of *V. harveyi* are homologs to the *A. fischeri* systems AinS-AinR and LuxS-LuxPQ, respectively. The third signal of *V. harveyi* is CAI-1 molecule produced by CqsA and interacts with a membrane bound histidine kinase sensor, CqsS. All three systems, LuxN, LuxQ and CqsS are two component system that contain a histidine kinase domain and a response regulator domain but no DNA-binding domain [81]. At LCD and when the AI level is not high enough to be detected by their cognate sensors, the three receptors (LuxN, LuxQ and CqsS) act as kinases. The receptors get autophosphorylated to subsequently transfer the phosphoryl group to the LuxU, and subsequently to the response regulator LuxO. The phosphorylated LuxO is activated and together with the sigma factor-54 induces the transcription of five small regulatory RNAs, Qrr1-5. The Qrrs together with RNA chaperon Hfq, destabilize and degrade the mRNA of the master regulator *luxR*, a homolog of *A. fischeri* LitR. At LCD the Qrrs also simultaneously activate production of another transcription factor, AphA [83]. The expression of LuxR is required for light production and hence no light is produced at low cell density. At HCD the AIs accumulate and bind to the corresponding receptors, inhibiting their kinase activities.

LuxU gets dephosphorylated and the phosphoryl groups are drained from the cascade. As LuxO become inactivated, the downstream cascade to induce Qrr sRNA is inhibited, eliminating the activation of *aphA* expression and allowing the production of LuxR. Hence *luxR* represses the production of AphA at HCD while the *aphA* represses the transcription of LuxR at LCD [81, 83, 88].

1.3.2.3 The QS systems of V. anguillarum

In the fish pathogen *V. anguillarum*, two QS circuits similar to *V. harveyi* systems LuxM-LuxN and LuxS-LuxPQ and a third which is a homolog to *V. cholerae* CqsA-CqsS were identified. VanM a homolog of LuxM, synthesizes an N-hexanoyl-L-homoserine lactone, (C6-HSL) and 3OC6-HSL and is assumed to be on the top of the QS hierarchy. The molecules are sensed by VanN, a hybrid sensor kinase. VanS, a LuxS homolog is responsible for production of AI-2 which is sensed by VanP and the hybrid sensor kinase VanQ. All systems, regulate the expression of the master regulator VanT, which is a homolog to LuxR in *V. harveyi* [81]. At LCD, the phosphoryl group is transmitted via VanU (LuxU homolog) to the VanO (LuxO homolog), which together with sigma factor-54 initiated transcription of sRNAs to repress the expression of QS master regulator, VanT. At HCD, the VanT expression is induced and the master regulator positively regulates pigment, metalloprotease and biofilm formation [89]. *V. anguillarum* also possesses and VanI-VanR system similar to LuxI-LuxR of *A. fischeri.* VanI is responsible for the synthesis of N-3-oxo-decanoyl-L-homoserine lactone, (3OC10-HSL) which is sensed by the transcription regulator VanR. VanR binds the 3OC10-HSL and regulates *vanI*. The VanI-VanR system is also connected to the phosphorelay cascade [81, 89, 90].

1.3.2.4 The QS systems of A. salmonicida

Based on the complete genome sequence of *A. salmonicida* LFI1238, genes of five QS systems have been identified: LuxI-LuxR, AinS-AinR, LuxM-LuxN, LuxS-LuxPQ and VarS-VarA [49]. However, it is believed that only the LuxI-LuxR and AinS-AinR are functional while the other QS systems are silent or incomplete. The *luxM* synthase is missing from the LuxM-LuxN system and frame-shift deletions were identified in the *luxN* histidine sensor kinase as well as in *luxP* which is part of the LuxS-LuxPQ system [49]. *A. salmonicida* produces eight AHLs, where the LuxI is responsible for production of seven AHLs (C4-HSL, 3OC4-HSL, C6-HSL, 3OC6-HSL, C8-HSL, 3OC8-HSL and 3OC10-HSL), and AinS only one AHL, 3OHC10-HSL [91, 92]. The diversity of the AHL production in *A. salmonicida* believed to have various biological function and fitness benefits [91, 92], still there is limited knowledge concerning the eight AHLs of this bacterium.

The LuxI-LuxR system and the *lux* operon of *A. salmonicida* differ from the one described in *A. fischeri* in several ways: the *luxR* gene in *A. salmonicida* is found in two copies, *luxR1* (*VSAL_II0965*)

and *luxR2* (*VSAL_II0958*), similar to the related *A. logei* [93]. The *luxR2* gene is located on the other end of the *lux* operon and transcribed in antisense orientation (Figure 4). The inactivation of *luxR1* and *luxR2* showed no significant production of LuxI AHLs and both mutants were able to produce only the AinS AHL, proposing that both proteins function as heterodimers [91]. Although *A. salmonicida* carry the genes for luminescence (*lux* operon) they do not produce a detectable level of light in culture and referred to as cryptically bioluminescence. Cultures of *A. salmonicida* become visibly luminous only in the presence of an exogenous aliphatic aldehyde, which induces the synthesis of luciferase as cells approach stationary phase [94]. This defect in light production was proposed to be due to a 11 base pair (bp) deletion in the intergenic space between the *luxC* and *luxD* genes that includes the A and T nucleotides of the *luxD* start codon ATG [15].

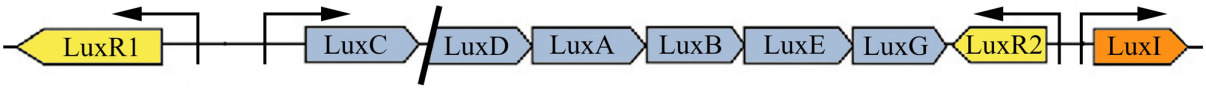

Figure 4 The schematic arrangement of the *lux* operon and the *luxR1/luxR2* genes in *A. salmonicida* LFI1238. The *luxA* and *luxB* genes respectively, encode the alpha and beta subunits of luciferase, the enzyme responsible for luminescence. The *luxC*, *luxD*, and *luxE* genes each encode an enzyme required for the synthesis of an aliphatic-aldehyde substrate. *luxG* is not essential for luminescence and is believed to increase the capacity of the cell to synthesize flavin mononucleotide. *luxR* encodes LuxR, an activator of *lux* operon transcription, and *luxI* encodes LuxI synthase, which produce autoinducers [95].

In *A. salmonicida* it is believed that the LuxS-LuxPQ and AinS-AinR systems transduce the information from the autoinducers AI-2 and 3OHC10-HSL to the histidine phosphotransferase protein LuxU and finally to the response regulator LuxO. The level of phosphorylated LuxO depends on the autoinducer concentrations. The phosphorylated LuxO controls the expression of small regulatory RNAs Qrrs that together with the RNA chaperon Hfq, destabilize the transcript of the master regulator LitR. The master regulator, LitR has been shown to be involved in the regulation of several activities that may be important for host pathogen interaction and virulence. For example, the inactivation of LitR led to biofilm formation, enhanced motility, wrinkled colony morphology, adhesiveness and a significant reduction in the production of 3OC6-HSL (LuxI-AHL) and 3OHC10-HSL (AinS-AHL) [57, 91, 96]. Atlantic salmon infected with an *A. salmonicida ΔlitR* mutant also showed lower rate of mortality compared to fish infected with the wild type, highlighting the impotence of LitR for pathogenicity of *A. salmonicida.* Furthermore, deletion of *litR* decreased the induced bioluminescence of *A. salmonicida* [57].

1.4 Phenotypic traits regulated by QS

Most bacteria depend on QS to regulate important cellular processes that are essential for survival, adaptation to the environment and virulence-related factors, like biofilm formation, adhesion, motility, iron-sequestering system and others. Below are some examples of these processes and the role of QS in their regulation.

1.4.1 Biofilm formation

Bacteria in aquatic environments are rarely found in the planktonic or free-swimming phase. Rather, they are found in association with a solid surface in a sessile state. The first observation of surface adherent bacteria was made by Anthony van Leeuwenhoek in 1684, when he observed the plaque of his own teeth and discovered what would later be known as "bacterial biofilm". The term "biofilm", however was not used until 1978 and in 1999 Costerton and co-authors defined the biofilm as "*a structured community of bacterial cells enclosed in a self-produced polymeric matrix and adherent to an inert or living surface*" [97-101]. Biofilms are found everywhere from drinking water to medical devices and cause the most problematic bacterial infections such as urinary tract infections, dental plaque and upper respiratory tract infections [102-105].

Biofilms can be either single or multilayered and can contain either homologs or heterologs population of bacteria. In most biofilm formations, unicellular organism come together to form a community. This community become attached to either biotic or abiotic surfaced and embedded in a self-produced matrix. The matrix is generally referred to as *extracellular polymeric substance* (EPS) which is a mixture of polysaccharides, proteins (composed primarily of D-amino acids), fatty acid and extracellular nucleic acids (eDNA) [99, 106, 107]. Most of the biomasses of a biofilm is composed of more EPS (90%) than microbial cells (10%) [108]. EPS is built of water channels that facilitate exchange of nutrients, waste products and oxygen to all parts of the structure. EPS is also involved in facilitating surface adherence, aggregation and maintaining the three-dimensional architecture of the biofilm. Furthermore, the EPS surrounding the biofilm serves as a barrier protecting the bacterial cells against various stress factors, such as antimicrobial compounds, host immune systems, oxidation and metallic cations, hence enhancing growth and survival by providing nutrients and protecting from predators. Thus, the biofilm is the preferred lifestyle among vibrios and other microbes, providing several advantages such as virulence in *V. cholerae*, *V. vulnificus* and *V. parahaemolyticus*, and host colonization by *A. fischeri* [108-112].

Figure 5 demonstrates the stages of biofilm formation, that can be divided into four stages (i) surface attachment; (ii) microcolony formation; (iii) biofilm maturation; and (iv) dispersal and detachment [106].

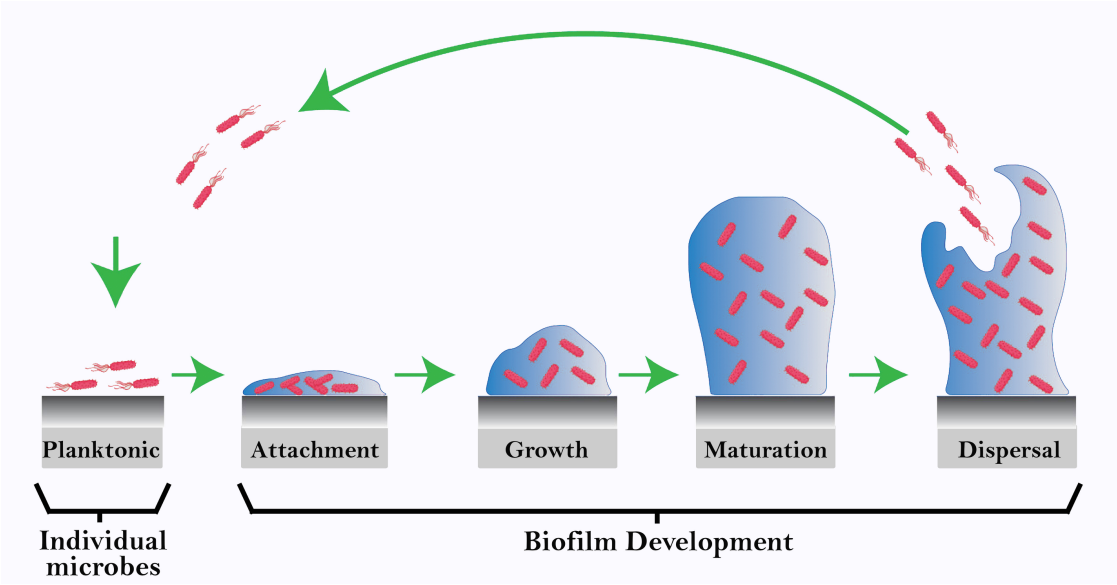

Figure 5 The steps of biofilm life cycle. Biofilm formation is a multistage process that involves (i) attachment of cells to a surface, (ii) secretion of adhesins and EPS that result in irreversible attachment of the biofilm and the growth of cells (iii) maturation of the biofilm into mushroom structure (iv) dispersal of single cells that return to a planktonic phase.

Surface attachment

Surface attachment is the turning point from a planktonic lifestyle to the biofilm mode and could be categorized as a two-stage process: initial reversible attachment and irreversible attachment. When planktonic cells come in contact with a surface, they adhere either by using a physical force of by bacterial appendages such as pili or flagella. This surface attachment is termed "reversible attachment". The initial attachment to the surface is dynamic and can be reversed due to weak interaction between bacteria and the surface. In this case the bacteria can detach and rejoin the planktonic population if perturbed by repulsive forced or in response to nutrient availability. There are several interaction forces that help the bacteria to adhere to a surface such as hydrophobic interaction, protein adhesion, electrostatic interactions and Van der Waal force. When the attractive force is greater that the repulsive force, some of the attached cells become immobilized and attach irreversibly [107, 113-115].

Microcolony formation

Following the irreversible attachment, surface associated bacterial cells come together and start to proliferate and produce biofilm matrix components, forming small aggregates to generate multi-layer microcolonies. At this stage bacterial cells enhance the production of EPS and repress flagellar-mediated swimming motility [114, 116].

Biofilm maturation

The multi-layer microcolonies undergo a maturation process involving two stages: stage I involves inter-cell communication and the production of autoinducer signal molecules such as AHLs. In stage II the microcolonies grow through cell proliferation, increase in size and gradually mature forming macrocolonies. At this stage the macrocolonies are encased in a self-produced EPS matrix that stabilizes the biofilm network and is essential to build the three-dimensional mushroom-like structure [107, 117].

Dispersal and detachment

Inside the mature biofilm, bacteria exchange and share products that play an essential role in maintaining the biofilm structure and providing a suitable and favorable environment for the bacterial colony. As the biofilm matures, resources such as nutrients and oxygen become limited and at the same time toxic products accumulate. In order to survive, expand, get nutrients and eliminate stress, the dispersal become an option and some cells of the biofilm disperse and return to a planktonic lifestyle and may subsequently colonize other surfaces to form new biofilms. For example, *Pseudomonas putida* biofilms can dissolve rapidly once the medium flow in the chambers stops, suggesting that nutrient limitation leads to biofilm dispersal [118]. In addition to nutrient limitation previous studies show that increase in nutrient availability can lead to dispersal of parts of a biofilm. For example *Pseudomonas aeruginosa* induces dispersal with increasing nutrient availability in the environment [119]. The dispersal stage is the final stage of biofilm life cycle as well as the start of a new cycle through dispersal. This can occur passively through dynamic forces or actively through the production of matrix-degrading enzymes and induction of flagella motility. In general, the mature biofilm is built of two distinct layers. The base film layer where the bacterial cells exist and the surface film layer where the bacterial cells get dispersed into their surroundings. Hence the dispersal could occur in the whole biofilm or just in a part of it [114, 117].

Biofilm formation is a highly regulated process, in which bacteria have to synchronize their gene expression to be able to create the overall biofilm structure. To achieve this, bacteria use several regulatory mechanisms such as QS, c-di-GMP signaling, alternative sigma factors, sRNAs and two-component regulators.

QS is associated with almost all stages of biofilm development from attachment to dispersal. For some species bacterial QS systems regulate flagellar activity and adhesion, which in turn influences the attachment of bacteria to surface and microcolony aggregation [120]. For example, in *Staphylococcus aureus* the *agr* QS system regulates surface adhesion, which influence the attachment to the host [121]. In *P. aeruginosa* QS regulates other aspects of biofilm formation,

including biofilm structure. The *lasI* mutant, which is defective in the synthesis of N-3-oxo-dodecanoyl-L-homoserine lactone (3OC12-HSL), formed thin (about 20% of the wild type thickness) and densely packed biofilms lacking water channels and mushroom structure [66, 122]. Similarly, in *V. cholerae* QS tightly regulate the transcription of genes involved in the production of exopolysaccharides which is necessary for biofilm maturation and the formation of the three-dimensional architecture [123]. Furthermore, QS plays a critical role in dispersal of detached bacteria from mature biofilm to trigger a new cycle of biofilm formation [124].

An intracellular second messenger, bis-(3-5)-cyclic dimeric guanosine monophosphate (c-di-GMP) plays a critical role in several stages of the bacterial biofilm formation. At early stages, the high intercellular concentration c-di-GMP is involved in the bacterial decision between remaining as planktonic cells or entering the biofilm lifestyle [125]. In *V. cholerae* and other bacterial spp. the increased level of c-di-GMP enhance biofilm formation and at the same time represses motility, while the low level of c-di-GMP inhibit biofilm formation and promote motility [126, 127]. C-di-GMP has been shown to be controlled by QS, where changes in cell density is one of the environmental factors sensed by the second messenger [128].

Alternative sigma factors and their role in QS and biofilm formation will be presented later in this thesis, whereas other regulatory factors are beyond the scope of this work.

1.4.2 Colony morphology and the production of polysaccharides

Some bacterial species show two distinct phenotypic morphological colony states: the rugose colony morphology (wrinkled) or smooth colony morphology. The rugose variant shows elevated resistance to acidic and saltwater environments as well as increased survival in chlorinated water [129-131]. In *V. cholerae* studies have shown that production of smooth and rugose colony phenotypes is a defensive mechanism against predation by protozoan grazing, a leading cause of bacterial mortality in natural aquatic environments [132]. In *Vibrio* and other bacterial species, the rugose colony morphology is associated with increase production of exopolysaccharides and is linked to robust biofilms. In *V. cholerae* the production of polysaccharides depends on the expression of *vibrio polysaccharide* genes also known as *vps* genes or operon. The *vps* operon consists of 17 genes, that are clustered in two regions the *vps-I* and the *vps-II.* The *vps-I* and *vps-II* regions are separated by the *rbmABCDEF* genes that encode biofilm matrix proteins [129, 133]. The expression of *vps* genes is positively regulated by transcription activators VpsR and VpsT. C-di-GMP binds VpsT and activates the transcription of *vps* genes required for biofilm formation and for rugose colony development [123, 126, 134-136]. QS and changes in cell density also play an essential role in regulating the *vps* genes and the rugose phenotype in *V. cholerae.* At LCD the AphA transcription factors is active, enhancing the expression of the biofilm activator VpsT allowing

biofilm and wrinkled colony formation. At HCD, the HapR is active and repressing the VpsT expression, leading to biofilm repression and formation of smoot colony morphology [78, 137].

V. parahaemolyticus isolates display variation in colony morphology, alternating between opaque (not clear colonies) and translucent (flat and clear/smooth colonies) cell types [138]. The opaque colonies produce more extracellular polysaccharide than translucent colonies [139]. In *V. parahaemolyticus* the polysaccharide biosynthesis locus (a homolog to "*vps*" operon of *V. cholerae*) is made up of 11 genes and located in two operons. The locus is known as *cps* for *capsular polysaccharides* and its genes code for proteins responsible for CPS production [130]. Besides opaque and translucent morphotypes, *V. parahaemolyticus* also forms rugose colonies that exhibit increased CPS production compared to parental translucent or opaque strains [140]. The production of CPS is regulated by the QS master regulator OpaR. Unlike the negative regulation of HapR on biofilm and rugosity in *V. cholerae*, the OpaR induces colony opacity, which indicate an enhanced production of CPS. The inactivation of OpaR resulted in translucent colony morphology, mimicking the low cell density regulatory state [141].

The switch from translucent to opaque colony morphology was also reported for *V. vulnificus.* The bacterium can also form rugose colony morphology in response to certain environmental conditions [142, 143]. The expression of *brp* cluster (renamed from *wcr*), involved in EPS production and group I *cps* operon are required for these switch events in colony morphology and for determining the size of the biofilm [144-147]. An additional exopolysaccharide locus, *rbd* was characterized in *V. vulnificus* and found to enhance biofilm formation and cell aggregation phenotypes, though its polysaccharide production did not appear to be required for the development or maintenance of the rugose colony phenotype [148]. These morphological variations are regulated by QS and the master regulator SmcR in a cell density dependent manner [149, 150].

In *A. fischeri* the production of polysaccharides depends upon 18 genes separated in four operons and known as *symbiotic polysaccharides* or *syp* genes. The expression of *syp* operon results in wrinkled colonies and biofilm matrix production. The *syp* locus is also required for symbiotic association with the host (squid). Production of polysaccharides via *syp* is controlled by two-component signaling cascade involving one or more regulators. The overexpression of one of such regulators the RscS (sensor kinase), is sufficient to induce biofilm and rugose colony formation by activating the downstream response regulators, the SypG and SypE. One of the response regulators "SypG" is a transcriptional regulator that directly regulate expression of the *syp* operon at its four promoters [151-153]. Similar to *V. parahaemolyticus,* the master regulator of *A. fischeri* (LitR), is a positive regulator of biofilm formation and colony rugosity at high cell density [75].

Biofilm and winkled colony formation in *A. salmonicida* LFI1238 involve the production of exopolysaccharides through *syp* operon (18-gene), which is located on the second chromosome and organized in four transcription units (Figure 6) [49, 96].

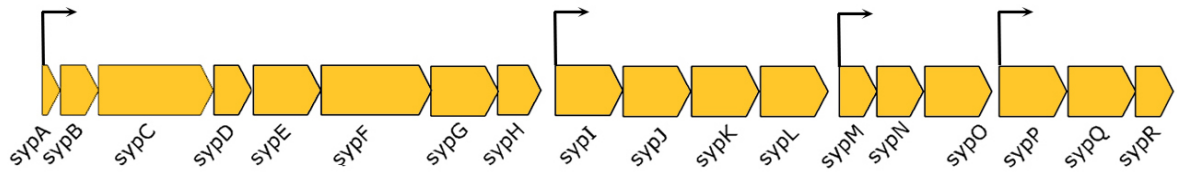

Figure 6 The schematic origination of the *syp* operon in *A. salmonicida* LFI1238. The *syp* operon is 22.453 bp, located on chromosome II from *VSAL_II0295* (*sypR*) to *VSAL_II0312* (*sypA*). Yellow arrows indicate genes and their direction of transcription. Black arrows indicate the start of each transcription unit.

Similar to *V. cholerae* the inactivation of QS master regulator (LitR) in *A. salmonicida*, enhanced biofilm formation and wrinkled colony morphology, indicating a negative regulation of the master regulator on the *syp* operon [96].

1.4.3 Flagellar-mediated motility

1.4.3.1 Flagellar structure and regulation

Many bacterial cells exhibit several ways of motility ranging from swimming in liquid with a polar flagellum or swarming over solid or viscous surfaces with lateral flagella. Among the wide range of different strategies for bacterial movement, flagellum-mediated motility is the most studied form [154]. Flagella are filamentous organelles that extend from inside-out (from cytoplasm to exterior of the cell) and can be subdivided into three substructures. The first component is the basal body, which anchors the flagellum to the cell membrane. The second component is the hook, which is connected to the basal body. The third component is the helical filament which is composed of the protein flagellin. The basal body functions as a rotary motor and can be divided into two major components: the stationary part (stator) and the rotary part (rotor). The *rotor* is connected to the basal body and polymerized from monomers of FliG proteins. The *stator* complex is composed of MotA and MotB proteins, which serve as an ion channels that provide the energy potential to rotate the flagellum. The interaction between the stator and rotors are responsible for generating a torques which drives flagellar rotation [155-158]. In *Vibrio* spp. the structure and function of the flagellum is similar to those of other bacterial species with the exception of the stator complex which consists of two additional motor proteins the MotX and MotY [159]. The

flagellar filament itself is a long structure of helical shape, which functions as a propellers [160]. The number of flagellin genes varies among flagellated bacterial species, where some bacteria possessing only one flagellin gene, while others possess multiple. For example, *V. parahaemolyticus* possesses six flagellin genes and *V. cholerae* and *V. anguillarum* possess five flagellin genes each. For these bacteria the chromosomal organization of the flagellin genes is similar [161-163]. *A. salmonicida* possesses six flagellin genes which are located at two separated chromosomal loci. *flaABCDE* genes are found in one locus and *flaF* in a different locus [56].

All *Vibrio* spp. possess two chromosomes and are highly motile with single or multiple polar flagella at the cell pole. All genes responsible for the polar flagellar assembly are located on the large chromosome, while the small chromosome contains genes involved in the later flagellar system [164]. The construction of functional flagellum in vibrios is a complex process involving more than 50 gene products [156]. The flagellum is assembled is a step-wise manner starting from the basal body, followed by hook assembly and finally by filament formation. Any defect in gene products that disrupts the basal body or the hook formation inhibits the filament [164]. The flagellar assembly of vibrios has been mostly studied in *V. cholerae* and showed to be organized in four hierarchical levels (classes). Class I encodes the regulatory protein FlrA, which together with sigma factor-54 controls expression of Class II flagellar genes. FlrA is the master regulator of the flagellar hierarchy and without it no flagellar genes are expressed. Class II proteins FlrB and FlrC are important for controlling transcription of Class III genes necessary for synthesis of hook, basal body, and filaments. Class II sigma factor-28 (FliA) regulates transcription of Class IV genes associated with the production of motor components [164-168].

The regulation of motility through QS has been studied in several members of the *Vibrionaceae* family. For example, in *V. harveyi,* QS positively regulate flagellar motility, where the inactivation of all three autoinducer synthases (in a triple mutant and single mutants) showed significantly lower swimming motility than the wild type. Moreover, the LuxR master regulator of QS, showed a positive regulation on motility, where upon its deletion the motility was reduced [169]. In other vibrios and allivibrios such as *A. salmonicida*, *A. fischeri* and *V. alginolyticus* QS has been shown to negatively regulate motility [57, 170, 171].

1.4.3.2 The role of flagella in biofilm formation

Traditionally flagella have been considered only as a motility organelle but it has become evident that they also possess several other functions such as participation in biofilm formation, virulence and adhesion [172-174]. Flagellar-mediated motility enables bacteria to move toward favorable environments and avoiding unfavorable conditions. When facing unfavorable conditions, bacteria can escape by forming biofilms. A relationship between motility and biofilm formation was

established in several bacterial species, where motility was shown to be involved in all steps of biofilm formation [174, 175]. Flagellar-mediated motility has been demonstrated to accelerate the surface attachments for several bacteria. Bacterial mutants exhibiting a non-motile phenotype are often defective of attachments to surfaces. Motility is known to enhance the initial interaction of bacterium to a surface in order to overcome the repulsive force and increasing the chance of close contact [174-178]. The disruption of the flagellar biosynthesis is known to alter biofilm architecture. For example in *P. aeruginosa* the loss of flagella did not affect the initial attachment of the biofilm formation, but the motility mutants formed biofilms with different structural characteristics compared to the wild type [179]. The presence of flagella was also required for mature biofilm formation in the *Xanthomonas axonopodis pv. citri* (*Xac*) which also showed reduced virulence due to the lack of motility [180]. Loss of motility also affected the biofilm architecture in *Escherichia coli*, where poorly motile strains formed flatter biofilms compared to highly motile strains, which displayed more mature vertical biofilm structures [181].

1.5 Alternative sigma factors

The bacterial core RNA polymerase (RNAP) complex consists of five subunits (ββ'α2ω). These subunits are sufficient for transcription elongation and termination, but is unable to initiate transcription. The initiation of transcription from promoter requires a sixth dissociable subunit, known as sigma factor. Sigma factors are class of proteins that bind to the core RNAP complex to form the holoenzyme. Once the RNAP holoenzyme is bound to the promoter, the initiation of transcription occurs [182, 183]. Sigma factors can be classified into two major families: the sigma-70 family and the sigma-54 family. The sigma-70 family contains the largest group of sigma factors, which includes primary sigma factors and alternative sigma factors. The sequence alignment of the sigma-70 family members reveals four conserved regions (region 1, region 2, region 3 and region 4) that are further divided into subregions. Only region 2 and 4 are well conserved among all sigma-70 family members. These regions contain subregions (region 2.4 and region 4.2) for core RNAP complex recognition as −10 and −35 promoter recognition residues, respectively. Alternative sigma factors direct gene transcription in response to various stimuli that occur in their natural environment or within the host. In Gram-negative bacteria the alternative sigma factor, RpoS is the general stress-responsive, which is critical for survival during stationary growth phase [184, 185]. Phylogenetic analysis of alternative sigma factors in *Vibrionaceae* revealed that a number of *Vibrio* species possess additional RpoS-like sigma factors. For example, a divergent copy of putative RpoS-like sigma factor has been identified in *Vibrio splendidus*, *Vibrio* sp. MED222, *Vibrio campbellii* and *V. alginolyticus* [186, 187]. Additionally, an RpoS-like sigma factor was identified in *A. fischeri* and named RpoQ due to its activation of the AinS-AinR QS system. RpoQ of *A. fischeri* has 45% amino acid identity to the RpoS protein in this

species. [188, 189]. A homolog of *A. fischeri rpoQ* is found in *A. salmonicida. rpoQ* (*VSAL_II0319*) of *A. salmonicida* showed a 40% protein sequence similarity to the *rpoS* gene (*VSAL_I2506*) in the same species. To date homologs of RpoQ sigma factor are found only among aliivibrios. The RpoQ of *A. salmonicida* shares a high amino acid sequence identity (99%) with its homolog in *A. logei* (*A. logei* S5-186 GeneBank accession no AJY02000108.1), whereas the amino acid sequence identity is 72% with *A. fischeri* ES114, 73% with *A. finisterrensis* and 69% with *A. wodanis* 06/09/139 [190].

1.5.1 The role of RpoS and RpoS-like sigma factors in Vibrionaceae

Most *Vibrio* species analyzed to date contain a copy of the *E. coli* RpoS homolog [186]. The role of RpoS has been characterized and shown to be involved in stress conditions. Moreover, a connection between RpoS and QS was established in several *Vibrio* species. Early studies with *V. cholerae* have shown that inactivation of RpoS resulted in bacterial strains sensitive to several environmental stress factors such as carbon starvation, hyperosmolarity and oxidative stress [191]. The loss of RpoS also interfered with the ability of *V. cholerae* to colonize the small intestine of infected mice [192]. Additionally, QS and the master regulator, HapR have been reported to increase the expression of RpoS, which in turn positively affect the expression of HapR-dependent *hapA* gene encoding hemagglutinin (HA)/protease [193, 194]. RpoS together with HapR also initiates the mucosa escape program which denotes a later stage of infection, when the bacterium detaches from the epithelial surfaces. This step requires expression of genes involved in motility and chemotaxis. Deletion of RpoS elevated the cholera toxin virulence factor and downregulated motility and chemotaxis genes. These results suggest that RpoS is involved in repression of virulence and promotion of motility to facilitate transmission [195, 196]. RpoS sigma factors provide the main line of response to changes in the environment and are important for determining the entry into the biofilm. However recently RpoS and QS have been shown to also be important for *V. cholerae* dispersion from the biofilm [197, 198].

In addition to *V. cholerae,* RpoS has been studied in other vibrios. In *V. parahaemolyticus*, RpoS plays an important role in the survival and viability under conditions of cold stress and hyperosmolarity [199]. RpoS was also connected to QS and together with the master regulator, OpaR showed positive regulation of the virulence factor PrtA [200]. Analysis of an *rpoS* deletion in *V. vulnificus* showed that RpoS was important for protecting the bacterium from acid stress, oxidative stress and nutrient starvation. RpoS was also shown to be essential for survival under certain environmental conditions and for host colonization through positive regulation of extracellular enzymes such as albuminase, caseinase and elastase [201, 202]. In the fish pathogen *V. anguillarum,* RpoS and QS system work together to control survival and stress response by

inducing the expression of VanT the master regulator of QS in a manner independent of VanO. Moreover, the deletion of the *rpoS* gene led to reduced metalloprotease production and virulence in this species [203]. In *V. harveyi* RpoS does not affect QS system regulation, but the *rpoS* deletion mutant showed increased sensitivity to stationary phase stress as well as high concertation of ethanol compared to the wild type [204]. In the marine bacterium *V. alginolyticus* the deletion of *rpoS* resulted in strains that are more sensitive than the wild type to ethanol, hyperosmolarity, heat and hydrogen peroxide changes. RpoS was also shown to be a part of the regulatory network of virulence and LuxS quorum sensing system [205]. Recently RpoS has been shown to regulate bacterial adhesion in response to changes in temperature, pH and nutrient content [206]. The RpoS-like sigma factor of *V. alginolyticus* (RpoX) was found to be involved in biofilm formation and stress responses, additionally it was shown to be a part of RpoE regulon and play an essential role in motility and hemolytic activities [187, 207]. RpoQ of *A. fischeri* was found to be involved in regulating bioluminescence, motility and chitinase activity by LuxO via LitR [188, 189]. The microarray analysis of *A. salmonicida ΔlitR* mutant revealed a number of differentially expressed genes (DEGs) that were up and downregulated in the mutant relative to the wild type. *rpoQ* sigma factor was among the positively regulated genes in both biofilm and suspension samples [96].

2 AIMS OF THIS THESIS

Main objective:

The aim of this study was to expand the knowledge concerning QS systems and its role in controlling several phenotypic traits, such as biofilm formation, colony rugosity and motility in *A. salmonicida*.

Sub-objectives:

1. To investigate the role of, RpoQ sigma factor and the impact of temperature changes on regulating cellular activities (biofilm formation, wrinkled colony morphology and motility) related to QS mechanism in *A. salmonicida*.

2. To explore the differential gene expression of Δ*litR* and Δ*rpoQ* and their role in regulating phenotypic traits related to QS, as well as to determine the influence of cell density changes on gene expression in *A. salmonicida*.

3. To determine the influence of AHLs on biofilm formation and to explore the regulatory effect of *luxI* and *ainS* autoinducer synthases on gene expression at different cell densities.

3 SUMMARY OF PAPERS

3.1 Paper I

The alternative sigma factor RpoQ regulates colony morphology, biofilm formation and motility in the fish pathogen *Aliivibrio salmonicida*

Miriam Khider, Nils Peder Willassen and Hilde Hansen // BMC Microbiology., 12 September 2018., **18**:16.

Quorum sensing (QS) is a cell-to cell communication system, which synchronously controls expression of a vast range of genes in response to changes in cell density, and is mediated by autoinducers that act as extracellular signals. LitR, the master regulator of QS in *Aliivibrio salmonicida*, has been shown to regulate a number of activities such as virulence, motility, biofilm formation, colony morphology and production of N-acyl-homoserine lactones (AHLs). LitR was also found to be a positive regulator of *rpoQ,* a gene encoding RpoS-like sigma factor. The role of RpoQ in biofilm formation, colony morphology, and motility at different temperature was analyzed by constructing a complete deletion mutant and a complementary strain using allelic exchange. The overexpression of *rpoQ* was also studied in both the wild type and the *Δ litR* mutant. The results indicated that RpoQ is a negative regulator of colony rugosity and biofilm formation, where the regulation of these traits is pronounced at low temperatures. The deletion of *rpoQ* significantly reduced the motility compared to the wild type, suggesting a positive regulation of RpoQ on motility in *A. salmonicida*. The overexpression of the *rpoQ* in the Δ*litR* mutant disrupted the biofilm produced and lowered the motility, whereas the overexpression of *rpoQ* in the wild type resulted in non-motile strains. Our results confirmed that RpoQ functions downstream of the LitR master regulator in the QS cascade and is a regulator of colony rugosity, biofilm formation and motility. We hypothesize that the negative regulation from LitR to the *syp* operon (polysaccharide biosynthesis locus), required for biofilm formation, is operated *via* RpoQ in a temperature dependent manner.

3.2 Paper II

Differential expression profiling of *ΔlitR* and *ΔrpoQ* mutants reveals insight into QS regulation of motility, adhesion and biofilm formation in *Aliivibrio salmonicida*

Miriam Khider, Erik Hjerde, Hilde Hansen and Nils Peder Willassen // BMC Genomics., 15 March 2019., **20**:220

Aliivibrio salmonicida, the causative agent of cold-water vibriosis in Atlantic salmon, uses quorum sensing (QS) to regulate several activities such as motility, biofilm formation, adhesion and rugose colony morphology, in a cell density dependent manner. In addition to QS, the expression of pathogenic and virulence factors for disease development requires seawater temperatures below 10°C. Our previous studies showed that LitR and RpoQ are involved in regulation of biofilm formation and rugose colony morphology, where the *syp* operon responsible for polysaccharide production was suggested to be regulated by LitR via *rpoQ*. To identify genes responsible for the observed phenotypic traits regulated by LitR and RpoQ, transcriptome profiling was used to compare *ΔrpoQ* and *ΔlitR* transcriptome to *A. salmonicida* wild type at high and low cell densities. Additionally, a comparative transcriptome of *A. salmonicida* at high cell density (HCD) relative to low cell density (LCD), was analyzed in order to map the changes in gene expression due to changes in cell density. We found that changes in cell density significantly altered the gene expression of *ΔrpoQ* and *ΔlitR* mutants as well as *A. salmonicida* wild type. The comparative transcriptome of *A. salmonicida* at HCD compared to LCD revealed 1013 differentially expressed genes that were distributed among 21 functional groups. Among the upregulated genes at HCD in the *A. salmonicida* wild type transcriptome were *litR* and *rpoQ*, while a downregulation was observed in flagellar biosynthesis genes and genes of the *tad* operon known to mediate adhesion. The transcriptome of *ΔrpoQ* mutant revealed a significant downregulation among flagellin genes with high abundance in the *flaA* gene. The *syp* operon and the *tad* operon were among the upregulated genes in the *ΔrpoQ* mutant compared to the wild type. Our results show that RpoQ-mediated activity negatively regulates the expression of the *syp* operon, confirming our hypothesis in Paper I. The results also indicate that RpoQ positively regulate the expression of several motility genes. However, the results were unable to solve the complicity of the motility regulation apparatus, which remains unknown and requires further studies.

3.3 Paper III

Exploring the transcriptome of *luxI*$^{-}$ and *ΔainS* mutants and the impact of N-3-oxo-hexanoyl-L- and N-3-hydroxy-decanoyl-L-homoserine lactones on biofilm formation in *Aliivibrio salmonicida*

Miriam Khider, Hilde Hansen, Jostein A. Johansen, Erik Hjerde and Nils Peder Willassen // PeerJ., 30 April 2019., 7:e6845

Aliivibrio salmonicida the causative agent of cold-water vibriosis in Atlantic salmon, possesses two quorum sensing (QS) systems, the LuxI-LuxR and AinS-AinR, which are responsible for the production of eight acyl-homoserine lactones (AHLs) in a cell density dependent manner. Previous studies demonstrated that inactivation of LitR, the master regulator of the QS, resulted in biofilm formation, similar to the biofilm formed by the AHL deficient mutant *ΔainSluxI*$^{-}$. In order to explore the role of AinS and LuxI, global gene expression patterns of *luxI* and *ainS* autoinducer synthases mutants were studied using transcriptomic profiling. The transcriptome profiling of *ΔainS* and *luxI*$^{-}$ mutants relative to the wild type revealed 29 and 500 differentially expressed genes (DEGs), respectively, which were involved in bacterial motility and chemotaxis, exopolysaccharide production and surface structures related to adhesion. Inactivation of *luxI*, but not *ainS* genes resulted in wrinkled colony morphology. While inactivation of both genes (*ΔainSluxI*$^{-}$) resulted in strains able to form wrinkled colonies and mushroom structured biofilm. When the *ΔainSluxI*$^{-}$ mutant was supplemented with N-3-oxo-hexanoyl-L- homoserine lactone (3OC6-HSL) or N-3-hydroxy-decanoyl-L-homoserine lactone (3OHC10-HSL), the biofilm did not develop. It has been demonstrated that LuxI is necessary for motility and repression of EPS production, where repression of EPS is likely operated through the RpoQ-sigma factor. These findings imply that the LuxI and AinS autoinducer synthases play a critical role in the regulation of biofilm formation, EPS production and motility.

4 RESULTS AND DISCUSSION

Quorum sensing is associated with various physiological processes most notably influencing the virulence system of many pathogenic bacteria [61, 208]. The work presented here was dedicated to expand the knowledge concerning the QS systems of *A. salmonicida*, in particular to study the role of QS in regulating phenotypic traits that may be important for survival and host interaction. It has been previously demonstrated that LitR, the master regulator of QS in *A. salmonicida*, regulates a number of activities such as virulence, motility, biofilm formation, colony morphology as well as production of AHLs. LitR was also found to be a positive regulator of *rpoQ*, a gene encoding RpoS-like sigma factor [57, 91, 96]. These studies led us to suspect that RpoQ acts downstream of LitR and may be involved in regulating some of the phenotypes related to QS in *A. salmonicida* LFI1238. In the context of QS, the role of RpoQ sigma factor was characterized in this study to gain insight into the regulation of biofilm formation, colony rugosity and motility (Paper I and II). Additionally, the QS autoinducer synthases, LuxI and AinS were previously shown to regulate AHL production and biofilm formation synergistically in *A. salmonicida* [91]. In Paper III we aimed to study the influence of AHLs on biofilm formation and the role of *ain* and *lux* QS systems in regulation of QS-dependent phenotypes.

This section represents a general discussion on five selected topics from this study that I found particularly interesting. First, I will discuss the role of RpoQ sigma factor in regulating polysaccharide production, which is essential for rugose colony morphology and biofilm formation. Next, I will discuss the importance of AHLs in downregulating biofilm development and then the role of flagellar-mediated motility in altering colony morphology. Finally, the influence of temperature variation and medium composition on QS-dependent phenotypes will be reviewed.

4.1 RpoQ sigma factor is vital for regulation of exopolysaccharide production and rugose colony phenotype

Alternative sigma factors such as RpoS provide the main line of responses to changes in the environment by altering gene transcription [209-211]. Several studies have shown a connection between RpoS and QS system in different vibrios [195, 203, 205, 212]. RpoQ, an RpoS-like sigma factor was initially studied in *A. fischeri* and showed to be regulated by LuxO via QS master regulator, LitR [188]. Likewise, our previous microarray results suggested that LitR is a positive regulator of *rpoQ* in *A. salmonicida* [96]. Hence, we proposed that RpoQ may be a component of

QS system and involved in controlling some of QS-related phenotypes similar to LitR. To reveal the role of RpoQ sigma factor in regulating colony morphology and other QS-related behaviors (see section 4.2 and 4.4 for further discussion), an in-frame deletion of the *rpoQ* coding sequence was constructed and compared to the wild type and complementary strains. Results in Paper I demonstrate that inactivation of *rpoQ* led to a strong and early rugose colony morphology as compared to Δ*litR*. The complimentary strain behaved similarly to the wild type and produced smooth colonies (see Figure 1 in Paper I). For several members of the *Vibrionaceae* family, including *A. salmonicida*, the ability to form rugose colonies is associated with enhanced exopolysaccharide production [96, 129, 139, 150]. Thus, the formation of rugose phenotype exhibited by the *ΔrpoQ* mutant is expected to be a consequence of enhanced polysaccharide production.

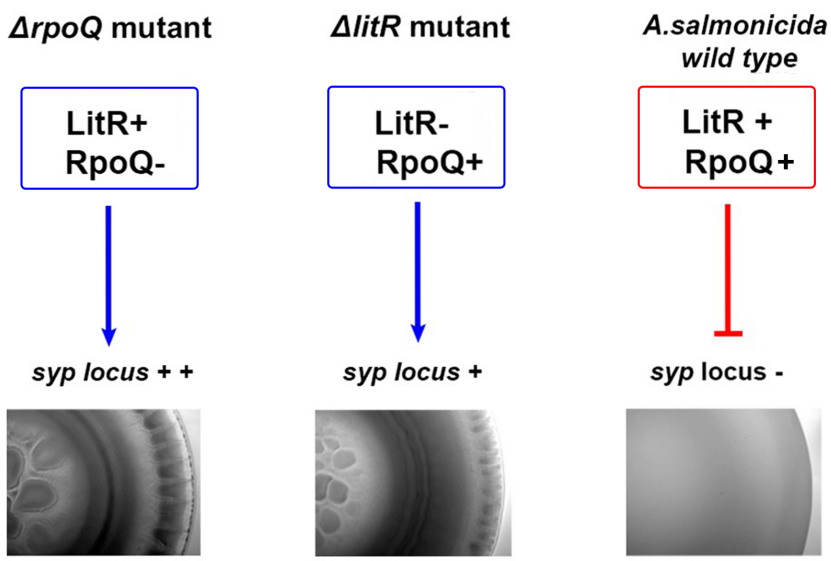

Figure 7 Conceptual model for regulation of *syp* operon by *A. salmonicida* LitR and RpoQ. Blue arrows indicate positive, inducing effects, and red bars indicate negative, inhibitory ones. (see discussion for explanation).

In several *Vibrio* species, homologs of the polysaccharide biosynthesis gene cluster, *syp* are conserved and contribute to rugose colony development [129, 139, 150, 213]. We know from our previous microarray that LitR represses the expression of, *syp* operon and that inactivation of three *syp* genes in the *ΔlitR* background resulted in smooth colonies [96]. Hence, stronger and earlier rugosity demonstrated by *ΔrpoQ* mutant, led us to speculate that LitR performs its activity on *syp* through RpoQ, and that RpoQ-dependent activity leads to a stronger repression of *syp*. The formation of weaker colony rugosity by *ΔlitR* mutant suggests a couple of potential explanations (Figure 7): (i) In *ΔlitR* mutant the *rpoQ* gene is downregulated and some expression of *rpoQ* still

occurs. This low level of LitR-independent *rpoQ* expression, results probably in repression of the *syp* expression via RpoQ leading to a weaker colony rugosity. (ii) In the *ΔrpoQ* mutant the expression of *rpoQ* is decreased to zero, resulting in absence of RpoQ-dependent repression on the *syp* expression and the *ΔrpoQ* mutant forms colonies with stronger rugosity.

As the project progressed, several QS-related mutants were analyzed for their rugose colony phenotype. In Paper III, the insertional inactivation of *luxI*, encoding an autoinducer synthase (responsible for synthesis of seven AHLs), led to strains with strong wrinkled colony morphology similar to that of the *ΔrpoQ* mutant. Hence, to further support the results obtained from the knock-out experiments (Paper I and III), a global transcriptome profiling analysis was performed (Paper II and III). Samples from *A. salmonicida ΔrpoQ*, *ΔlitR* and *luxI*$^{-}$ mutants were collected at early logarithmic phase at OD_{600} = 0.3 (optical density measured at 600 nm) and late exponential phase at OD_{600} = 1.2, from three independent cultures. The RNA sequencing (RNA-seq) was done using the TruSeq standard mRNA library prep kit (Illumina), and sequenced using the Illumina NextSeq 500 platform with mid output reagents to produce 75 bp paired-end reads. Differential expression analysis for genes between the reference genome of *A. salmonicida* wild type and *ΔlitR*, *ΔrpoQ* and *luxI*$^{-}$ mutants was performed using the DESeq2 package [214]. Genes were defined as significantly differentially expressed genes based on a *p*-value ≤0.05 and differentially expression values (fold change values) of ≥2 and ≤ −2. The transcriptome of the *ΔrpoQ* mutant relative to the wild type (*ΔrpoQ*/wt) demonstrated that 13 out of 18 *syp* genes were upregulated at HCD (see Table 4 in Paper II). Similar results have been obtained for *V. cholerae,* in which the transcription of the *vps* genes was greater in rugose-associated colonies, and in the absence of *vps* genes smooth colonies were formed [215]. In order to determine whether *syp* genes are responsible for the observed rugose phenotype in *ΔrpoQ* mutant, double mutants of *rpoQ* and *syp* genes were constructed. In Paper II, three *syp* genes (*sypQ*, *sypP* and *sypC*) were separately inactivated in the *ΔrpoQ* mutant by insertional mutation and the double mutants were characterized for colony morphology phenotype (Paper II). As reported in Paper II the characterized double mutants lacking the *syp* genes (*ΔrpoQsypQ*$^{-}$, *ΔrpoQsypP*$^{-}$ and *ΔrpoQsypC*$^{-}$) were unable to form rugose colony morphology and the colonies appeared smooth and similar to the wild type (see Figure S1 in Paper II). The lack of the *syp*-encoded EPS production upon the inactivation of the *sypQ*, *sypP* and *sypC* genes in the *ΔrpoQ* mutant suggests the importance of these genes in rugose phenotype formation. The *sypQ* and *sypP* genes are predicted to encode glycosyltransferase, which are enzymes that catalyze the sequential transfer of specific sugars to the undecaprenyl phosphate carrier lipid during the early steps of polysaccharide synthesis [216]. The *sypC* gene is predicted to encode polysaccharide biosynthesis exporter protein and may play a role in polysaccharide production. These results are in accordance with the situation in *V. vulnificus* where inactivation of *brpA* and *brpI* genes

(predicted to encode glycosyltransferase) and the *brpD* gene (predicted to encode polysaccharide export periplasmic protein), resulted in lack of EPS production and formation of smooth colonies, indicating the importance of these genes in rugose colony development [217]. In *V. cholerae,* strains containing in-frame deletion of *vpsD*, *vpsI*, and *vpsL* genes encoding glycosyltransferase exhibited flat and smooth colony morphology and were unable to produce VPS [133]. As mentioned above, the *luxI*$^{-}$ mutant also exhibited rugose colony phenotype (Paper III). The *luxI*$^{-}$ transcriptome, when compared to the wild type (*luxI*$^{-}$/wt), revealed an upregulation in 11 out of 18 *syp* genes (see Table 3 in Paper III). Interestingly, in addition to the *syp* genes, the transcriptome of *luxI*$^{-}$ mutant demonstrated a strong LuxI-dependent downregulation of the *rpoQ* gene. These results suggest that wrinkled colony morphology exhibited by, *luxI*$^{-}$ mutant and the expression of *syp* genes in this mutant is also operated through RpoQ. The transcriptome of *ΔlitR*, compared to the wild type (*ΔlitR*/wt) did not reveal a significant differential expression among *syp* gene and only *sypA* (*VSAL_II0312*- fold change 2.19) and *sypC* (*VSAL_II0310*- fold change 2.26) were differentially expressed at HCD with fold change value close to threshold (fold change values ≥2 and ≤ −2, *p*-value ≤0.05). Results from the *ΔlitR* mutant showed patterns different to those previously shown using microarray experiments [96]. One potential explanation is differing culturing conditions between the two studies, which may have contributed to the observed differences. The change of media composition and/or culturing conditions has been reported to influence the exopolysaccharide production and colony rugosity in *A. salmonicida* [96](see section 4.5).

Alternative sigma factors such as RpoS, are known to function as activators [183]. Most of the previous studies have focused mainly on the positive RpoS-dependent transcription of genes and the physiological implication of the under-expression of these genes in *rpoS*-mutant strains. For example, it was recently demonstrated that RpoS sigma factor is a positive regulator of polysaccharide production by direct binding to the promoter sequence of *pea* cluster (exopolysaccharide gene cluster) in *P. putida* [218]. Similar results were obtained in *P. aeruginosa*, where RpoS was shown to be a transcriptional factor that positively regulates the expression of *psI* operon (polysaccharide synthesis locus), and by *rpoS* inactivation the polysaccharide production was reduced [219]. However, little is known regarding the mechanism(s) of RpoS-mediated repression, and a direct repression by a sigma factor is considered to be a rare mechanism. Our study is among the few that mention genes negatively regulated by RpoS and to the consequence of their overexpression [215, 220-222]. By RNA-seq it was recently determined that RpoS represses 197 out of 729 differentially expressed genes in the fish pathogen *Edwardsiella piscicida* [223]. RpoS of *E. piscicida,* has been found to downregulate expression of *esrB* gene (encoding EsrB transcription activator) and thereby reducing expression of virulence-

associated genes. Further analysis demonstrated that RpoS repression of *esrB* gene involves a direct interaction between RpoS residue R99 and the -6G nucleotide in the *esrB* promoter discriminator which appears to be critical for inhabitation of *esrB* expression [223]. Yin et al. suggested that a similar mechanism of direct RpoS repression of gene expression uncovered in *E. piscicida* may be shared among several Gram-negative bacteria, since RpoS repressed genes often contain −6G in their respective promoter discriminator [223]. For example, in *Salmonella enterica* it was reported that four of RpoS repressed genes also contain −6G in their respective promoter discriminators [224]. In the work presented in Paper I and II, RpoQ is found to be necessary for the repression of polysaccharide production, where upon its inactivation the polysaccharides are overproduced. Based on the interpretation of Yin et al. [223], we may expect a similar mechanism of direct RpoQ repression of gene expression (e.g *syp*) in *A. salmonicida*. Additionally, another mechanistic explanation of repression by RpoQ is that RpoQ activates the transcription of a repressor, whose expression represses target genes. As the mechanism behind this repressive activity remains unknown, I choose throughout the discussion to term this negative regulation of RpoQ on some genes as "RpoQ-dependent repression".

Bacteria use several survival strategies to adapt to their surroundings, both inside and outside their host, where this adaptation to environmental factors and stress is mediated by RpoS sigma factors [211]. Polysaccharides and the rugose phenotype are believed to have an important role in the association of *Vibrio* species with the marine biotic surface. They are also proposed to contribute to bacterial survival during environmental stress and persistence in the environment [225, 226]. With this in mind, we can speculate about the importance of RpoQ in regulating polysaccharide production as a protective strategy used by *A. salmonicida*, when the bacterium is exposed to harsh and unfavorable environments. We therefore suggest that RpoQ is regulated by a QS-dependent mechanism involving either or both LitR and LuxI. Additionally, environmental factors may influence RpoQ regulation and thereby the expression of *syp* operon and a vast range of other genes.

Altogether, the results obtained in this part of the study (Paper I, II and III) confirm that RpoQ plays an important role in controlling colony rugosity through regulating expression of *syp* genes, either directly or indirectly. The results also confirm that in the absence of RpoQ, the production of polysaccharides is enhanced. Hence, *ΔrpoQ* is believed to mimic a low cell density regulatory state in *A. salmonicida*. Under a low cell density condition (low AHL concentration), LitR is not activated, and consequently RpoQ levels are low and insufficient to activate repression of *syp* genes which would result in upregulation of polysaccharide production and formation of rugose colony. Whereas at high cell density, LitR is activated in response to high AHL concentrations, leading to expression of *rpoQ.* The increased level of RpoQ activity then results in RpoQ-dependent

repression on polysaccharide production via *syp* and formation of smooth colonies (wild type state). Despite the results that give a clear evidence of RpoQ-dependent repression of *syp* genes, the detailed regulatory mechanism of RpoQ on *syp* genes is still not completely understood. Moreover, the influence of various environmental factors can not be excluded as factors influencing the regulation of RpoQ on polysaccharide production. As the current study does not focus on the effect of environmental factors (except temperature variation discussed in section 4.5) on the expression of *rpoQ,* more research is needed to highlight the detailed regulatory mechanism of this sigma factor on *syp* operon expression.

4.2 Biofilm maturation by *A. salmonicida* depends on polysaccharides and other matrix components encoded by LitR-dependent genes

Biofilm formation by the fish pathogen *A. salmonicida* is suggested to be a strategy to protect the bacterium from hostile conditions present in the marine environment, as well as hostile conditions inside the fish host due to processes induced by the immune system [57]. The ability to form biofilm and rugose colonies are often correlated features in vibrios [110, 129]. Hence, in addition to the role of RpoQ in regulating colony rugosity it was of interest to investigate its role in biofilm formation. Using artificial seawater based medium (SWT) and static conditions the *ΔrpoQ* mutant was allowed to form biofilm. Paper I demonstrated that RpoQ is a negative regulator of biofilm formation in *A. salmonicida,* however, the biofilm formed by the *ΔrpoQ* mutant was morphologically different from the biofilm formed by *ΔlitR* [57]. The biofilm of the *ΔrpoQ* mutant was more flat, compact and granulated with a heavy slimy substance and without large mushroom structures, indicating that complete biofilm maturation did not occur in this mutant (see Figure 2 in Paper I). Although polysaccharides are critical for biofilm formation in *A. salmonicida* and other species [96, 227, 228], the production of polysaccharides alone by the *ΔrpoQ* mutant is not sufficient to develop the well-structured, three-dimensional mushroom biofilm structure, which we refer to as "mature biofilm". This finding suggests that other key factors are needed for biofilm maturation in *A. salmonicida.* Similarly, Park et al. demonstrated that exopolysaccharides alone were not sufficient for maturation of the biofilm in *V. vulnificus* and the additional factor, CabA was necessary to develop the mature structure [229]. Previous analysis of the *ΔlitR* three-dimensional biofilm in *A. salmonicida* revealed that the biofilm matrix is composed of polysaccharides (encoded mainly by the *syp* locus) and proteins. When the *syp* genes were inactivated in the *ΔlitR* background, the three-dimensional biofilm structure was not formed, but the quantified biomass from the *ΔlitRsyp*$^{-}$ biofilm indicated that some biofilm formation matrix was present [96]. Based on the obtained results (Paper I), a model for QS-dependent regulation of mature biofilm formation was hypothesized (i) LitR regulates *syp* locus

involved in polysaccharide production via RpoQ and (ii) LitR regulates a set of unknown genes that encode other matrix components (e.g. eDNA, protein and lipoproteins) through an unknown mechanism and independent of RpoQ regulation (Figure 8). Given this, the defect in biofilm maturation exhibited by the *ΔrpoQ* mutant can be explained as following: in the *ΔrpoQ* mutant, LitR is active and the expression of genes that encode other matrix components (lipoproteins and filament structures) are perhaps repressed by LitR itself. This repression of other matrix components by LitR, results in only polysaccharide production via *syp* (due to *rpoQ* inactivation), which is not enough to build the three-dimensional, mushroom-shaped biofilm architecture.

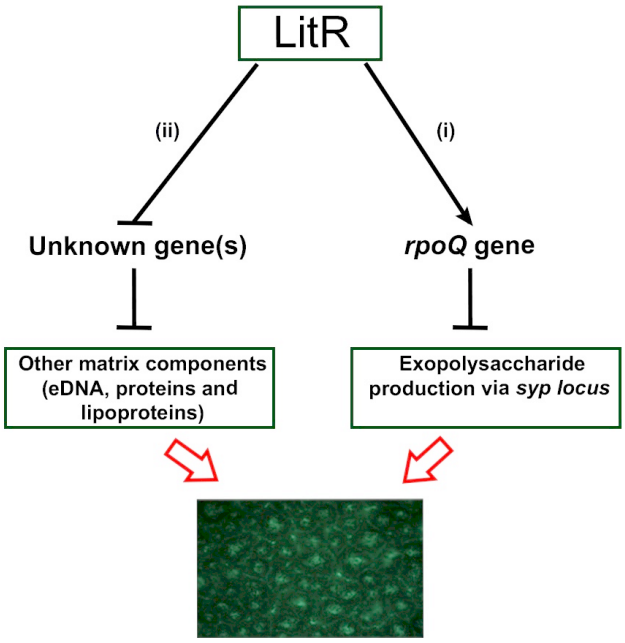

Figure 8 Proposed model for mature biofilm regulation in *A. salmonicida*. (i) LitR acts as a positive regulator of *rpoQ* expression and probably downregulates the expression of exopolysaccharides via RpoQ. The *ΔlitR* mutant shows a mature biofilm with mushroom shaped structures, whereas the *ΔrpoQ* biofilm is flat and regular. Thus, in addition to repression of exopolysaccharides via RpoQ, (ii) LitR represses other biofilm matrix components independent of RpoQ that are required for building mature mushroom structures (e.g. lipoproteins, protein filaments). Therefore, at high cell densities both RpoQ dependent and independent processes are needed for downregulation of the mature biofilm. Arrows and lines with bar end indicate pathways of positive and negative regulation, respectively, and may consist of several steps. The thicker, empty red arrows indicate the resulting phenotype (mature biofilm formation).

To further confirm that *rpoQ* is positively regulated by LitR, *rpoQ* was overexpressed in the *ΔlitR* mutant. For this purpose, an overexpression plasmid was constructed by cloning the *rpoQ* gene under the control of an IPTG-inducible *Ptrc* promoter on pTM214 plasmid. The plasmid was

transferred to the *ΔlitR* and *A. salmonicida* wild type through bacterial conjugation. The overexpression of *rpoQ* from an inducible promoter was compared to the parental strain (*ΔlitR* harboring pTM214 control vector). Results in Paper I demonstrate that RpoQ inhibits the formed biofilm by *ΔlitR*, whereas the *ΔlitR* biofilm formation was unaffected by the presence of the control vector (see Figure 4 in Paper I). These results confirmed that *rpoQ* functions downstream of LitR and has a negative effect on biofilm formation at high cell density most probably through the RpoQ-dependent repression of *syp* genes.

V. cholerae, the etiological agent of cholera, is closely related to *A. salmonicida*. Both species are pathogens and their QS-dependent biofilm formation and rugose colony morphology seem to have similarities. The *V. cholerae* QS system can downregulate biofilm formation and virulence gene expression at high cell density [79, 80, 230]. Likewise, *A. salmonicida* was proposed to regulate biofilm formation in response to changes in cell density [57]. During the infection in a nutrient rich environment such as fish tissue, cell density increases and autoinducers accumulate leading to expression of *litR*. A high LitR level downregulates biofilm formation [57]. This downregulation is proposed to be necessary for adequate disease development, consistent to what was reported for the role of HapR in *V. cholerae* [79, 231]. Whereas at low cell density the bacteria perform an opposite reaction and due to low autoinducer concentration the *litR* transcription is repressed, allowing biofilm formation [57]. In addition to the changes in cell density, environmental factors that are known to be sensed by RpoS sigma factors, influence the production of substances that facilitate biofilm formation [232]. Hence, in *A. salmonicida* biofilm formation and the elevated level of polysaccharides are thought to be expressed in response to stress-related conditions that are frequently present in the aquatic environment which may be sensed by RpoQ. While RpoS and QS are known for their importance in determining entry into a biofilm in response to stress, recently it became clear that RpoS and QS are also important for *V. cholerae* dispersion from biofilm [198, 232]. Singh et al. showed that *V. cholerae* involve a dual sensory input, by integrating information about local cell density through QS and stress response, which can be induced via starvation to control active dispersal [198]. Even though, the role of RpoS in *V. cholerae* in regulating stress response and virulence may differ from *A. salmonicida*, we may expect a similar scenario for the role of RpoQ in altering gene transcription in response to QS and stress including various environmental conditions. The *ΔrpoQ* strain mimics low cell density behaviors and in the absence of RpoQ, the bacterium is captured in the early stage of biofilm formation. Our results in Paper I also show that the absence of RpoQ reduces motility and affects a number of flagellar biosynthesis genes (Paper I and II). These results are consistent with the early stages of biofilm formation, where cells inhibit motility and promote EPS production [116, 233]. Thus, it tempting to expect that at HCD the high levels of RpoQ will have a reverse effect on biofilm formation by

downregulating polysaccharide production that eventually leads to biofilm disruption. At the same time the high level of RpoQ would promote the motility required for dispersal and colonization of new environments to initiate a new biofilm growth cycle or reenter the planktonic lifestyle which is preferred for pathogenesis in the fish host.

In summary, the results presented in Paper I suggest that mature biofilm formation in *A. salmonicida* requires RpoQ-dependent expression of polysaccharide genes and RpoQ-independent expression of genes encoding other matrix components, which are mainly regulated by LitR. Bacteria are believed to sense and withstand stresses caused by changing environmental conditions. Quorum sensing, together with stress sensing factor, RpoQ, are probably two means by which *A. salmonicida* senses its environment to survive. However, how RpoQ tunes biofilm initiation and probably dispersal by integrating information from the stress response and QS mechanism remains unknown and requires further investigation.

4.3 *lux* and *ain* are two QS systems, operated at different cell densities and influence biofilm formation synergistically

The inactivation of *ain* and *lux* autoinducer synthases in *A. salmonicida,* resulted in no AHL production and a mature biofilm formation similar to the biofilm formed by the *ΔlitR* mutant [57, 91]. The fact that biofilm formation in *A. salmonicida* is regulated by QS at high cell density, led to the speculation that AHLs play a critical role in the downregulation of biofilm formation at high cell density which may operate through the QS master regulator, LitR. Paper III revealed that inactivation of *ainS* alone resulted in presence of smooth colonies, indistinguishable from those formed by the wild type (see Figure 2 in Paper III) and additionally confirmed the absence of biofilm formation in this mutant (*ΔainS*) as previously reported [91]. Nevertheless, the introduction of *luxI* mutation to a *ΔainS* background, resulted in a strain (*ΔainSluxI*$^{-}$) with three-dimensional biofilm architecture and wrinkled colony morphology. Hence, when both systems *luxI* and *ainS* were inactivated simultaneously a mature biofilm was formed. These results confirm that both LuxI and AinS regulate biofilm formation synergistically through a common pathway.

In *V. cholerae* the deficiency in AHL synthesis, led to the elevated EPS expression, which is the underlying reason for colony rugosity and enhanced biofilm formation [234]. Similarly, a three-dimensional biofilm structure similar to the biofilm of *ΔlitR* was formed only when AHL production by LuxI and AinS was completely inhibited in *A. salmonicida* [91]. This suggests that the deficiency in AHL production (*ΔainSluxI*$^{-}$) led to *litR* inactivation and thereby no repression is achieved on either the polysaccharide production via *syp* operon or other matrix components (Figure 8). When the AHL profiling of the *ΔlitR* was analyzed a significant reduction in AHL

production was observed for 3OC6-HSL (LuxI product) and 3OHC10-HSL (AinS product) compared to the wild type (see Table 2 in Paper III and [91]). Therefore, the possible effects of 3OC6-HSL and 3OHC10-HSL on biofilm formation were investigated, and the exogenous addition of either AHL to the *ΔainSluxI*$^{-}$ mutant, completely inhibited biofilm formation. Addition of the same AHLs to *ΔlitR* mutant did not interfere with the biofilm formation (see Figure 1 in Paper III). This confirms that both *lux* and *ain* systems regulate biofilm formation, where 3OHC10-HSL (AinS product) and 3OC6-HSL (LuxI product) functions through LitR as a common pathway. Thus, in the absence of *litR* the downregulation of biofilm cannot be achieved. The role of AHLs in the downregulation of biofilm is not restricted to *A. salmonicida:* in a previous study on *P. aeruginosa*, the addition of culture extract containing AHLs also inhibited biofilm formation [235]. Similarly, biofilm development in *Salmonella enterica* was inhibited by cell-free culture supernatant (CFS) containing AHLs of *P. aeruginosa* [236]. Furthermore, the addition of CFS from *Pseudomonas fluorescens* also significantly inhibited the biofilm development of *Shewanella baltica*, suggesting that some biofilm related gene products in *S. baltica* such as EPS and motility, could be affected by AHLs presented in the CFS [237].

As stated earlier (see Figure 8, section 4.2), the biofilm formation in *A. salmonicida* is proposed to depend on both polysaccharide production and other matrix components. By repressing either the polysaccharides or other matrix components the mature biofilm is not formed. Hence, the inhibition of biofilm formation by exogenous addition of AHLs may further confirm the proposed model in Figure 8 (see section 4.2) and can be explained as following: the addition of 3OHC10-HSL (AinS product) alone may result in inhibiting other matrix components through LitR-dependent genes which are independent of *rpoQ* expression. Whereas by the addition of 3OC6-HSL (LuxI product) the polysaccharide production is inhibited through RpoQ-dependent repression of *syp* expression. Hence, adding any of these two AHLs, inhibits the biofilm due to the downregulation of either polysaccharides or other matrix components through LitR as a common regulator. The remaining six AHLs showed no influence on biofilm formation and may regulate other QS activities in *A. salmonicida*.

The *luxI*$^{-}$ mutant produced rugose colonies, while the *ΔainS* mutant only showed smooth colony phenotype similar to the wild type (see Figure 2 in Paper III). This suggests that the *lux* system is more essential for the production of polysaccharides compared to the *ain* system. In *V. cholerae* the exopolysaccharide production is the first step in biofilm formation as cells switch from a motile planktonic state to being non-motile and surface attached [233]. Likewise, the *luxI*$^{-}$ mutant is non-motile and enhances the exopolysaccharide production probably to mediate the initial step of biofilm formation. At the stage of early biofilm formation, *ainS* is probably neither required nor fully active. This suggests that the *ain* system may play a role in later stages of biofilm formation.

These results propose that the *lux* system may operate at lower threshold cell density than the *ain* system in *A. salmonicida* LFI1238. This proposed delay in *ain* system compared to the *lux* system is consistent to what was previously shown concerning the production of AHLs by LuxI and AinS autoinducer synthases [91]. The production of the 3OHC10-HSL by AinS was delayed relative to the production of 3OC6-HSL by LuxI. This is opposite to how *ain* and *lux* systems work in *A. fischeri*. Here the *ain* was functional and essential for initiation of early colonization of the squid (*E. scolopes*), whereas the *lux* system was not required until later in the symbiosis [171].

In conclusion, the results presented in this part of the work demonstrate that both *luxI* and *ainS* are required to form a three-dimensional mature biofilm in *A. salmonicida* LFI1238. Addition of either LuxI-3OC6-HSL or AinS-3OHC10-HSL inhibit biofilm formation, where both systems operate through a common pathway. It was further demonstrated that *luxI*, but not *ainS* is essential for formation of wrinkled colonies. The results confirm that the biofilm formation is a low cell density phenotype, which is downregulated due to AHL production at high cell densities.

4.4 Does the absence of flagellum-mediated motility alter colony morphology in *A. salmonicida*?

The results presented in Paper I and III demonstrated that the *ΔrpoQ* and *luxI*$^{-}$mutants which are able to form wrinkled colonies, also showed a significant reduction in motility (see Figure 3 in Paper I and Figure 6 in Paper III). Based on this observation it was hypothesized that the wrinkled colony morphology and the polysaccharide production correlated with motility and flagellar biosynthesis genes.

To further investigate this hypothesis, flagellar mutants constructed by Dr. Simen Foyn Nørstebø [55], were allowed to form colonies on SWT plates at 8°C and their morphology was investigated (experimental conditions were similar to the morphology assay of the *ΔrpoQ* and *luxI*$^{-}$ mutants, presented in Paper I, II and III). The results showed that only *ΔflaA* strains were able to form colonies with wrinkled morphology similar to those formed by the *ΔrpoQ* and *luxI*$^{-}$ mutants (Figure 9). The complementary strain *ΔflaAc* formed smooth colonies similar to the wild type. Additionally, the inactivation of *flaD* had no significant effect on motility in *A. salmonicida* [55] and the mutants formed a smooth colony morphology indistinguishable from those formed by the wild type on SWT plates (Figure 9).

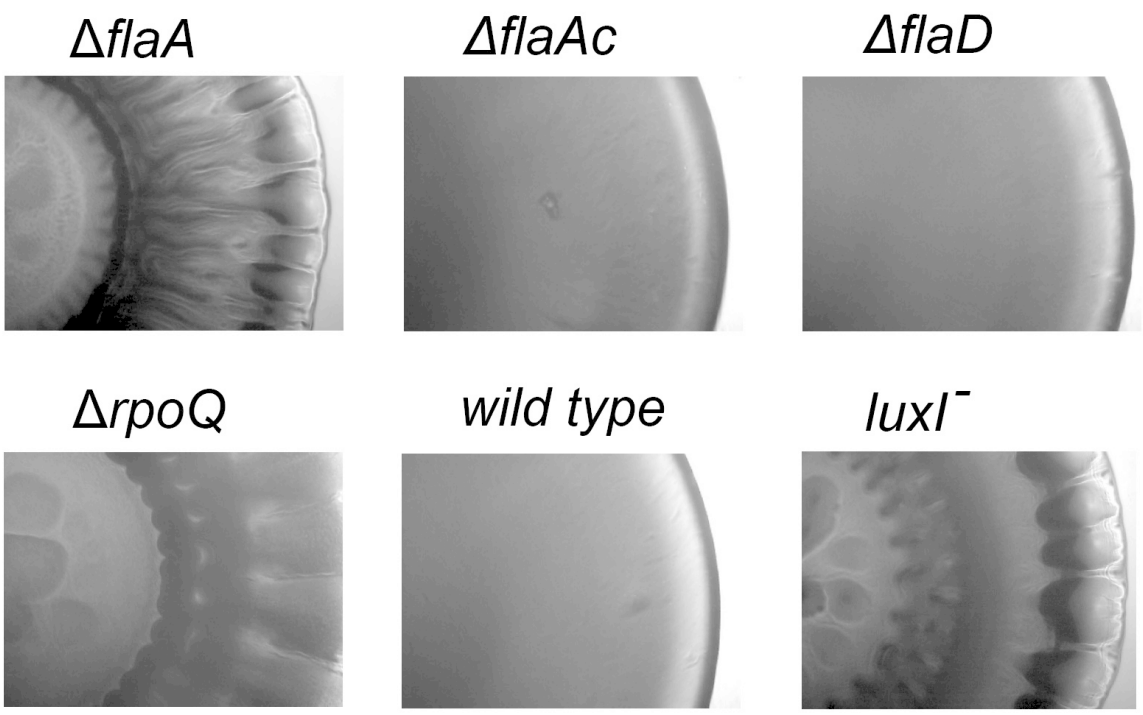

Figure 9 Colony morphology of *A. salmonicida* mutants and the wild type on SWT agar at 8°C. The colonies of *A. salmonicida* strains (*ΔflaA, ΔflaAc, ΔflaD, ΔrpoQ,* wild type LFI1238 and *luxI*$^-$) were allowed to form on SWT plates for 12 days at 8°C. The colonies were viewed microscopically with Zeiss Primo Vert and photographed with AxioCam ERc5s at x4 magnification.

Previous studies reported a link between flagellum motility and exopolysaccharide production in several microorganisms [174, 215, 226, 238-241]. For example, evidence for inverse regulation of motility and exopolysaccharide synthesis is seen in *V. cholerae* [240], where the inactivation of *flaA* and *flaC* genes resulted in non-motile strains and induced exopolysaccharide production [240]. These results proposed that under conditions that favour surface attachment, the *flaA* and *flaC* genes are not expressed. As the environmental conditions favour the search for new surfaces, the bacteria will tend to induce the expression of *flaA* and *flaC* to facilitate motility [240]. Furthermore, the rugose variant of *V. cholerae* revealed a downregulation of several flagellar biosynthesis genes. By contrast the smooth colony variant was motile and no significant differential gene expression of the flagellar genes was reported [215]. Like *V. cholerae*, the opaque variant of *V. parahaemolyticus* has been reported to show reduced motility [174]. In *V. vulnificus,* the rugose isolates also were less motile than their opaque or translucent counterparts [241]. The results obtained in this study (Paper I and III) indicate that the flagellar biosynthesis and exopolysaccharides assumed to be inversely regulated in *A. salmonicida*. Results obtained from Paper I and III propose that *ΔrpoQ* and *luxI*$^-$ mutants mimic the low cell density behaviors. Being non-motile and able to produce elevated level of polysaccharides further suggested that both

mutants (*ΔrpoQ* and *luxI*-) resemble an early biofilm state, where motility seems not to be essential. Motility in *A. salmonicida* may be more important during the aquatic lifestyle. During the transition from a planktonic lifestyle in seawater to the adherence and colonization of the surface, the bacteria tend to turn off the motility apparatus. The downregulation of motility in *A. salmonicida* at this stage of the biofilm life cycle may be for its energetic reason, as cells need to use sources on EPS production rather than maintaining the motility apparatus.

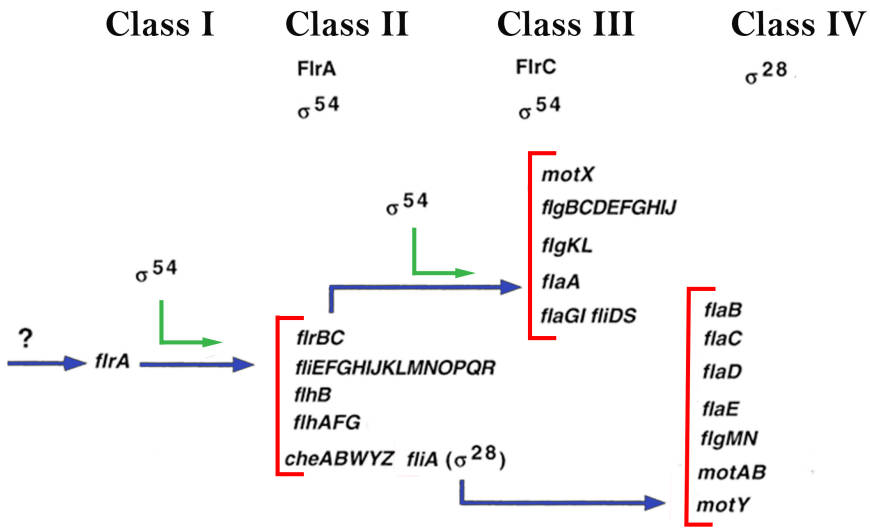

Figure 10 The hierarchal classes of flagellar gene transcription. In vibrios flagellar genes fall into four different hierarchical classes: class I encode the regulatory protein FlrA, which together with sigma factor-54 controls expression of class II genes. Class II proteins FlrB and FlrC are important for controlling transcription of class III genes necessary for synthesis of hook, basal body, and filaments. Class II sigma factor-28 (FliA) regulates transcription of class IV genes associated with the production of motor components [168]. The figure is modified from Prouty et al. [168].

Since both *ΔrpoQ* and *luxI*- strains exhibited the rugose variant and are proposed to mimic a non-motile biofilm state, their transcription profile was analyzed with regards to the expression of the flagellar genes. A hierarchical transcriptional arrangement controlling flagellar gene expression in *A. salmonicida* so far remains poorly understood. However it can be assumed that it is similar to the regulatory network of *V. cholerae,* where genes are organized in four hierarchical classes (Figure 10) [168]. Results in Paper II demonstrated that the expression of some of class III and class IV genes was significantly low in the *ΔrpoQ* mutant relative to the wild type. In contrast the expression of genes that belong to class I and class II were not significantly affected in the two strains (*ΔrpoQ* and wild type). A similar result was demonstrated by the microarray analysis of the rugose variant of *V. cholerae.* The transcriptome analysis in *V. cholerae* revealed a significant downregulation of some flagellar genes that belong to class III and IV compared to the smooth

variant. No significant expression was reported for class I and II in the same strain [215]. The expression profile of the *luxI*$^{-}$ mutant presented in Paper III showed downregulation of motility and chemotaxis genes that belong to all four regulatory classes, including the master regulator *flrA* (the only gene of class I). Given the present results it remains unclear what is the reason of decreased flagellar gene expression and formation of rugose colonies and at which regulatory level this occurs. Our RNA-seq results presented in Paper II and III, showed that among the genes that had a greatest transcript abundance were genes encoding flagellin A protein, *flaA* (fold change of -61.99 at LCD and -17.36 at HCD) and flagellin C protein, *flaC* (fold change of -13134 at LCD and -1129 at HCD) in *ΔrpoQ* and *luxI*$^{-}$ strains, respectively. Even though only the *ΔflaA* mutant was analyzed for the rugose phenotype (Figure 9), we strongly believe that both FlaA and FlaC contribute considerably to the rugose phenotype in *A. salmonicida* through a mechanism that requires further investigation.

Overall, the current work present evidence suggesting that the absence of motility or downregulation of flagellar biosynthesis genes lead to increased exopolysaccharide production in *in vitro* colonies, where these two functions may be coordinately regulated during biofilm development in *A. salmonicida*. This opposite regulation of motility and rugosity in *A. salmonicida* have supported the previously proposed regulation of RpoQ on biofilm formation (see section 4.2), where *A. salmonicida* decreases motility to promote biofilm formation by allowing the production of polysaccharides at low cell density. On the other hand, when cell density is high, the *rpoQ* is activated through LitR. This activation induces RpoQ-dependent repression of *syp* genes, inhibiting the biofilm formation. In addition, the high level of RpoQ may promote flagellar gene expression late in the biofilm cycle to induce dispersion from the mature biofilm to colonize a new surface.

4.5 Environmental factors important for regulation of traits associated with virulence

The marine pathogen *A. salmonicida* causes cold-water vibriosis in Atlantic salmon when seawater temperature is below 10°C [40]. Environmental factors such as salinity and temperature have been shown to influence several cellular activities in this bacterium. For example iron is often the rate limiting element in marine environments and sequestration of iron has been shown to be significantly affected by temperatures below 10°C [58]. Colquhoun and co-authors examined the effect of water temperature on growth, virulence and antigen expression in *A. salmonicida* and have demonstrated that the highest rate of cell division occurred at 15°C. The same authors also demonstrated that optimal cultivation temperature in liquid media is 10°C [47]. Furthermore,

temperature is an important factor for production of AHLs. When the bacteria are grown at temperatures above the disease limit the production of AHLs is drastically reduced [91]. The inactivation of the QS master regulator, LitR also resulted in adhesive wrinkled colonies and formed biofilm at temperatures below 14°C [57, 96]. Our results presented in Paper I show that biofilm formation and wrinkling colony morphology were highly pronounced in the *ΔrpoQ* mutant at low temperatures (4-14°C). As temperature was raised above the threshold of disease development, the phenotypic changes of the *rpoQ* deletion mutant were absent and the mutant behaved similar to the wild type. Our results may suggest that *syp* locus may alter its expression in response to temperature variation which is associated with the temperature dependent cold-water vibriosis in *A. salmonicida*. This is consistent to what was shown for *V. vulnificus*, where the expression of *brp* locus known to be responsible for the rugose phenotype was temperature dependent. The change in rugosity in response to temperature variation was suggested to be due to ecological and pathological relevance. *V. vulnificus* is most prevalent in oyster at temperatures below 20°C, a range that supports *brp* expression, biofilm formation, and host colonization [242-245]. *V. cholerae* was also studied for the impact of temperature on the switch from smooth to rugose colony phenotype and on the increase of biofilm formation [246, 247]. Considering the importance of low temperature in the development of cold-water vibriosis and based on the effect of temperature on rugosity, adhesion and biofilm formation presented in Paper I, we cultured the *A. salmonicida* at 8°C in Paper II and III. This is in order to obtain results relevant to the associated disease and thereby the phenotypic traits related to it.

In addition to the importance of temperature, salinity is also considered as an essential factor for *A. salmonicida.* For example, the motility and flagellin protein production were increased in medium with 2.5% (wt/vol) salt compared to 1% salt *in vitro* experiments [56] . Salinity was also reported to be important for the regulation of the QS, master regulator, LitR [57]. Earlier studies also showed that both thick, mature biofilm and colony rugosity were formed by *A. salmonicida ΔlitR* mutant in SWT medium and L-15 rather than LB (Luria Broth) [57, 96]. Therefore, in this thesis an SWT medium containing 2.5% (wt/vol) concentration of sea salt was used in all experiments. SWT medium was considered a suitable alternative to mimic the physiological characteristics of natural seawater. In Paper I the *ΔrpoQ* mutant formed colony rugosity and a heavy slimy substance in the biofilm only when grown on SWT medium and under low temperatures as mentioned above (Paper I). The rugose phenotype was neither formed on blood agar nor on LA (Luria Agar) plates supplemented with 2.5% NaCl (wt/vol), additionally no biofilm was observed after growth in LB with 2.5% NaCl (data not shown). This confirms our previously reported results [96] that sea salt concentration in addition to other medium composition are essential to favour the rugosity and biofilm formation in *A. salmonicida.* The impact of sea salt

and media composition also showed an effect on colony morphology in other vibrios, in a recent study using *A. fischeri* it has been shown that wild type strains demonstrated ability to form substantial wrinkled colonies only when grown on the nutrient dense LBS medium containing NaCl. The presence of both yeast and tryptone as nutrients, as well as salt were essential for the rugosity and biofilm formation, suggesting that media composition may have increased *syp* operon expression [248]. Similarly, in *V. vulnificus* a *syp*-like polysaccharide biosynthesis locus is upregulated in the artificial seawater based medium [249]. This suggests that in some *Vibrio* spp., there may be a common mechanism involving seawater salts and other components that governs *syp* locus activation and may play an important role in environmental persistence, but which remains unknown.

Although SWT medium was considered as suitable medium, it does not entirely replace all the natural conditions present in the ocean environment or conditions that bacteria would experience inside its natural host. Collectively our results obtained from the current *in vitro* study (Paper I), suggest that QS and the phenotypic traits associated with adaption to a particular environment are temperature and medium dependent confirming the previously reported results [96]. However how RpoQ and other genes in *A. salmonicida* sense changes in the environment and initiate biofilm formation and colony rugosity remains to be determined.

5 CONCLUDING REMARKS

1. The alternative sigma factor RpoQ regulates motility, winkled colony morphology and biofilm formation. This indicates that RpoQ is involved in the regulatory hierarchy influencing a large panel of genes some of which are seems to be connected to QS system.

2. The formation of the mature biofilm in *A. salmonicida* depends on polysaccharide production regulated by RpoQ and on genes encoding other matrix components (e.g. lipoproteins and filament structures) mainly regulated by LitR and are RpoQ-independent. A disruption of either routes, prevents the mature three-dimensional biofilm development.

3. *rpoQ* operates downstream of LitR in the QS cascade. RpoQ is assumed to be the main regulator of the polysaccharide production through *syp* operon in *A. salmonicida.*

4. Motility and rugose-associated exopolysaccharides are respectively, negatively and positively regulated by LuxI and RpoQ at low cell density. The mutants are captured in a non-motile early biofilm state where motility and colony rugosity are reversely regulated.

5. The colony rugosity and biofilm formation in *A. salmonicida* are shown to be elevated at low temperatures, indicating an association of these traits to the temperature dependent cold-water vibriosis.

6. The inactivation of *ainS* and *luxI* simultaneously, results in mature mushroom biofilm structure. Exogenous addition of either 3OC6-HSL (LuxI-AHL) or 3OHC10-HSL (AinS-AHL) inhibits biofilm formation in the double mutant *ΔainSluxI*$^{-}$. This indicates that the three-dimensional biofilm structure is regulated by AinS and LuxI synergistically through a common pathway and is downregulated at high cell densities.

6 FURTHER PRESPECTIVES

Vibrios has been a significant threat in aquaculture and for human health, worldwide. Many pathogenic vibrios employ QS to control the production of virulence factors in addition to the regulation of various physiological processes [61, 79]. Among these physiological processes is biofilm formation, which plays an important role in the bacterial life cycle. Identifying key regulators of *A. salmonicida* biofilm formation is necessary to fully understand how this mode of growth is controlled in response to different genes and environmental factors. Despite the results presented in this thesis, knowledge of QS and the traits regulated through this system is limited. Further studies will be required to determine detailed regulatory mechanisms.

The expression of *syp* genes was elevated in the *ΔrpoQ* mutant, hypothesizing that RpoQ-dependent repression of *syp* expression occur either directly or indirectly. A reporter fusion strains can be constructed in order to better understand the molecular mechanism(s) underlying RpoQ-dependent repression. Additionally, the expression of *syp* genes can be measured in response to temperature and to the different minerals/components, presented in the SWT medium. This may allow us map which component(s) trigger *syp* expression and the rugose phenotype. Lack of rugose colony morphology was demonstrated by inactivation of three *syp* genes. To determine if all *syp* gene products are required for rugose phenotype, an in-frame deletion mutant for each *syp* gene in the *ΔrpoQ* or *ΔlitR* rugose background can be investigated. 3OC6-HSL and 3OHC10-HSL are shown to inhibit biofilm formation, although it is still unclear which genes and mechanism(s) these two AHLs affect. Comparing the transcripts from the AHL-deficient mutant, with and without exogenous addition of these AHLs, could elucidated their regulation. Finally, the reverse regulation of motility and colony rugosity, presented in this work, was only for the *flaA* mutant. It would be interesting to explore the role of flagellar genes in influencing the polysaccharide production and vice versa, which may explore the role of motility and EPS production in the pathogenicity of *A. salmonicida.*

7 REFERENCES

1. Veron M. The taxonomic position of *Vibrio* and certain comparable bacteria. C R Acad Sci Hebd Seances Acad Sci D. 1965;261(23):5243-6.

2. National Center for Biotechnology Information. NCBI *Vibrionaceae* taxonomy database. Available: https://www.ncbi.nlm.nih.gov/Taxonomy/Browser/wwwtax.cgi?id=641

3. Thompson FL, Iida T, Swings J. Biodiversity of vibrios. Microbiol Mol Biol Rev. 2004;68(3):403-31.

4. Reen FJ, Almagro-Moreno S, Ussery D, Boyd EF. The genomic code: inferring *Vibrionaceae* niche specialization. Nat Rev Microbiol. 2006;4(9):697-704.

5. Grimes DJ, Johnson CN, Dillon KS, Flowers AR, Noriea NF, 3rd, Berutti T. What genomic sequence information has revealed about *Vibrio* ecology in the ocean-a review. Microb Ecol. 2009;58(3):447-60.

6. Okada K, Iida T, Kita-Tsukamoto K, Honda T. Vibrios commonly possess two chromosomes. J Bacteriol. 2005;187(2):752-7.

7. Xu Q, Dziejman M, Mekalanos JJ. Determination of the transcriptome of *Vibrio cholerae* during intraintestinal growth and midexponential phase *in vitro*. Proc Natl Acad Sci U S A. 2003;100(3):1286-91.

8. Urbanczyk H, Ast JC, Higgins MJ, Carson J, Dunlap PV. Reclassification of *Vibrio fischeri*, *Vibrio logei*, *Vibrio salmonicida* and *Vibrio wodanis* as *Aliivibrio fischeri* gen. nov., comb. nov., *Aliivibrio logei* comb. nov., *Aliivibrio salmonicida* comb. nov. and *Aliivibrio wodanis* comb. nov. Int J Syst Evol Microbiol. 2007;57(Pt 12):2823-9.

9. Beaz-Hidalgo R, Doce A, Balboa S, Barja JL, Romalde JL. *Aliivibrio finisterrensis* sp. nov., isolated from Manila clam, Ruditapes philippinarum and emended description of the genus *Aliivibrio*. Int J Syst Evol Microbiol. 2010;60(Pt 1):223-8.

10. Yoshizawa S, Karatani H, Wada M, Yokota A, Kogure K. *Aliivibrio sifiae* sp. nov., luminous marine bacteria isolated from seawater. J Gen Appl Microbiol. 2010;56(6):509-18.

11. Urbanczyk H, Ast JC, Dunlap PV. Phylogeny, genomics, and symbiosis of *Photobacterium*. FEMS Microbiol Rev. 2011;35(2):324-42.

12. Hunt DE, Gevers D, Vahora NM, Polz MF. Conservation of the chitin utilization pathway in the *Vibrionaceae*. Appl Environ Microbiol. 2008;74(1):44-51.

13. Vital M, Fuchslin HP, Hammes F, Egli T. Growth of *Vibrio cholerae* O1 Ogawa Eltor in freshwater. Microbiology. 2007;153(Pt 7):1993-2001.

14. Shandera WX, Johnston JM, Davis BR, Blake PA. Disease from infection with *Vibrio mimicus*, a newly recognized *Vibrio* species. Clinical characteristics and edipemiology. Ann Intern Med. 1983;99(2):169-71.

15. Manukhov IV, Khrul'nova SA, Baranova A, Zavilgelsky GB. Comparative analysis of the *lux* operons in *Aliivibrio logei* KCh1 (a Kamchatka Isolate) and *Aliivibrio salmonicida*. J Bacteriol. 2011;193(15):3998-4001.

16. Fendrihan S, Negoiţă TG. Psychrophilic Microorganisms as Important Source for Biotechnological Processes. In: Adaption of Microbial Life to Environmental Extremes: Novel Research Results and Application. Edited by Stan-Lotter H, Fendrihan S. Cham: Springer International Publisher. 2017. p. 147-99.

17. Rosenberg E, Ben-Haim Y. Microbial diseases of corals and global warming. Environ Microbiol. 2002;4(6):318-26.

18. Heidelberg JF, Heidelberg KB, Colwell RR. Bacteria of the gamma-subclass *Proteobacteria* associated with zooplankton in Chesapeake Bay. Appl Environ Microbiol. 2002;68(11):5498-5507.

19. Ruby EG. Lessons from a cooperative, bacterial-animal association. the *Vibrio fischeri-Euprymna scolopes* light organ symbiosis. Annu Rev Microbiol. 1996;50:591-624.

20. Jones BW, Nishiguchi MK. Counterillumination in the Hawaiian bobtail squid, *Euprymna scolopes* Berry (Mollusca: Cephalopoda). Marin Biol. 2004;144(6):1151-5.

21. Levine WC, Griffin PM. *Vibrio* infections on the Gulf Coast results of first year of regional surveillance. Gulf Coast *Vibrio* Working Group. J Infect Dis. 1993;167(2):479-83.

22. Baker-Austin C, Oliver JD, Alam M, Ali A, Waldor MK, Qadri F, Martinez-Urtaza J. *Vibrio* spp. infections. Nat Rev Dis Primers. 2018;4(1):8.

23. Watson JT, Gayer M, Connolly MA. Epidemics after natural disasters. Emerg Infec Dis 2007;13(1):1-5.

24. Somboonwit C, Menezes LJ, Holt DA, Sinnott JT, Shapshak P. Current views and challenges on clinical cholera. Bioinformation. 2017;13(12):405-9.

25. Rivera IN, Chun J, Huq A, Sack RB, Colwell RR. Genotypes associated with virulence in environmental isolates of *Vibrio cholerae*. Appl Environ Microbiol. 2001;67(6):2421-9.

26. Letchumanan V, Chan KG, Lee LH. *Vibrio parahaemolyticus*: a review on the pathogenesis, prevalence, and advance molecular identification techniques. Front Microbiol. 2014;5:705.

27. Daniels NA, MacKinnon L, Bishop R, Altekruse S, Ray B, Hammond RM, Thompson S, Wilson S, Bean NH, Griffin PM et al. *Vibrio parahaemolyticus* infections in the United States, 1973-1998. J Infect Dis. 2000;181(5):1661-6.

28. Makino K, Oshima K, Kurokawa K, Yokoyama K, Uda T, Tagomori K, Iijima Y, Najima M, Nakano M, Yamashita A et al. Genome sequence of *Vibrio parahaemolyticus*: a pathogenic mechanism distinct from that of *Vibrio cholerae*. Lancet. 2003;361(9359):743-9.

29. Park KS, Ono T, Rokuda M, Jang MH, Okada K, Iida T, Honda T. Functional characterization of two type III secretion systems of *Vibrio parahaemolyticus*. Infect Immun. 2004;72(11):6659-65.

30. Zhang L, Orth K. Virulence determinants for *Vibrio parahaemolyticus* infection. Curr Opin Microbiol. 2013;16(1):70-7.

31. Horseman MA, Surani S. A comprehensive review of *Vibrio vulnificus*: an important cause of severe sepsis and skin and soft-tissue infection. Int J Infect Dis. 2011;15(3):e157-66.

32. Horseman MA BR, Lujan-Francis B, Matthew E. Infections Caused by *Vibrionaceae*. Infec Dis Clin Prac. 2013;21(4).

33. Austin B, Zhang XH. *Vibrio harveyi*: a significant pathogen of marine vertebrates and invertebrates. Lett Appl Microbiol. 2006;43(2):119-24.

34. Soto-Rodriguez SA, Gomez-Gil B, Lozano-Olvera R, Betancourt-Lozano M, Morales-Covarrubias MS. Field and experimental evidence of *Vibrio parahaemolyticus* as the causative agent of acute hepatopancreatic necrosis disease of cultured shrimp (*Litopenaeus vannamei*) in Northwestern Mexico. Appl Environ Microbiol. 2015;81(5):1689-99.

35. Austin B, Austin, AD. Bacterial Fish Pathogens Disease of Farmed and Wild Fish, 6th ed. Berlin: Springer-Verlag KG; 2016.

36. Bergman AM. Die rote Beulenkrankheit des Aals. Bericht aus der Koniglichen Bayerischen Versuchsstation. 1909;2:10-54.

37. Frans I, Michiels CW, Bossier P, Willems KA, Lievens B, Rediers H. *Vibrio anguillarum* as a fish pathogen: virulence factors, diagnosis and prevention. J Fish Dis. 2011;34(9):643-61.

38. Toranzo AE MB, Avendano-Herrera B. Vibriosis: *Vibrio anguillarum*, *V. ordalii* and *Aliivibrio salmonicida*. Fish Virus Bact. 2017; dio:10.1079/9781780647784.0314.

39. Schiewe MH, Trust TJ, Crosa JH. *Vibrio ordalii* sp. nov.: A causative agent of vibriosis in fish. Curr Microbiol. 1981;6(6):343-8.

40. Egidius E, Andersen K, Clausen E, Raa J. Cold-water vibriosis or "Hitra disease" in Norwegian salmonid farming. J Fish Dis. 1981;4(4):353-4.

41. Egidius E, Wiik R, Andersen K, Hoof KA, Hjeltnes B. *Vibrio salmonicida* sp. nov., a new fish pathogen. Int J Syst Bacteriol. 1986;36:518-20.

42. Holm K, Strøm E, Stensvaag K, Raa J, Jørgensen T. Characterestics of a *Vibrio* sp. Associated with the "Hitra Disease" of Atlantic Salmon in Norwegian Fish Farms. Fish Pathol. 1985;20(2-3):125-9.

43. Sørum H, Hvaal AB, Heum M, Daae FL, Wiik R. Plasmid profiling of *Vibrio salmonicida* for epidemiological studies of cold-water vibriosis in Atlantic salmon (*Salmo salar*) and cod (*Gadus morhua*). Appl Environ Microbiol. 1990;56(4):1033-7.

44. Kashulin A, Seredkina N, Sørum H. Cold-water vibriosis. The current status of knowledge. J Fish Dis. 2017;40(1):119-26.

45. Toranzo AE, Magariños B, Romalde JL. A review of the main bacterial fish diseases in mariculture systems. Aquaculture. 2005;246(1):37-61.

46. Enger O, Husevåg B, Goksøyr J. Presence of the fish pathogen *Vibrio salmonicida* in fish farm sediments. Appl Environ Microbiol. 1989;55(11):2815-18.

47. Colquhoun DJ, Alvheim K, Dommarsnes K, Syvertsen C, Sørum H. Relevance of incubation temperature for *Vibrio salmonicida* vaccine production. J Appl Microbiol. 2002;92(6):1087-96.

48. Enger O, Husevåg B, Goksøyr J. Seasonal variation in presence of *Vibrio salmonicida* and total bacterial counts in Norwegian fish-farm water. Can J Microbiol. 1991;37(8):618-23.

49. Hjerde E, Lorentzen MS, Holden MT, Seeger K, Paulsen S, Bason N, Churcher C, Harris D, Norbertczak H, Quail MA et al. The genome sequence of the fish pathogen *Aliivibrio salmonicida* strain LFI1238 shows extensive evidence of gene decay. BMC Genomics. 2008;9:616.

50. Kashulin A, Sørum H, Hjerde E, Willassen NP. IS elements in *Aliivibrio salmonicida* LFI1238: occurrence, variability and impact on adaptability. Gene. 2015;554(1):40-9.

51. Nelson EJ, Tunsjø HS, Fidopiastis PM, Sørum H, Ruby EG. A novel *lux* operon in the cryptically bioluminescent fish pathogen *Vibrio salmonicida* is associated with virulence. Appl Environ Microbiol. 2007;73(6):1825-33.

52. Josenhans C, Suerbaum S. The role of motility as a virulence factor in bacteria. Int J Med Microbiol. 2002;291(8):605-14.

53. Milton DL, O'Toole R, Horstedt P, Wolf-Watz H. Flagellin A is essential for the virulence of *Vibrio anguillarum*. J Bacteriol. 1996;178(5):1310-9.

54. Bjelland AM, Johansen R, Brudal E, Hansen H, Winther-Larsen HC, Sørum H. *Vibrio salmonicida* pathogenesis analyzed by experimental challenge of Atlantic salmon (*Salmo salar*). Microb Pathog. 2012;52(1):77-84.

55. Nørstebø SF, Paulshus E, Bjelland AM, Sørum H. A unique role of flagellar function in *Aliivibrio salmonicida* pathogenicity not related to bacterial motility in aquatic environments. Microb Pathog. 2017;109:263-73.

56. Karlsen C, Paulsen SM, Tunsjø HS, Krinner S, Sørum H, Haugen P, Willassen NP. Motility and flagellin gene expression in the fish pathogen *Vibrio salmonicida*: effects of salinity and temperature. Microb Pathog. 2008;45(4):258-64.

57. Bjelland AM, Sørum H, Tegegne DA, Winther-Larsen HC, Willassen NP, Hansen H. LitR of *Vibrio salmonicida* is a salinity-sensitive quorum-sensing regulator of phenotypes involved in host interactions and virulence. Infect Immun. 2012;80(5):1681-9.

58. Colquhoun DJ, Sørum H. Temperature dependent siderophore production in *Vibrio salmonicida*. Microb Pathog. 2001;31(5):213-9.

59. Winkelmann G, Schmid DG, Nicholson G, Jung G, Colquhoun DJ. Bisucaberin-a dihydroxamate siderophore isolated from *Vibrio salmonicida*, an important pathogen of farmed Atlantic salmon (*Salmo salar*). Biometals. 2002;15(2):153-60.

60. Nørstebø SF, Lotherington L, Landsverk M, Bjelland AM, Sørum H. *Aliivibrio salmonicida* requires O-antigen for virulence in Atlantic salmon (*Salmo salar L.*). Microb Pathog. 2018;124:322-31.

61. Miller MB, Bassler BL. Quorum sensing in bacteria. Annu Rev Microbiol. 2001;55:165-99.

62. Abisado RG, Benomar S, Klaus JR, Dandekar AA, Chandler JR. Bacterial Quorum Sensing and Microbial Community Interactions. mBio. 2018;9(3).

63. Waters CM, Bassler BL. Quorum sensing: cell-to-cell communication in bacteria. Annu Rev Cell Dev Biol. 2005;21:319-46.

64. Federle MJ, Bassler BL. Interspecies communication in bacteria. J Clin Invest. 2003; 112(9):1291-9.

65. Bassler BL. Small talk. Cell-to-cell communication in bacteria. Cell. 2002;109(4):421-4.

66. Whitehead NA, Barnard AM, Slater H, Simpson NJ, Salmond GP. Quorum-sensing in Gram-negative bacteria. FEMS Microbiol Rev. 2001;25(4):365-404.

67. Churchill ME, Chen L. Structural basis of acyl-homoserine lactone-dependent signaling. Chem Rev. 2011;111(1):68-85.

68. Yates EA, Philipp B, Buckley C, Atkinson S, Chhabra SR, Sockett RE, Goldner M, Dessaux Y, Camara M, Smith H et al. N-acylhomoserine lactones undergo lactonolysis in a pH-, temperature-, and acyl chain length-dependent manner during growth of *Yersinia pseudotuberculosis* and *Pseudomonas aeruginosa*. Infect Immun. 2002;70(10):5635-46.

69. Nealson KH, Platt T, Hastings JW. Cellular control of the synthesis and activity of the bacterial luminescent system. J Bacteriol. 1970;104(1):313-22.

70. Hawver LA, Jung SA, Ng WL. Specificity and complexity in bacterial quorum-sensing systems. FEMS Microbiol Rev. 2016;40(5):738-52.

71. Engebrecht J, Nealson K, Silverman M. Bacterial bioluminescence: isolation and genetic analysis of functions from *Vibrio fischeri*. Cell. 1983;32(3):773-81.

72. Engebrecht J, Silverman M. Identification of genes and gene products necessary for bacterial bioluminescence. Proc Natl Acad Sci U S A. 1984;81(13):4154-8.

73. Verma SC, Miyashiro T. Quorum sensing in the squid-*Vibrio* symbiosis. Int J Mol Sci. 2013;14(8):16386-401.

74. Li YH, Tian X. Quorum sensing and bacterial social interactions in biofilms. Sensors (Basel). 2012;12(3):2519-38.

75. Fidopiastis PM, Miyamoto CM, Jobling MG, Meighen EA, Ruby EG. LitR, a new transcriptional activator in *Vibrio fischeri*, regulates luminescence and symbiotic light organ colonization. Mol Microbiol. 2002;45(1):131-43.

76. Lupp C, Urbanowski M, Greenberg EP, Ruby EG. The *Vibrio fischeri* quorum-sensing systems *ain* and *lux* sequentially induce luminescence gene expression and are important for persistence in the squid host. Mol Microbiol. 2003;50(1):319-31.

77. Lupp C, Ruby EG. *Vibrio fischeri* LuxS and AinS: comparative study of two signal synthases. J Bacteriol. 2004;186(12):3873-81.

78. Waters CM, Lu W, Rabinowitz JD, Bassler BL. Quorum sensing controls biofilm formation in *Vibrio cholerae* through modulation of cyclic di-GMP levels and repression of *vpsT*. J Bacteriol. 2008;190(7):2527-36.

79. Zhu J, Miller MB, Vance RE, Dziejman M, Bassler BL, Mekalanos JJ. Quorum-sensing regulators control virulence gene expression in *Vibrio cholerae.* Proc Natl Acad Sci U S A. 2002;99(5):3129-34.

80. Miller MB, Skorupski K, Lenz DH, Taylor RK, Bassler BL. Parallel quorum sensing systems converge to regulate virulence in *Vibrio cholerae*. Cell. 2002;110(3):303-14.

81. Milton DL. Quorum sensing in vibrios: complexity for diversification. Int J Med Microbiol. 2006;296(2-3):61-71.

82. Camara M, Hardman A, Williams P, Milton D. Quorum sensing in *Vibrio cholerae*. Nat Genet. 2002;32(2):217-18.

83. Rutherford ST, van Kessel JC, Shao Y, Bassler BL. AphA and LuxR/HapR reciprocally control quorum sensing in vibrios. Genes Dev. 2011;25(4):397-408.

84. Jung SA, Chapman CA, Ng WL. Quadruple quorum-sensing inputs control *Vibrio cholerae* virulence and maintain system robustness. PLoS Pathog. 2015;11(4):e1004837.

85. Herzog R, Peschek N, Frohlich KS, Schumacher K, Papenfort K. Three autoinducer molecules act in concert to control virulence gene expression in *Vibrio cholerae*. Nucleic Acids Res. 2019;47(6):3171-83.

86. Mok KC, Wingreen NS, Bassler BL. *Vibrio harveyi* quorum sensing: a coincidence detector for two autoinducers controls gene expression. EMBO J. 2003;22(4):870-81.

87. Lilley BN, Bassler BL. Regulation of quorum sensing in *Vibrio harveyi* by LuxO and sigma-54. Mol Microbiol. 2000;36(4):940-54.

88. Henke JM, Bassler BL. Three parallel quorum-sensing systems regulate gene expression in *Vibrio harveyi*. J Bacteriol. 2004;186(20):6902-14.

89. Croxatto A, Chalker VJ, Lauritz J, Jass J, Hardman A, Williams P, Camara M, Milton DL. VanT, a homologue of *Vibrio harveyi* LuxR, regulates serine, metalloprotease, pigment, and biofilm production in *Vibrio anguillarum*. J Bacteriol. 2002;184(6):1617-29.

90. Milton DL, Hardman A, Camara M, Chhabra SR, Bycroft BW, Stewart GS, Williams P. Quorum sensing in *Vibrio anguillarum*: characterization of the *vanI/vanR* locus and identification of the autoinducer N-(3-oxodecanoyl)-L-homoserine lactone. J Bacteriol. 1997;179(9):3004-12.

91. Hansen H, Purohit AA, Leiros HK, Johansen JA, Kellermann SJ, Bjelland AM, Willassen NP. The autoinducer synthases LuxI and AinS are responsible for temperature-dependent AHL production in the fish pathogen *Aliivibrio salmonicida*. BMC Microbiol. 2015;15:69.

92. Purohit AA, Johansen JA, Hansen H, Leiros HK, Kashulin A, Karlsen C, Smalås A, Haugen P, Willassen NP. Presence of acyl-homoserine lactones in 57 members of the *Vibrionaceae* family. J Appl Microbiol. 2013;115(3):835-47.

93. Khrulnova SA, Baranova A, Bazhenov SV, Goryanin, II, Konopleva MN, Maryshev IV, Salykhova AI, Vasilyeva AV, Manukhov IV, Zavilgelsky GB. *Lux*-operon of the Marine

Psychrophilic Bacteria *Aliivibrio logei*: a Comparative Analysis of the LuxR1/LuxR2 Regulatory Activity in *Escherichia coli* cells. Microbiology. 2016.

94. Fidopiastis PM, Sørum H, Ruby EG. Cryptic luminescence in the cold-water fish pathogen *Vibrio salmonicida*. Arch Microbiol. 1999;171(3):205-09.

95. Swartzman A, Kapoor S, Graham AF, Meighen EA. A new *Vibrio fischeri lux* gene precedes a bidirectional termination site for the *lux* operon. J Bacteriol. 1990;172(12):6797-6802.

96. Hansen H, Bjelland AM, Ronessen M, Robertsen E, Willassen NP. LitR is a repressor of *syp* genes and has a temperature-sensitive regulatory effect on biofilm formation and colony morphology in *Vibrio* (*Aliivibrio*) *salmonicida*. Appl Environ Microbiol. 2014;80(17):5530-41.

97. Donlan RM. Biofilms: microbial life on surfaces. Emerg Infec Dis. 2002;8(9):881-90.

98. Costerton JW, Lewandowski Z, Caldwell DE, Korber DR, Lappin-Scott HM. Microbial biofilms. Annu Rev Microbiol. 1995;49:711-45.

99. Costerton JW, Stewart PS, Greenberg EP. Bacterial biofilms: a common cause of persistent infections. Science. 1999;284(5418):1318-22.

100. Costerton JW, Geesey GG, Cheng KJ. How bacteria stick. Sci Am. 1978;238(1):86-95.

101. Costerton JW, Cheng KJ, Geesey GG, Ladd TI, Nickel JC, Dasgupta M, Marrie TJ. Bacterial biofilms in nature and disease. Annu Rev Microbiol. 1987;41:435-64.

102. Foxman B. The epidemiology of urinary tract infection. Nat Rev Urol. 2010;7(12):653-60.

103. Kuramitsu HK, Wang BY. The whole is greater than the sum of its parts: dental plaque bacterial interactions can affect the virulence properties of cariogenic *Streptococcus* mutans. Am J Dent. 2011;24(3):153-4.

104. Boucher RC. An overview of the pathogenesis of cystic fibrosis lung disease. Adv Drug Deliv Rev. 2002;54(11):1359-71.

105. Percival SL, Suleman L, Vuotto C, Donelli G. Healthcare-associated infections, medical devices and biofilms: risk, tolerance and control. J Med Microbiol. 2015;64(Pt 4):323-34.

106. Bjarnsholt T. The role of bacterial biofilms in chronic infections. APMIS Suppl. 2013;(136):1-51.

107. Gupta P, Sarkar S, Das B, Bhattacharjee S, Tribedi P. Biofilm, pathogenesis and prevention-a journey to break the wall: a review. Arch Microbiol. 2016;198(1):1-15.

108. Flemming HC, Wingender J. The biofilm matrix. Nat Rev Microbiol. 2010;8(9):623-33.

109. Flemming HC, Neu TR, Wozniak DJ. The EPS matrix: the "house of biofilm cells". J Bacteriol. 2007;189(22):7945-7.

110. Yildiz FH, Visick KL. *Vibrio* biofilms: so much the same yet so different. Trends Microbiol. 2009;17(3):109-18.

111. Hall-Stoodley L, Costerton JW, Stoodley P. Bacterial biofilms: from the natural environment to infectious diseases. Nat Rev Microbiol. 2004;2(2):95-108.

112. Donlan RM, Costerton JW. Biofilms: survival mechanisms of clinically relevant microorganisms. Clin Microbiol Rev. 2002;15(2):167-93.

113. Armbruster CR, Parsek MR. New insight into the early stages of biofilm formation. Proc Natl Acad Sci U S A. 2018;115(17):4317-9.

114. Kostakioti M, Hadjifrangiskou M, Hultgren SJ. Bacterial biofilms: development, dispersal, and therapeutic strategies in the dawn of the postantibiotic era. Cold Spring Harb Perspect Med. 2013;3(4):a010306.

115. Renner LD, Weibel DB. Physicochemical regulation of biofilm formation. MRS Bull. 2011;36(5):347-55.

116. Maunders E, Welch M. Matrix exopolysaccharides; the sticky side of biofilm formation. FEMS Microbiol Lett. 2017;364(13).

117. Rabin N, Zheng Y, Opoku-Temeng C, Du Y, Bonsu E, Sintim HO. Biofilm formation mechanisms and targets for developing antibiofilm agents. Future Med Chem. 2015;7(4):493-512.

118. Gjermansen M, Ragas P, Sternberg C, Molin S, Tolker-Nielsen T. Characterization of starvation-induced dispersion in *Pseudomonas putida* biofilms. Environ Microbiol. 2005;7(6):894-906.

119. Sauer K, Cullen MC, Rickard AH, Zeef LA, Davies DG, Gilbert P. Characterization of nutrient-induced dispersion in *Pseudomonas aeruginosa* PAO1 biofilm. J Bacteriol 2004;186(21):7312-26.

120. Pratt LA, Kolter R. Genetic analysis of *Escherichia coli* biofilm formation: roles of flagella, motility, chemotaxis and type I pili. Mol Microbiol. 1998;30(2):285-93.

121. Kong KF, Vuong C, Otto M. *Staphylococcus* quorum sensing in biofilm formation and infection. Int J Med Microbiol. 2006;296(2-3):133-9.

122. Davies DG, Parsek MR, Pearson JP, Iglewski BH, Costerton JW, Greenberg EP. The involvement of cell-to-cell signals in the development of a bacterial biofilm. Science. 1998;280(5361):295-8.

123. Beyhan S, Bilecen K, Salama SR, Casper-Lindley C, Yildiz FH. Regulation of Rugosity and Biofilm Formation in *Vibrio cholerae*: Comparison of VpsT and VpsR Regulons and Epistasis Analysis of *vpsT*, *vpsR*, and *hapR*. J Bacteriol. 2007;189(2):388-402.

124. Kaplan JB. Biofilm dispersal: mechanisms, clinical implications, and potential therapeutic uses. J Dent Res. 2010;89(3):205-18.

125. Hengge R. Principles of c-di-GMP signalling in bacteria. Nat Rev Microbiol. 2009, 7(4):263-73.

126. Beyhan S, Tischler AD, Camilli A, Yildiz FH. Transcriptome and phenotypic responses of *Vibrio cholerae* to increased cyclic di-GMP level. J Bacteriol. 2006;188(10):3600-13.

127. Tischler AD, Camilli A. Cyclic diguanylate (c-di-GMP) regulates *Vibrio cholerae* biofilm formation. Mol Microbiol. 2004;53(3):857-69.

128. Srivastava D, Waters CM. A tangled web: regulatory connections between quorum sensing and cyclic Di-GMP. J Bacteriol. 2012;194(17):4485-93.

129. Yildiz FH, Schoolnik GK. *Vibrio cholerae* O1 El Tor: identification of a gene cluster required for the rugose colony type, exopolysaccharide production, chlorine resistance, and biofilm formation. Proc Natl Acad Sci U S A. 1999;96(7):4028-33.

130. Guvener ZT, McCarter LL. Multiple regulators control capsular polysaccharide production in *Vibrio parahaemolyticus*. J Bacteriol. 2003;185(18):5431-41.

131. Chang C, Jin X, Chaoqun H. Phenotypic and genetic differences between opaque and translucent colonies of *Vibrio alginolyticus*. Biofouling. 2009;25(6):525-31.

132. Matz C, McDougald D, Moreno AM, Yung PY, Yildiz FH, Kjelleberg S. Biofilm formation and phenotypic variation enhance predation-driven persistence of *Vibrio cholerae*. Proc Natl Acad Sci U S A. 2005;102(46):16819-24.

133. Fong JC, Syed KA, Klose KE, Yildiz FH. Role of Vibrio polysaccharide (*vps*) genes in VPS production, biofilm formation and *Vibrio cholerae* pathogenesis. Microbiology. 2010;156(Pt 9):2757-69.

134. Casper-Lindley C, Yildiz FH. VpsT is a transcriptional regulator required for expression of *vps* biosynthesis genes and the development of rugose colonial morphology in *Vibrio cholerae* O1 El Tor. J Bacteriol. 2004;186(5):1574-8.

135. Yildiz FH, Dolganov NA, Schoolnik GK. VpsR, a Member of the Response Regulators of the Two-Component Regulatory Systems, Is Required for Expression of *vps* Biosynthesis Genes and EPS(ETr)-Associated Phenotypes in *Vibrio cholerae* O1 El Tor. J Bacteriol. 2001;183(5):1716-26.

136. Teschler JK, Zamorano-Sanchez D, Utada AS, Warner CJ, Wong GC, Linington RG, Yildiz FH. Living in the matrix: assembly and control of *Vibrio cholerae* biofilms. Nat Rev Microbiol. 2015;13(5):255-68.

137. Yang M, Frey EM, Liu Z, Bishar R, Zhu J. The virulence transcriptional activator AphA enhances biofilm formation by *Vibrio cholerae* by activating expression of the biofilm regulator VpsT. Infect Immun. 2010;78(2):697-703.

138. Enos-Berlage JL, Guvener ZT, Keenan CE, McCarter LL. Genetic determinants of biofilm development of opaque and translucent *Vibrio parahaemolyticus*. Mol Microbiol. 2005;55(4):1160-82.

139. Enos-Berlage JL, McCarter LL. Relation of capsular polysaccharide production and colonial cell organization to colony morphology in *Vibrio parahaemolyticus*. J Bacteriol. 2000;182(19):5513-20.

140. Boles BR, McCarter LL. *Vibrio parahaemolyticus scrABC*, a novel operon affecting swarming and capsular polysaccharide regulation. J Bacteriol. 2002;184(21):5946-54.

141. McCarter LL. OpaR, a homolog of *Vibrio harveyi* LuxR, controls opacity of *Vibrio parahaemolyticus*. J Bacteriol. 1998;180(12):3166-73.

142. Garrison-Schilling KL, Grau BL, McCarter KS, Olivier BJ, Comeaux NE, Pettis GS. Calcium promotes exopolysaccharide phase variation and biofilm formation of the resulting phase variants in the human pathogen *Vibrio vulnificus*. Environ Microbiol. 2011;13(3):643-54.

143. Hilton T, Rosche T, Froelich B, Smith B, Oliver J. Capsular polysaccharide phase variation in *Vibrio vulnificus*. Appl Environ Microbiol. 2006;72(11):6986-93.

144. Grau BL, Henk MC, Garrison KL, Olivier BJ, Schulz RM, O'Reilly KL, Pettis GS. Further characterization of *Vibrio vulnificus* rugose variants and identification of a capsular and rugose exopolysaccharide gene cluster. Infect Immun. 2008;76(4):1485-97.

145. Chatzidaki-Livanis M, Jones MK, Wright AC. Genetic variation in the *Vibrio vulnificus* group 1 capsular polysaccharide operon. J Bacteriol. 2006;188(5):1987-98.

146. Wright AC, Powell JL, Kaper JB, Morris JG, Jr. Identification of a group 1-like capsular polysaccharide operon for *Vibrio vulnificus*. Infect Immun. 2001;69(11):6893-6901.

147. Guo Y, Rowe-Magnus DA. Identification of a c-di-GMP-regulated polysaccharide locus governing stress resistance and biofilm and rugose colony formation in *Vibrio vulnificus*. Infect Immun. 2010;78(3):1390-1402.

148. Guo Y, Rowe-Magnus DA. Overlapping and unique contributions of two conserved polysaccharide loci in governing distinct survival phenotypes in *Vibrio vulnificus*. Environ Microbiol. 2011;13(11):2888-2990.

149. Chodur DM, Rowe-Magnus DA. Complex Control of a Genomic Island Governing Biofilm and Rugose Colony Development in *Vibrio vulnificus*. J Bacteriol. 2018;200(16).

150. Lee KJ, Kim JA, Hwang W, Park SJ, Lee KH. Role of capsular polysaccharide (CPS) in biofilm formation and regulation of CPS production by quorum-sensing in *Vibrio vulnificus*. Mol Microbiol. 2013;90(4):841-57.

151. Yip ES, Geszvain K, DeLoney-Marino CR, Visick KL. The symbiosis regulator *rscS* controls the *syp* gene locus, biofilm formation and symbiotic aggregation by *Vibrio fischeri*. Mol Microbiol. 2006;62(6):1586-1600.

152. Hussa EA, Darnell CL, Visick KL. RscS functions upstream of SypG to control the *syp* locus and biofilm formation in *Vibrio fischeri*. J Bacteriol. 2008;190(13):4576-83.

153. Norsworthy AN, Visick KL. Signaling between two interacting sensor kinases promotes biofilms and colonization by a bacterial symbiont. Mol Microbiol. 2015;96(2):233-48.

154. Jarrell KF, McBride MJ. The surprisingly diverse ways that prokaryotes move. Nat Rev Microbiol. 2008;6(6):466-76.

155. Zhou J, Lloyd SA, Blair DF. Electrostatic interactions between rotor and stator in the bacterial flagellar motor. Proc Natl Acad Sci U S A. 1998;95(11):6436-41.

156. Macnab RM. How bacteria assemble flagella. Annu Rev Microbiol. 2003;57:77-100.

157. Zhao X, Norris SJ, Liu J. Molecular architecture of the bacterial flagellar motor in cells. Biochemistry. 2014;53(27):4323-33.

158. Terashima H, Kojima S, Homma M. Flagellar motility in bacteria structure and function of flagellar motor. Int Rev Cell Mol Biol. 2008;270:39-85.

159. Terashima H, Fukuoka H, Yakushi T, Kojima S, Homma M. The *Vibrio* motor proteins, MotX and MotY, are associated with the basal body of Na-driven flagella and required for stator formation. Mol Microbiol. 2006;62(4):1170-80.

160. Namba K, Vonderviszt F. Molecular architecture of bacterial flagellum. Q Rev Biophys. 1997;30(1):1-65.

161. McCarter LL. Polar flagellar motility of the *Vibrionaceae*. Microbiol Mol Biol Rev. 2001;65(3):445-62.

162. McGee K, Hörstedt P, Milton DL: Identification and characterization of additional flagellin genes from Vibrio anguillarum. J Bacteriol 1996, 178(17):5188-5198.

163. Klose KE, Mekalanos JJ. Differential regulation of multiple flagellins in *Vibrio cholerae*. J Bacteriol. 1998;180(2):303-16.

164. Zhu S, Kojima S, Homma M. Structure, gene regulation and environmental response of flagella in *Vibrio*. Front Microbiol. 2013;4:410.

165. Echazarreta MA, Klose KE. *Vibrio* Flagellar Synthesis. Front Cell Infect Microbiol. 2019;9(131).

166. Klose KE, Mekalanos JJ. Distinct roles of an alternative sigma factor during both free-swimming and colonizing phases of the *Vibrio cholerae* pathogenic cycle. Mol Microbiol. 1998;28(3):501-20.

167. Syed KA, Beyhan S, Correa N, Queen J, Liu J, Peng F, Satchell KJ, Yildiz F, Klose KE. The *Vibrio cholerae* flagellar regulatory hierarchy controls expression of virulence factors. J Bacteriol. 2009;191(21):6555-70.

168. Prouty MG, Correa NE, Klose KE. The novel sigma54- and sigma28-dependent flagellar gene transcription hierarchy of *Vibrio cholerae*. Mol Microbiol. 2001;39(6):1595-1609.

169. Yang Q, Defoirdt T. Quorum sensing positively regulates flagellar motility in pathogenic *Vibrio harveyi*. Environ Microbiol. 2015;17(4):960-8.

170. Tian Y, Wang Q, Liu Q, Ma Y, Cao X, Guan L, Zhang Y. Involvement of LuxS in the regulation of motility and flagella biogenesis in *Vibrio alginolyticus*. Biosci Biotechnol Biochem. 2008;72(4):1063-71.

171. Lupp C, Ruby EG. *Vibrio fischeri* uses two quorum-sensing systems for the regulation of early and late colonization factors. J Bacteriol. 2005;187(11):3620-9.

172. Utada AS, Bennett RR, Fong JCN, Gibiansky ML, Yildiz FH, Golestanian R, Wong GCL. *Vibrio cholerae* use pili and flagella synergistically to effect motility switching and conditional surface attachment. Nat Commun. 2014;5:4913.

173. Haiko J, Westerlund-Wikstrom B. The role of the bacterial flagellum in adhesion and virulence. Biology (Basel). 2013;2(4):1242-67.

174. Guttenplan SB, Kearns DB. Regulation of flagellar motility during biofilm formation. FEMS Microbiol Rev. 2013;37(6):849-71.

175. Davey ME, O'Toole G A. Microbial biofilms: from ecology to molecular genetics. Microbiol Mol Biol Rev. 2000;64(4):847-67.

176. Lemon KP, Higgins DE, Kolter R. Flagellar motility is critical for *Listeria monocytogenes* biofilm formation. J Bacteriol. 2007;189(12):4418-24.

177. Kirov SM, Castrisios M, Shaw JG. *Aeromonas* flagella (polar and lateral) are enterocyte adhesins that contribute to biofilm formation on surfaces. Infect Immun. 2004;72(4):1939-45.

178. O'Toole GA, Kolter R. Flagellar and twitching motility are necessary for *Pseudomonas aeruginosa* biofilm development. Mol Microbiol. 1998;30(2):295-304.

179. Klausen M, Heydorn A, Ragas P, Lambertsen L, Aaes-Jorgensen A, Molin S, Tolker-Nielsen T. Biofilm formation by *Pseudomonas aeruginosa* wild type, flagella and type IV pili mutants. Mol Microbiol. 2003;48(6):1511-24.

180. Malamud F, Torres PS, Roeschlin R, Rigano LA, Enrique R, Bonomi HR, Castagnaro AP, Marano MR, Vojnov AA. The *Xanthomonas axonopodis* pv. *citri* flagellum is required for mature biofilm and canker development. Microbiology. 2011;157(Pt 3):819-29.

181. Wood TK, Gonzalez Barrios AF, Herzberg M, Lee J. Motility influences biofilm architecture in *Escherichia coli*. Appl Microbiol Biotechnol. 2006;72(2):361-7.

182. Saecker RM, Record MT, Jr., Dehaseth PL. Mechanism of bacterial transcription initiation: RNA polymerase - promoter binding, isomerization to initiation-competent open complexes, and initiation of RNA synthesis. J Mol Biol. 2011;412(5):754-71.

183. Paget MS. Bacterial Sigma Factors and Anti-Sigma Factors: Structure, Function and Distribution. Biomolecules. 2015;5(3):1245-65.

184. Paget MS, Helmann JD. The sigma70 family of sigma factors. Genome Biol. 2003;4(1):203.

185. Osterberg S, del Peso-Santos T, Shingler V. Regulation of alternative sigma factor use. Annu Rev Microbiol. 2011;65:37-55.

186. Boyd EF, Carpenter MR, Chowdhury N, Cohen AL, Haines-Menges BL, Kalburge SS, Kingston JJ, Lubin JB, Ongagna-Yhombi SY, Whitaker WB. Post-Genomic Analysis of Members of the Family *Vibrionaceae*. Microbiol Spectr. 2015;3(5).

187. Zhao JJ, Chen C, Zhang LP, Hu CQ. Cloning, identification, and characterization of the rpoS-like sigma factor *rpoX* from *Vibrio alginolyticus*. J Biomed Biotechnol. 2009; 2009:126986.

188. Cao X, Studer SV, Wassarman K, Zhang Y, Ruby EG, Miyashiro T. The novel sigma factor-like regulator RpoQ controls luminescence, chitinase activity, and motility in *Vibrio fischeri*. mBio. 2012;3(1).

189. Mandel MJ, Stabb EV, Ruby EG. Comparative genomics-based investigation of resequencing targets in *Vibrio fischeri*: focus on point miscalls and artefactual expansions. BMC Genomics. 2008;9:138.

190. Hjerde E, Karlsen C, Sørum H, Parkhill J, Willassen NP, Thomson NR. Co-cultivation and transcriptome sequencing of two co-existing fish pathogens *Moritella viscosa* and *Aliivibrio wodanis*. BMC Genomics. 2015;16:447.

191. Yildiz FH, Schoolnik GK. Role of *rpoS* in stress survival and virulence of *Vibrio cholerae*. J Bacteriol. 1998;180(4):773-84.

192. Merrell DS, Tischler AD, Lee SH, Camilli A. *Vibrio cholerae* requires *rpoS* for efficient intestinal colonization. Infect Immun. 2000;68(12):6691-6.

193. Silva AJ, Benitez JA. Transcriptional regulation of *Vibrio cholerae* hemagglutinin/protease by the cyclic AMP receptor protein and RpoS. J Bacteriol. 2004;186(19):6374-82.

194. Wang H, Wu JH, Ayala JC, Benitez JA, Silva AJ. Interplay among cyclic diguanylate, HapR, and the general stress response regulator (RpoS) in the regulation of *Vibrio cholerae* hemagglutinin/protease. J Bacteriol. 2011;193(23):6529-38.

195. Ringgaard S, Hubbard T, Mandlik A, Davis BM, Waldor MK. RpoS and quorum sensing control expression and polar localization of *Vibrio cholerae* chemotaxis cluster III proteins *in vitro* and *in vivo*. Mol Microbiol. 2015;97(4):660-75.

196. Nielsen AT, Dolganov NA, Otto G, Miller MC, Wu CY, Schoolnik GK. RpoS controls the *Vibrio cholerae* mucosal escape response. PLoS Pathog. 2006;2(10):e109.

197. Wang H, Ayala JC, Benitez JA, Silva AJ. The LuxR-type regulator VpsT negatively controls the transcription of *rpoS*, encoding the general stress response regulator, in *Vibrio cholerae* biofilms. J Bacteriol. 2014;196(5):1020-30.

198. Singh PK, Bartalomej S, Hartmann R, Jeckel H, Vidakovic L, Nadell CD, Drescher K. *Vibrio cholerae* Combines Individual and Collective Sensing to Trigger Biofilm Dispersal. Curr Biol. 2017;27(21):3359-66 e3357.

199. Vasudevan P, Venkitanarayanan K. Role of the *rpoS* gene in the survival of *Vibrio parahaemolyticus* in artificial seawater and fish homogenate. J Food Prot. 2006;69(6):1438-42.

200. Chang SC, Lee CY. OpaR and RpoS are positive regulators of a virulence factor PrtA in *Vibrio parahaemolyticus.* Microbiology. 2018;164(2):221-31.

201. Rosche TM, Smith DJ, Parker EE, Oliver JD. RpoS involvement and requirement for exogenous nutrient for osmotically induced cross protection in *Vibrio vulnificus*. FEMS Microbiol Ecol. 2005;53(3):455-62.

202. Hulsmann A, Rosche TM, Kong IS, Hassan HM, Beam DM, Oliver JD. RpoS-dependent stress response and exoenzyme production in *Vibrio vulnificus*. Appl Environ Microbiol. 2003;69(10):6114-20.

203. Weber B, Croxatto A, Chen C, Milton DL. RpoS induces expression of the *Vibrio anguillarum* quorum-sensing regulator VanT. Microbiology. 2008;154(Pt 3):767-80.

204. Lin YH, Miyamoto C, Meighen EA. Cloning, sequencing, and functional studies of the *rpoS* gene from *Vibrio harveyi*. Biochem Biophys Res Commun. 2002;293(1):456-62.

205. Tian Y, Wang Q, Liu Q, Ma Y, Cao X, Zhang Y. Role of RpoS in stress survival, synthesis of extracellular autoinducer 2, and virulence in *Vibrio alginolyticus*. Arch Microbiol. 2008;190(5):585-94.

206. Huang L, Guo L, Xu X, Qin Y, Zhao L, Su Y, Yan Q. The role of *rpoS* in the regulation of *Vibrio alginolyticus* virulence and the response to diverse stresses. J Fish Dis. 2019;42(5):703-12.

207. Gu D, Zhang J, Hao Y, Xu R, Zhang Y, Ma Y, Wang Q. Alternative sigma factor RpoX is a part of RpoE regulon and plays distinct roles in stress response, motility, biofilm formation and hemolytic activities in the marine pathogen *Vibrio alginolyticus*. Appl Environ Microbiol. 2019;85(14).

208. Rutherford ST, Bassler BL. Bacterial quorum sensing: its role in virulence and possibilities for its control. Cold Spring Harb Perspec Med. 2012;2(11).

209. Ron EZ. Bacterial Stress Response. In: The Prokaryotes: Prokaryotic Physiology and Biochemistry. Edited by Rosenberg E, DeLong EF, Lory S, Stackebrandt E, Thompson F. Berlin: Springer Berlin Heidelberg; 2013. p. 589-603.

210. Battesti A, Majdalani N, Gottesman S. The RpoS-mediated general stress response in *Escherichia coli.* Annu Rev Microbiol. 2011;65:189-213.

211. Landini P, Egli T, Wolf J, Lacour S. sigmaS, a major player in the response to environmental stresses in *Escherichia coli*: role, regulation and mechanisms of promoter recognition. Environ Microbiol Rep. 2014;6(1):1-13.

212. Joelsson A, Kan B, Zhu J. Quorum sensing enhances the stress response in *Vibrio cholerae*. Appl Environ Microbiol. 2007;73(11):3742-46.

213. Yip ES, Grublesky BT, Hussa EA, Visick KL. A novel, conserved cluster of genes promotes symbiotic colonization and sigma-dependent biofilm formation by *Vibrio fischeri*. Mol Microbiol. 2005;57(5):1485-98.

214. Love MI, Huber W, Anders S. Moderated estimation of fold change and dispersion for RNA-seq data with DESeq2. Genome Biol. 2014;15(12):550.

215. Yildiz FH, Liu XS, Heydorn A, Schoolnik GK. Molecular analysis of rugosity in a *Vibrio cholerae* O1 El Tor phase variant. Mol Microbiol. 2004;53(2):497-515.

216. Whitfield C. Biosynthesis and assembly of capsular polysaccharides in *Escherichia coli*. Annu Rev Biochem. 2006;75:39-68.

217. Garrison-Schilling KL, Kaluskar ZM, Lambert B, Pettis GS. Genetic analysis and prevalence studies of the *brp* exopolysaccharide locus of *Vibrio vulnificus*. PLoS One. 2014;9(7):e100890.

218. Liu H, Yan H, Xiao Y, Nie H, Huang Q, Chen W. The exopolysaccharide gene cluster *pea* is transcriptionally controlled by RpoS and repressed by AmrZ in *Pseudomonas putida* KT2440. Microbiol Res. 2019;218:1-11.

219. Irie Y, Starkey M, Edwards AN, Wozniak DJ, Romeo T, Parsek MR. *Pseudomonas aeruginosa* biofilm matrix polysaccharide Psl is regulated transcriptionally by RpoS and post-transcriptionally by RsmA. Mol Microbiol. 2010;78(1):158-72.

220. Ionescu M, Belkin S. Overproduction of exopolysaccharides by an *Escherichia coli* K-12 *rpoS* mutant in response to osmotic stress. Appl Environ Microbiol. 2009;75(2):483-92.

221. Dudin O, Geiselmann J, Ogasawara H, Ishihama A, Lacour S. Repression of flagellar genes in exponential phase by CsgD and CpxR, two crucial modulators of *Escherichia coli* biofilm formation. J Bacteriol. 2014;196(3):707-15.

222. Caimano MJ, Eggers CH, Gonzalez CA, Radolf JD. Alternate sigma factor RpoS is required for the *in vivo*-specific repression of *Borrelia burgdorferi* plasmid lp54-borne *ospA* and *lp6.6* genes. J Bacteriol. 2005;187(22):7845-52.

223. Yin K, Guan Y, Ma R, Wei L, Liu B, Liu X, Zhou X, Ma Y, Zhang Y, Waldor MK et al. Critical role for a promoter discriminator in RpoS control of virulence in *Edwardsiella piscicida*. PLoS Pathog. 2018;14(8):e1007272.

224. Levi-Meyrueis C, Monteil V, Sismeiro O, Dillies MA, Kolb A, Monot M, Dupuy B, Duarte SS, Jagla B, Coppee JY et al. Repressor activity of the RpoS/sigmaS-dependent RNA polymerase requires DNA binding. Nucleic Acids Res. 2015;43(3):1456-68.

225. Wai SN, Mizunoe Y, Takade A, Kawabata SI, Yoshida SI. *Vibrio cholerae* O1 strain TSI-4 produces the exopolysaccharide materials that determine colony morphology, stress resistance, and biofilm formation. Appl Environ Microbiol. 1998;64(10):3648-55.

226. Ali A, Rashid MH, Karaolis DK. High-frequency rugose exopolysaccharide production by *Vibrio cholerae*. Appl Environ Microbiol. 2002;68(11):5773-78.

227. Watnick PI, Kolter R. Steps in the development of a *Vibrio cholerae* El Tor biofilm. Mol Microbiol. 1999;34(3):586-95.

228. Danese PN, Pratt LA, Kolter R. Exopolysaccharide production is required for development of *Escherichia coli* K-12 biofilm architecture. J Bacteriol. 2000;182(12):3593-96.

229. Park JH, Jo Y, Jang SY, Kwon H, Irie Y, Parsek MR, Kim MH, Choi SH. The *cabABC* Operon Essential for Biofilm and Rugose Colony Development in *Vibrio vulnificus*. PLoS Pathog. 2015;11(9):e1005192.

230. Zhu J, Mekalanos JJ. Quorum sensing-dependent biofilms enhance colonization in *Vibrio cholerae*. Dev Cell. 2003;5(4):647-56.

231. Liu Z, Miyashiro T, Tsou A, Hsiao A, Goulian M, Zhu J. Mucosal penetration primes *Vibrio cholerae* for host colonization by repressing quorum sensing. Proc Natl Acad Sci U S A. 2008;105(28):9769-74.

232. Dorman MJ, Dorman CJ. Regulatory Hierarchies Controlling Virulence Gene Expression in *Shigella flexneri* and *Vibrio cholerae*. Front Microbiol. 2018;9:2686.

233. Silva AJ, Benitez JA. *Vibrio cholerae* Biofilms and Cholera Pathogenesis. PLoS Negl Trop Dis. 2016;10(2):e0004330.

234. Biswas S, Mukherjee P, Manna T, Dutta K, Guchhait KC, Karmakar A, Karmakar M, Dua P, Panda AK, Ghosh C. Quorum Sensing Autoinducer(s) and Flagellum Independently Mediate EPS Signaling in *Vibrio cholerae* Through LuxO-Independent Mechanism. Microb Ecol 2019;77(3):616-30.

235. Zhang QQ, Ye KP, Wang HH, Xiao HM, Xu XL, Zhou GH. Inhibition of biofilm formation of *Pseudomonas aeruginosa* by an acylated homoserine lactones-containing culture extract. Technologie. 2014; 57(1):230-35.

236. Wang HH, Ye KP, Zhang QQ, Dong Y, Xu XL, Zhou GH. Biofilm formation of meat-borne *Salmonella enterica* and inhibition by the cell-free supernatant from *Pseudomonas aeruginosa.* Food Contr. 2013;32(2):650-8.

237. Zhao A, Zhu J, Ye X, Ge Y, Li J. Inhibition of biofilm development and spoilage potential of *Shewanella baltica* by quorum sensing signal in cell-free supernatant from *Pseudomonas fluorescens*. Int J Food Microbiol. 2016;230:73-80.

238. Prigent-Combaret C, Vidal O, Dorel C, Lejeune P. Abiotic surface sensing and biofilm-dependent regulation of gene expression in *Escherichia coli*. J Bacteriol. 1999;181(19):5993-6002.

239. Garrett ES, Perlegas D, Wozniak DJ. Negative control of flagellum synthesis in *Pseudomonas aeruginosa* is modulated by the alternative sigma factor AlgT (AlgU). J Bacteriol. 1999;181(23):7401-4.

240. Watnick PI, Lauriano CM, Klose KE, Croal L, Kolter R. The absence of a flagellum leads to altered colony morphology, biofilm development and virulence in *Vibrio cholerae* O139. Mol Microbiol. 2001;39(2):223-35.

241. Grau BL, Henk MC, Pettis GS. High-frequency phase variation of *Vibrio vulnificus* 1003: isolation and characterization of a rugose phenotypic variant. J Bacteriol. 2005;187(7):2519-25.

242. Chodur DM, Guo L, Pu M, Bruger E, Fernandez N, Waters C, Rowe-Magnus DA. The Proline Variant of the W[F/L/M][T/S]R Cyclic Di-GMP Binding Motif Suppresses Dependence on Signal Association for Regulator Function. J Bacteriol. 2017;199(19).

243. Koenig KL, Mueller J, Rose T. *Vibrio vulnificus*. Hazard on the half shell. West J Med. 1991;155(4):400-3.

244. Motes ML, DePaola A, Cook DW, Veazey JE, Hunsucker JC, Garthright WE, Blodgett RJ, Chirtel SJ. Influence of water temperature and salinity on *Vibrio vulnificus* in Northern Gulf and Atlantic Coast oysters (*Crassostrea virginica*). Appl Environ Microbiol. 1998;64(4):1459-65.

245. Kelly MT. Effect of temperature and salinity on *Vibrio* (*Beneckea*) *vulnificus* occurrence in a Gulf Coast environment. Appl Environ Microbiol. 1982;44(4):820-4.

246. Rahman M, Jubair M, Alam MT, Weppelmann TA, Azarian T, Salemi M, Sakharuk IA, Rashid MH, Johnson JA, Yasmin M et al. High-frequency rugose exopolysaccharide production by *Vibrio cholerae* strains isolated in Haiti. PLoS One. 2014;9(11):e112853.

247. Townsley L, Yildiz FH. Temperature affects c-di-GMP signalling and biofilm formation in *Vibrio cholerae*. Environ Microbiol. 2015;17(11):4290-4305.

248. Marsden AE, Grudzinski K, Ondrey JM, DeLoney-Marino CR, Visick KL. Impact of Salt and Nutrient Content on Biofilm Formation by *Vibrio fischeri*. PLoS One. 2017;12(1):e0169521.

249. Williams TC, Blackman ER, Morrison SS, Gibas CJ, Oliver JD. Transcriptome sequencing reveals the virulence and environmental genetic programs of *Vibrio vulnificus* exposed to host and estuarine conditions. PLoS One. 2014;9(12):e114376.

SCIENTIFIC PAPERS I-III

Paper I

The alternative sigma factor RpoQ regulates colony morphology, biofilm formation and motility in the fish pathogen *Aliivibrio salmonicida*

Miriam Khider, Nils Peder Willassen and Hilde Hansen // BMC Microbiology., 12 September 2018., **18**:16.

Khider et al. BMC Microbiology (2018) 18:116
https://doi.org/10.1186/s12866-018-1258-9

BMC Microbiology

RESEARCH ARTICLE Open Access

The alternative sigma factor RpoQ regulates colony morphology, biofilm formation and motility in the fish pathogen *Aliivibrio salmonicida*

Miriam Khider, Nils Peder Willassen and Hilde Hansen*

Abstract

Background: Quorum sensing (QS) is a cell-to cell communication system that bacteria use to synchronize activities as a group. LitR, the master regulator of QS in *Aliivibrio salmonicida,* was recently shown to regulate activities such as motility, rugosity and biofilm formation in a temperature dependent manner. LitR was also found to be a positive regulator of *rpoQ*. RpoQ is an alternative sigma factor belonging to the sigma −70 family. Alternative sigma factors direct gene transcription in response to environmental signals. In this work we have studied the role of RpoQ in biofilm formation, colony morphology and motility of *A. salmonicida* LFI1238.

Results: The *rpoQ* gene in *A. salmonicida* LFI1238 was deleted using allelic exchange. We found that RpoQ is a strong repressor of rugose colony morphology and biofilm formation, and that it controls motility of the bacteria. We also show that overexpression of *rpoQ* in a Δ*litR* mutant of *A. salmonicida* disrupts the biofilm produced by the Δ*litR* mutant and decreases its motility, whereas *rpoQ* overexpression in the wild-type completely eliminates the motility.

Conclusion: The present work demonstrates that the RpoQ sigma factor is a novel regulatory component involved in modulating motility, colony morphology and biofilm formation in the fish pathogen *A. salmonicida*. The findings also confirm that RpoQ functions downstream of the QS master regulator LitR. However further studies are needed to elucidate how LitR and RpoQ work together in controlling phenotypes related to QS in *A. salmonicida*.

Keywords: *Aliivibrio salmonicida*, Sigma factors, RpoQ, Temperature, Quorum sensing, Motility, Biofilm, Overexpression

Background

Aliivibrio salmonicida belongs to the *Vibrionaceae* family, which is widely distributed in the environment, mainly in the aquatic habits. Members of this family may exist in symbiotic or pathogenic relations with their hosts [1]. According to current taxonomy, *A. salmonicida* belongs to the *Aliivibrio* genus together with its three most closely related species *Aliivibro logei*, *Aliivibrio wodanis* and *Aliivibrio fischeri* [2].

A. salmonicida causes cold water vibriosis or Hitra disease in farmed Atlantic salmon (*Salmo salar L*), Atlantic cod (*Gadus morhua*) and rainbow trout (*Oncorhynchus mykiss*). The disease occurs mainly during late autumn and winter seasons when the seawater temperature is below 12°C. *A. salmonicida* is a gram-negative psychrophilic bacterium with a rod shape and nine polar flagella for motility and colonization [3–5].

Members of the *Vibrionaceae* family use quorum sensing (QS) for cell-to-cell communication to regulate gene expression in response to cell density by secretion and sensing of extracellular signals called auto-inducers (AIs). As the bacterial population density increases, AIs accumulate in the environment. When the AI concentration increases above a certain threshold, the bacteria detect this and modulate gene expression [6, 7]. N-acyl homoserine lactones (AHLs) are the major class of AIs in gram-negative bacteria, and were first described in *A. fischeri* [8, 9] and *Vibrio harveyi* [10]. The QS systems in

* Correspondence: hilde.hansen@uit.no
Norwegian Structural Biology Center and the Department of Chemistry, Faculty of Science and Technology, UiT-The Arctic University of Norway, N-9037 Tromsø, Norway

A. fischeri control properties such as motility, squid colonization and bioluminescence [11–13]. *A. fischeri* has two AHL based systems, LuxI/LuxR and AinS/AinR, which are primarily responsible for regulating bioluminescence and colonization factors [14]. In addition to the LuxI/LuxR and AinS/AinR systems, *A. fischeri* has the LuxS/LuxPQ QS system [14, 15]. LuxI is responsible for the synthesis of the autoinducer N-3-(oxo-hexanoyl)-homoserine lactone (3-oxo-C6-HSL) which binds the cytoplasmic receptor LuxR. LuxR then functions as a transcription activator for the luciferase *luxICDABE* operon [16]. LuxS and AinS synthesize signal molecules which are sensed by LuxPQ and AinR, respectively. The two signal systems work in parallel and convey the signal responses to LuxU-LuxO. At low cell density when AIs are not produced, LuxPQ and AinR act as kinases and relay phosphates to LuxU, which in turns phosphorylates LuxO. Phosphorylated LuxO activates the transcription of *qrr* which binds and destabilizes the mRNA of the master QS regulator LitR [12, 15, 17]. At high cell density, the AI produced by AinS (C8-HSL) accumulates in the environment and results in dephosphorylation of LuxO. When LuxO is dephosphorylated, the *qrr* level decreases and allows LitR translation. In turn, LitR activates the transcription of *luxR* which contributes to bioluminescence [12, 13].

A. salmonicida has three QS systems similar to those in *A. fischeri*: LuxS/LuxPQ, LuxI/LuxR and AinS/AinR [18]. LuxI is responsible for the synthesis of a total of seven AHLs, while AinS synthesizes only one AHL. This AHL diversity may suggest a complex sensing system which allows more fine-tuned responses to changes in the environment [19]. *A. salmonicida* does not produce bioluminescence per se [20], but regulates activities such as virulence, motility, colony morphology, adhesion, and biofilm formation by QS in a temperature dependent manner [21, 22].

Sigma factors are essential dissociable subunits of prokaryotic RNA polymerase that control promoter recognition and transcription initiation [23, 24]. Primary sigma factors (RpoD, σ^{70} family) direct transcription from the promoters of genes required for basic cellular functions. In addition to the primary sigma factors, bacteria have a variable number of alternative sigma factors whose activities increase in response to certain environmental conditions or stress [25].

Several alternative sigma factors have been identified or predicted in vibrios and aliivibrios [26], and recently a divergent copy of a putative RpoS-like sigma factor was identified in *A. fischeri* and named RpoQ due to its activation by the AinS/AinR QS system [27]. RpoQ was later found to regulate bioluminescence, motility and chitinase activity in *A. fischeri* through LuxO via LitR [28]. Pfam analysis of RpoQ identified four conserved domains (σ^{70} regions) where all were significant except for region 3. Phylogenetic analysis further revealed that region 3 in RpoQ is clearly divergent from the corresponding region in RpoD and RpoS [27, 28]. This less conserved region 3 is involved in binding the core RNA polymerase and recognition of the extended −10 promoter [29]. An RpoS-like sigma factor (RpoX) lacking region 3 has been described in *Vibrio alginolyticus,* and shown to be involved in biofilm formation and stress responses [30].

A. salmonicida strain LFI1238 encodes an *rpoQ* homolog (*VSAL_II0319*) similar to the one in *A. fischeri* [18, 28]. In a previous study we analyzed the transcriptomes of an *A. salmonicida ΔlitR* mutant and the isogenic wild-type strain LFI1238. The *rpoQ* gene was found to be downregulated in the *ΔlitR* mutant [31] suggesting that LitR is a positive regulator of *rpoQ* in *A. salmonicida*. In the work presented here we have studied the impact of this putative RpoS-like sigma factor in *A. salmonicida* with regard to different phenotypic traits such as biofilm formation, motility and colony morphology.

Methods

Bacterial strains, plasmids and culture conditions

Bacterial cells and plasmids used in this study are listed in Table 1. The wild-type *A. salmonicida* LFI1238 and the constructed mutants were grown from frozen glycerol stocks on blood agar base no. 2 (Oxiod, Cambridge, United Kingdom) with a final concentration of 2.5% NaCl (wt/vol) and 5% bovine blood (BA2.5) or on Luria-Bertani agar (Difco, BD Diagnostics, Sparks, MD) with a final concentration of 2.5% NaCl (wt/vol) (LA2.5). The primary cultures (2 ml) of *A. salmonicida* and the constructed mutants were grown from single colonies in LB2.5 at 12°C and 220 rpm for 48 h. Secondary cultures were made by diluting the primary cultures 1:20 in LB2.5 and incubated for additional 24 h, unless otherwise indicated.

The *Escherichia coli* strains S17λpir, CC118λpir, JM109, PIR2, DH5α λpir and DH5α were cultivated in LA or LB with 1% (wt/vol) NaCl (LA1 and LB1 respectively) and incubated at 37°C. The suicide plasmids pDM4 (GenBank: KC795686.1) and pNQ705 (GenBank: KC795685.1) were propagated in S17λpir cells. The TA plasmid vector pGEM-T was propagated in JM109 and DH5α cells. The conjugation helper pEVS104 plasmid was propagated in the *E. coli* helper strain CC118λpir [32]. The pTM214 and pVSV102 (GFP) expression plasmids were propagated in the donor strains PIR2 and DH5αλpir, respectively [32, 33]. For selection of *E. coli* transformants, chloramphenicol (final concentration 25 μg/ml) or ampicillin (final concentration 100 μg/ml) was added to the medium. The potential *A. salmonicida* transconjugants were selected either on BA2.5 or LA2.5 supplemented with 2 μg/ml of chloramphenicol or 150 μg/ml of kanamycin.

Table 1 Bacterial strains and plasmids used in this study

Bacterial strains or plasmids	Description	Source
A. salmonicida		
LFI1238	Wild-type, isolated from Atlantic cod	[18]
ΔlitR	LFI1238 containing an in-frame deletion in *litR*	[22]
ΔrpoQ	LFI1238 containing an in-frame deletion in *rpoQ*	This study
ΔrpoQ$_c$	*ΔrpoQ* strain complemented with wild-type copy of the *rpoQ* gene, Cm^r	This study
ΔlitR-rpoQ$^-$	*ΔlitR* stain with an insertional disruption in *rpoQ*, Cm^r	This study
LFI1238-pVSV102	LFI1238 carrying pVSV102, Kn^r	This study
ΔlitR-pVSV102	*ΔlitR* carrying pVSV102, Kn^r	This study
ΔrpoQ-pVSV102	*ΔrpoQ* carrying pVSV102, Kn^r	This study
LFI1238-pTM214	LFI1238 carrying pTM214, Cm^r	This study
LFI1238-*Ptrc-rpoQ*	LFI1238 carrying pTM214-*rpoQ*, Cm^r	This study
ΔlitR-pTM214	*ΔlitR* carrying pTM214, Cm^r	This study
ΔlitR-Ptrc-rpoQ	*ΔlitR* carrying pTM214-*rpoQ*, Cm^r	This study
E. coli		
S17λpir	Donor strain for conjugation	[65]
JM109	Strain for subcloning pGEM-T constructs	[66]
DH5α	Strain for cloning	Thermo Fisher
C118λpir	Helper strain containing pEVS104	[32]
DH5αλpir	Donor strain for conjugation harboring pVSV102	[32]
PIR2	Donor strain for conjugation harboring pTM214	[33]
Plasmids		
pDM4	Suicide vector with an R6K origin, *sacBR* and Cm^r	[35]
pNQ705	Suicide vector with an R6K origin, Cm^r	[35]
pDM4-*ΔrpoQ*	pDM4 containing a fragment of *rpoQ* harboring an internal deletion	This study
pNQ705-*rpoQ*$_c$	pNQ705 containing a full length *rpoQ* and flanking sequences	This study
pNQ705-*rpoQ*$^-$	pNQ705 containing an internal 304 bp fragment of *rpoQ*	This study
pTM214	pVSV105, *Ptrc-mCherry*, Cm^r	[33]
pVSV102	pES213, constitutive GFP, Kn^r	[67]
pEVS104	Helper plasmid, R6K origin, RP4, *oriT, trb, tra* and Kn^r	[32]
pTM214-*rpoQ*	pVSV105, *Ptrc-rpoQ* (a full length *rpoQ* copy), Cm^r	This study
pGEM-T	TA cloning vector, white/blue screening, Amp^r	Promega

A seawater-based medium (SWT) was used for biofilm and morphology assays. The medium contains 5 g/L of bacto peptone (BD), 3 g/L of yeast extract (Sigma) and 28 g of a synthetic sea salt (Instant Ocean, Aquarium Systems) per liter. The SWT medium was solidified with 1.5% (wt/vol) agar (Fluka).

All biological assays were carried out in triplicate.

DNA extraction, PCR and DNA sequencing

DNA extraction, recombinant DNA techniques and transformations were performed according to standard protocols [34]. Restriction digestion, ligation, genomic DNA extraction and plasmid purification were performed as recommended by the manufacturers (NEB Biolabs, Sigma and Promega). PCR was performed using Phusion polymerase (NEB) or Taq polymerase master mix (WVR). DNA sequencing was performed using Big Dye (Applied Biosystems) with custom made primers synthesized by Sigma. The primers used for PCR and sequencing are listed in Table 2.

Construction of *A. salmonicida* LFI1238 Δ*rpoQ* mutant and the complementary strain

The *rpoQ* gene (*VSAL_II0319*) was deleted in *A. salmonicida* by allelic exchange as previously described [22]. In brief, the pDM4-*ΔrpoQ* was constructed by fusion of two PCR products amplified from sequences downstream and upstream *rpoQ* in the genomic DNA of *A.*

Table 2 The primers used in this study

Primers	Sequence (5–3′)	Source
RpoQ-A fwd	AATAACTCGAGCAAACGAATGACATGCAGACA	This study
RpoQ-B rev	ATCAATGCTGTTTCTTGGTTCTTC	This study
RpoQ-C fwd	AGAAACAGCATTGATCTAGGCCAAGATCTTCAA	This study
RpoQ-D rev	TATATACTAGTCGATCTCATTATCTTCGTAATACA	This study
RpoQ-G fwd	AGTTCAGGTGATCGTGTTA	This study
RpoQ-H rev	GATTTTGCGTATTGGTAACT	This study
RpoQ-E fwd	CTCGAGAACAGCATTGATGCTTACTCA	This study
RpoQ-F rev	ACTAGTATCCACCATACCGCGTAA	This study
pTM214-*rpoQ* fwd	TCGAGCTCAGAGGAGAAATTAAGCATGTTGAATATAGAATGTTCA	This study
pTM214-*rpoQ* rev	AGGTCGACCTAATTTAAAGCATTTCTAAA	This study
pNQ-fwd	TAACGGCAAAAGCACCGCCGGACATCA	Milton, D.
pNQ-rev	TGTACACCTTAACACTCGCCTATTGTT	Milton, D.

salmonicida LFI1238. The RpoQ-A and RpoQ-B primers were used to amplify the region upstream *rpoQ* (558 bp), and RpoQ-C and RpoQ-D primers for amplification of the region downstream *rpoQ* (729 bp). The downstream region contained the last 40 C-terminal codons of the *rpoQ* open reading frame. Primers RpoQ-B and RpoQ-C contain complementary sequences that enable fusion of the upstream and downstream PCR products by a second overlap-extension PCR. This fusion of the two PCR products results in removing 254 codons (including the start codon) from the *rpoQ* open reading frame. A'overhangs were added to the PCR product and ligated into pGEM-T, and transformed into *E. coli* JM109 competent cells. The insert (PCR overlap product) was digested from the pGEM-T plasmid using *Spe*I and *Xho*I, as restriction sites are included in RpoQ-A and RpoQ-D primers respectively. The digested overlap PCR product was then ligated into the corresponding restriction sites of the suicide vector pDM4 before being transformed directly to *E. coli* S17λpir cells. The resulting plasmid is named pDM4-*ΔrpoQ*.

The complementary strain $\Delta rpoQ_c$ was constructed by insertion of a full-length copy of the wild-type *rpoQ* gene into the original locus of the *ΔrpoQ*. The complete gene and flanking regions was amplified by PCR using RpoQ-A and RpoQ-D primers, digested as above, and ligated into the *Spe*I and *Xho*I restriction sites of the pNQ705. The resulting plasmid is named pNQ705-$rpoQ_c$.

The pDM4-*ΔrpoQ* was transferred to *A. salmonicida* LFI1238, while the pNQ705-$rpoQ_c$ construct was transferred to the *ΔrpoQ* mutant by bacterial conjugation mainly as described elsewhere [22, 35]. Briefly, donor cells *E. coli* S17λpir harboring the pDM4-*ΔrpoQ* or pNQ705-$rpoQ_c$ were mated with their respective recipient cells (*A. salmonicida* wild-type or the *ΔrpoQ* mutant), at a 1:1 ratio. The donor cells were grown to mid-exponential phase to OD_{600} (optical density) of 0.7 and the recipient to an early stationary phase (OD_{600} 1.2) before they were harvested by centrifugation and washed twice in LB1 medium. The washed bacterial pellets were mixed and spotted onto BA2.5 agar plates. The plates were incubated at 20°C for 6 h followed by an additional incubation for 17 h at 12°C. The spotted cells were suspended in 2 ml LB2.5 and incubated overnight at 12°C with agitation at 220 rpm. Potential transconjugants were selected after 5 days on BA2.5 supplemented with chloramphenicol. To complete the allelic exchange needed to generate the *ΔrpoQ* mutant, transconjugants (*A. salmonicida*-pDM4-*ΔrpoQ*), were streaked onto LA2.5 plate supplemented with 5% sucrose. Cells that are able to grow after the sucrose selection were selected based on the sensitivity to chloramphenicol. Chloramphenicol-sensitive cells were analyzed for deletion by PCR and verified by sequencing.

Construction of the double mutant *A. salmonicida* Δ*litR-rpoQ*$^-$

Construction of *A. salmonicida* LFI1238 containing a *litR* in-frame deletion *(ΔlitR)* is described elsewhere [22]. The double mutant *ΔlitR-rpoQ*$^-$ (Table 1) was constructed mainly as described by others [35]. Briefly, the pNQ705-*rpoQ*$^-$ plasmid was constructed by cloning a (304 bp) PCR product amplified from an internal part of the *rpoQ* gene using the forward and reverse primer pair RpoQ-E and RpoQ-F (Table 2). The restrictions enzyme sites *Spe*I and *Xho*I were added to the 5' end of the forward (RpoQ-E) and reverse (RpoQ-F) primers respectively in order to ligate the digested PCR product into the pNQ705 suicide plasmid. Hence, both the pNQ705 plasmid and the amplified PCR product were digested with *Spe*I and *Xho*I and ligated using T4 DNA ligase. The ligated construct (pNQ705-*rpoQ*$^-$) was transformed into *E. coli* S17λpir. Next pNQ705-*rpoQ* was transferred to the *ΔlitR* mutant by bacterial conjugation

as described above. The resulting double mutant strain was named *ΔlitR-rpoQ*⁻.

Construction of *rpoQ* overexpression strains

A full length (882 base pairs) copy of the *A. salmonicida rpoQ* gene was amplified by PCR using the primer pair pTM214-*rpoQ* fwd and pTM214-*rpoQ* rev, containing the *SacI* and *SalI* restriction sites, respectively (Table 2). The resulting PCR product and the pTM214 expression vector (provided by Dr. Tim Miyashiro) were digested using *SacI* and *SalI* restriction enzymes. The digested PCR product was cloned downstream of the tryptophan promoter in the pTM214 expression vector, replacing the native *mCherry* gene. The construct was transformed to *E. coli* S17λpir cells and selected on LA1 plates. The resulting plasmid is referred to as pTM214-*rpoQ*.

The pTM214-*rpoQ* and pTM214 (control vector) was transferred to LFI1238 and *ΔlitR* by tri-parental mating using the conjugative helper strain CC118λpir carrying pEVS104 (helper plasmid) as described by others [32], with some modifications. Briefly, *E. coli* S17λpir harboring pTM214-*rpoQ* or PIR2 harboring pTM214 and helper strain CC118λpir carrying pEVS104 were grown to the mid-exponential phase at 37°C. The recipient cells LFI1238 and *ΔlitR* were grown to the early stationary phase. The donor, helper and recipient cells were mated at a 1:1:1 ratio after being harvested by centrifugation for 1 min at 4°C and washed with LB1 twice. The pelleted cells were mixed and spotted onto BA2.5 and incubated ON (overnight) at 16°C. The spotted cells were resuspended in 2 ml LB2.5 and incubated ON at 12°C and 220 rpm. Transconjugants were selected on plates with chloramphenicol. The resulting strains are named LFI1238-pTM214, LFI1238-*Ptrc-rpoQ*, *ΔlitR*-pTM214 and *ΔlitR-Ptrc-rpoQ*.

Construction of green fluorescent *A. salmonicida* LFI1238, Δ*litR* and Δ*rpoQ*

The pVSV102 plasmid encoding the green fluorescent protein (GFP) and kanamycin resistance was transferred from *E. coli* DH5αλpir to *A. salmonicida* LFI1238, *ΔlitR* and *ΔrpoQ* using the conjugative helper strain CC118λpir carrying pEVS104 as described above. The potential tagged strains were selected on BA2.5 after 5 days. The resulting strains were named LFI1238-pVSV102, *ΔlitR*-pVSV102 and *ΔrpoQ*-pVSV102. The GFP expression was confirmed microscopically using Nikon Eclipse TS100.

Growth rate assay

The overnight secondary cultures were diluted to OD_{600} of 0.05 in a total volume of 60 ml SWT. The cultures were grown further in 250 ml baffled flask at 8°C and 220 rpm. The optical density was measured every 3 h using Ultrospec 10 cell density meter (Amersham Biosciences).

Motility assay

The motility assay was performed using soft agar plates containing 0.25% agar and 2.5% NaCl and with or without 1 mM isopropyl β-D-1-thiogalactopyranoside (IPTG). The primary cultures were diluted 1:40 and incubated overnight at 12°C with agitation. The cultures were diluted to an OD_{600} of 0.4. Then 3 μl of each culture was spotted on the soft agar plates and incubated at 4, 8, 12, 14 and 16°C for 5 days. The motility zones were monitored every 24 h for 5 days by measuring the diameter of the motile cells in the soft agar.

Colony morphology and adhesion

The colony morphology assay was carried out as described previously [31, 36]. A 250 μl of each bacterial culture was harvested by centrifugation, and the pellet was re-suspended in 250 μl SWT. Then, 2 μl of each culture was spotted onto SWT agar plates, and incubated at 4, 8, 12, and 14°C for up to 3 weeks. The colonies were viewed microscopically with Zeiss Primo Vert and photographed with AxioCam ERc5s at × 4 magnification. The same (three weeks old) colonies were also tested for their ability to adhere to the SWT agar. This was done by touching the colonies using a sterile plastic loop mainly as previously described [22], but the grading of the adherence was only recorded as "none" for smooth and creamy colonies, "weak" for slightly adherent and "strong" for colonies that were impossible to separate from the agar plate.

Static biofilm assay

The biofilm assay was performed as previously described [31]. The overnight secondary cultures were diluted to an OD_{600} of 1.3 in LB2.5 The cultures were further diluted 1:10 in SWT and a total volume of 300 μl was added to each well in flat-bottom, non-tissue culture-treated Falcon 24-well plates (BD Bioscience). For the overexpression biofilm assay a total of 1 mM IPTG was added. The plates were incubated statically at 4, 8, 12, 14 and 16°C, for 72 h and the biofilm was visualized using Nikon Eclipse TS100 microscope at 10× magnification and photographed with Nikon DS-5Mc.

Phylogenic analyses and software

The amino acid sequences were aligned using ClustalW. The aligned sequences were then used to construct a neighbor-joining (NJ) tree using the MEGA version 7.0 [37]. Gaps in pairwise sequence comparison were deleted and the p-distance model was used. Bootstrap analyses with 500 replicates were conducted to provide confidence levels for the tree topology. Search for

conserved sigma factor domains was performed using Pfam at EMBL-EBI (https://pfam.xfam.org/).

Results

Our previous studies show that *A. salmonicida* LitR is involved in regulating a number of activities that may be important for host interactions [22], and by using microarray we identified a number of genes regulated by LitR [31]. The regulation of LitR on downstream genes could proceed either directly or indirectly. One of the genes found to be regulated by LitR was the *rpoQ* gene (*VSAL_II0319*). We therefore sought to analyze the role of RpoQ in the different phenotypes known to be regulated by LitR and QS in *A. salmonicida*. To this end we constructed an in-frame deletion mutant (*ΔrpoQ*) of the wild-type strain LFI1238 by removing 254 of the 294 amino acids in RpoQ. A complementation mutant ($\Delta rpoQ_c$) was constructed to verify whether the observed phenotypes were due to the mutation of *rpoQ*. We do not expect the in-frame deletion (*ΔrpoQ*) or the insertion (*ΔrpoQc*) of *rpoQ* to have any polar effect(s) on downstream genes. However, it should be noted that this possibility cannot be excluded since the expression of the downstream genes in the operon was not analyzed in this work. Since temperature is an important factor involved in regulating AHL production and phenotypes related to QS in *A. salmonicida* [22, 31], the experiments were performed at different temperatures (4–16°C).

Deletion of *rpoQ* does not alter the growth of *A. salmonicida*

To analyze if the *rpoQ* mutation affected the vitality of *A. salmonicida* LFI1238, a growth curve assay was performed. The bacterial growth of all strains (LFI1238, *ΔrpoQ* and the complementary strain) was monitored in triplicate at 8°C for 72 h. The *ΔrpoQ* mutant showed the same growth rate as the wild-type strain LFI1238 and the complementary strain $\Delta rpoQ_c$ (Additional file 1: Figure S1).

RpoQ shows temperature dependent rugose colony morphology

The ability to form rugose colonies and biofilm are often correlated features in vibrios [38–40], and a rugose colony phenotype usually indicates high production of exopolysaccharides [39].

To compare colony morphologies of the wild-type LFI1238, and the *ΔrpoQ* and *ΔlitR* mutants a spot colony assay was performed on SWT agar incubated at different temperatures (4 to 14°C). The LFI1238 produced smooth colony morphology at all temperatures as previously reported [31]. The *ΔrpoQ* mutant started to form wrinkled colonies after 7 days of incubation, and at day 12 a strong rugose colony morphology with wrinkled edges was observed after growth at 4 and 8°C (Fig. 1). When incubated at 12°C, the *ΔrpoQ* colony remained smooth in the central part whereas the edges became wrinkled. No wrinkling was observed for *ΔrpoQ* at 14°C. The *ΔlitR* mutant was used as positive control [31] and, compared to *ΔrpoQ,* it showed a weaker rugose colony morphology. A strong *ΔlitR* rugose colony morphology similar to the wrinkled *ΔrpoQ* colonies was observed after 3 weeks (Additional file 2: Figure S2). As previously reported the wrinkling of *ΔlitR* colonies is absent after growth at 14°C [31].

The wrinkled colonies formed by the *ΔrpoQ* and *ΔlitR* mutants were found to be adhesive on the SWT agar, and the adhesiveness was stronger at low temperatures (4 to 8°C). No colonies were adhesive after growth at 14°C (Additional file 3: Table S1). The complementary strain (*ΔrpoQc*) behaved similar to the wild-type and produced non-adhesive, smooth and creamy colonies at all temperatures.

RpoQ is involved in biofilm formation

In order to investigate whether *rpoQ* is involved in biofilm formation, the *ΔrpoQ* mutant was allowed to form biofilm in SWT medium at different temperatures using static conditions (Additional file 4: Figure S3). To better visualize the biofilm, GFP-tagged strains were used. The tagged strains were constructed by transferring a constitutive GFP expressing plasmid (pVSV102) into the different mutants and the wild-type strain. As shown in Fig. 2, *ΔrpoQ* produced a biofilm at 8 and 14°C, which could be clearly visualized after 72 h. Little or no biofilm was observed at 16°C for the different strains. The biofilm produced by the *ΔrpoQ* mutant does not show large mushroom shaped structures similar to those produced by *ΔlitR* (Fig. 2 and [31]); instead the *ΔrpoQ* mutant formed a more regular and flat biofilm with smaller micro-colonies and structures. Above the microscopically visual *ΔrpoQ* biofilm structures is a thick and slimy extracellular matrix without or with few embedded bacteria (Additional file 5: Figure S4). The complementary strain *ΔrpoQc* behaved similar to the wild-type, whereas the double mutant $\Delta litR\text{-}rpoQ^-$ produced a biofilm with mushroom structure similar to the one produced by the *ΔlitR* mutant (Additional file 4: Figure S3).

RpoQ regulates motility in *A. salmonicida*

The flagellum is required for motility of bacteria, mediating their movements towards favorable environments or away from harmful conditions [41, 42]. Previous studies have shown that *A. salmonicida* is more motile at 12°C than at 4°C, and that LitR is a negative regulator of motility [22]. Here we analyzed the influence of RpoQ on the motility of *A. salmonicida* at different temperatures (4 to 16°C). Deletion of *rpoQ* resulted in a strain

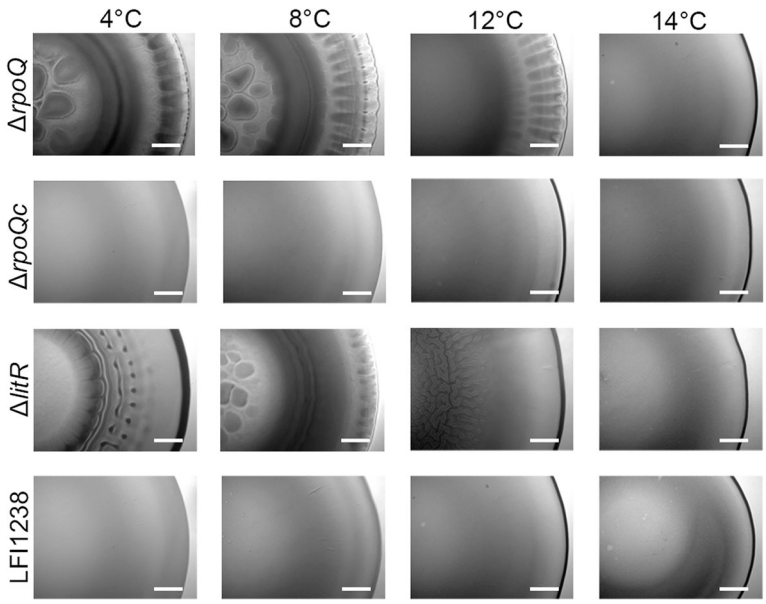

Fig. 1 Colony morphology of *ΔrpoQ*, *ΔrpoQ*$_c$, *ΔlitR* and LFI1238 at different temperatures. The colonies were allowed to form on SWT plates for 12 days at 4, 8, 12 and 14°C. The colonies were viewed in a Zeiss Primo Vert microscope at 4× magnification. Scale bars represent 0.5 mm

with reduced motility compared to the wild-type and the *ΔlitR* mutant at all tested temperatures (Fig. 3 and Additional file 6: Table S2). After 5 days of incubation at 4°C the *ΔrpoQ* mutant was almost non-motile and the motility zone was only 6.0 ± 1.0 mm. At higher temperatures (8 to 16°C) the motility of the *ΔrpoQ* mutant was between 36 and 51% compared to the motility of wild-type. Hence, the incubation temperature did not seem to affect the regulatory effect of RpoQ on the motility. Similar to the wild-type and *ΔlitR*, the *ΔrpoQ* mutant shows highest motility at 14°C. The *ΔrpoQc* behaved similar to the wild-type (Fig. 3a and b).

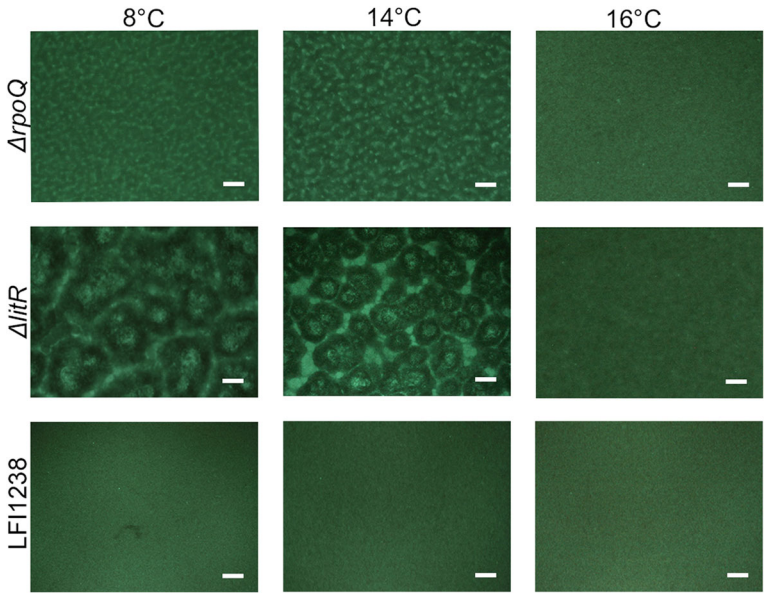

Fig. 2 Biofilm formation of GFP-tagged *ΔrpoQ*, *ΔlitR* and LFI1238 at different temperatures. The GFP tagged strains (LFI1238-pVSV102, *ΔrpoQ*-pVSV102 and *ΔlitR*-pVSV102) were allowed to form biofilms in SWT media at 8, 14 and 16°C. The biofilms were viewed, after 72 h of incubation, in a Nikon Eclipse TS100 microscope at 10× magnification and photographed with Nikon DS-5Mc. Scale bars represent 20 μm

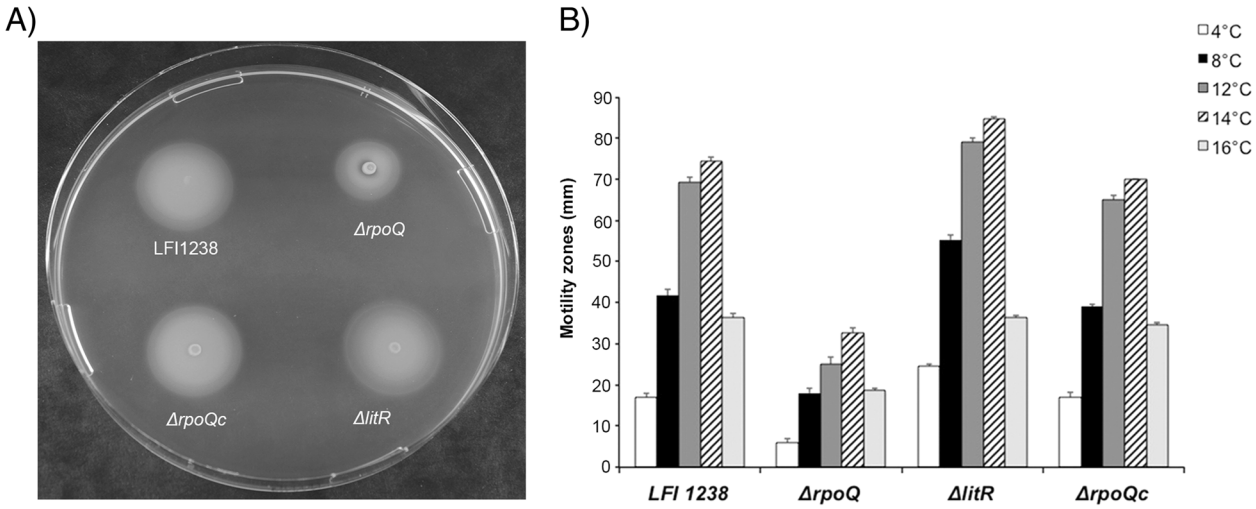

Fig. 3 Motility of LFI1238, *ΔrpoQ*, *ΔrpoQ*$_c$ and *ΔlitR* at different temperatures. **a** Soft agar plate showing motility zones of LFI1238, *ΔrpoQ*, *ΔrpoQ*$_c$ and *ΔlitR* after 5 days incubation at 8°C. **b** Motility zones (mm) of LFI1238, *ΔrpoQ*, *ΔlitR*, and *ΔrpoQ*$_c$ measured after 5 days incubation at different temperatures (4–16°C). The error bars present the standard deviation of biological triplicate

RpoQ is a negative regulator of biofilm

RpoQ is believed to function downstream of LitR in the QS cascade in *A. salmonicida* [31], and as shown above, deletion of *rpoQ* resulted in increased biofilm formation (Fig. 2). Hence, it was of interest to examine the influence of overexpressing *rpoQ* on the *ΔlitR* biofilm formation. For this purpose, the control vector (pTM214) and the inducible *rpoQ* vector (pTM214-*rpoQ*) were separately transferred to the *ΔlitR* mutant strain and the wild-type LFI1238 by conjugation. The biofilm assay was performed as before in SWT medium (4 to 16°C) but with 1 mM IPTG to induce expression of *rpoQ*.

As shown in Fig. 4, overexpression of *rpoQ* disrupted or inhibited the biofilm formation produced by *ΔlitR* (*ΔlitR-Ptrc-rpoQ* at 4 to 14°C) leaving small aggregates in the wells, whereas the *ΔlitR* biofilm formation was unaffected by the presence of the control vector (*ΔlitR*-pTM214) at all temperatures. Biofilm formation does not occur at 16°C, and hence no effects of the overproduced *rpoQ* was observed. Neither was any

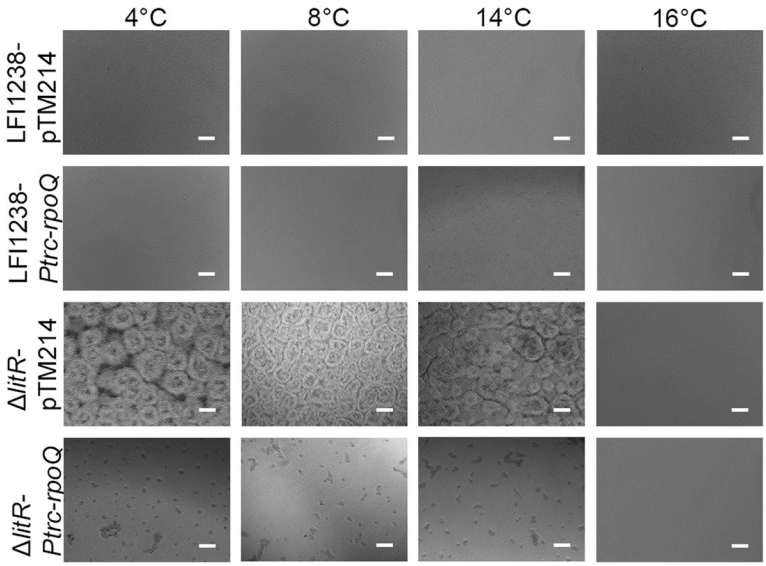

Fig. 4 The effect of the RpoQ on the biofilm formation of LFI1238 and *ΔlitR*. The biofilms of LFI1238 and *ΔlitR* harboring the pTM214 (control vector) and LFI1238 and *ΔlitR* harboring the P_{trc}-*rpoQ* (*rpoQ* overexpression vector) were allowed to form in SWT medium supplemented with 1 mM IPTG. The biofilms were incubated for 72 h at different temperatures (4 to 16°C). The biofilms were viewed in Nikon Eclipse TS100 microscope at 10× magnification and photographed with Nikon DS-5Mc. Scale bars represent 20 μm

changes observed when *rpoQ* was overexpressed in wild-type cells (LFI1238-*Ptrc-rpoQ*) (Fig. 4).

Overexpression of RpoQ decreases motility in *A. salmonicida*

In the experiments performed above we show that *rpoQ* is required for full wild- type motility at all temperatures (Fig. 3) and that overexpression of *rpoQ* has a negative effect on the biofilm forming ability of the *ΔlitR* mutant (Fig. 4). It therefore was of interest to analyze if overexpressed *rpoQ* also affected the motility of the wild-type and the *ΔlitR* mutant. As shown in Fig. 5, overexpression of *rpoQ* repressed the motility in both strains. Most notable, overexpression of *rpoQ* in the wild-type resulted in a completely non-motile strain when incubated at 4 and 8°C, and the size of the spotted LFI1238-*Ptrc-rpoQ* colony (5 mm) did not change at any of the two temperatures during the 5 days of the experiment (Fig. 5a and b). At 12, 14 and 16°C small motility zones (7–9 mm) were observed for LFI1238-*Ptrc-rpoQ* showing that overexpression of *rpoQ* in the wild-type does not result in complete shutdown of the motility at these temperatures. Overexpression of *rpoQ* in the *ΔlitR* also resulted in clearly diminished motility zones at all temperatures (Fig. 5b and Additional file 7: Table S3).

Discussion

Bacteria continually face changes in their environment such as temperature fluctuations, nutrient accessibility and pH changes. In order to adapt to these changes and often challenging conditions, bacteria have developed various responses. Alternative sigma factors such as RpoS provide a main line of responses to changes in the environment by altering gene transcription [43, 44]. Several studies have shown a connection between RpoS and QS in different vibrios [38, 45–48]. When Cao et al. (2012) described the alternative sigma factor RpoQ in *A. fischeri* a homologue was only found in *A. salmonicida* [28]. However, since then the genomes of *A. wodanis* [49] and *A. logei* (*A.logei* S5–186 GeneBank accession no. AJY02000108.1) have become available. Analysis show that they also encode an RpoQ homolog with four conserved domains (σ^{70} regions 1–4). RpoQ of *A. salmonicida* shares a high amino acid sequence identity (99%) with its homolog in *A. logei* whereas the amino acid sequence identity is 72% with *A. fischeri* and 69% with *A. wodanis.* Region 2 and region 4 of the putative RpoQ are well conserved between the four species, whereas region 3 is less conserved (Additional file 8: Figure S5).

RpoQ is regulated by LuxO through LitR in *A. fischeri* [28]. Similarly, our previous microarray results suggested that LitR is a positive regulator of RpoQ in *A. salmonicida* [31]. In the study presented here, we show that RpoQ is involved in regulation of colony morphology, adhesion, biofilm and motility similar to LitR. However, since RpoQ is suspected to act downstream of the master regulator LitR, one can expect that the *ΔlitR* mutant expresses phenotypes that are independent of RpoQ regulation.

The *ΔrpoQ* mutant demonstrated a stronger and an earlier onset of the rugose colony morphology as compared to the *ΔlitR* mutant. A rugose colony phenotype usually develops when the bacteria produce high amounts of polysaccharides, suggesting that more polysaccharides

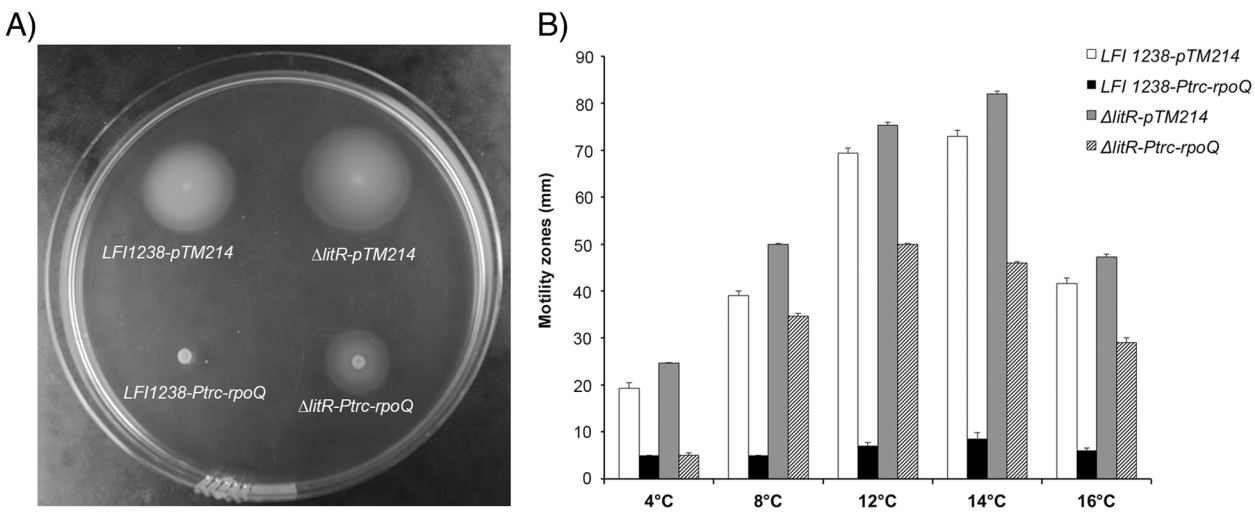

Fig. 5 Motility assay on soft agar supplemented with 1 mM IPTG. **a** Soft agar plate showing motility zones of LFI1238 and *ΔlitR* harboring the pTM214 (control vector) and LFI1238 and *ΔlitR* harboring the P_{trc}-*rpoQ* (*rpoQ* overexpression vector) at 8°C after 5 days. **b** Motility zones (mm) of LFI1238-pTM214, *ΔlitR*-pTM214, LFI1238-P_{trc}-*rpoQ* and *ΔlitR*-P_{trc}-*rpoQ* after 5 days of incubation at temperatures ranging from 4 to 16°C. The error bars present the standard deviation of biological triplicate

are made by the *ΔrpoQ* mutant. We know from our previous work that LitR represses the expression of the *symbiosis polysaccharide* (*syp*) operon, and that inactivation of *syp* (*sypC, sypP* and *sypQ*) in the *ΔlitR* mutant results in smooth colonies [31]. Hence, it is likely that LitR performs its activity on *syp* through RpoQ and that activation of RpoQ leads to a strong(er) repression of *syp*. The weaker rugose colony morphology of the *ΔlitR* mutant may be due to low levels of LitR-independent *rpoQ* expression, consistent with our previous microarray results that show expression of *rpoQ* in the *ΔlitR* mutant [31]. Hence, some repression of *syp* via RpoQ probably occurs in the *ΔlitR* mutant. Whereas in the *ΔrpoQ* mutant there is zero expression of *rpoQ* resulting in no or low *syp* repression and stronger rugosity.

Both LitR and RpoQ are negative regulators of biofilm formation in *A. salmonicida*. However, the *ΔrpoQ* mutant formed a biofilm morphologically different from the *ΔlitR* mutant. The biofilm produced by the *ΔrpoQ* was less mature and relatively flat and compact, without the large mushroom structures exhibited by the *ΔlitR* mutant. Additionally, the biofilm produced by *ΔrpoQ* contained a heavy and slimy extracellular matrix substance above the biofilm cells attached to the substratum (Additional file 5: Figure S4). This slimy matrix is likely due to high amounts of polysaccharides (i.e. *syp* expression as discussed above) that are common components of the extracellular matrix of biofilms, together with proteins and eDNA [50]. When we previously analyzed the *ΔlitR* biofilm we found that major components were polysaccharides and proteins, and by using electron microscopy we were able to see a network of fibers that connected biofilm cells together. The microarray analysis identified, in addition to *syp*, some lipoprotein, pili, flagella, and curli genes that were upregulated in the *ΔlitR* mutant [31]. Hence, LitR may repress some lipoproteins or filament structures needed to build up this mushroom-shaped biofilm architecture. Thus, one explanation for the observed biofilm morphology of the *ΔrpoQ* mutant may be that polysaccharide production is obtained through expression of *syp*, whereas expression of a functional LitR down-regulates genes involved in building mushroom shaped structures. When we inactivated *syp* in the *ΔlitR* mutant we found that although the rugose colony morphology reverted to wild-type morphology (smooth), some biofilm formation still occurred when using SWT medium [31]. Indeed, the biofilms produced by the *ΔlitRsyp*$^-$ mutants resembles the biofilm produced by *ΔrpoQ* but without the slimy extracellular matrix. We therefore believe that the pathway through which LitR represses genes responsible for building the mushroom-shaped structures is different from the pathway through which LitR represses *syp* (via RpoQ) resulting in rugose colony morphology (Fig. 6).

Both mutants produce biofilms that are loosely attached; however, in contrast to the *ΔlitR* biofilm, the *ΔrpoQ* biofilm is not able to withstand the washing steps required after staining with crystal violet. To our knowledge RpoQ, has not been shown to be involved in biofilm formation of *A. fischeri* or any other aliivibrios. However, studies have shown that RpoS is able to enhance or repress biofilm formation in *E. coli* and other bacteria [51–53]. Additionally, RpoS has been shown to be involved in cell attachment and the maturation of biofilm [30, 54, 55], and inactivation RpoX in *V. alginolyticus* results in cells with decreased ability to form biofilm [29]. Likewise, inactivation of *rpoQ* in *A. salmonicida* may have reduced the ability of the bacteria to attach to the abiotic surface and to build a mature biofilm. Another explanation is that the *ΔrpoQ* biofilm contains a higher amount of a heavy, extracellular, slimy polysaccharide matrix that tears the biofilm away from the substratum when the medium or wash solutions is being poured out or a combination of both.

Thus, as shown in Fig. 6 we propose that RpoQ and LitR function in the same pathway, where RpoQ functions

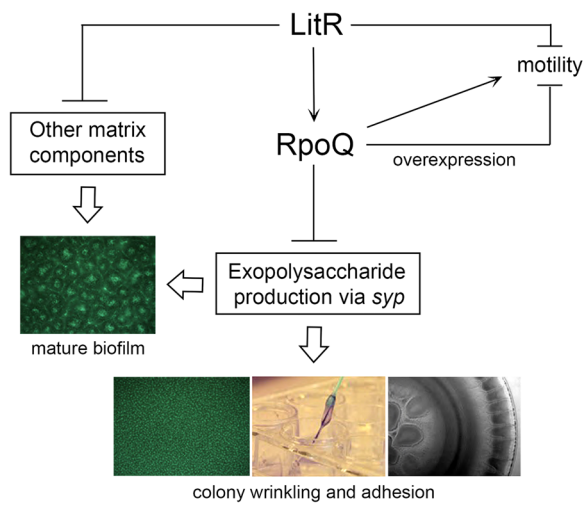

Fig. 6 Proposed model for regulation of QS related phenotypes in *A. salmonicida*. At high cell densities, LitR is produced in response to AHLs and acts as a positive regulator of *rpoQ* expression. LitR, probably via RpoQ, downregulates motility and expression of exopolysaccharides. The *ΔlitR* mutant shows a mature biofilm with mushroom shaped structures, whereas the *ΔrpoQ* biofilm is more flat and regular. Thus, in addition to repression of exopolysaccharides via RpoQ, LitR represses other biofilm matrix components independent of RpoQ that are required for building mature mushroom structures (e.g. lipoproteins, protein filaments). Therefore, at high cell densities both RpoQ dependent and independent processes are needed for down regulation of the mature biofilm. The *ΔrpoQ* mutant shows decreased motility suggesting that RpoQ may also act as a positive activator of motility. Arrows and lines with bar ends indicate pathways of positive and negative regulation, respectively, and may consist of several steps. The thicker, empty arrows indicate the resulting phenotypes

downstream of the LitR and is involved in repression of biofilm and the wrinkled colony morphology in *A. salmonicida*. The negative regulation cascade of extracellular polysaccharide matrix from LitR to the *syp* operon is probably operated through RpoQ, either directly or indirectly. The phenotypes are likely regulated in a cell density manner as previously discussed, where the development of a mushroom shaped biofilm structures and wrinkled colony morphology are initiated when neither AinS or LuxI AHLs are present at low cell density [19, 22, 31]. At high cell density when AHLs are produced, LitR represses genes required for building a mature biofilm structure, and activates *rpoQ* leading to repression of *syp*.

Inactivation of either *rpoQ* or *litR* had the opposite effect on motility in *A. salmonicida*. Unlike the *ΔlitR* mutant, which is more motile than the wild-type strain, the *ΔrpoQ* mutant exhibited significantly reduced motility. The complementary strain *ΔrpoQc* showed wild-type motility, suggesting that the termination of motility is due to *rpoQ* deletion and not to other factors. Reduced motility due to disruption of sigma factors has been reported for other bacteria, and inactivation of *rpoS* in *Y. pseudotuberculosis* results in decreased motility due to downregulation of the flagella master regulatory gene *flhDC* [51]. Thus, RpoQ may work in a similar manner by altering transcription of genes responsible for flagellar assembly or flagellar biosynthesis in *A. salmonicida*. Flagellum-mediated motility is important for specific stages of biofilm formation and surface attachment in several bacteria [56–58], and disruption of flagella biosynthesis is known to decrease attachment and alter biofilm architecture [59–62]. For example, loss of motility in *E. coli* affected the biofilm architecture, where poorly motile strains formed flatter biofilms compared to highly motile strains, which displayed more mature vertical biofilm structures [63]. Thus, it is tempting to speculate that the decreased motility of the *ΔrpoQ* mutant resulted in cells with reduced ability to attach and form mature biofilms.

Furthermore, overexpression of *rpoQ* resulted in non-motile wild-type cells and *ΔlitR* cells with reduced motility. These results are similar to those obtained with *A. fischeri*, where the overexpression of *rpoQ* in the wild-type and *ΔlitR* mutant resulted in non-motile strains [28]. The finding that both deletion and overexpression of *rpoQ* in *A. salmonicida* resulted in bacteria with reduced motility is interesting, but at the same time difficult to interpret. We know that RpoQ functions downstream of LitR and that LitR is a negative regulator of motility at high cell density [22, 31]. Thus, we may have expected to observe a similar effect on motility when we knocked out *rpoQ*. However, the *ΔrpoQ* mutant show decreased motility compared to the wild-type indicating that RpoQ is a positive regulator of motility (Fig. 6). This may suggest that at low cell densities some *litR* independent expression of *rpoQ* occurs and that RpoQ activates genes involved in flagellar biosynthesis. As the cell population increases *litR* will be expressed leading to increased levels of RpoQ. High RpoQ levels (overexpression of *rpoQ*) then turns down motility probably by acting as an activator of genes involved in down regulation of the flagellar apparatus. Hence, RpoQ probably controls genes responsible for both promoting or repressing motility depending on growth phase, environmental conditions and stress factors. Our results show that regulation of motility in *A. salmonicida* is complex similar to other vibrios [64] and probably involves several regulatory genes and factors, which is still unrevealed.

Temperature is an important factor in developing cold-water vibriosis and for production of AHLs in *A. salmonicida.* When the bacteria is grown at temperature above the disease limit (16°C), the production of AHLs is nearly absent [19]. Our results from the biofilm and colony morphology assays show that the *ΔrpoQ* mutant behaves as the wild-type strain and the *ΔlitR* mutant when the assays are performed at 16°C, and neither of the strains forms rugose colonies or biofilm at this temperature. This shows that RpoQ, similar to LitR, represses formation of biofilm and rugose colonies more at low temperatures (4–14°C), and at 16°C the effect of the *rpoQ* deletion is absent with regard to these phenotypes. Interestingly, this temperature effect was not observed when the motility of the *ΔrpoQ* mutant was analyzed, and at 16°C the motility of the *ΔrpoQ* mutant was still clearly reduced compared to the wild-type. This implies that RpoQ is expressed and is able to regulate motility in *A. salmonicida* at temperatures above the limit for developing cold water vibriosis, and at conditions when AHL concentrations are expected to be low.

Conclusion

In this work we have shown that the alternative sigma factor RpoQ regulates motility, colony morphology and biofilm formation in *A. salmonicida*. This broad range of different phenotypes suggests that RpoQ is involved in a regulatory hierarchy influencing expression of a large panel of genes. Overexpression of RpoQ led to disruption of the biofilm produced by *ΔlitR*, paralyzed the motility of the wild-type *A. salmonicida* and caused a reduction in *ΔlitR* motility. These findings confirm that the RpoQ is a novel factor in the QS and functions downstream of the LitR. However, further studies are needed to understand exactly how LitR and RpoQ work together or independently to regulate the QS dependent phenotypes investigated here, and to identify genes regulated by RpoQ.

Additional files

Additional file 1: Figure S1. The figure shows growth curves of *A. salmonicida* wild type and *rpoQ* mutants. (DOCX 126 kb)

Additional file 2: Figure S2. The figure shows colony morphology of Δ*litR* after 3 weeks of incubation. (DOCX 101 kb)

Additional file 3: Table S1. The table lists grading of adherence of *A. salmonicida* wild-type and mutants on SWT agar. (DOCX 16 kb)

Additional file 4: Figure S3. The figure shows biofilm formation of *A. salmonicida* wild-type LFI1238 and mutants. (DOCX 642 kb)

Additional file 5: Figure S4. The figure shows the slimy extracellular matrix formed by Δ*rpoQ* in the biofilm assay. (DOCX 701 kb)

Additional file 6: Table S2. The table lists motility zones of LFI1238, Δ*rpoQ*, Δ*rpoQc* and Δ*litR* formed on soft agar plates. (DOCX 15 kb)

Additional file 7: Table S3. The table lists motility zones formed on soft agar plates supplemented with 1 mM IPTG. (DOCX 16 kb)

Additional file 8: Figure S5. The figure shows alignment and phylogeny of RpoQ, RpoS and RpoX. (DOCX 699 kb)

Abbreviations
IPTG: Isopropyl β-D-1-thiogalactopyranoside; min: Minutes; OD_{600}: Optical density measured at 600 nm; ON: Overnight; PCR: Polymerase chain reaction; QS: Quorum sensing; rpm: Rounds per minute

Acknowledgements
We thank Dr. Debra Milton (Umeå University) for the pDM4 and pNQ705 plasmids, Dr. Eric V. Stabb (University of Georgia) and Dr. Tim Miyashiro (Penn State University) for the pVSV102, pTM214 and pEVS104 plasmids. We also thank Prof. Richard Engh (UiT The Arctic University of Norway) for proofreading parts of this manuscript.

Funding
This work was financed by UiT The Arctic University of Norway. UiT was not involved in designing the study, analysis, collection, data interpretation and in writing the manuscript. The publication charges for this article have been funded by a grant from the publication fund of UiT The Arctic University of Norway.

Availability of data and materials
The datasets used and/or analyzed during the current study are available from the corresponding author on reasonable request.

Authors' contributions
MK, HH and NPW conceived and designed the experiments. MK and HH constructed the mutants. MK constructed the GFP-tagged and overexpression mutants. MK performed the motility, morphology and biofilm assays. MK and HH wrote the paper. All authors read and approved the final manuscript.

Ethics approval and consent to participate
The experimental work carried in this study does not have any human or animal subjects. We do not see any ethical issues.

Consent for publication
Not applicable.

Competing interests
The authors declare that they have no competing interest.

Publisher's Note
Springer Nature remains neutral with regard to jurisdictional claims in published maps and institutional affiliations.

Received: 16 April 2018 Accepted: 4 September 2018
Published online: 12 September 2018

References
1. Thompson FL, Iida T, Swings J. Biodiversity of vibrios. Microbiol Mol Biol Rev. 2004;68(3):403–31.
2. Urbanczyk H, Ast JC, Higgins MJ, Carson J, Dunlap PV. Reclassification of *Vibrio fischeri*, *Vibrio logei*, *Vibrio salmonicida* and *Vibrio wodanis* as *Aliivibrio fischeri* gen. Nov., comb. nov., *Aliivibrio logei* comb. nov., *Aliivibrio salmonicida* comb. nov. and *Aliivibrio wodanis* comb. nov. Int J Syst Evol Microbiol. 2007;57(Pt 12):2823–9.
3. Egidius E, Andersen K, Clausen E, Raa J. Cold-water vibriosis or "Hitra disease" in Norwegian salmonid farming. J Fish Dis. 1981;4(4):353–4.
4. Holm K, Strøm E, Stensvaag K, Raa J, Jørgensen T. Characteristics of a *Vibrio* sp. associated with the "Hitra disease" of Atlantic Salmon in Norwegian fish farms. Fish Pathology. 1985;20(2–3):125–9.
5. Egidius E, Wiik R, Andersen K, Hoof KA, Hjeltnes B. *Vibrio salmonicida* sp. nov., a new fish pathogen. Int J Syst Evol Microbiol. 1986;36(4):518–20.
6. Miller MB, Bassler BL. Quorum sensing in bacteria. Annu Rev Microbiol. 2001;55:165–99.
7. Ng WL, Bassler BL. Bacterial quorum-sensing network architectures. Annu Rev Genet. 2009;43:197–222.
8. Ruby EG. Lessons from a cooperative, bacterial-animal association: the *Vibrio fischeri-Euprymna scolopes* light organ symbiosis. Annu Rev Microbiol. 1996; 50:591–624.
9. Hastings JW, Nealson KH. Bacterial bioluminescence. Annu Rev Microbiol. 1977;31:549–95.
10. Bassler BL, Wright M, Showalter RE, Silverman MR. Intercellular signalling in *Vibrio harveyi*: sequence and function of genes regulating expression of luminescence. Mol Microbiol. 1993;9(4):773–86.
11. Lupp C, Ruby EG. *Vibrio fischeri* uses two quorum-sensing systems for the regulation of early and late colonization factors. J Bacteriol. 2005; 187(11):3620–9.
12. Fidopiastis PM, Miyamoto CM, Jobling MG, Meighen EA, Ruby EG. LitR, a new transcriptional activator in *Vibrio fischeri*, regulates luminescence and symbiotic light organ colonization. Mol Microbiol. 2002;45(1):131–43.
13. Miyashiro T, Wollenberg MS, Cao X, Oehlert D, Ruby EG. A single *qrr* gene is necessary and sufficient for LuxO-mediated regulation in *Vibrio fischeri*. Mol Microbiol. 2010;77(6):1556–67.
14. Lupp C, Ruby EG. *Vibrio fischeri* LuxS and AinS: comparative study of two signal synthases. J Bacteriol. 2004;186(12):3873–81.
15. Miyashiro T, Ruby EG. Shedding light on bioluminescence regulation in *Vibrio fischeri*. Mol Microbiol. 2012;84(5):795–806.
16. Engebrecht J, Silverman M. Identification of genes and gene products necessary for bacterial bioluminescence. Proc Natl Acad Sci U S A. 1984; 81(13):4154–8.
17. Verma SC, Miyashiro T. Quorum sensing in the squid-*Vibrio* symbiosis. Int J Mol Sci. 2013;14(7):16386–401.
18. Hjerde E, Lorentzen MS, Holden MT, Seeger K, Paulsen S, Bason N, Churcher C, Harris D, Norbertczak H, Quail MA, et al. The genome sequence of the fish pathogen *Aliivibrio salmonicida* strain LFI1238 shows extensive evidence of gene decay. BMC Genomics. 2008;9:616.
19. Hansen H, Purohit AA, Leiros HK, Johansen JA, Kellermann SJ, Bjelland AM, Willassen NP. The autoinducer synthases LuxI and AinS are responsible for temperature-dependent AHL production in the fish pathogen *Aliivibrio salmonicida*. BMC Microbiol. 2015;15:69.
20. Fidopiastis PM, Sørum H, Ruby EG. Cryptic luminescence in the cold-water fish pathogen *Vibrio salmonicida*. Arch Microbiol. 1999;171(3):205–9.
21. Hmelo LR. Quorum sensing in marine microbial environments. Annu Rev Mar Sci. 2017;9:257–81.
22. Bjelland AM, Sørum H, Tegegne DA, Winther-Larsen HC, Willassen NP, Hansen H. LitR of *Vibrio salmonicida* is a salinity-sensitive quorum-sensing regulator of phenotypes involved in host interactions and virulence. Infect Immun. 2012;80(5):1681–9.
23. Borukhov S, Nudler E. RNA polymerase holoenzyme: structure, function and biological implications. Curr Opin Microbiol. 2003;6(2):93–100.
24. Davis MC, Kesthely CA, Franklin EA, MacLellan SR. The essential activities of the bacterial sigma factor. Can J Microbiol. 2017;63(2):89–99.
25. Tripathi L, Zhang Y, Lin Z. Bacterial sigma factors as targets for engineered or synthetic transcriptional control. Front Bioeng Biotechnol. 2014;2:33.

26. Boyd EF, Carpenter MR, Chowdhury N, Cohen AL, Haines-Menges BL, Kalburge SS, Kingston JJ, Lubin JB, Ongagna-Yhombi SY, Whitaker WB. Post-genomic analysis of members of the family *Vibrionaceae*. Microbiol Spectr. 2015;3:5.
27. Mandel MJ, Stabb EV, Ruby EG. Comparative genomics-based investigation of resequencing targets in *Vibrio fischeri*: focus on point miscalls and artefactual expansions. BMC Genomics. 2008;9:138.
28. Cao X, Studer SV, Wassarman K, Zhang Y, Ruby EG, Miyashiro T. The novel sigma factor-like regulator RpoQ controls luminescence, chitinase activity, and motility in *Vibrio fischeri*. mBio. 2012;3:e00285–11.
29. Paget MS, Helmann JD. The sigma70 family of sigma factors. Genome Biol. 2003;4(1):203.
30. Zhao JJ, Chen C, Zhang LP, Hu CQ. Cloning, identification, and characterization of the *rpoS*-like sigma factor *rpoX* from *Vibrio alginolyticus*. J Biomed Biotechnol. 2009;2009:126986.
31. Hansen H, Bjelland AM, Ronessen M, Robertsen E, Willassen NP. LitR is a repressor of *syp* genes and has a temperature-sensitive regulatory effect on biofilm formation and colony morphology in *Vibrio (Aliivibrio) salmonicida*. Appl Environ Microbiol. 2014;80(17):5530–41.
32. Stabb EV, Ruby EG. RP4-based plasmids for conjugation between *Escherichia coli* and members of the *Vibrionaceae*. Methods Enzymol. 2002;358:413–26.
33. Miyashiro T, Klein W, Oehlert D, Cao X, Schwartzman J, Ruby EG. The *N*-acetyl-D-glucosamine repressor NagC of *Vibrio fischeri* facilitates colonization of *Euprymna scolopes*. Mol Microbiol. 2011;82(4):894–903.
34. Shubeita HE, Sambrook JF, McCormick AM. Molecular cloning and analysis of functional cDNA and genomic clones encoding bovine cellular retinoic acid-binding protein. Proc Natl Acad Sci U S A. 1987;84(16):5645–9.
35. Milton DL, O'Toole R, Horstedt P, Wolf-Watz H. Flagellin a is essential for the virulence of *Vibrio anguillarum*. J Bacteriol. 1996;178(5):1310–9.
36. Lim B, Beyhan S, Meir J, Yildiz FH. Cyclic-diGMP signal transduction systems in *Vibrio cholerae*: modulation of rugosity and biofilm formation. Mol Microbiol. 2006;60(2):331–48.
37. Saitou N, Nei M. The neighbor-joining method: a new method for reconstructing phylogenetic trees. Mol Biol Evol. 1987;4(4):406–25.
38. Yildiz FH, Liu XS, Heydorn A, Schoolnik GK. Molecular analysis of rugosity in a *Vibrio cholerae* O1 El Tor phase variant. Mol Microbiol. 2004;53(2):497–515.
39. Yildiz FH, Schoolnik GK. *Vibrio cholerae* O1 El Tor: identification of a gene cluster required for the rugose colony type, exopolysaccharide production, chlorine resistance, and biofilm formation. Proc Natl Acad Sci U S A. 1999; 96(7):4028–33.
40. Casper-Lindley C, Yildiz FH. VpsT is a transcriptional regulator required for expression of *vps* biosynthesis genes and the development of rugose colonial morphology in *Vibrio cholerae* O1 El Tor. J Bacteriol. 2004;186(5): 1574–8.
41. Utada AS, Bennett RR, Fong JCN, Gibiansky ML, Yildiz FH, Golestanian R, Wong GCL. *Vibrio cholerae* use pili and flagella synergistically to effect motility switching and conditional surface attachment. Nat Commun. 2014;5:4913.
42. Wadhams GH, Armitage JP. Making sense of it all: bacterial chemotaxis. Nat Rev Mol Cell Biol. 2004;5(12):1024–37.
43. Marles-Wright J, Lewis RJ. Stress responses of bacteria. Curr Opin Struct Biol. 2007;17(6):755–60.
44. Aertsen A, Michiels CW. Stress and how bacteria cope with death and survival. Crit Rev Microbiol. 2004;30(4):263–73.
45. Joelsson A, Kan B, Zhu J. Quorum sensing enhances the stress response in *Vibrio cholerae*. Appl Environ Microbiol. 2007;73(11):3742–6.
46. Ringgaard S, Hubbard T, Mandlik A, Davis BM, Waldor MK. RpoS and quorum sensing control expression and polar localization of *Vibrio cholerae* chemotaxis cluster III proteins *in vitro* and *in vivo*. Mol Microbiol. 2015;97(4): 660–75.
47. Weber B, Croxatto A, Chen C, Milton DL. RpoS induces expression of the *Vibrio anguillarum* quorum-sensing regulator VanT. Microbiology. 2008; 154(Pt 3):767–80.
48. Tian Y, Wang Q, Liu Q, Ma Y, Cao X, Zhang Y. Role of RpoS in stress survival, synthesis of extracellular autoinducer 2, and virulence in *Vibrio alginolyticus*. Arch Microbiol. 2008;190(5):585–94.
49. Hjerde E, Karlsen C, Sørum H, Parkhill J, Willassen NP, Thomson NR. Co-cultivation and transcriptome sequencing of two co-existing fish pathogens *Moritella viscosa* and *Aliivibrio wodanis*. BMC Genomics. 2015;16:447.
50. Flemming HC, Neu TR, Wozniak DJ. The EPS matrix: the "house of biofilm cells". J Bacteriol. 2007;189(22):7945–7.
51. Guan J, Xiao X, Xu S, Gao F, Wang J, Wang T, Song Y, Pan J, Shen X, Wang Y. Roles of RpoS in *Yersinia pseudotuberculosis* stress survival, motility, biofilm formation and type VI secretion system expression. J Microbiol. 2015;53(9): 633–42.
52. Corona-Izquierdo FP, Membrillo-Hernandez J. A mutation in *rpoS* enhances biofilm formation in *Escherichia coli* during exponential phase of growth. FEMS Microbiol Lett. 2002;211(1):105–10.
53. Sheldon JR, Yim MS, Saliba JH, Chung WH, Wong KY, Leung KT. Role of *rpoS* in *Escherichia coli* O157:H7 strain H32 biofilm development and survival. Appl Environ Microbiol. 2012;78(23):8331–9.
54. Adams JL, McLean RJ. Impact of *rpoS* deletion on *Escherichia coli* biofilms. Appl Environ Microbiol. 1999;65(9):4285–7.
55. Ito A, May T, Kawata K, Okabe S. Significance of *rpoS* during maturation of *Escherichia coli* biofilms. Biotechnol Bioeng. 2008;99(6):1462–71.
56. Guttenplan SB, Kearns DB. Regulation of flagellar motility during biofilm formation. FEMS Microbiol Rev. 2013;37(6):849–71.
57. Lemon KP, Higgins DE, Kolter R. Flagellar motility is critical for *Listeria monocytogenes* biofilm formation. J Bacteriol. 2007;189(12):4418–24.
58. O'Toole GA, Kolter R. Flagellar and twitching motility are necessary for *Pseudomonas aeruginosa* biofilm development. Mol Microbiol. 1998;30(2): 295–304.
59. Klausen M, Heydorn A, Ragas P, Lambertsen L, Aaes-Jørgensen A, Molin S, Tolker-Nielsen T. Biofilm formation by *Pseudomonas aeruginosa* wild type, flagella and type IV pili mutants. Mol Microbiol. 2003;48(6):1511–24.
60. Watnick PI, Kolter R. Steps in the development of a *Vibrio cholerae* El Tor biofilm. Mol Microbiol. 1999;34(3):586–95.
61. Malamud F, Torres PS, Roeschlin R, Rigano LA, Enrique R, Bonomi HR, Castagnaro AP, Marano MR, Vojnov AA. The *Xanthomonas axonopodis* pv. citri flagellum is required for mature biofilm and canker development. Microbiology. 2011;157(Pt 3):819–29.
62. Merritt PM, Danhorn T, Fuqua C. Motility and chemotaxis in *Agrobacterium tumefaciens* surface attachment and biofilm formation. J Bacteriol. 2007; 189(22):8005–14.
63. Wood TK, Gonzalez Barrios AF, Herzberg M, Lee J. Motility influences biofilm architecture in *Escherichia coli*. Appl Microbiol Biotechnol. 2006;72(2):361–7.
64. Macnab RM. How bacteria assemble flagella. Annu Rev Microbiol. 2003;57:77–100.
65. Simon R, Priefer U, Puhler A. A broad host range mobilization system for in vivo genetic engineering: transposon mutagenesis in gram negative bacteria Nat. Biotech. 1983;1:784–91.
66. Messing J, Crea R, Seeburg PH. A system for shotgun DNA sequencing. Nucleic Acids Res. 1981;9(2):309–21.
67. Dunn AK, Millikan DS, Adin DM, Bose JL, Stabb EV. New *rfp*- and pES213-derived tools for analyzing symbiotic *Vibrio fischeri* reveal patterns of infection and *lux* expression *in situ*. Appl Environ Microbiol. 2006;72(1):802–10.

Additional file 1

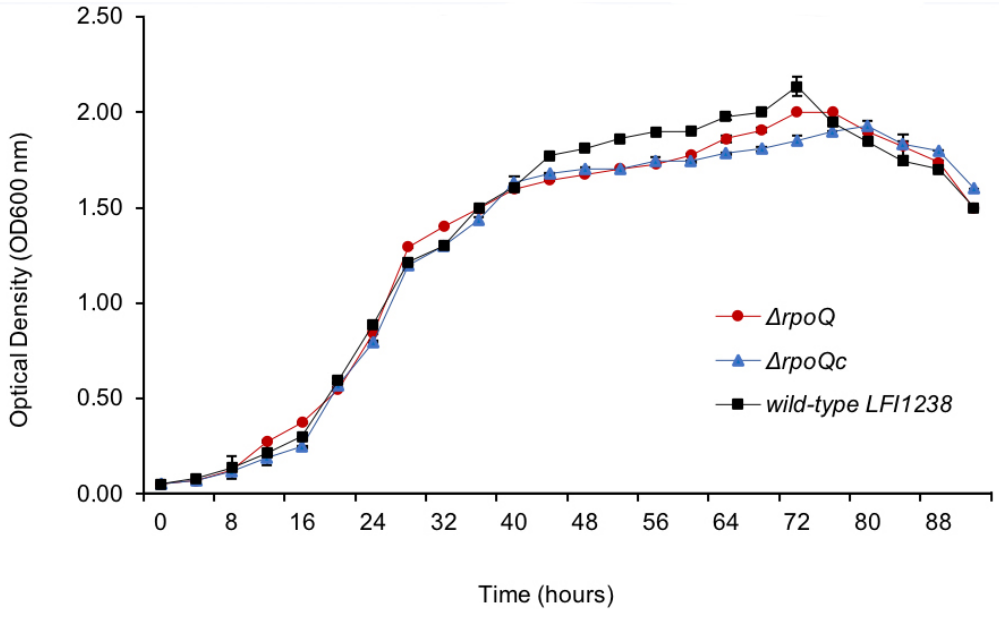

Figure S1. **Growth curves of *ΔrpoQ, ΔrpoQc* and wild-type LFI1238.** The bacterial cultures were grown in SWT medium for 92 hours at 8°C and 200 rpm. The bacterial cultures were diluted to a starting OD_{600} of 0.05. The OD_{600} measurements were performed at 4 hours intervals. The error bars represent the standard deviation of biological triplicates.

Additional file 2

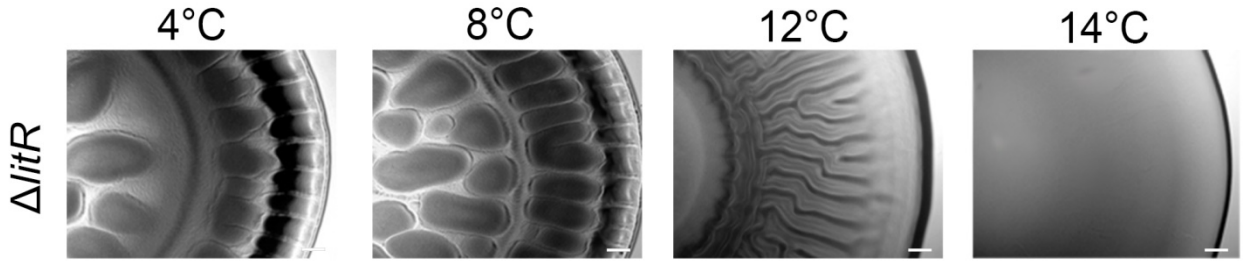

Figure S2. **Colony morphology of *ΔlitR* at different temperatures.** The colonies were allowed to form on SWT plates for 3 weeks at 4, 8, 12 and 14°C. The colonies were viewed in a Zeiss Primo Vert microscope at 4x magnification. Scale bars present 0.5mm.

Additional file 3

Table S1. **Grading of adherence of LFI1238, *ΔrpoQ*, *ΔrpoQ*$_c$ and *ΔlitR* to SWT agar.** The adherence of the colonies was analyzed after 3 weeks incubation at the different temperatures.

Bacterial strains	**4°C**	**8°C**	**12°C**	**14°C**
LFI1238	none	none	none	none
ΔrpoQ	strong	strong	weak	none
ΔlitR	strong	strong	weak	none
ΔrpoQ$_c$	none	none	none	none

Additional file 4

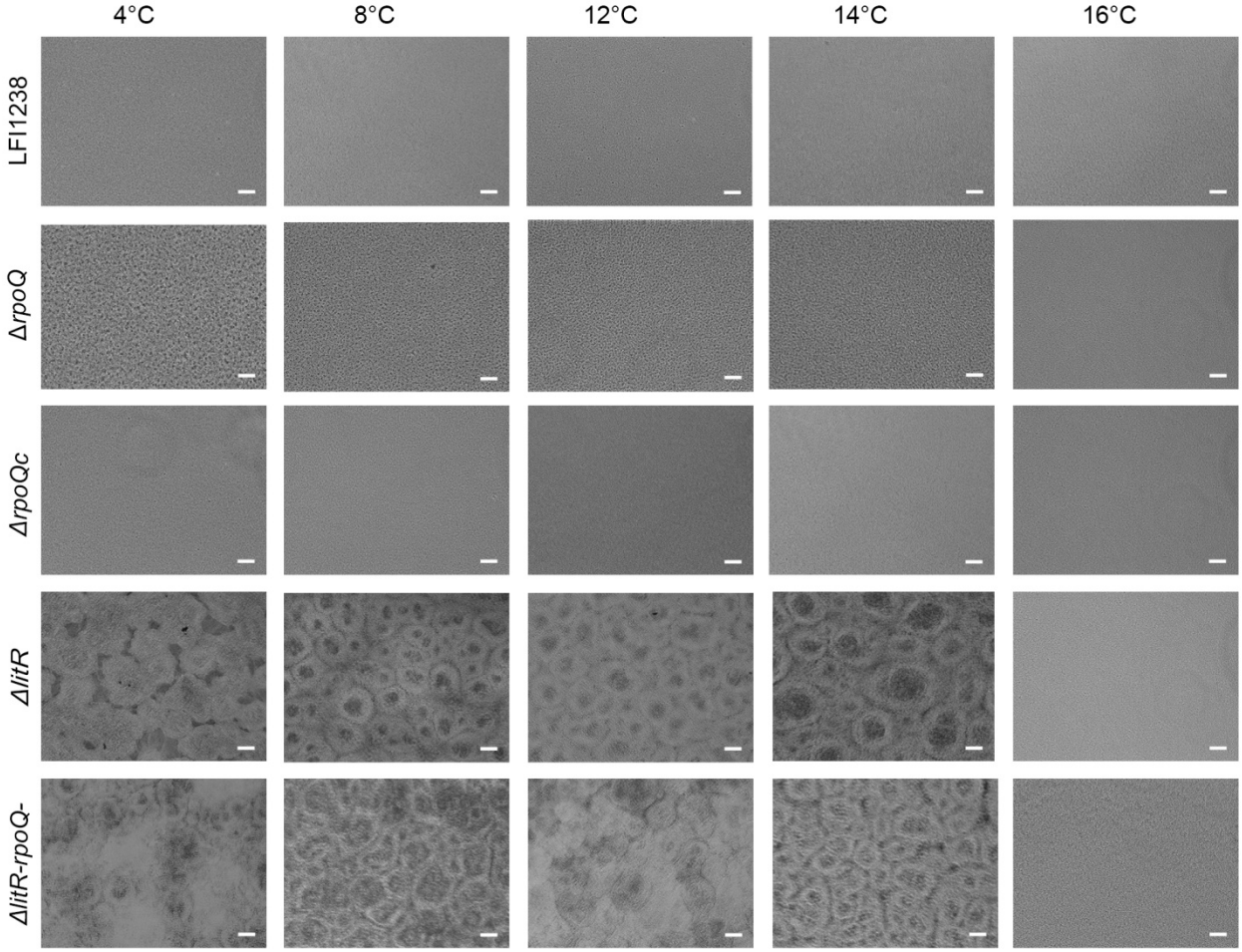

Figure S3. **Biofilm formation of *A. salmonicida* wild-type LFI1238 and mutants.** The different strains (LFI1238, *ΔrpoQ, ΔrpoQc, ΔlitR* and *ΔlitR-rpoQ*$^{-}$) were incubated and allowed to form biofilms in SWT medium at different temperatures (4-16°C). The biofilms formed after 72 hours of incubation were viewed in a Nikon Eclipse TS100 microscope at x10 magnification and photographed by Nikon DS-5Mc. Scale bars present 20µm.

Additional file 5

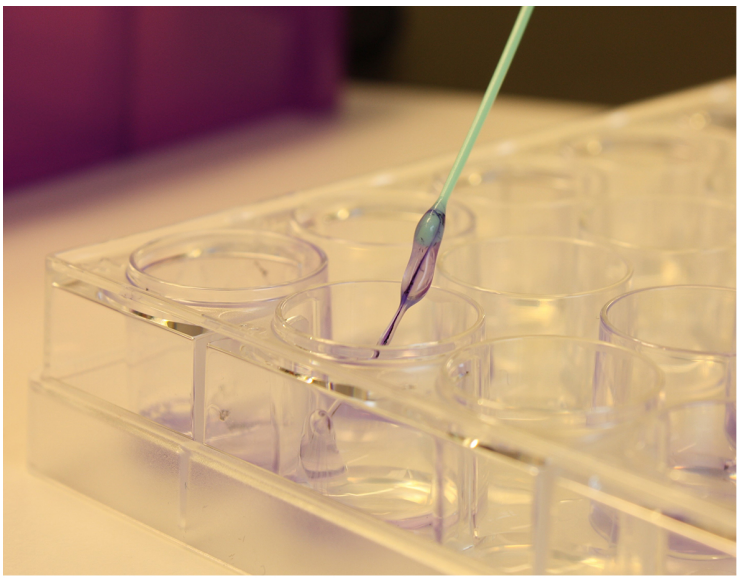

Figure S4. **The extracellular slimy substance of the *ΔrpoQ* biofilm.** *ΔrpoQ* was allowed to form biofilm in SWT medium. After 72 hours incubation a small amount of crystal violet was added into the well to improve the visualization. The picture shows the slimy substance lifted from the well using a plastic-loop. Images were photographed using a Canon camera.

Additional file 6

Table S2. **Motility zones of LFI1238, *ΔrpoQ*, *ΔrpoQ*$_c$ and *ΔlitR* formed on soft agar plates.** Each value represents the average (mm) of biological triplicates ± standard deviation.

Bacterial strains	**4°C**	**8°C**	**12°C**	**14°C**	**16°C**
LFI1238	17.0 ± 1.0	41.6 ± 1.5	69.3 ± 1.1	74.3 ± 1.1	36.3 ± 1.1
ΔrpoQ	6.0 ± 1.0	18.0 ± 1.3	25.0 ± 1.7	32.6 ± 1.1	18.6 ± 0.6
ΔlitR	24.6 ± 0.6	55.3 ± 1.1	79.0 ± 1.0	84.6 ± 0.6	36.3 ± 0.6
ΔrpoQ$_c$	17.0 ± 1.1	39.0 ± 0.5	65.0 ± 1.0	70.0 ± 0.0	34.6 ± 0.6

* The original size of the spotted colony was 5.0 mm.

Additional file 7

Table S3. **Motility zones formed on soft agar plates supplemented with 1mM IPTG.** The values represent the average (mm) of biological triplicates ± standard deviation*

Bacterial strains	**4°C**	**8°C**	**12°C**	**14°C**	**16°C**
LFI1238-pTM214	19.3 ± 1.1	39.0 ± 1.0	69.3 ± 1.1	73 ± 1.2	41.6 ± 1.1
LFI1238-Ptrc-rpoQ	5.0 ± 0.0	5.0 ± 0.0	7.0 ± 0.5	7.4 ± 1.3	6.0 ± 0.6
ΔlitR-pTM214	24.6 ± 0.0	50.0 ± 0.2	75.3 ± 0.5	82.0 ± 0.6	47.3 ± 0.6
ΔlitR-Ptrc-rpoQ	5.0 ± 0.0	34.6 ± 0.6	50.0 ± 0.1	46.0 ± 0.2	30.0 ± 1.0

* The original size of the spotted colony was 5.0 mm.

Additional file 8

A)

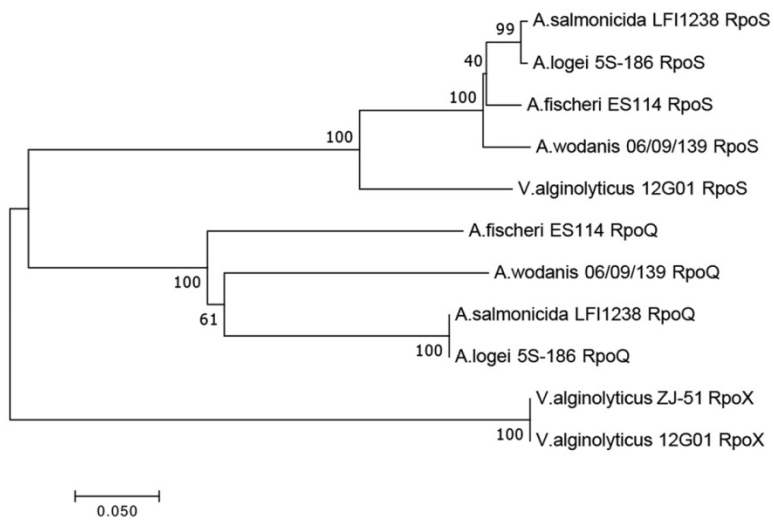

B)

```
                                        Region 1
A.fischeri      MAYAKLDMRVCEEQGLNDSYSLYLKEINRYQLLTAEEELAYSRLYKKGDVSARNTLIESN 60
A.salmonicida   MLNIECS-KKEEPRNSIDAYSLYLKEINKYKLLTASEELEHSRNYLSGDLKSRNVLIESN 59
A.logei         MLNIECS-KKEEPRNSIDAYSLYLKEINKYKLLTASEELEHSRNYLSGDLKSRNVLIESN 59
A.wodanis       MASVKIN-DKSDSYVGGDLYSKYLKEINKYQLLAASEELIYSRKYHDGDILSRNILIESN 59
                *   : .    :     * ** ******:*:**:*.*** :** * .**: :** *****
                                        Region 2
A.fischeri      LRLVVKVANKYRKRNQTDLAILDIIEEGNLGLIKAIDKFNPELGYRFSTYAVWWIRESIE 120
A.salmonicida   LRLVVKIANKYRHRNQRELAPLDIIEEGNLGLMKAVNKFDPELGYRFSTYAVWWIKESIE 119
A.logei         LRLVVKIANKYRHRNQRELAPLDIIEEGNLGLMKAVNKFDPELGYRFSTYAVWWIKESIE 119
A.wodanis       LRLVVKVANKYRGRNQTDLAPLDIIEEGNLGLIKAIDKFDPDLGYRFSTYAVWWIKEAIE 119
                ******:***** *** :*  ***********:**::**:*:*************:*:**
                                                Region 3
A.fischeri      SALFNHSRTVRLPVHITKELNTYLRAARELSKSLKREPSIRDISTYCEEEQIKVSKIISL 180
A.salmonicida   SALFNHSRTVRLPVHITKELNVYLRAARDLSRTLKKEPSISEISVHCNKDYKKVNKILGL 179
A.logei         SALFNHSRTVRLPVHITKELNVYLRAARDLSRTLKKEPSISEISVHCNKDYKKVNKILGL 179
A.wodanis       SALFNHSRTVRLPVHITKELNTYLRASRELSKSLKKEPSISDISKHCGVDAIKVNKIMRL 179
                *********************.****:*:**::**:**** :** :*  :  **.**: *

A.fischeri      IPNQLTCHSACSDELSPKFFELSSNNKALEPDSSLSQNNLEMNLSSWIDSLNYREKEIII 240
A.salmonicida   VPSSSTCHSASSDDMSSNLIELCADDHEQEPAQSLSKSNLESNLSSWLNLLQCREKQIII 239
A.logei         VPSSSTCHSASSDDMSSNLIELCADDHEQEPAQSLSKSNLESNLSSWLNLLQCREKQIII 239
A.wodanis       SSGGFMGYSASSDDALPQLIDSCVNKKENNPDNLLSKSNLEDNLSSWLNLlQGREKQIIV 239
                  .    :**.**:   :::: . :.:  :* . **:.*** *****:: *: ***:**:
                                Region 4
A.fischeri      NRYGLFGCKVKTLEDLGKDLDLSKERVRQIQSETLIKLNTIFKKNKLDLEIALG-      294
A.salmonicida   NRYGLFGTDVKTLEELGQDLQLSKERVRQIQTETLTKLNTIFKKNKLNLEIALN-      293
A.logei         NRYGLFGTDVKTLEELGQDLQLSKERVRQIQTETLTKLNTIFKKNKLNLEIALN-      293
A.wodanis       NRFGLFDSDIKTLEQLGKELQLSKERVRQIQSETLIKLNSIFIKNKLNDDVVLNF      293
                **:***. .:****:**::*:**********:*** ***:** ****: ::.*.
```

Figure S5. **Alignment and phylogenetic analyses of RpoQ, RpoS and RpoX amino acid sequences. A)** The phylogenetic tree was constructed using neighbor joining and clustalW aligned amino acid sequences of RpoQ from *A. salmonicida* LFI1238 (acc.no. WP_012551679, *VSAL_II0319*), *A. fischeri* ES114 (acc.no. YP_206973, *VF_A1015*), *A. logei* S5-186 (acc.no. OEF11440, *A1Q5_19865*) and *A. wodanis* 06/09/139 (acc.no. CED57794, *AWOD_II1179*); RpoS from *A. salmonicida* (acc.no. WP_012550978, *VSAL_I2506*), *A. fischeri* ES114 (acc.no. YP_205450, *VF_2067*), *A. logei* S5-186 (acc.no. OEF20103, *A1Q5_16955*), *A. wodanis* 06/09/139 (acc.no. CED72209, *AWOD_I_2147*) and *V. alginolyticus* 12G01 (acc.no. EAS74640, *V12G01_13719*); and RpoX from *V. alginolyticus* ZJ-51 (acc.no. ACJ09227, locus tag not available) and *V. alginolyticus* 12G01 (acc.no. ZP_01261551, *V12G01_06616*) was included as an outgroup. Numbers shown on the branch points of phylogenic tree represent the bootstrap values (%). The scale bar (0.050) represents amino acid substitutions per site. **B)** ClustalW alignment of RpoQ amino acid sequences from *A. fischeri* ES114, *A. salmonicida* LFI1238, *A. logei* 5S-186 and *A. wodanis* 06/09/136. (*) indicates a full conserved residue, (:) indicates a fully conserved strong group and (.) indicates a fully conserved weak group. The four conserved regions (region 1-4) in RpoQ are highlighted in grey color.

Paper II

Differential expression profiling of *ΔlitR* and *ΔrpoQ* mutants reveals insight into QS regulation of motility, adhesion and biofilm formation in *Aliivibrio salmonicida*

Miriam Khider, Erik Hjerde, Hilde Hansen and Nils Peder Willassen // BMC Genomics., 15 March 2019., **20**:220

Khider et al. BMC Genomics (2019) 20:220
https://doi.org/10.1186/s12864-019-5594-4

BMC Genomics

RESEARCH ARTICLE Open Access

Differential expression profiling of *ΔlitR* and *ΔrpoQ* mutants reveals insight into QS regulation of motility, adhesion and biofilm formation in *Aliivibrio salmonicida*

Miriam Khider[1*], Erik Hjerde[1,2], Hilde Hansen[1] and Nils Peder Willassen[1,2*]

Abstract

Background: The coordination of group behaviors in bacteria is achieved by a cell-cell signaling process called quorum sensing (QS). QS is an intercellular communication system, which synchronously controls expression of a vast range of genes in response to changes in cell density and is mediated by autoinducers that act as extracellular signals. *Aliivibrio salmonicida,* the causative agent of cold-water vibriosis in marine aquacultures, uses QS to regulate several activities such as motility, biofilm formation, adhesion and rugose colony morphology. However, little is known about either genes or detailed mechanisms involved in the regulation of these phenotypes.

Results: Differential expression profiling allowed us to define the genes involved in controlling phenotypes related to QS in *A. salmonicida* LFI1238. RNA sequencing data revealed that the number of expressed genes in *A. salmonicida,* **Δ***litR* and **Δ***rpoQ* mutants were significantly altered due to changes in cell density. These included genes that were distributed among the 21 functional groups, mainly presented in cell envelope, cell processes, extrachromosomal/foreign DNA and transport-binding proteins functional groups. The comparative transcriptome of *A. salmonicida* wild-type at high cell density relative to low cell density revealed 1013 genes to be either up- or downregulated. Thirty-six downregulated genes were gene clusters encoding biosynthesis of the flagellar and chemotaxis genes. Additionally we identified significant expression for genes involved in acyl homoserine lactone (AHL) synthesis, adhesion and early colonization. The transcriptome profile of **Δ***rpoQ* compared to the wild-type revealed 384 differensially expressed genes (DEGs) that allowed us to assign genes involved in regulating motility, adhesion and colony rugosity. Indicating the importance of RpoQ in controlling several QS related activities. Furthermore, the comparison of the transcriptome profiles of **Δ***litR* and **Δ***rpoQ* mutants, exposed numerous overlapping DEGs that were essential for motility, exopolysaccharide production via *syp* operon and genes associated with *tad* operon.

Conclusion: Our findings indicate previously unexplained functional roles for LitR and RpoQ in regulation of different phenotypes related to QS. Our transcriptome data provide a better understanding of the regulation cascade of motility, wrinkling colony morphology and biofilm formation and will offer a major source for further research and analysis on this important field.

Keywords: *Aliivibrio salmonicida*, LitR, RpoQ, High cell density, Low cell density, Differentially expressed genes and quorum sensing

* Correspondence: miriam.khider@uit.no; nils-peder.willassen@uit.no
[1]Norwegian Structural Biology Centre, UiT - The Arctic University of Norway, N-9037 Tromsø, Norway
Full list of author information is available at the end of the article

Background

Quorum sensing (QS) is a cell to cell communication process that allows bacteria to adjust gene expression in response to cell density [1]. The communication in QS depends on the production, accumulation and detection of signaling autoinducers such as acyl homoserine lactone (AHL) [2]. QS regulates a number of traits such as motility, biofilm formation, colonization, adhesion, virulence factor secretion and bioluminescence, which are required for survival and/or virulence in several bacteria [1]. The QS controlled activities, become costly when undertaken by an individual bacterium and are more beneficial when carried out by a group. Therefore, the QS system allows bacteria to switch between two states of gene expression: the low cell density (LCD) favoured for individuals and high cell density (HCD) favoured for groups [3–6].

Vibrio, species including the fish pathogen *Aliivibrio salmonicida*, are gram-negative, rod-shaped bacteria that live in different aqueous environments, including marine and freshwater [7]. *Vibrios* are known to regulate gene expression using QS system [8]. *A. salmonicida* possesses two QS systems the LuxI/R and AinS/R which are responsible for the production of eight AHLs in a cell density dependent manner [9].

Numerous studies have shown the ability of *Vibrio* species to move using flagella, mediating their movement to favorable environments and avoiding harmful conditions [10, 11]. When facing unfavorable conditions, bacteria can escape by forming biofilms [12]. A biofilm is a structured microbial community, which serves as a reservoir protecting the bacteria from being destroyed by external treatments, as well as being the main approach for survival in various harsh environmental conditions [13–15]. The development of the biofilm is a complex mechanism involving several steps. In the initial step the planktonic bacterial cells attach to the abiotic or biotic surface using physical force or bacterial appendages (flagella or pilli). Following the adhesion micro-colonies form and grow further to a three-dimensional mature biofilm structure [5, 16]. The forms of mature biofilms can vary from flat to multi-layered high mushroom-like structures, where numerous factors have been shown to influence the architecture of biofilm, including motility and extracellular polymeric substance (EPS) matrix production [4, 17]. Differing from the free-living planktonic state, cells in the biofilm are embedded in an EPS matrix, which provides strength to the interaction of the bacteria in the biofilm. EPS is mainly composed of polysaccharides in addition to proteins, lipids and nucleic acids [14, 18]. The EPS loci have been identified in several pathogenic and symbiotic vibrios [14]. For example, *A. salmonicida* and *Aliivibrio fischeri* (*A. fischeri*) produces EPS-dependent biofilm and wrinkled colonies involving an 18-gene cluster known as *symbiosis polysaccharides* (*syp*) [19, 20]. In *Vibrio cholerae* (*V. cholerae*) the *vibrio polysaccharide* (*vps*) locus encodes proteins responsible for EPS production, which is associated with rugose colony morphology and three-dimensional biofilm structure [21, 22]. The regulation of EPS biosynthesis involves several transcription regulators such as QS which sense and respond in a cell density dependent manner [14]. HapR, the QS transcription regulator of *V. cholerae* regulates expression of VpsT and VpsR regulators of biofilm [23]. At LCD *hapR* is not expressed in turn both *vpsT* and *vpsR* are upregulated allowing expression of genes involved in biofilm formation. Whereas at HCD *hapR* is expressed which results in *vpsT* and *vpsR* repression, causing the downregulation of the biofilm [23–26]. Likewise LitR (a homolog of HapR) of *A. salmonicida* is a negative regulator of biofilm formation and rugosity through *syp* repression [19, 27]. Conversely, transcription regulators OpaR, LitR and SmcR of *Vibrio parahaemolyticus* (*V. parahaemolyticus*), *A. fischeri* and *Vibrio vulnificus* (*V. vulnificus*) respectively, are positive regulators of biofilm formation and colony opacity at HCD [28–31].

In our previous studies we were able to show that the inactivation of the LitR master regulator of QS enhanced biofilm formation, rugose colony morphology, adhesiveness and motility [19, 27]. By microarray analysis we identified a number of LitR regulated genes, among these genes were genes of the *syp* operon (*VSAL_II0295-VSAL_II0312*) and *rpoQ* sigma factor (*VSAL_II0319*) homologs of the *A. fischeri syp* and *rpoQ* genes [19, 32]. The inactivation of the *rpoQ* gene in *A. salmonicida* LFI1238 resulted in phenotypic traits somewhat different from the *ΔlitR* [33] . The *ΔrpoQ* mutant showed reduced motility, slimy biofilm without mushroom structure and formed an early and strong rugose colony morphology [33]. Neverless we were not able to answer how LitR and RpoQ work together to regulate QS related traits. In the present study the transcriptome expression profiles of *ΔlitR* and *ΔrpoQ* mutants were compared to the isogenic *A. salmonicida* LFI1238 wild-type, in order to gain a better understanding on how LitR and RpoQ work together and to identify the major differences in the gene expression profiles associated with the modulation of the QS related activities. Triplicates from each mutant were grown at low temperature (8°C) and harvested at two cell densities (LCD, $OD_{600} = 0.3$ and HCD, $OD_{600} = 1.2$). Low temperatures play an important role both in the development of cold-water vibriosis and the production of AHLs [9, 27]. Previously, we were able to show that the phenotypes exhibited by *ΔlitR* and *ΔrpoQ* (rugosity and biofilm formation) were absent at temperatures above the threshold of disease development mainly above 14°C [19,

27, 33]. Moreover, the concentration of the eight known *A. salmonicida* AHLs were also declined at high temperatures (above 16°C) [9]. Additionally, we assume that changes in cell density may affect the gene expression involved in regulating phenotypes related to QS mechanism.

Methods

Bacterial strains, culture conditions and supplements

Bacterial strains used in this study are listed in Table 1. *A. salmonicida* LFI1238 strain and the constructed *A. salmonicida* mutants were grow on blood agar base no. 2 (Oxoid, Thermo Scientific) with a total concentration of 5% blood and 2.5% NaCl (BA2.5) or in Luria Bertani broth (Difco, BD Diagnostics) with a total concentration of 2.5% NaCl (LB2.5). *A. salmonicida* strains were cultivated from a single colony in 2 ml (LB2.5) at 12°C, 220 rpm for 2 days.

The GFP constitutive plasmid pVSV102, helper plasmid pEVS104 and suicide plasmid pNQ705 were propagated in *Escherichia coli* (*E. coli*), DH5αλpir, CC118λpir and S17.1λpir respectively. The *E. coli* strains were cultivated in LB or Luria Agar (LA) containing 1% NaCl (LB1 and LA1 respectively) and incubated at 37°C and 220 rpm. The potential transconjugants were selected on BA2.5 supplemented with 2 μl/ml chloramphenicol or 150 μl/ml kanamycin.

A seawater-based medium (SWT) was used for the transcriptomics, biofilm and morphology assays. The medium consists of 5 g/L of bacto peptone (BD Biosciences), 3 g/L of yeast extract (Sigma-Aldrich) and 28 g/L of a synthetic sea salt (Instant Ocean, Aquarium Systems).

Transcriptomics

Sample collection

Three biological replicates were used for all *A. salmonicida* strains. Cultures were grown from an individual

Table 1 Bacterial strains and plasmids used in this study

Bacterial strains or plasmids	Description	Source
A. salmonicida		
LFI1238	Wild-type, isolated from Atlantic cod	[36]
Δ*litR*	LFI1238 containing an in-frame deletion in *litR*	[27]
Δ*rpoQ*	LFI1238 containing an in-frame deletion in *rpoQ*	[33]
Δ*rpoQ-sypQ*$^-$	Δ*rpoQ* stain with an insertional disruption in *sypQ*, Cm^r	This study
Δ*rpoQ-sypP*$^-$	Δ*rpoQ* stain with an insertional disruption in *sypP*, Cm^r	This study
Δ*rpoQ-sypC*$^-$	Δ*rpoQ* stain with an insertional disruption in *sypC*, Cm^r	This study
LFI1238-*sypQ*$^-$	LFI1238 containing an insertional disruption in *sypQ*, Cm^r	This study
LFI1238-*sypP*$^-$	LFI1238 containing an insertional disruption in *sypP*, Cm^r	This study
LFI1238-*sypC*$^-$	LFI1238 containing an insertional disruption in *sypC*, Cm^r	This study
LFI1238- pVSV102	*A. salmonicida* LFI1238 carrying pVSV102, Kn^r	[33]
Δ*rpoQ*-pVSV102	Δ*rpoQ* carrying pVSV102, Kn^r	[33]
Δ*rpoQ-sypQ*$^-$-pVSV102	Δ*rpoQ-sypQ*$^-$ carrying pVSV102, Kn^r	This study
Δ*rpoQ-sypP*$^-$-pVSV102	Δ*rpoQ-sypP*$^-$ carrying pVSV102, Kn^r	This study
Δ*rpoQ-sypC*$^-$-pVSV102	Δ*rpoQ-sypC*$^-$ carrying pVSV102, Kn^r	This study
LFI1238-*sypQ*$^-$-pVSV102	LFI1238-*sypQ*$^-$ carrying pVSV102, Kn^r	This study
LFI1238-*sypP*$^-$-pVSV102	LFI1238-*sypP*$^-$ carrying pVSV102, Kn^r	This study
LFI1238-*sypC*$^-$-pVSV102	LFI1238-*sypC*$^-$ carrying pVSV102, Kn^r	This study
E. coli		
C118λpir	Helper strain containing pEVS104	[37]
DH5αλpir	*E. coli* strain containing GFP plasmid pVSV102	[37]
Plasmids		
pNQ705-*sypQ*$^-$	pNQ705 containing an internal fragment of *sypQ*$^-$	[19]
pNQ705-*sypP*$^-$	pNQ705 containing an internal fragment of *sypP*$^-$	[19]
pNQ*705-sypC*$^-$	pNQ705 containing an internal fragment of *sypC*$^-$	[19]
pVSV102	pES213, constitutive GFP, Kn^r	[37]
pEVS104	R6Korigin, RP4, *oriT, trb tra* and Kn^r	[64]

colony in 2 ml LB2.5 medium at 12°C and 220 rpm for 2 days. The 2 days culture was diluted 1:20 and grown overnight before being diluted to $OD_{600} = 0.05$ (optical density measured at 600 nm) in a total volume of 70 ml SWT media supplemented with 2.5% sea salt. The cultures were grown further at 8°C and 220 rpm in 250 ml baffled flask. Samples (10 ml) at low cell density $OD_{600} = 0.30$ and (2.5 ml) at high cell density $OD_{600} = 1.20$ were harvested (13,000 x g, 2 min, 4°C) (Heraeus 3XR, Thermo Scientific). Samples were persevered in 5th of their volume in RNA-*later* and stored at −80°C until RNA extraction.

Total RNA isolation and rRNA depletion

The total RNA was extracted from the cell pellets following the standard protocols by manufactures (Masterpure DNA & RNA purification kit, Epicenter). The quality of total RNA was determined using a Bioanalyzer and Total RNA nano chip (Agilent Technologies). The ribosomal rRNA was removed from the samples using Ribo-Zero rRNA Removal kit for bacteria (Illumina) following manufactures instructions. The quality of RNA after depletion was determined using Bioanalyzer and Total RNA pico chip (Agilent Technologies).

RNA sequencing and data analysis

The rRNA depleted samples were used to generate RNA-sequencing libraries using TruSeq strandard mRNA library prep kit (Illumina), and sequenced at the Norwegian Sequencing Center using the Illumina NextSeq 500 with mid output reagents with 75 bp read length and paired end reads.

The sequencing quality of FASTQ files was assessed using FastQC. Further analysis of the RNA-Seq data was performed using a Galaxy pipeline consisting of EDGE-pro v1.0.1 [34] and DESeq2 [35]. EDGE-pro was used to align the reads to the *A. salmonicida* LFI1238 genome [36], and to estimate gene expression. Differences in gene expression between the reference genome of *A. salmonicida* wild-type and *ΔlitR* and *ΔrpoQ* mutants were determined using DESeq2. Log2 fold changes of the genes were recalculated to × differential expression values (i.e., Δ*litR*/wt) and genes were defined as significantly differentially expressed genes (DEGs) based on a *p*-value ≤0.05 and differentially expression values (fold change values) of ≥2 × and ≤ −2 × equal to $\log_2$ fold ≥1 and ≤ −1. tRNA and rRNA reads was filtered out before analysis.

The sequences from this study have been deposited in the European Nucleotide Archive (www.ebi.ac.uk/ena) under study accession number PRJEB28385.

Construction of *A. salmonicida* LFI1238 and Δ*rpoQ* double mutants

A. salmonicida harboring in-frame deletion in the *rpoQ* genes (*ΔrpoQ*) is described in our recent study [33]. The pNQ705-*sypQ*⁻, pNQ705-*sypP*⁻ and pNQ705-*sypC*⁻ plasmids used to construct the mutants were described previously [19]. The LFI1238 and *ΔrpoQ* double mutants (Table 1) were constructed by transferring the pNQ705 plasmids carrying the targeted genes (*sypQ, sypP* and *sypC*) to LFI1238 wild-type or the *ΔrpoQ* mutant by bacterial conjugation. The conjugation of *E. coli* S17λpir harboring different pNQ705 suicide constructs to recipient cells was done as described by others [19]. The resulting mutant strains were named LFI1238-*sypQ*⁻, LFI1238-*sypP*⁻, LFI1238-*sypC*⁻, *ΔrpoQ-sypQ*⁻, *ΔrpoQ-sypP*⁻ and *ΔrpoQ-sypC*⁻.

Construction of GFP tagged *A. salmonicida* strains

The transfer of green fluorescence protein (GFP) into *A. salmonicida* was performed by tri-parental mating as described by others [37]. Briefly, the pVSV102 plasmid carrying the gene encoding for GFP and kanamycin was transferred from *E. coli* DH5α to the mutant strains (LFI1238-*sypQ*⁻, LFI1238-*sypP*⁻, LFI1238-*sypC*⁻, *ΔrpoQ-sypQ*⁻, *ΔrpoQ-sypP*⁻ and *ΔrpoQ-sypC*⁻) using the conjugative helper strain CC118λpir harboring pEVS104. Donor and helper cells were grown to mid-log phase (OD_{600} = 0.7) in LB1. Recipient strains (*A. salmonicida*) were grown to early stationary phase ($OD_{600} = 1.2$) in LB2.5. The donor, helper and recipient were harvested (13,000 x g, 1 min) and washed twice with LB1 before they were mixed in 1 to 1 ratio and spotted onto BA2.5 plates, followed by overnight incubation at 16°C. The spotted cells were re-suspended in LB2.5 and incubated for 24 h at 12°C with agitation (220 rpm). The potential tagged strains were selected on BA2.5 after 5 days. The tagged strains were confirmed microscopically with Nikon Eclipse TS100.

Static biofilm assay

The biofilm assay was performed as described previously [19]. The overnight secondary cultures were grown to an OD_{600} of 1.3 in LB2.5. The secondary cultures were further diluted 1:10 in SWT and a total volume of 300 μl was added to each well in flat-bottom, non-tissue culture-treated Falcon 24-well plates (BD, Bioscience). The plates were incubated statically at 8°C, for 72 h and the biofilm was visualized using Nikon Eclipse TS100 microscope at 10x magnification and photographed with Nikon DS-5Mc.

Colony morphology assay

The colony morphology assay was performed as described previously [19, 33]. The overnight secondary cultures were grown to an OD_{600} of 1.2 in LB2.5. From each secondary overnight culture, a 250 μl was harvested by centrifugation, and the pellet was re-suspended in 250 μl SWT. Then, 2 μl of each culture was spotted onto SWT agar plates, and incubated at 8°C for 12 days. The colonies were viewed microscopically with Zeiss Primo

Vert and photographed with AxioCam ERc5s at 4x magnification.

Results

Expression profiling of the *A. salmonicida* transcriptome

The total assembled transcriptome of *A. salmonicida* wild-type LFI1238 generated an average of 9.87 million reads at LCD ($OD_{600} = 0.3$) and 9.56 million at HCD ($OD_{600} = 1.2$). The average of mapped reads to the reference genome (*A. salmonicida* LFI1238) was 88.7% at LCD and 91.4% at HCD, with an average mapping coverage of 140.6 and 141.0 respectively, indicating that the transcriptome data were sufficient for further analysis (Additional file 1: Table S1). The detailed transcriptome data of *ΔlitR* and *ΔrpoQ* are listed in Table S1 in the supplementary material (Additional file 1: Table S1).

Cell density alters the expression pattern in *A. salmonicida* wild-type

We identified one thousand and thirteen genes to be differentially expressed in a cell density dependent manner. The majority of DEGs (70%) came from chromosome I, where the essential genes are located. The comparison (wt1.2/wt0.3) list of all DEGs are given in Table S2 in the supplementary material (Additional file 2: Table S2).

The comparison revealed that 597 (58.8%) and 416 (41.0%) of 1013 genes were significantly up- and down-regulated, respectively. The 1013 DEGs were classified into different functional groups according to MultiFun [38]. Figure 1 shows a graphical presentation of the functional classes and the number of the differentially expressed genes of wild-type at HCD relative to LCD (wt1.2/wt0.3). A large number of significantly upregulated genes fell into *cell envelop* ($n = 97$, 16.2%) where the genes with highest fold change values were *VSAL_II0321* (28.25 fold-change) and *VSAL_II0322* (28.74 fold-change) encoding for putative glycosyl transferase and membrane protein, respectively. Genes with *unknown function* were next largest functional group ($n = 94$, 15.7%). Within this group, the highest fold change was observed in a number of genes coding for transposases. Among these were *VSAL_II0030* (1975.26-fold change), *VSAL_I0514* (529.36-fold--change), *VSAL_I1911* (237.06-fold change) and *VSAL_1339* (129.70-fold change). Additionally a high fold change was also observed among genes coding for arginine/ornithine periplasmic binding protein (*VASL_I1958*, 32.83-fold change) and L-amino acid binding periplasmic protein (*VSAL_I2057*, 51.77-fold change) that fell into *transport/binding proteins* functional group ($n = 73$, 12.2%).

The comparison of wild-type transcriptome at HCD relative to LCD revealed an upregulation among genes known to be associated with AHL production. The *luxI* autoinducer synthase (*VSAL_II0957*) responsible for the production of seven AHLs and its receptor *luxR1*

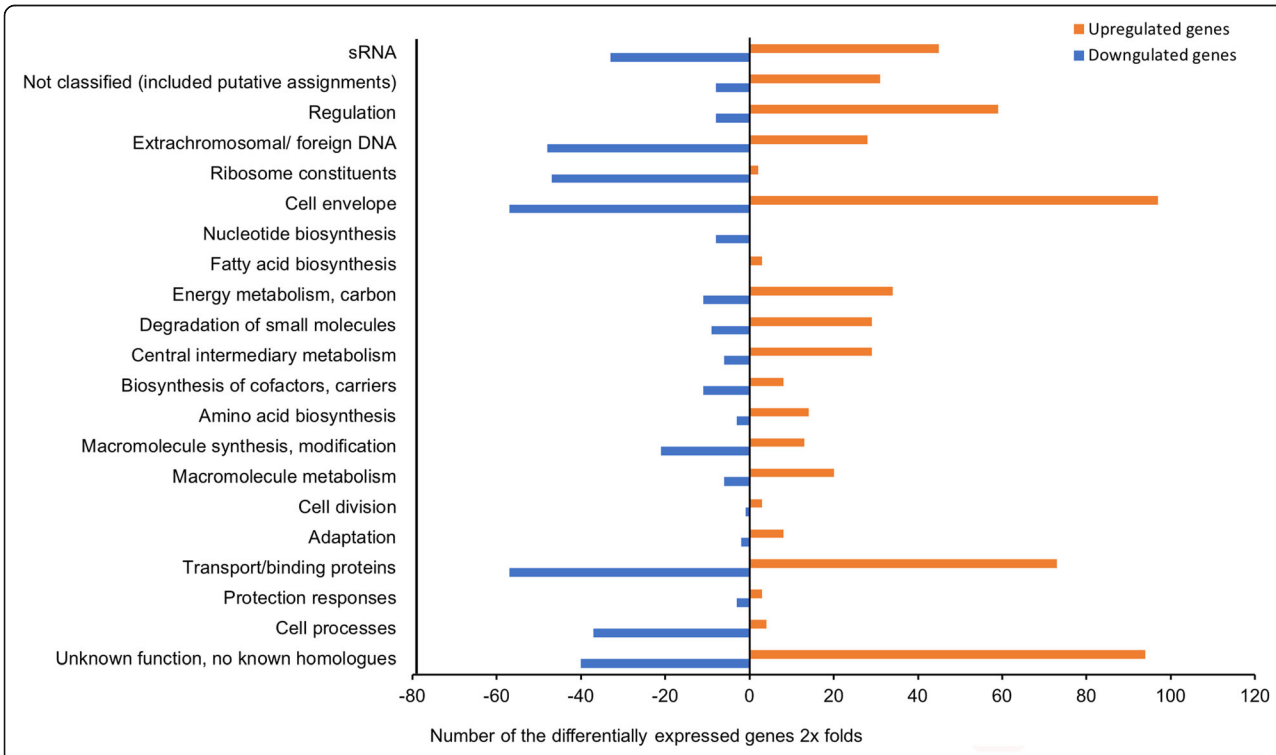

Fig. 1 Functional distribution of genes between *A. salmonicida* wild-type at HCD compared to LCD that are ≥2 × differentially expressed

(*VSAL_II0965*) [9], were significantly differensially expressed with a fold change values of 3.72 and 3.23, respectively.

Fifty-nine (9.8%) genes were classified into *regulation* functions, where we were able to identify the *rpoQ* sigma factor (*VSAL_II0319*) and 4 other genes from the same locus coding for putative response regulators (*VSAL_II0315*, *VSAL_II0316*, *VSAL_II0320*, *VSAL_II0329*). An additional 14 genes located close to *rpoQ* or within the same operon were also highly upregulated in the wt1.2 compared to wt0.3 and fell into other functional groups such as *cell envelope*, *extrachromosomal DNA* and *central intermediary metabolism*, in addition to some hypothetical proteins with unknown or unclassified functions. *litR*, a transcription regulator of QS (*VSAL_I2619*), was also within the 59 upregulated genes involved in regulation with a fold change of 3.43.

Even though the *fatty acid and amino acid group* showed only 3 upregulated genes, these genes exhibited high fold change values. *VSAL_I2833* coding for acetyl-coenzyme A synthetase was among the highest with 290.53-fold change value. Other highly expressed genes were grouped in *central metabolism* such as *VSAL_I2438* (57.86-fold change) and *VSAL_I2439* (61.58-fold change) coding for isocitrate lyase and malate synthase A, respectively. Among the genes that fell into a group with *not classified functions* were genes coding for putative PrkA serine protein kinase (*VSAL_I2208*, 56.64-fold change), putative anti-sigma F factor antagonist (*VSAL_II0328*, 47.87-fold change), and putative nucleotidyltransferases (*VSAL_ 2831*, 38.11-fold change) (Fig. 1 and Additional file 2: Table S2). The remaining upregulated DEGs were grouped in other functional groups (Fig. 1 and Additional file 3: Table S3).

The majority of the downregulated genes fell into *cell envelope* and *transport/ binding proteins* with 57 significantly DEGs. Among the top 5 downregulated genes within *transport/binding protein* functional group were genes of the PTS system (*VSAL_II0577*, *VSAL_II0894*, *VSAL_II0995* and *VSAL_II0966*) with fold changes ranging from −44.43 to −8.34 (Additional file 3: Table S3).

Six genes (*VSAL_II0366*, *VSLA_II0367*, *VSAL_II0368*, *VSAL_II0369*, *VSAL_II0370* and *VSAL_II0373*) located within the tight adherence (Tad) loci also known as *tad* operon were grouped in *cell envelop* and *extrachromosomal DNA* (subgroup *pathogenicity island-related functions*) functional groups. For all 6 genes the expression level ranging from −8.44 to −2.03 fold change at HCD (wt1.2) in comparison with that at LCD (wt0.3).

Thirty-six genes out of 37 genes that fell into *cell processes* were genes involved in cell motility and chemotaxis. Figure 2 shows the organization of the flagellar genes in the *A. salmonicida* genome, and Table 2 summarizes in detail the differentially expressed genes and operons. We were able to identify 28 genes coding for flagellar

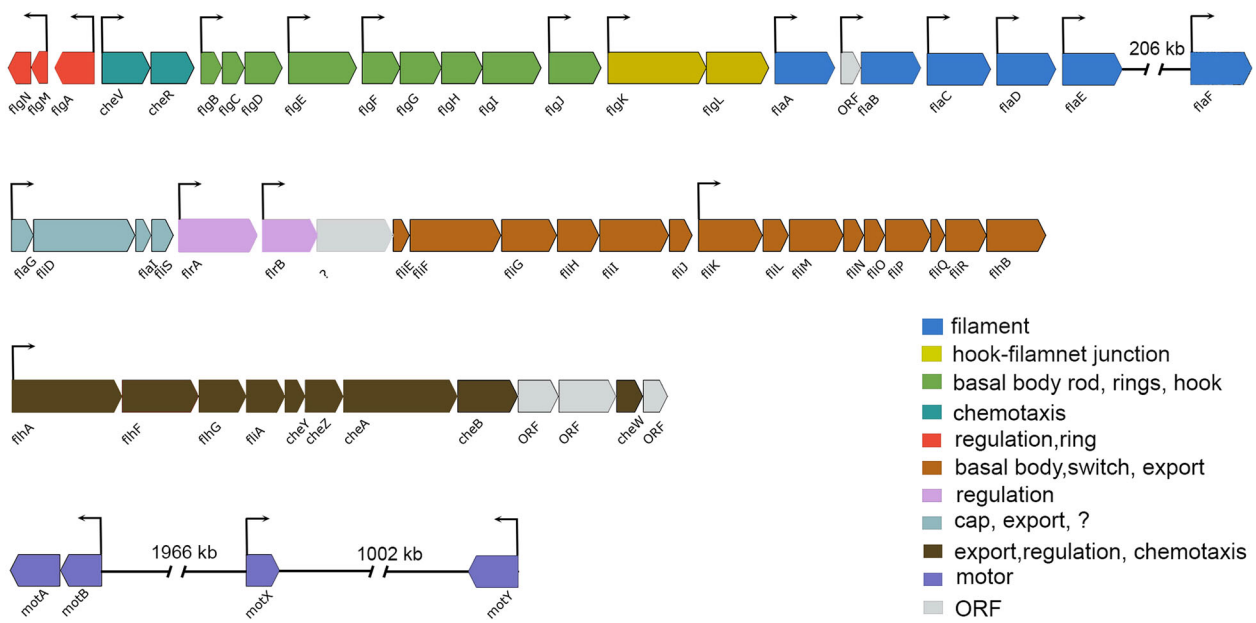

Fig. 2 Organization of flagellar genes in *A. salmonicida* LFI1238. Arrows indicate genes and their direction of transcription. Color code provided in the image represents the different functions of each group in the flagellar apparatus. All *A. salmonicida* flagellar related genes are located on the large chromosome (first chromosome) and are organized in five chromosomal regions with clusters of flagellar genes. The six flagellin genes are located at two separated chromosomal loci. *flaABCDE* genes are found in one locus and *flaF* in a different locus. Genes encoding the flagellar motor components (*motABXY*) are located at three additional loci. Additional chemotaxis genes are scattered throughout the genome. 206 kb, 1966 kb and 1002 kb are distances between genes

Table 2 Thirty-six differentially expressed genes involved in motility and chemotaxis in wt1.2/wt0.3

VSAL_ID	FC	p-adjusted	Gene	Function
VSAL_I0799	−2.55	3.1217E-13		methyl-accepting chemotaxis protein
VSAL_I1822	−2.42	9.1448E-06		methyl-accepting chemotaxis protein
VSAL_I1863	−2.15	1.9114E-07	*motY*	sodium-type flagellar protein MotY precursor
VSAL_I2117	−2.26	4.7375E-06		methyl-accepting chemotaxis protein
VSAL_I2193	−2.96	1.4728E-16		methyl-accepting chemotaxis protein
VSAL_I2293	−2.18	9.8803E-11	*flhA*	polar flagellar assembly protein FlhA
VSAL_I2295	−2.23	1.0662E-10	*flhB*	polar flagellar assembly protein FlhB
VSAL_I2298	−2.17	2.498E-07	*flip*	polar flagellar assembly protein FliP
VSAL_I2299	−2.18	9.0124E-10	*fliO*	polar flagellar assembly protein FliO
VSAL_I2300	−2.11	3.8699E-09	*fliN*	polar flagellar switch protein FliN
VSAL_I2301	−2.02	2.1524E-08	*fliM*	polar flagellar motor switch protein FliM
VSAL_I2302	−2.27	1.8061E-10	*fliL*	polar flagellar protein FliL
VSAL_I2303	−2.05	9.5905E-09	*fliK*	polar flagellar hook-length control protein FliK
VSAL_I2304	−2.15	1.6591E-06	*fliJ*	polar flagellar assembly protein FliJ
VSAL_I2305	−2.12	2.5798E-07	*fliI*	polar flagellum-specific ATP synthase FliI
VSAL_I2306	−2.66	2.9148E-17	*fliH*	polar flagellar assembly protein FliH
VSAL_I2307	−2.61	5.6929E-15	*fliG*	polar flagellar motor switch protein FliG
VSAL_I2308	−2.73	7.0985E-17	*fliF*	polar flagellar M-ring protein FliF (pseudogene)
VSAL_I2309	−2.63	7.3748E-15	*fliE*	flagellar hook-basal body complex protein FliE
VSAL_I2313	−2.13	4.8203E-13	*fliS*	polar flagellar protein FliS
VSAL_I2314	−2.09	3.7432E-07	*flaI*	polar flagellar protein FlaI
VSAL_I2316	−2.06	3.2548E-06	*flaG*	polar flagellar protein FlaG (pseudogene)
VSAL_I2319	−2.68	1.6171E-16	*flaC*	flagellin subunit C
VSAL_I2327	−2.20	1.314E-05	*flaA*	flagellin subunit A
VSAL_I2328	−2.21	1.353E-08	*flgL*	flagellar hook-associated protein type 3 FlgL
VSAL_I2329	−2.33	3.2437E-10	*flgK*	hypothetical protein
VSAL_I2330	−2.14	5.0777E-09	*flgJ*	peptidoglycan hydrolase FlgJ
VSAL_I2335	−2.02	1.3131E-05	*flgE*	flagellar hook protein FlgE
VSAL_I2336	−2.13	1.3871E-10	*flgD*	flagellar basal-body rod protein FlgD
VSAL_I2337	−2.20	1.5834E-09	*flgC*	flagellar basal-body rod protein FlgC
VSAL_I2338	−2.29	8.8397E-09	*flgB*	flagellar basal-body rod protein FlgB
VSAL_I2517	−2.51	3.4203E-14	*flaF*	flagellin subunit F
VSAL_I2897	−2.40	6.0326E-09	*fliL*	putative flagellar basal body-associated protein FliL
VSAL_II0675	−2.38	0.00023876		methyl-accepting chemotaxis protein
VSAL_II0712	−3.87	8.4405E-30		methyl-accepting chemotaxis citrate transducer
VSAL_II1022	−2.60	8.1567E-05		methyl-accepting chemotaxis protein

components (flagellin, flagellar basal body rod, rings, hook, cap proteins and flagellar assembly proteins), 7 genes coding for methyl-accepting chemotaxis protein and one gene coding for motor component, *motY.*

The global comparison analysis of *A. salmonicida* wild-type at HCD compared to LCD resulted in an equal distribution of genes to be upregulated and downregulated. Additionally, the differentially expressed genes were distributed in all 21 functional classes (Fig. 1).

Expression profiles of *A. salmonicida* Δ*rpoQ* and Δ*litR* mutants compared to the wild-type at low and high cell densities

Expression profiling of A. salmonicida ΔlitR mutant

As shown in Fig. 3, the transcriptome of *ΔlitR* compared to the wild-type (*ΔlitR* /wt) resulted in a total of 62 DEGs at LCD, where half ($n = 31$, 50.0%) was upregulated and the other half ($n = 31$, 50.0%) was downregulated (Additional file 4: Table S4). At HCD we identified

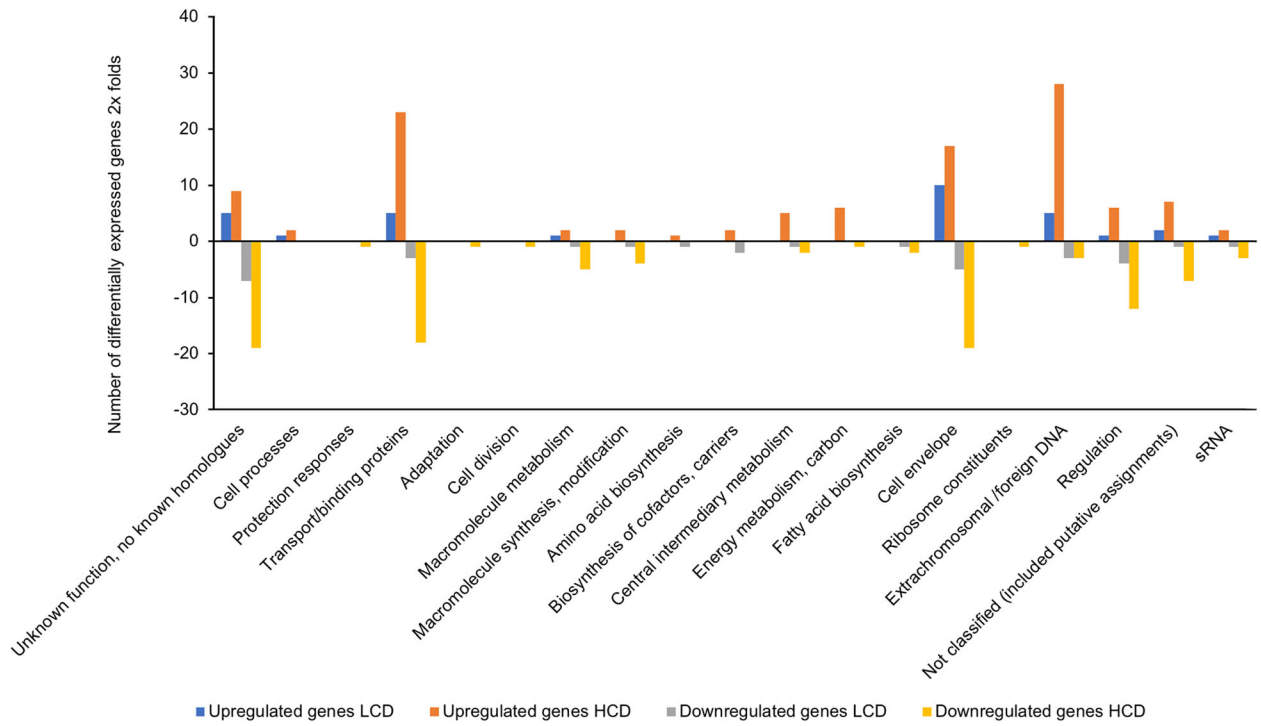

Fig. 3 Functional distribution of genes between *A. salmonicida* wild-type and Δ*litR* mutant at LCD and HCD that are ≥2 × differentially expressed

a total of 212 DEGs, 112 (53.9%) upregulated and 100 (46.0%) downregulated (Additional file 5: Table S5). The highest number of upregulated genes at LCD was represented in *cell envelope* with 10 genes (32.2%), where 4 of them were genes associated with *tad* operon. Five genes (16.1%) fell into each of *extrachromosomal/foreign DNA*, *transport/binding proteins* and genes of *unknown functions*. Other upregulated genes were involved in *transport/binding proteins*, *cell processes* mainly motility and chemotaxis, *macromolecule metabolism*, *regulation* and small RNA (*sRNA*) (Additional file 6: Table S6). The highest number of downregulated genes fell into three major groups, *unknown function* ($n = 7$, 22.5%), *cell envelope* ($n = 5$, 16.1%), and *transport/binding proteins* ($n = 3$, 9.6%). Four genes fell into the *regulation* functional group ($n = 4$, 12.9%), where the *rpoQ* sigma factor (*VSAL_II0319*) was among the significantly downregulated genes with −4.2 fold change value. The remaining downregulated genes were distributed in the other functional groups (Additional file 6: Table S6 and Fig. 3).

The 212 DEGs at HCD were distributed in 19 out of 21 functional classes (Fig. 3). The upregulated genes fell into 14 functional groups with highest number of genes in *extrachromosomal/foreign DNA*, *transport/binding proteins* and *cell envelope* groups with 28 (25%), 23 (20.5%) and 17 (15.1%) genes respectively. The downregulated genes were distributed in fewer functional groups with highest number of genes in *cell envelope* ($n = 19$), *unknown functions* ($n = 19$), *transport/ binding proteins* ($n = 18$), and *regulation* ($n = 12$). Other downregulated genes fell into other functional categories and range from 1 to 7 genes out of 100 downregulated genes (Additional file 6: Table S7).

In summary, the transcriptome of *ΔlitR* relative to the wild-type exhibited an equal gene distribution between upregulated and downregulated genes which suggests that LitR may act both as a positive and negative regulator in *A. salmonicida.*

Expression profiling of A. salmonicida ΔrpoQ mutant

Figure 4, represents the transcriptome of *ΔrpoQ* relative to the wild-type (*ΔrpoQ*/wt) at LCD and HCD. The LCD transcrimtome resulted in a total of 84 DEGs, where 43 (51.2%) were upregulated and 41 (48.8%) were downregulated (Additional file 7: Table S8). At HCD we identified in total 300 DEGs, 206 (68.6%) upregulated and 94 (31.3%) downregulated (Additional file 8: Table S9). The 84 DEGs at LCD were distributed into 8 functional groups (Fig. 4). Among the 43 upregulated genes (LCD), 18 genes (41.8%) were grouped within the *cell envelope* group, where *VSAL_II0252* annotated as hypothetical protein was among the genes with high fold change value (16.1-fold change). Nine genes (20.9%) fell into each of *unknown functions* and *extrachromosomal/foreign DNA*. Three genes (6.9%) were allocated to *regulation* and one gene (*VSAL_II0170*) codes for

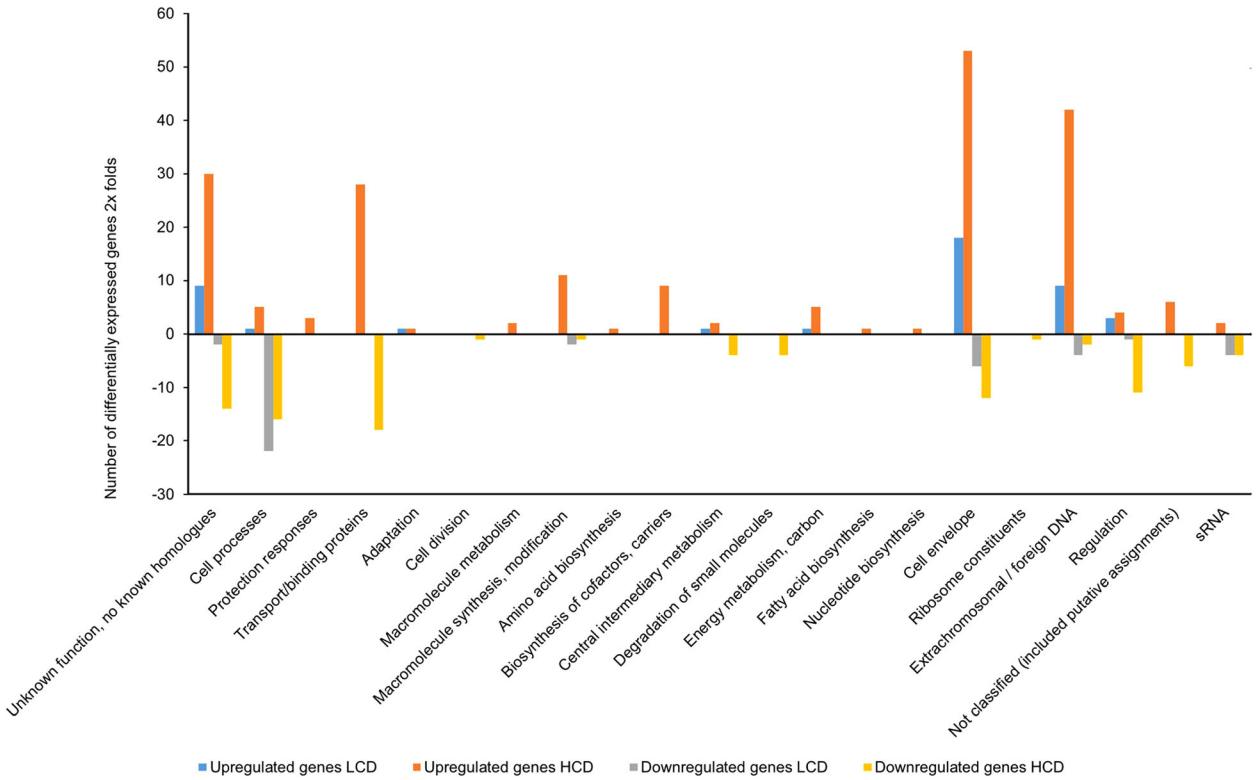

Fig. 4 Functional distribution of genes between *A. salmonicida* wild-type and Δ*rpoQ* mutant at LCD and HCD that are ≥2 × differentially expressed

methyl-accepting chemotaxis protein was grouped in *cell processes* (Additional file 9: Table S10). The 41 downregulated genes were distributed in 7 functional groups with highest number of genes within *cell processes* ($n = 22$, 53.6%). Other downregulated genes fell into *cell envelope* ($n = 6$, 14.6%), *sRNA* and *extrachromosomal/foreign DNA* with 4 genes (9.7%) in each group and *unknown functions* with 2 hypothetical genes *VSAL_I2061* and *VSAL_II1023*.

Figure 4 shows the 300 DEGs at HCD and their distribution among the 21 functional groups. Among the 206 (68.8%) upregulated genes, 53 (25.7%) genes were involved in *cell envelope*, 42 (20%) in *extrachromosomal/foreign DNA* and 30 (14.5%) *hypothetical genes* with unknown functions (Additional file 9: Table S11). The remaining upregulated genes were distributed among other functional groups with a percentage ranging from 13.5 to 0.4% (Additional file 9: Table S11). The 94 downregulated genes at HCD were mostly represented in *transport/binding proteins* ($n = 18$, 19%), *cell processes* ($n = 16$, 17%), *hypothetical proteins* with unknown functions ($n = 14$, 14.8%), *cell envelope* ($n = 12$, 12.7%) and genes involved in *regulation* ($n = 11$, 11.7%). The remaining genes fell into other functional categories and ranging from 1 to 6 genes out of 94 downregulated genes (Additional file 9: Table S11).

The transcriptome of *ΔrpoQ* compared to the wild-type, showed more upregulated genes (68.8%), than downregulated (31.2%) at HCD, which indicates that RpoQ acts more as a negative regulator in *A. salmonicida* at high cell density.

Deletion of *litR* and *rpoQ* impacts operons related to quorum sensing

A large number of genes that fell in the *cell processes* functional group in both *ΔlitR* and *ΔrpoQ* were genes involved in the signaling cascade of bacterial chemotaxis and flagellar biosynthesis. Transcriptional analysis of *ΔrpoQ* compared to the wild-type revealed 29 genes that were considerably downregulated at both low and high cell densities. Among the genes that had the greatest transcript abundance at LCD was the gene encoding flagellin A protein, *flaA* (−61.99-fold change). Other flagellin genes were either expressed with lower fold change values such as *flaB* (−2.05-fold change), *flaC* (−6.29-fold change) and *flaE* (−2.70-fold change) or filtered out due to the predetermined criteria for identifying DEGs (fold change value ≥2 and ≤ −2, p-value ≤0.05) such as, *flaD* (−1.98-fold change) and *flaF* (−1.8-fold change). In addition to the genes coding for flagellin proteins, genes coding for flagellar basal body rod, ring, hook and cap proteins (*fliD*, *flaG*, *flgB-flgL*) showed also reduced level

of expression compared to control (wild-type) (Additional file 7: Table S8). Likewise, at HCD 12 out of 16 downregulated genes grouped in *cell processes* were flagellar genes. In particular, the expression of *flaA* was highly decreased with a fold change value of −17.36. The remaining flagellin genes were expressed at a lower level as *flaC* (−2.04-fold change), while others such as *flaB* (−1.4-fold change), *flaD* (−1.4-fold change), *flaE* (−1.6-fold change) and *flaF* (1.17- fold change), were filtered out due to a fold change values below ≤2 and ≥ −2. Genes encoding flagellar basal body rod, ring and hook proteins (from *flgB* to *flgL*) were also downregulated with fold change values ranging from −3.53 to −11.69. In addition to the flagellar genes, 4 genes encoding methyl-accepting chemotaxis proteins were also downregulated such as *VSAL_I2193*, *VSAL_I0799* at LCD, *VSAL_I0712* at HCD and *VSAL_II1022* at both low and high cell densities (Additional file 8: Table S9).

In contrast to *ΔrpoQ* transcriptome (*ΔrpoQ*/wt), the *ΔlitR* transcription profiling (*ΔlitR*/wt) exhibited an increased level of expression among genes involved in cell motility and chemotaxis. One gene, *VSAL_I2117,* encoding methyl-chemotaxis accepting proteins was upregulated with fold change values of 3.84 and 3.46 at low and high cell densities, respectively. Only one flagellin gene, *flaC* gene (*VSAL_I2317*) was found to be upregulated with a fold change of 2.64 at HCD (Additional file 5: Table S5).

The second most highly expressed group of genes are those associated with the *tad* operon. The *tad* operon in *A. salmonicida* consists of 13 genes (*VSAL_II0366* to *VSAL_II0378*) and is located on the second chromosome, that harbours accessory genes [36] (Fig. 5).

The transcriptome of *ΔrpoQ* (*ΔrpoQ*/wt) at LCD showed that all 13 *tad* genes were highly upregulated (Table 3). Nine *tad* genes (*VSAL_II0369*, *VSAL_II0371*, *VSAL_II0372*, *VSAL_II0373*, *VSAL_II0374*, *VSAL_II375*, *VSAL_II0376*, *VSAL_II0377* and *VSAL_II0378*) were classified as *pathogenicity island-related* factors. The other 5 *tad* genes (*VSAL_II0366*, *VSAL_II0367* and *VSAL_II0368*) fell into *surface structures* group coding for Flp-type pilus protein. At HCD 8 out of 13 genes exhibiting an increased level of expression based on our criteria (fold change value ≥2 and ≤ −2, *p*-value ≤0.05). Four *tad* genes were classified within *pathogenicity island-related* functions (*VSAL_II0369*, *VSAL_II0371*, *VSAL_II0372* and *VSAL_II0373*), other 4 were divided into *surface structures* (*VSAL_II0366*, *VSAL_II0367*, *VSAL_II0368*) and *membrane exported lipoproteins* (*VSAL_II0370*). All 8 *tad* DEGs ranged from 11.09 to 5.6-fold change (Table 3).

In comparison to *ΔrpoQ*, the *ΔlitR* transcriptome relative to the wild-type revealed fewer *tad* genes to be differentially expressed in our analysis. An equal number of differentially expressed genes was present in both LCD and HCD with approximately similar fold change values (Table 3).

Exopolysaccharide genes are highly expressed in the Δ*litR* and Δ*rpoQ* mutants

The inactivation of either *rpoQ* or *litR* in *A. salmonicida* resulted in strains with enhanced extracellular polysaccharide production, which is involved in biofilm formation and wrinkled colony morphology [19, 33] . The biosynthesis of EPS in *A. salmonicida* likely requires the expression of *syp* operon (22,453 bp) located on the second chromosome [36]. The *syp* operon consists of 18

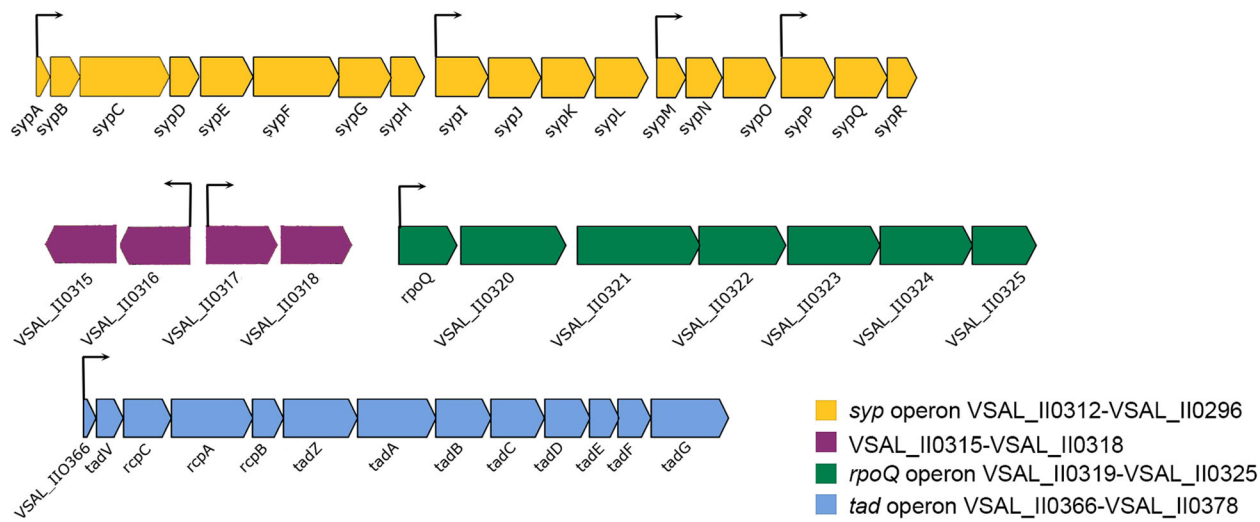

Fig. 5 Organization of *syp* genes, *rpoQ* genes and *tad* genes in *A. salmonicida* LFI1238. Arrows indicate genes and their direction of transcription. Color code represents the different operons and their start-end *VSAL* number

Table 3 Genes of the *tad* operon of Δ*litR*/wt and Δ*rpoQ*/wt at low and high cell densities

VSAL_ID	LCD		HCD		Gene	Function
	FC	p-adjusted	FC	p-adjusted		
Δ*rpoQ*/wt						
VSAL_II0366	**25.55**	1.58E-95	**11.88**	1.16E-09		fimbrial protein, Flp/Fap pilin component
VSAL_II0367	**24.82**	7.13E-119	**10.45**	8.51E-10	*tadV*	type IV leader peptidase
VSAL_II0368	**14.23**	1.86E-123	**6.78**	3.37E-14	*rcpC*	putative Flp pilus assembly protein
VSAL_II0369	**10.94**	5.17E-98	**7.24**	4.39E-16	*rcpA*	type II/III secretion system protein
VSAL_II0370	**14.26**	3.98E-113	**7.42**	5.14E-10	*rcpB*	putative lipoprotein
VSAL_II0371	**13.54**	2.15E-108	**6.16**	NA	*tadZ*	type II secretion system protein Z
VSAL_II0372	**12.73**	6.04E-118	**5.63**	1.76E-07	*tadA*	type II/IV secretion system protein, ATP binding domain
VSAL_II0373	**10.33**	1.16E-86	**6.99**	4.54E-16	*tadB*	bacterial type II secretion system protein F
VSAL_II0374	**4.65**	9.46E-64	1.49	5.18E-01	*tadC*	bacterial type II secretion system protein F
VSAL_II0375	**2.94**	1.16E-29	1.18	7.92E-01	*tadD*	putative secretion system protein
VSAL_II0376	**3.17**	1.38E-31	1.16	8.00E-01	*tadE*	membrane associated secretion system protein
VSAL_II0377	**3.11**	9.37E-30	1.06	9.18E-01	*tadF*	membrane associated secretion system protein
VSAL_II0378	**3.04**	1.68E-30	1.11	8.50E-01	*tadG*	membrane associated secretion system protein
Δ*litR*/wt						
VSAL_II0366	**12.23**	7.54E-75	**10.24**	2.94E-13		fimbrial protein, Flp/Fap pilin component
VSAL_II0367	**8.59**	3.94E-59	**6.44**	1.20E-12	*tadV*	type IV leader peptidase
VSAL_II0368	**4.30**	1.07E-38	**2.42**	NA	*rcpC*	putative Flp pilus assembly protein
VSAL_II0369	**3.45**	4.58E-30	**3.10**	6.14E-05	*rcpA*	type II/III secretion system protein
VSAL_II0370	**4.67**	1.77E-37	**2.74**	0.009798979	*rcpB*	putative lipoprotein
VSAL_II0371	**3.73**	1.31E-24	**2.38**	0.004220895	*tadZ*	type II secretion system protein Z
VSAL_II0372	**3.67**	2.53E-27	**2.43**	0.000108788	*tadA*	type II/IV secretion system protein, ATP binding domain
VSAL_II0373	**2.49**	1.89E-11	**2.53**	NA	*tadB*	bacterial type II secretion system protein F
VSAL_II0374	1.88	7.21E-09	1.06	0.926675356	*tadC*	bacterial type II secretion system protein F
VSAL_II0375	1.32	0.031001079	1.29	0.372370396	*tadD*	putative secretion system protein
VSAL_II0376	1.45	0.001283239	1.29	0.376863481	*tadE*	membrane associated secretion system protein
VSAL_II0377	1.53	0.000365049	1.35	0.33429395	*tadF*	membrane associated secretion system protein
VSAL_II0378	1.35	0.006750764	1.35	0.304804669	*tadG*	membrane associated secretion system protein

Values indicated in bold are differentially expressed genes with fold change values (FC) that are ≥2 and ≤ −2, *p*-value ≤0.05

genes (*VSAL_II0295* to *VSAL_II0312*) organized into four transcription units (Fig. 5).

The transcriptome of *ΔrpoQ* compared to the wild-type, showed that 13 *syp* genes were upregulated at HCD, whereas at LCD only *sypB* (*VSAL_II0311*) was differentially expressed with a fold change value of 2.03 (Table 4).

Next, we wanted to analyze the importance of *syp* genes in formation of colony rugosity and biofilm and for this 3 *syp* genes (*sypQ, sypP* and *sypC*) were separately inactivated in the wild-type LFI1238 and *ΔrpoQ* mutant by insertional inactivation. The constructed mutants were GFP tagged for better biofilm visualization. The inactivation of *sypQ, P* or *C* in *ΔrpoQ* resulted in strains similar to the wild-type strain with no biofilm formation and smooth colonies (Additional file 10: Figure S1). No difference was observed on biofilm formation or colony morphology after the inactivation of *syp* genes in *A. salmonicida* wild-type at the chosen conditions (Additional file 10: Figure S1).

The transcriptome of *ΔlitR* (*ΔlitR*/wt) did not show any significant upregulation of the *syp* genes, except for two genes; *sypA* (*VSAL_II0312*) and *sypC* (*VSAL_II0310*) encoding a putative anti-sigma factor and polysaccharide biosynthesis/export protein, respectively (Additional file 5: Table S5). Our results indicate that this operon is regulated in a cell density dependent manner, where RpoQ expression leads to a repression of large number of *syp* genes at HCD.

Comparative analysis of Δ*rpoQ* and Δ*litR* reveals genes regulated by QS

RpoQ and LitR were studied previously and shown to regulate phenotypes such as motility, adhesion, biofilm

Table 4 DEGs of *syp* locus at low and high cell densities in the Δ*rpoQ*/wt

VSAL_ID	LCD		HCD		Gene	Function
	FC	p-adjusted	FC	p-adjusted		
VSAL_II0295	1.22	0.74710921	**2.189**	0.07468146	*sypR*	sugar transferase
VSAL_II0296	1.07	0.89636775	**2.585**	0.00426114	*sypQ*	putative transmembrane glycosyl transferase
VSAL_II0297	1.10	0.84634234	**3.182**	0.0001044	*sypP*	putative glycosyl transferase
VSAL_II0298	−1.05	0.91873517	**2.462**	0.04236082	*sypO*	putative membrane protein
VSAL_II0299	1.14	0.81791828	**2.189**	0.11185209	*sypN*	putative glycosyl transferases
VSAL_II0300	1.43	0.17621734	**3.160**	0.00642603	*sypM*	hypothetical protein
VSAL_II0301	−1.25	0.56460157	1.778	0.44063722	*sypL*	O-antigen polymerase
VSAL_II0302	1.12	0.85566635	**2.713**	0.04069669	*sypK*	putative polysaccharide biosynthesis protein
VSAL_II0303	1.10	0.87199934	**2.928**	0.00991193	*sypJ*	putative glycosyl transferase
VSAL_II0304	1.23	0.60244622	**2.868**	0.00187435	*sypI*	putative glycosyl transferase
VSAL_II0305	−1.23	0.602336	1.035	0.96181635	*sypH*	putative glycosyl transferase
VSAL_II0306	−1.35	0.2022748	−1.647	0.06439411	*sypG*	two-component response regulator, transcriptional regulatory protein LuxO
VSAL_II0307	−1.17	0.69188251	−1.157	0.76925525	*sypF*	response regulator, histidine kinase
VSAL_II0308	1.25	0.4506543	1.021	0.97005546	*sypE*	putative response regulator
VSAL_II0309	1.20	0.73767376	**2.189**	0.08945561	*sypD*	putative capsular polysaccharide synthesis protein
VSAL_II0310	1.49	0.08145483	**3.811**	0.00016578	*sypC*	polysaccharide biosynthesis/export protein
VSAL_II0311	**2.03**	0.00119744	**4.377**	0.00012723	*sypB*	outer membrane protein, OmpA family
VSAL_II0312	1.94	0.01339391	**6.063**	5.41E-06	*sypA*	hypothetical protein, putative anti-sigma factor antagonist

Values indicated in bold are differentially expressed genes with fold change values (FC) that are ≥2 and ≤ −2, p-value ≤0.05

formation and colony morphology differently in *A. salmonicida* [19, 33]. To identify genes that are differentially expressed in *ΔrpoQ* relative to *ΔlitR,* we compared the RNA-Seq data for these mutants at low and high cell densities using DESeq. At LCD a differential expression analysis revealed 63 (53.3%) and 55 (46.6%) of the total 118 genes to be significantly up and downregulated respectively (Additional file 11: Table S12). Whereas at HCD the RNA-Seq revealed 107 genes where 55 (51.4%) were upregulated while 57 (53.2%) were downregulated. Figure 6 illustrates the number of DEGs that overlap between the *ΔrpoQ* and *ΔlitR* transcriptome where the majority of the differentially expressed genes at both cell densities came from chromosome I. At both low and high cell densities, genes associated with several phenotypes known to be related to QS were significantly

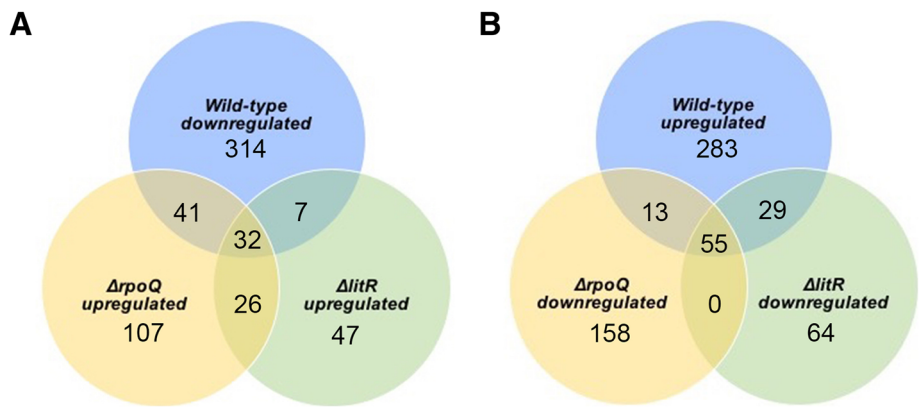

Fig. 6 Venn diagram of differentially expressed genes **a**) Venn diagram of upregulated genes in the Δ*litR* and Δ*rpoQ* mutants and downregulated genes in the wild-type at HCD. **b**) Venn diagram of downregulated genes in the Δ*litR* and Δ*rpoQ* mutants and upregulated genes in the wild-type at HCD. The sum of the numbers in each large circle represents total number of uniquely differentially expressed genes identified in each sample. The overlap part of the circles represents number of overlapping differentially expressed genes between combinations

expressed in the *ΔrpoQ* relative to *ΔlitR.* Among these were genes involved in motility and chemotaxis, genes associated with the *syp* operon such as (*VSAL_II0297*) encoding a putative glycosyl transferase, (*VSAL_II0300*) annotated as hypothetical protein, (*VASL_II0311*) coding for the outer membrane protein OmpA and (*VSAL_II0312*) coding for a putative anti-sigma factor, in addition to some genes associated with the *tad* operon (Additional file 11: Table S12 and Additional file 12: Table S13).

Discussion

Whole-transcriptome RNA sequencing analysis provides a powerful understanding of the gene expression patterns underlying the basic biology of the organism. In this work we studied the comparative transcriptome of *A. salmonicida* LFI1238, *ΔlitR* and *ΔrpoQ* mutants at low (OD_{600} = 0.3) and high (OD_{600} = 1.2) cell densities in SWT medium at 8°C. The SWT medium (2.5% salt concentration) and low temperature (8°C) were chosen as appropriated physiological conditions (similar to ocean environment) for *A. salmonicida* which is responsible for developing of cold-water vibriosis in Atlantic salmon at low seawater temperatures [39–41]. These conditions also favoured the development of several phenotypes (as motility, morphology and biofilm) related to QS in our *ΔlitR* and *ΔrpoQ* mutants in vitro [19, 33]. The differentially expressed genes identified in this work provide a new insight to explain mechanisms related to QS such as motility, bioluminescence, wrinkled colony morphology, adhesiveness and biofilm formation.

Changes in cell density impacts genes related to quorum sensing in *A. salmonicida* LFI1238

QS is known to be a cell density dependent mechanism allowing communication between bacteria and is regulated through master regulators, as VanT, HapR and LitR [28, 42, 43]. LitR was shown previously to regulate cryptic bioluminescence in *A. salmonicida*, where its inactivation resulted in less light production [44]. This led us to propose that cryptic bioluminescence is a high cell density dependen phenotype, where LitR is involved in its regulation. Herein, the transcriptome of *A. salmonicida* at HCD showed a significant upregulation of *lux* operon (Additional file 2: Table S2), confirming that the alteration in gene experession of this operon is affected by changes in population.

RpoS sigma factor aids in adaptation to environmental stress, mainly required for virulence, stress resistance and biofilm formation, additionally it has been shown to be required for full motility in some vibrios [45]. In this study *rpoQ* (RpoS-like sigma factor) was found to be upregulated in *A. salmonicida* at HCD compared to LCD. Moreover, the transcriptome of *A. salmonicida* demonstrated a downregulation in genes associated with motility and chemotaxis. This explains our previously obtained results, where the overexpression of RpoQ in the wild-type resulted in non-motile strains [33]. Hence, the expression of *rpoQ* leads to reduced motility in *A. salmonicida* at HCD. *So why do A. salmonicida reduce their motility at HCD?* It is believed that bacteria have different expression profiles during the different stages of life cycle. However, a complete life cycle of *A. salmonicida* is still unknown. But we assume that *A. salmonicida* similar to *V. cholerae*, is able to change from planktonic to biofilm life cycle which results in changes in genes expression required for motility and other functions [46, 47]. The high cell density transcriptome presented in this study exhibits the activities of the late exponential phase (OD_{600} = 1.2). During this phase nutrition accessibility is limited which favors the bacterial cells to enter the stationary phase and QS. Thus, at this time period the accumulation of autoinducers results in the expression of LitR, which in turn activates the *rpoQ* expression leading to activate regulators responsible for motility reduction, hence protecting the bacteria from excessive energy loss required to manage the motility apparatus. Additionally, it has been shown that *A. salmonicida* suppresses motility under the late stages of the host colonization (i.e., HCD) [48, 49]. In contrast to HCD, at LCD we believe that the expression of motility genes in *A. salmonicida* are upregulated resulting in motile strains able to swim and colonize new host or environment. However the mechanism by which flagellar biosynthesis is controlled in *A. salmonicida* seems to be complex and will require further studies.

LitR and RpoQ regulate genes vital for motility

A. salmonicida is motile by nine polar flagella [50], where genes required for flagellum biosynthesis and flagellar motility are organized in different loci (Fig. 2) in a similar manner to *A. fischeri* [49]. The expression of genes involved in the synthesis of flagella in vibrios is tightly regulated through a complex hierarchy requiring the presence of regulatory proteins and the production of the flagellin monomer the basic component of bacterial flagellum, such as, FlaA [10, 51]. RpoQ was shown to be a positive regulator of motility in *A. salmonicida* under our experimental conditions [33], and here we determine that the deletion of *rpoQ* resulted in a downregulation of several flagellar and chemotaxis genes, mainly *flaA* at both cell densities. Although *A. salmonicida* flagellar filament is composed of six flagellins (Fig. 2), it appears that the FlaA protein is mainly essential for motility and most likley regulated by RpoQ. The importance of FlaA for motility was reported in *V. cholerae,* where its deletion affected motility and thereby virulence [44]. Similarly, in *A. fischeri* the inactivation of *flaA*

resulted in strains with reduced motility and symbiotic competence [52]. Likewise, a considerable importance of FlaA for motility was recently documented in *A. salmonicida* LFI1238, where the complete deletion of *flaA* resulted in 62% reduced motility at 8°C [53]. A similar reduction in motility was observed for the *ΔrpoQ* using the same temperature and salt concentration [33]. RpoQ is similar to other sigma factors that functions as a gene activator, and most probably activates a regulator of *flaA* gene. In *V. cholerae* it was show that *flaA* transcription is regulated by sigma factor 54 which depends on and requires an additional regulator, FlrC [54, 55]. Thus, it is reasonable to speculate that RpoQ may work in the similar manner as *V. cholerae* by activating regulators responsible for motility, where in the *ΔrpoQ* mutant, *flaA* regulator is not activated resulting in decreased motility.

The quorum sensing master regulator LitR, has been shown to be associated with motility in *A. salmonicida* similar to other bacteria [27, 56]. The deletion of *litR* (*ΔlitR*) resulted in more motile strain than the wild-type [27]. This led us to conclude that LitR is a repressor of motility at HCD, where its deletion (*ΔlitR*) mimics the low cell density phenotype [27]. A similar conclusion was also applied to the role of RpoQ in motility [33]. However, *ΔrpoQ* transcriptome exhibited downregulation in motility genes regardless of growth phases. This proposes either that QS does not seem to be implicated in the RpoQ-dependent induction of motility and chemotaxis, or that *rpoQ* is critical for flagellar gene expression, where its deletion does not completely mimic the low cell density phenotype.

In summary, these results indicate the importance of RpoQ in controlling the *flaA* gene which has a direct impact on the motility. Additionally RpoQ seems to tightly regulates several genes essential for flagellar assembly of *A. salmonicida*. Furthermore, RpoQ is believed to be a stress regulator in *A. salmonicida* similar to RpoS which may have the ability to switch between motile and non-motile states in response to physical or chemical changes in the environment.

LitR and RpoQ repress genes associated with virulence

Among the differentially expressed transcripts of *ΔrpoQ* and *ΔlitR* we were able to identify a number of significantly upregulated genes that may play an important role in virulence. These included the genes encoding adhesion and fimbrial attachment proteins also known as *tad* genes or *tad* operon. Tad loci is a widespread colonization island that is found in numerous pathogenic and non pathogenic bacteria including vibrios such as *V. cholerae*, *A. fischeri*, *V.vulnificus* and *Vibrio parahaemolyticus* (*V. parahaemolyticus*) [36, 57]. The *A. salmonicida* genome encode a number of potential virulence factors. Among them is the Flp-type pilus (fimbrial –low molecular weight protein), which has high similarity to the Tad macromolecular transport system of *Actinobacillus actinomycetemcomitans* (*A. actinomycetemcomitans*) [36]. Tad operon is known to facilitate adhesion and, to play an important role in motility and biofilm formation [57]. Although the function of the *tad* operon was not investigated in detail in *A. salmonicida* and the inactivation of two *tad* genes (*VSAL_II0367* and *VSAL_II0368*) did not affect the architecture or amounts of biofilm formed [19], it is reasonable to assume that this widespread colonization island provides important functions for pathogenic bacteria (e.g., *A. salmonicida*) in the form of colonization and adhesion. Our previous microarray analyzes on the *ΔlitR* mutant did not reveal any *tad* genes to be differentially expressed [19], although the adhesion of the *ΔlitR* mutants to the agar plates was observed [27]. In the study presented here, DEGs related to Tad locus in *ΔrpoQ* and *ΔlitR* yielded highly similar findings, where a number of *tad* genes were significantly upregulated. Whereas, the transcriptome of *A. salmonicida* wild-type at HCD revealed opposite results, where *tad* genes were downregulated. Thus, the increased expression level of LitR and RpoQ at HCD, leads to a repression of *tad* genes in *A. salmonicida* wild-type. This, proposes the importance of this colonization island at early stages of life cycle (i.e., LCD). Although evidence for the physiological role of this colonization island in *Vibrionaceae* is scant, recently a correlation between *tad* genes and phenotypes in *V. vulnificus* was found to be associated with biofilm formation, auto-aggregation and initial surface attachment to the host [58]. *tad* genes were also found to mediate adherence, colonization and micro-colony formation in other bacteria [59–61]. Hypothetically, these findings also can be considered in *A. salmonicida,* where the *tad* operon is mainly required for the initial surface attachment of the cells to the biotic surface and formation of micro-colonies and less necessary in the later stages of biofilm or infection. However, further investigations are needed to confirm this hypothesis.

Biofilm formation and colony rugosity are low cell density phenotypes involving expression of *syp*

The ability to form rugose colonies and biofilm are often correlated features in vibrios, which is generally associated with enhanced production of exopolysaccharides [21, 25, 62]. Similarly, in *A. salmonicida* colony rugosity and biofilm formation requires the expression of *syp* genes responsible for the production of EPS [19, 33]. Our previous microarray analysis showed that the expression of 14 out of 18 *syp* genes was negatively regulated by LitR, where the majority, were genes significantly upregulated in the biofilm compared to the

suspension [19]. However, the data obtained from the current work did not show significant upregulation of the 14 *syp* genes previously identified [19], except *sypA* and *sypC* genes, that showed to be differentially expressed at HCD. We know from our previous results that changes in medium composition affects the biofilm morphology [19], and here we assume that changes in some compounds of the SWT medium have affected the transcriptome of *ΔlitR* and resulted in less differentially expressed *syp* genes. In contrast to the *ΔlitR* transcriptome, the *ΔrpoQ* presented an upregulation among 13 out of 18 *syp* genes at HCD. We have previously observed what we refere to as a "late and weak" wrinkling colony morphology exhibited by *ΔlitR* compared to *ΔrpoQ*, which demonstrated an earlier and stronger rugosity in addition to a heavy and slimy extracellular matrix substance in the biofilm [33]. This led us to propose that LitR performs its activity on *syp* through RpoQ, where its expression leads to a strong *syp* repression. Moreover, the mature biofilm formation exhibited by *ΔlitR* was proposed to be a result of two independent processes where the first results in repression of *syp* via RpoQ while the second is independent of *rpoQ* and represses other biofilm matrix components. When three *syp* genes were inactivated separately in the *rpoQ* mutant no biofilm and no wrinckeled colonies were formed, and the *ΔrpoQsyp* double mutants behaved similar to the wild-type (Additional file 10: Figure S1). However, the inactivation of the same *syp* genes in *ΔlitR*, resulted in some biofilm production using the same conditions [19]. Hence, the inactivation of *syp* genes in *ΔrpoQ* mutant inhibited colony rugosity and biofilm formation completely, which was not the case for the *ΔlitR*. Consequently, our results provide a clear evidence that the negative regulatory cascade from LitR to *syp* genes is operated through RpoQ in a cell density dependent manner. *Why is RpoQ involved in regulating exopolysaccharide production via syp?* The bacteria, whether it is in the host or in the aquatic environment, employes survival strategies, where sigma factors (e.g., RpoS or RpoQ) are believed to aid in adaptation to environmental stress such as osmotic shock and starvation [63]. Hence, for RpoQ to be involved in regulating this EPS locus (*syp* operon) may suggest that this sigma factor may play an important role in environmental persistence protecting the bacteria under starvation and during infection of the host. We therefore believe that in addition to the negative regulatory cascade operated from LitR to *syp* genes (via RpoQ), *rpoQ* is also influenced by other genes and environmental factors leading to repression of *syp* in a pathway that remains unknown (Fig. 7).

Even though the relationship between RpoQ and LitR is not well-studied in *A. salmonicida*, our current transcriptome and previous microarray data showed a positive regulation of LitR on *rpoQ*, confirming that RpoQ operates downstream of LitR in the QS regulatory hierarchy [19]. Furthermore, the overexpression of *rpoQ* in the *ΔlitR* mutant influenced phenotypes related to QS [33]. Consistent with the results demonstrated in *A. fischeri*, where the overexpression of RpoQ in *ΔlitR* mutant resulted in decreased motility [32].

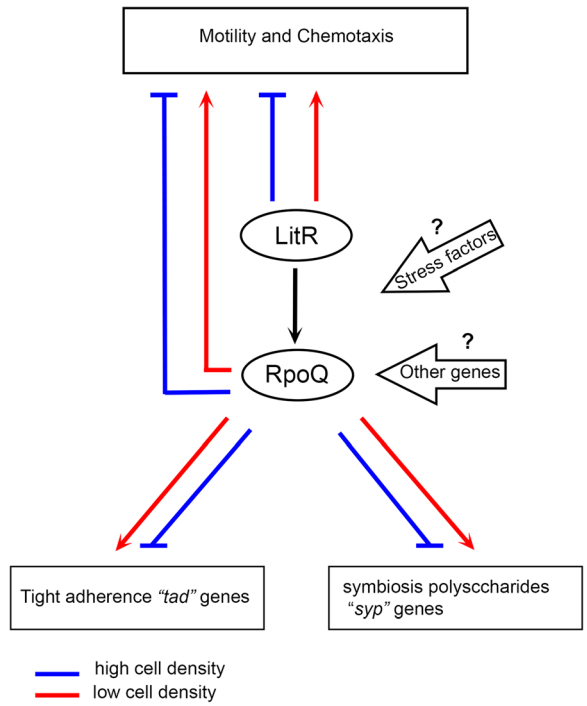

Fig. 7 Proposed model of QS and the possible LitR and RpoQ interaction in *A. salmonicida*. The expression of LitR signaling at high cell density represses motility, biofilm and activates transcription of RpoQ [19, 27]. The increased level of RpoQ activity leads to strong repression on biofilm formation, rugose colony morphology, motility and adhesion, through a negative regulatory cascade on EPS producing genes (i.e., *syp*), flagellar and *tad* genes, respectively. At low cell density the LitR is not activated, thereby RpoQ levels are low and not sufficient to repress either *tad* or *syp* genes, resulting in an upregulation leading to a strong adhesion to surface and thereby biofilm formation. However, the deletion of *rpoQ* results in reduced motility, where the regulation of flagellar genes maybe affected by other genes and environmental factor either dependent or independent of QS mechanism. Arrows and lines with bar end indicate positive and negative regulation respectively. Lines may also indirect direct or indicate pathways with several steps

Taken together, our data suggest a working model (Fig. 7) for *how LitR and RpoQ work together in A. salmonicida*, proposing that expression of genes in *A. salmonicida* is not always regulated by QS, and possibly involve other regulatory elements that act independently of the QS regulatory mechanism. Hence, the interaction between RpoQ and LitR and their roles in controlling motility, biofilm formation and rugose colony morphology,

may be directly or indirectly regulated by RpoQ independent of LitR and vice versa. Additionally, we assume that RpoQ is regulated by other gene(s) and stress factors rather than LitR alone.

Conclusion

In this work we have shown that the master regulator LitR and the alternative sigma factor RpoQ regulate genes involved in motility, rugose colony morphology and biofilm formation in *A. salmonicida*. Our results indicate that RpoQ is an activator of *flaA* gene either directly or indirectly. Moreover, the positive activation of LitR on *rpoQ* results in reduced motility, repression of genes involved in adhesion (e.g., *tad* genes) and exopolysaccharide production via *syp* operon at HCD in *A. salmonicida* wild-type. These findings confirm that LitR and RpoQ regulate phenotypic traits related to QS together (dependent) and also independent of each other, where other environmental factors and genes are probably also involved. However further studies are needed to map the elements and factors affecting gene expression and influencing the observed phenotypes during different life cycles.

Additional files

Additional file 1: Table S1. The table lists the summary of RNA sequencing data for *A. salmonicida* LFI1238, Δ*litR* and Δ*rpoQ*. (XLSX 10 kb)

Additional file 2: Table S2. The table lists the differentially expressed genes of *A. salmonicida* wild-type at HCD compared to LCD. (XLSX 82 kb)

Additional file 3: Table S3. The table lists the functional distribution of the differenatially expressed gene of *A. salmonicida* at HCD relative to LCD. (DOCX 16 kb)

Additional file 4: Table S4. The table lists the differentially expressed genes of Δ*litR* mutant compared to wild-type at LCD. (XLSX 13 kb)

Additional file 5: Table S5. The table lists the differentially expressed genes of Δ*litR* mutant compared to wild-type at HCD. (XLSX 24 kb)

Additional file 6: Table S6 and **Table S7.** The tables list the functional distribution of Δ*litR*/wt at LCD and HCD. (DOCX 18 kb)

Additional file 7: Table S8. The table lists the differentially expressed genes of Δ*rpoQ* mutant compared to wild-type at LCD. (XLSX 15 kb)

Additional file 8: Table S9. The table lists the differentially expressed genes of Δ*rpoQ* mutant compared to wild-type at HCD. (XLSX 28 kb)

Additional file 9: Table S10 and **Table S11.** The tables list the functional distribution of Δ*rpoQ*/wt at LCD and HCD. (DOCX 18 kb)

Additional file 10: Figure S1. Colony morpgology and biofilm formation of Δ*rpoQ* and LFI1238 *syp* mutants. (DOCX 1263 kb)

Additional file 11: Table S12. The table lists the differentially expressed genes of Δ*rpoQ* compared to Δ*litR* at LCD. (XLSX 19 kb)

Additional file 12: Table S13. The table lists the differentially expressed genes of Δ*rpoQ* compared to Δ*litR* at HCD. (XLSX 17 kb)

Abbreviations

DEGs: Differentially expressed genes; EPS: Exopolysaccharide; HCD: High cell density; LCD: Low cell density; min: Minutes; OD_{600}: Optical density measured at 600 nm; ON: Overnight; QS: Quorum sensing; rpm: Rounds per minute

Acknowledgements

We thank Dr. Eric V. Stabb (University of Georgia) for the pVSV102 and pEVS104 plasmids. We also thank researcher Adele Kim Willamson (UiT The Arctic University of Norway) for proofreading the manuscript.

Funding

This work was financed by UiT The Arctic University of Norway. The publication charges have been funded by a grant from the publication fund of UiT The Arctic University of Norway. The funders had no role in study design, data collection and analysis, decision to publish, or preparation and writing of the manuscript.

Availability of data and materials

All data generated or analysed during this study are included in this published article and its supplimentary materials. The transcriptome data have been deposited to the European Nucleotide Archive (www.ebi.ac.uk/ena) under study accession number PRJEB28385.

Author's contributions

MK, NPW, and HH conceived and designed the experiments. MK and HH constructed the mutants. MK performed the experiments and analyzed the transcriptomics data. EH analyzed the transcriptomics data. MK and NP wrote the paper. NP coordinated the research. All authors read and approved the final manuscript.

Ethics approval and consent to participate

Not applicable

Consent for publication

Not applicable.

Competing interests

The authors declare that they have no competing interest.

Publisher's Note

Springer Nature remains neutral with regard to jurisdictional claims in published maps and institutional affiliations.

Author details

[1]Norwegian Structural Biology Centre, UiT - The Arctic University of Norway, N-9037 Tromsø, Norway. [2]Centre for Bioinformatics, Department of Chemistry, Faculty of Science and Technology, UiT - The Arctic University of Norway, N-9037 Tromsø, Norway.

Received: 28 September 2018 Accepted: 11 March 2019
Published online: 15 March 2019

References

1. Miller MB, Bassler BL. Quorum sensing in bacteria. Annu Rev Microbiol. 2001; 55:165–99.
2. Bassler BL. How bacteria talk to each other: regulation of gene expression by quorum sensing. Curr Opin Microbiol. 1999;2(6):582–7.
3. Ng WL, Bassler BL. Bacterial quorum-sensing network architectures. Annu Rev Genet. 2009;43:197–222.
4. Parsek MR, Greenberg EP. Sociomicrobiology: the connections between quorum sensing and biofilms. Trends Microbiol. 2005;13(1):27–33.
5. Li YH, Tian X. Quorum sensing and bacterial social interactions in biofilms. Sensors (Basel). 2012;12(3):2519–38.
6. Waters CM, Bassler BL. Quorum sensing: cell-to-cell communication in bacteria. Annu Rev Cell Dev Biol. 2005;21:319–46.
7. Johnson CN. Fitness factors in vibrios: a mini-review. Microb Ecol. 2013;65(4): 826–51.
8. Milton DL. Quorum sensing in vibrios: complexity for diversification. Int J of Med Microbiol. 2006;296(2–3):61–71.
9. Hansen H, Purohit AA, Leiros HK, Johansen JA, Kellermann SJ, Bjelland AM, Willassen NP. The autoinducer synthases LuxI and AinS are responsible for temperature-dependent AHL production in the fish pathogen *Aliivibrio salmonicida*. BMC Microbiol. 2015;15:69.
10. Zhu S, Kojima S, Homma M. Structure, gene regulation and environmental response of flagella in *Vibrio*. Front Microbiol. 2013;4:410.

11. McCarter LL. Polar flagellar motility of the *Vibrionaceae*. Microbiol Mol Biol Rev. 2001;65(3):445–62 table of contents.
12. Guttenplan SB, Kearns DB. Regulation of flagellar motility during biofilm formation. FEMS Microbiol Rev. 2013;37(6):849–71.
13. Donlan RM, Costerton JW. Biofilms: survival mechanisms of clinically relevant microorganisms. Clin Microbiol Rev. 2002;15(2):167–93.
14. Yildiz FH, Visick KL. *Vibrio* biofilms: so much the same yet so different. Trends Microbiol. 2009;17(3):109–18.
15. Nistico L, Gieseke A, Stoodley P, Hall-Stoodley L, Kerschner JE, Ehrlich GD. Fluorescence "in situ" hybridization for the detection of biofilm in the middle ear and upper respiratory tract mucosa. Methods Mol Biol. 2009;493: 191–213.
16. Jamal M, Ahmad W, Andleeb S, Jalil F, Imran M, Nawaz MA, Hussain T, Ali M, Rafiq M, Kamil MA. Bacterial biofilm and associated infections. J Chin Med Assoc. 2018;81(1):7–11.
17. Klausen M, Aaes-Jorgensen A, Molin S, Tolker-Nielsen T. Involvement of bacterial migration in the development of complex multicellular structures in *Pseudomonas aeruginosa* biofilms. Mol Microbiol. 2003;50(1):61–8.
18. Gupta P, Sarkar S, Das B, Bhattacharjee S, Tribedi P. Biofilm, pathogenesis and prevention--a journey to break the wall: a review. Arch Microbiol. 2016; 198(1):1–15.
19. Hansen H, Bjelland AM, Ronessen M, Robertsen E, Willassen NP. LitR is a repressor of syp genes and has a temperature-sensitive regulatory effect on biofilm formation and colony morphology in *Vibrio* (*Aliivibrio*) *salmonicida*. Appl Environ Microbiol. 2014;80(17):5530–41.
20. Yip ES, Geszvain K, DeLoney-Marino CR, Visick KL. The symbiosis regulator *rscS* controls the syp gene locus, biofilm formation and symbiotic aggregation by *Vibrio fischeri*. Mol Microbiol. 2006;62(6):1586–600.
21. Yildiz FH, Schoolnik GK. Vibrio cholerae O1 El Tor: identification of a gene cluster required for the rugose colony type, exopolysaccharide production, chlorine resistance, and biofilm formation. Proc Natl Acad Sci U S A. 1999; 96(7):4028–33.
22. Fong JC, Syed KA, Klose KE, Yildiz FH. Role of Vibrio polysaccharide (*vps*) genes in VPS production, biofilm formation and *Vibrio cholerae* pathogenesis. Microbiology. 2010;156(Pt 9:2757–69.
23. Beyhan S, Odell LS, Yildiz FH. Identification and characterization of cyclic diguanylate signaling systems controlling rugosity in Vibrio cholerae. J Bacteriol. 2008;190(22):7392–405.
24. Waters CM, Lu W, Rabinowitz JD, Bassler BL. Quorum sensing controls biofilm formation in *Vibrio cholerae* through modulation of cyclic di-GMP levels and repression of *vpsT*. J Bacteriol. 2008;190(7):2527–36.
25. Yildiz FH, Liu XS, Heydorn A, Schoolnik GK. Molecular analysis of rugosity in a *Vibrio cholerae* O1 El Tor phase variant. Mol Microbiol. 2004;53(2):497–515.
26. Hammer BK, Bassler BL. Quorum sensing controls biofilm formation in *Vibrio cholerae*. Mol Microbiol. 2003;50(1):101–4.
27. Bjelland AM, Sørum H, Tegegne DA, Winther-Larsen HC, Willassen NP, Hansen H. LitR of *Vibrio salmonicida* is a salinity-sensitive quorum-sensing regulator of phenotypes involved in host interactions and virulence. Infect Immun. 2012;80(5):1681–9.
28. Fidopiastis PM, Miyamoto CM, Jobling MG, Meighen EA, Ruby EG. LitR, a new transcriptional activator in *Vibrio fischeri*, regulates luminescence and symbiotic light organ colonization. Mol Microbiol. 2002;45(1):131–43.
29. Lee JH, Rhee JE, Park U, Ju HM, Lee BC, Kim TS, Jeong HS, Choi SH. Identification and functional analysis of *vibrio vulnificus* SmcR, a novel global regulator. J Microbiol Biotechnol. 2007;17(2):325–34.
30. McCarter LL. OpaR, a homolog of *Vibrio harveyi* LuxR, controls opacity of *Vibrio parahaemolyticus*. J Bacteriol. 1998;180(12):3166–73.
31. Enos-Berlage JL, McCarter LL. Relation of capsular polysaccharide production and colonial cell organization to colony morphology in *Vibrio parahaemolyticus*. J Bacteriol. 2000;182(19):5513–20.
32. Cao X, Studer SV, Wassarman K, Zhang Y, Ruby EG, Miyashiro T. The novel sigma factor-like regulator RpoQ controls luminescence, chitinase activity, and motility in *Vibrio fischeri*. mBio. 2012;3(1):e00285–11.
33. Khider M, Willassen NP, Hansen H. The alternative sigma factor RpoQ regulates colony morphology, biofilm formation and motility in the fish pathogen *Aliivibrio salmonicida*. BMC Microbiol. 2018;18(1):116.
34. Magoc T, Wood D, Salzberg SL. EDGE-pro: estimated degree of gene expression in prokaryotic genomes. Evol Bioinformatics Online. 2013;9: 127–36.
35. Love MI, Huber W, Anders S. Moderated estimation of fold change and dispersion for RNA-seq data with DESeq2. Genome Biol. 2014;15(12):550.
36. Hjerde E, Lorentzen MS, Holden MT, Seeger K, Paulsen S, Bason N, Churcher C, Harris D, Norbertczak H, Quail MA, et al. The genome sequence of the fish pathogen *Aliivibrio salmonicida* strain LFI1238 shows extensive evidence of gene decay. BMC Genomics. 2008;9:616.
37. Dunn AK, Millikan DS, Adin DM, Bose JL, Stabb EV. New *rfp*- and pES213-derived tools for analyzing symbiotic *Vibrio fischeri* reveal patterns of infection and *lux* expression *in situ*. Appl Environ Microbiol. 2006;72(1):802–10.
38. Serres MH, Riley M. MultiFun, a multifunctional classification scheme for *Escherichia coli* K-12 gene products. Microb Comp Genomics. 2000;5(4):205–22.
39. Hoff KA. Survival of *Vibrio anguillarum* and *Vibrio salmonicida* at different salinities. Appl Environ Microbiol. 1989;55(7):1775–86.
40. Colquhoun DJ, Sørum H. Cloning, characterisation and phylogenetic analysis of the fur gene in *Vibrio salmonicida* and *Vibrio logei*. Gene. 2002; 296(1–2):213–20.
41. Kashulin A, Seredkina N, Sørum H. Cold-water vibriosis. The current status of knowledge. J Fish Dis. 2017;40(1):119–26.
42. Buchholtz C, Nielsen KF, Milton DL, Larsen JL, Gram L. Profiling of acylated homoserine lactones of *Vibrio anguillarum in vitro* and *in vivo*: influence of growth conditions and serotype. Syst Appl Microbiol. 2006;29(6):433–45.
43. Zhu J, Miller MB, Vance RE, Dziejman M, Bassler BL, Mekalanos JJ. Quorum-sensing regulators control virulence gene expression in *Vibrio cholerae*. Proc Natl Acad Sci U S A. 2002;99(5):3129–34.
44. Klose KE, Mekalanos JJ. Differential regulation of multiple flagellins in *Vibrio cholerae*. J Bacteriol. 1998;180(2):303–16.
45. Hulsmann A, Rosche TM, Kong IS, Hassan HM, Beam DM, Oliver JD. RpoS-dependent stress response and exoenzyme production in *Vibrio vulnificus*. Appl Environ Microbiol. 2003;69(10):6114–20.
46. Moorthy S, Watnick PI. Identification of novel stage-specific genetic requirements through whole genome transcription profiling of *Vibrio cholerae* biofilm development. Mol Microbiol. 2005;57(6):1623–35.
47. Moorthy S, Watnick PI. Genetic evidence that the *Vibrio cholerae* monolayer is a distinct stage in biofilm development. Mol Microbiol. 2004;52(2):573–87.
48. Bjelland AM, Johansen R, Brudal E, Hansen H, Winther-Larsen HC, Sørum H. *Vibrio salmonicida* pathogenesis analyzed by experimental challenge of Atlantic salmon (*Salmo salar*). Microbial Pathog. 2012;52(1):77–84.
49. Karlsen C, Paulsen SM, Tunsjo HS, Krinner S, Sørum H, Haugen P, Willassen NP. Motility and flagellin gene expression in the fish pathogen *Vibrio salmonicida*: effects of salinity and temperature. Microb Pathog. 2008;45(4): 258–64.
50. Egidius EWR, Andersen K, Hoof KA, Hjeltnes B. *Vibrio salmonicida* sp. nov., a new fish pathogen. Int J Syst Bacteriol. 1986;36:518–20.
51. Macnab RM. How bacteria assemble flagella. Annu Rev Microbiol. 2003;57: 77–100.
52. Millikan DS, Ruby EG. *Vibrio fischeri* flagellin a is essential for normal motility and for symbiotic competence during initial squid light organ colonization. J Bacteriol. 2004;186(13):4315–25.
53. Norstebø SF, Paulshus E, Bjelland AM, Sørum H. A unique role of flagellar function in *Aliivibrio salmonicida* pathogenicity not related to bacterial motility in aquatic environments. Microbial Pathog. 2017;109:263–73.
54. Syed KA, Beyhan S, Correa N, Queen J, Liu J, Peng F, Satchell KJ, Yildiz F, Klose KE. The *Vibrio cholerae* flagellar regulatory hierarchy controls expression of virulence factors. J Bacteriol. 2009;191(21):6555–70.
55. Correa NE, Lauriano CM, McGee R, Klose KE. Phosphorylation of the flagellar regulatory protein FlrC is necessary for *Vibrio cholerae* motility and enhanced colonization. Mol Microbiol. 2000;35(4):743–55.
56. Kim SM, Lee DH, Choi SH. Evidence that the *Vibrio vulnificus* flagellar regulator FlhF is regulated by a quorum sensing master regulator SmcR. Microbiology. 2012;158(Pt 8:2017–25.
57. Tomich M, Planet PJ, Figurski DH. The tad locus: postcards from the widespread colonization island. Nat Rev Microbiol. 2007;5(5):363–75.
58. Pu M, Rowe-Magnus DA. A tad pilus promotes the establishment and resistance of *Vibrio vulnificus* biofilms to mechanical clearance. NPJ Biofilms Microbiomes. 2018;4:10.
59. Nika JR, Latimer JL, Ward CK, Blick RJ, Wagner NJ, Cope LD, Mahairas GG, Munson RS Jr, Hansen EJ. Haemophilus ducreyi requires the *flp* gene cluster for microcolony formation in vitro. Infect Immun. 2002;70(6):2965–75.
60. Watnick PI, Kolter R. Steps in the development of a *Vibrio cholerae* El Tor biofilm. Mol Microbiol. 1999;34(3):586–95.
61. O'Toole GA, Kolter R. Flagellar and twitching motility are necessary for *Pseudomonas aeruginosa* biofilm development. Mol Microbiol. 1998;30(2): 295–304.

62. Casper-Lindley C, Yildiz FH. VpsT is a transcriptional regulator required for expression of *vps* biosynthesis genes and the development of rugose colonial morphology in *Vibrio cholerae* O1 El Tor. J Bacteriol. 2004;186(5): 1574–8.
63. Trastoy R, Manso T, Fernandez-Garcia L, Blasco L, Ambroa A, Perez Del Molino ML, Bou G, Garcia-Contreras R, Wood TK, Tomas M. Mechanisms of bacterial tolerance and persistence in the gastrointestinal and respiratory environments. Clin Microbiol Rev. 2018;31(4).
64. Stabb EV, Ruby EG. RP4-based plasmids for conjugation between Escherichia coli and members of the *Vibrionaceae*. Methods Enzymol. 2002; 358:413–26.

Additional file 1

Table S1 Summary of RNA seqeucing data

RNA seqeuncing	*ΔlitR*						*ΔrpoQ*						WT					
	LCD OD_{600} = 0.3			HCD OD_{600} = 1.2			LCD OD_{600} = 0.3			HCD OD_{600} = 1.2			LCD OD_{600} = 0.3			HCD OD_{600} = 1.2		
	Replicate 1	Replicate 2	Replicate 3	Replicate 1	Replicate 2	Replicate 3	Replicate 1	Replicate 2	Replicate 3	Replicate 1	Replicate 2	Replicate 3	Replicate 1	Replicate 2	Replicate 3	Replicate 1	Replicate 2	Replicate 3
Total no. of reads	11666026	9398860	10001066	9917818	8676412	8760004	8776832	10447656	10041794	9885060	10106286	10376302	10069440	9175370	10357454	8998582	9383042	10313296
Total no. of reads mapped to *A. salmonicida* LFI1238	9228085	7165163	7715927	7386004	6525387	6198972	6956522	7574291	8454444	6597776	7606996	8165643	9145064	8622094	8440288	8493760	8547012	9154082
Percent mapped reads to A. salmonicida LFI1238	95.14%	96.18%	93.94%	92.40%	92.77%	93.28%	93.21%	87.09%	92.98%	90.16%	77.55%	91.40%	90.82%	93.97%	81.49%	94,39 %	91,09 %	88,76 %
Average mapping coverage	149	115	124	119	105	100	112	122	136	106	123	132	147	139	136	137	138	148

Additional file 2 Table S2. The table lists the differentially expressed genes of *A. salmonicida* wild-type at HCD compared to LCD.

VSAL_nr	Function	Fold Change	p-value	p-adjusted
VSAL_II0130	transposase	-457,47	3,37051E-13	3,2997E-12
VSAL_I1441	transposase	-63,55	0,125753462	0,200757496
VSAL_II0577	PTS system, trehalose-specific EIIBC component	-44,43	4,2477E-153	2,1994E-150
VSAL_I0286	transposase	-33,58	0,195559546	0,287910754
VSAL_II0578	trehalose-6-phosphate hydrolase	-31,04	9,0389E-245	2,1061E-241
VSAL_I0456	transposase	-29,79	0,211404154	0,307185331
VSAL_I2323	transposase	-27,34	0,223294859	0,320170475
VSAL_II0038	maltodextrin phosphorylase	-27,08	2,27413E-71	2,40851E-69
VSAL_I1745	transposase	-12,46	0,12513574	0,20011412
VSAL_II0134	hypothetical protein	-10,00	5,8142E-102	1,3547E-99
VSAL_II0995	PTS system, fructose-like permease IIC component	-9,76	3,58544E-06	1,60965E-05
VSAL_II0366	fimbrial protein, Flp/Fap pilin component	-8,44	1,46051E-06	6,9662E-06
VSAL_II0894	PTS system, IIBC component	-8,42	3,41863E-25	7,77112E-24
VSAL_II0996	PTS system, permease-specific phosphorylation site EIIA compo	-8,34	0,001479377	0,004211299
VSAL_I2160	sodium/proton antiporter (fragment)	-7,46	1,81272E-44	8,79924E-43
VSAL_II0135	putative cytochrome b561	-6,98	8,38751E-51	5,011E-49
VSAL_II0039	4-alpha-glucanotransferase	-6,81	8,62248E-50	4,90009E-48
VSAL_II0895	mannose-6-phosphate isomerase	-6,28	1,56957E-32	4,81197E-31
VSAL_I2127	hypothetical protein	-5,87	0,019758142	0,042469069
VSAL_I0798	nitrite reductase (NAD(P)H) large subunit	-5,49	1,0754E-05	4,48243E-05
VSAL_II0500	inosine-guanosine kinase	-4,93	2,95171E-33	9,35711E-32
VSAL_I4069s	srna	-4,88	7,5473E-18	1,04363E-16
VSAL_I2625	pyruvate dehydrogenase E1 component	-4,87	3,68885E-44	1,73637E-42
VSAL_I2626	pyruvate dehydrogenase complex repressor	-4,85	2,35082E-54	1,50066E-52
VSAL_I2624	dihydrolipoyllysine-residue acetyltransferase component of pyr	-4,70	6,97213E-36	2,44578E-34
VSAL_II0969	putative exported protein	-4,69	2,96971E-11	2,48008E-10
VSAL_I2839	DNA-binding protein Fis	-4,43	1,40679E-40	6,01436E-39
VSAL_II0090	PTS system, fructose-specific IIA/FPR component	-4,20	0,026048219	0,054020784
VSAL_I1493	microbial collagenase precursor (pseudogene)	-4,15	6,58936E-33	2,06083E-31
VSAL_II1034	cold shock-like protein CspG	-4,14	5,00047E-13	4,86476E-12
VSAL_II0367	type IV leader peptidase	-4,08	7,10172E-07	3,5169E-06

VSAL_I0797	nitrite reductase (NAD(P)H) small subunit	-3,97	5,22089E-06	2,30174E-05
VSAL_I2494	putative transcriptional regulator	-3,94	1,59678E-17	2,14439E-16
VSAL_II2030s	srna	-3,93	0,012354322	0,027951228
VSAL_II0712	methyl-accepting chemotaxis citrate transducer	-3,87	2,95237E-31	8,44052E-30
VSAL_I0861	5-methyltetrahydropteroyltriglutamate--homocyst eine methylt	-3,87	3,89607E-09	2,56436E-08
VSAL_I1813	sodium/dicarboxylate symporter	-3,79	0,000532179	0,001668878
VSAL_I1030	membrane protein, putative phage gene	-3,77	0,009483656	0,022196804
pVSAL840_11	conjugative transfer protein TraU	-3,76	1,96696E-11	1,67569E-10
VSAL_I1001	transposase	-3,73	0,609893781	0,714276204
VSAL_II0564	hypothetical protein, putative phage gene	-3,72	1,02261E-24	2,25846E-23
VSAL_II0439	cold-shock DEAD box protein A (ATP-independent RNA helicase)	-3,67	8,21226E-12	7,2755E-11
VSAL_II0968	putative exported protein	-3,62	0,006228675	0,01524806
VSAL_II2014s	srna	-3,61	1,2506E-15	1,47913E-14
VSAL_II0218	ABC transporter, ATP-binding protein	-3,56	2,06505E-13	2,05623E-12
VSAL_II0599	membrane protein	-3,55	2,46515E-25	5,68693E-24
VSAL_I2838	tRNA-dihydrouridine synthase B	-3,51	8,18323E-33	2,52542E-31
VSAL_I1186	putative lysine exporter protein	-3,41	2,11244E-10	1,61112E-09
VSAL_II0592	membrane protein, putative nucleoside transporter	-3,40	1,05051E-16	1,35232E-15
VSAL_I2390	phosphoribosylformylglycinamidine cyclo-ligase (phosphoribosy	-3,38	5,09808E-18	7,24301E-17
VSAL_I2138	putative diaminobutyrate--2-oxoglutarate aminotransferase	-3,35	3,60534E-12	3,29429E-11
VSAL_II0142	putative ATP-dependent RNA helicase (DEAD/DEAH box helicas	-3,29	1,88495E-15	2,19597E-14
VSAL_I1490	hypothetical protein	-3,28	0,018244002	0,039506065
VSAL_I4053s	srna	-3,27	0,391337944	0,502655684
VSAL_I0796	formate/nitrite transporter	-3,27	4,75914E-10	3,49253E-09
VSAL_I2695	conserved hypothetical protein	-3,25	2,0308E-29	5,37701E-28
VSAL_I1377	putative lipoprotein	-3,21	4,39682E-11	3,60091E-10
VSAL_I4023s	srna	-3,20	1,46314E-05	5,96001E-05
VSAL_I0552	S-adenosylmethionine synthetase	-3,19	1,16634E-07	6,4321E-07
VSAL_I2986	thiamine biosynthesis protein ThiS	-3,19	0,00033783	0,001096302
VSAL_I1036	probable rRNA transcription initiatior protein, putative phage g	-3,19	0,003142482	0,008287473
VSAL_I2763	hypothetical protein	-3,14	4,24913E-21	7,58371E-20
VSAL_II1063	putative HTH-type transcriptional regulator (fragment)	-3,14	0,002857282	0,0076216

VSAL_II0365	hypothetical protein	-3,14	0,325050083	0,433772448
VSAL_I2215	translation initiation factor IF-1	-3,12	9,80217E-25	2,17803E-23
VSAL_I0714	inositol-1-monophosphatase	-3,11	4,243E-19	6,63503E-18
VSAL_II0643	transposase	-3,09	0,461560509	0,574792082
VSAL_I1234	sodium-dependent nucleoside transport protein	-3,06	3,27757E-10	2,43985E-09
VSAL_I2764	30S ribosomal subunit protein S18	-3,05	1,00527E-23	2,11971E-22
VSAL_II0370	putative lipoprotein	-3,05	1,13971E-05	4,72852E-05
VSAL_I2765	primosomal replication protein N	-3,04	9,81514E-25	2,17803E-23
VSAL_I2270	outer membrane protein transport protein	-3,03	7,92577E-14	8,26266E-13
VSAL_I0287	fructose-1,6-bisphosphatase class II GlpX	-3,02	6,78174E-18	9,4337E-17
VSAL_I1974	ABC transporter, ATP-binding component	-3,01	0,000455327	0,001444401
VSAL_I2766	30S ribosomal protein S6	-3,00	1,09296E-26	2,59857E-25
VSAL_I4121s	srna	-2,99	0,000141476	0,000491631
VSAL_I1029	phage terminase, endonuclease subunit	-2,98	0,000514723	0,001615224
VSAL_I0737	inosine-5'-monophosphate dehydrogenase	-2,98	3,43115E-16	4,25243E-15
VSAL_I0886	D-methionine transport ATP-binding protein MetN	-2,96	4,2638E-21	7,58371E-20
VSAL_I2193	methyl-accepting chemotaxis protein	-2,96	1,08725E-17	1,47284E-16
VSAL_I1312	putative helicase (DEAD/DEAH box helicase)	-2,94	7,69715E-15	8,64307E-14
VSAL_I2466	peptidase	-2,94	7,828E-10	5,57775E-09
VSAL_II0911	ABC transporter ATP-binding protein	-2,92	1,48247E-11	1,28407E-10
VSAL_I2744	50S ribosomal protein L31	-2,92	3,17483E-18	4,59462E-17
VSAL_II0051	inner membrane protein	-2,91	0,014786281	0,032842739
VSAL_I0190	50S ribosomal protein L33	-2,91	2,86068E-20	4,74404E-19
VSAL_II0091	1-phosphofructokinase	-2,90	0,043306014	0,083253311
VSAL_I0577	30S ribosomal protein S20	-2,90	1,36046E-14	1,4917E-13
VSAL_I1995	phospholipase A1 precursor	-2,89	1,57368E-15	1,84255E-14
VSAL_I0739	putative ion transporter	-2,88	4,56083E-10	3,35758E-09
VSAL_I4143s	srna	-2,87	2,86035E-14	3,07126E-13
pVSAL840_12	hypothetical protein, putative conjugative transfer protein TrbC	-2,87	0,000114305	0,000402921
VSAL_I1037	hypothetical protein, putative phage gene	-2,86	0,001530367	0,004337902
VSAL_I0553	hypothetical protein	-2,86	6,34928E-05	0,000233157
VSAL_II0755	membrane protein	-2,85	7,69679E-13	7,38005E-12

VSAL_II0119	putative exported protein	-2,83	0,000338267	0,001096956
VSAL_II2052s	srna	-2,82	2,09522E-07	1,12098E-06
VSAL_I1990	putative cobalt transport protein	-2,82	2,60937E-15	3,01729E-14
VSAL_I2663	30S ribosomal protein S9	-2,82	1,44119E-18	2,15255E-17
VSAL_I0652	50S ribosomal protein L19	-2,81	9,4752E-27	2,26433E-25
VSAL_I0136	siderophore biosynthesis protein	-2,81	5,27768E-10	3,85486E-09
VSAL_II0265	hypothetical protein	-2,79	0,00045254	0,001437517
VSAL_II0811	extracellular solute-binding protein	-2,79	2,24975E-10	1,71305E-09
VSAL_II0899	putative exported protein (pseudogene)	-2,79	7,29926E-05	0,000265531
VSAL_II0118	membrane protein	-2,76	0,000226314	0,00076146
VSAL_II0369	type II/III secretion system protein	-2,75	2,89806E-09	1,94316E-08
VSAL_I2308	polar flagellar M-ring protein FliF (pseudogene)	-2,73	4,98114E-18	7,09851E-17
VSAL_I0321	50S ribosomal protein L4	-2,73	1,37605E-26	3,25502E-25
VSAL_II0145	multidrug resistance protein D	-2,72	8,44308E-15	9,41263E-14
VSAL_I2664	50S ribosomal protein L13	-2,72	2,15188E-20	3,64646E-19
VSAL_I1219	hypothetical protein (fragment)	-2,71	0,06261954	0,113676298
VSAL_I2950	putative signaling protein (pseudogene)	-2,71	3,06593E-20	5,0485E-19
VSAL_I1262	conserved hypothetical protein	-2,71	5,28017E-06	2,32128E-05
VSAL_I1042	hypothetical protein, putative phage gene	-2,71	0,034606194	0,068975562
VSAL_I1796	sodium/alanine symporter	-2,69	2,49269E-10	1,88877E-09
VSAL_II0785	putative exported protein	-2,69	1,64569E-10	1,28673E-09
VSAL_I0322	50S ribosomal protein L23	-2,69	1,69541E-24	3,67471E-23
VSAL_I0323	50S ribosomal protein L2	-2,68	6,54826E-27	1,58108E-25
VSAL_I2319	hypothetical protein	-2,68	1,19718E-17	1,61706E-16
VSAL_II0815	hypothetical protein	-2,67	1,10554E-13	1,13227E-12
VSAL_II0721	PTS system permease for N-acetylglucosamine and glucose	-2,67	3,09985E-07	1,63224E-06
VSAL_I1018	hypothetical protein, putative phage gene	-2,67	0,008064671	0,019203561
VSAL_I2306	polar flagellar assembly protein FliH	-2,66	1,97656E-18	2,9148E-17
VSAL_I1313	hypothetical protein	-2,66	1,56184E-15	1,8333E-14
VSAL_I0325	50S ribosomal subunit protein L22	-2,66	1,17926E-23	2,46429E-22
VSAL_I0191	50S ribosomal protein L28	-2,65	2,09743E-22	4,05562E-21
VSAL_II1122s	srna	-2,65	4,17332E-06	1,86102E-05

VSAL_I0784	GTP-dependent nucleic acid-binding protein EngD	-2,65	1,85192E-18	2,73967E-17
VSAL_I2294	putative type IV pilus assembly (PilZ) protein	-2,65	8,40569E-15	9,39341E-14
VSAL_I0210	5'guanylate kinase	-2,65	1,28856E-08	7,98494E-08
VSAL_II0598	MFS transporter	-2,64	5,88324E-07	2,94162E-06
VSAL_I0319	30S ribosomal subunit protein S10	-2,64	9,80267E-26	2,2955E-24
VSAL_I2309	flagellar hook-basal body complex protein FliE	-2,63	6,14037E-16	7,37478E-15
VSAL_II0813	aminotransferase class III	-2,63	5,51008E-12	4,95695E-11
VSAL_I0337	30S ribosomal protein S5	-2,63	1,24882E-20	2,17145E-19
VSAL_I0004	ribonuclease P protein component (RNase P protein)	-2,62	1,9357E-10	1,49097E-09
VSAL_I2843	phosphoribosylamine--glycine ligase	-2,62	2,28531E-16	2,8551E-15
VSAL_I2307	polar flagellar motor switch protein FliG	-2,61	4,67894E-16	5,69292E-15
VSAL_I1216	putative HTH-type transcriptional regulator	-2,61	2,53912E-08	1,53268E-07
VSAL_I0320	50S ribosomal protein L3	-2,60	5,36046E-23	1,09082E-21
VSAL_I2467	ferredoxin	-2,60	2,41706E-06	1,11189E-05
VSAL_I0651	tRNA(guanine-N1)methyltransferase	-2,60	2,61305E-22	5,01103E-21
VSAL_II1022	methyl-accepting chemotaxis protein	-2,60	2,04094E-05	8,15674E-05
VSAL_I0361	50S ribosomal protein L21	-2,59	7,51954E-20	1,2167E-18
VSAL_II0150	ferrichrome transport ATP-binding protein FhuC	-2,59	1,39064E-07	7,5794E-07
VSAL_I2868	50S ribosomal subunit protein L10	-2,58	1,09473E-21	2,00057E-20
VSAL_I0327	50S ribosomal subunit protein L16	-2,58	1,57447E-23	3,26091E-22
VSAL_I2427	30S ribosomal protein S2	-2,58	6,34845E-18	8,85742E-17
VSAL_I1337	tyrosine-specific transport protein (tyrosine permease)	-2,57	4,03839E-09	2,65429E-08
VSAL_I0324	30S ribosomal protein S19	-2,57	7,07751E-23	1,4216E-21
VSAL_I0345	50S ribosomal protein L17	-2,55	7,58349E-23	1,51022E-21
VSAL_II0368	putative Flp pilus assembly protein	-2,55	1,66679E-08	1,02606E-07
VSAL_I1862	ribonuclease T	-2,55	1,88663E-08	1,15226E-07
VSAL_I2869	50S ribosomal protein L1	-2,55	4,55624E-18	6,53295E-17
VSAL_I0799	methyl-accepting chemotaxis protein	-2,55	2,914E-14	3,12166E-13
VSAL_I1038	hypothetical protein, putative phage gene	-2,54	0,014303288	0,031952696
VSAL_I0005	50S ribosomal protein L34	-2,54	3,79357E-10	2,8105E-09
VSAL_I0326	30S ribosomal subunit protein S3	-2,54	6,38786E-22	1,18595E-20
VSAL_II0168	putative exported protein	-2,54	0,019008149	0,040970387

VSAL_I1043	hypothetical protein, putative phage gene	-2,53	0,002380459	0,006455697
VSAL_I0338	50S ribosomal protein L30	-2,53	1,59011E-16	2,02456E-15
pVSAL840_06	conjugative transfer protein TraB	-2,53	2,85343E-05	0,000111552
VSAL_I2870	50S ribosomal protein L11	-2,53	4,22392E-16	5,16627E-15
VSAL_I0137	TonB-dependent iron-siderophore receptor precursor	-2,52	1,19063E-07	6,55832E-07
VSAL_I0328	50S ribosomal protein L29	-2,52	1,35357E-20	2,34485E-19
VSAL_I2237	50S ribosomal protein L32	-2,52	2,03665E-17	2,72724E-16
VSAL_I1989	ABC transporter ATP-binding protein	-2,51	1,43396E-14	1,56493E-13
VSAL_I0135	siderophore biosynthetis protein	-2,51	1,89193E-08	1,15398E-07
VSAL_I0340	preprotein translocase SecY subunit	-2,51	1,40169E-22	2,733E-21
VSAL_I2517	hypothetical protein	-2,51	2,99102E-15	3,42035E-14
VSAL_II0812	putative aminotransferase class-V	-2,50	7,23415E-10	5,20234E-09
VSAL_I0856	conserved hypothetical protein	-2,50	1,67088E-10	1,30424E-09
VSAL_I1446	membrane-bound lytic murein transglycosylase C	-2,49	2,94135E-10	2,2072E-09
VSAL_I1699	outer membrane protein, OmpA-like	-2,49	1,10127E-16	1,41375E-15
VSAL_II1033	hypothetical protein	-2,49	5,53019E-12	4,96545E-11
VSAL_II0008	transposase	-2,49	0,706531614	0,790015834
VSAL_II1023	hypothetical protein	-2,48	3,59235E-05	0,00013835
VSAL_I1015	hypothetical protein, putative phage gene	-2,48	0,001913377	0,005307343
VSAL_I0339	50S ribosomal protein L15	-2,48	2,53798E-21	4,60195E-20
VSAL_I0336	50S ribosomal protein L18	-2,48	2,89938E-22	5,53735E-21
VSAL_II0487	ABC transporter, ATP binding protein	-2,47	1,52405E-09	1,04596E-08
VSAL_I2867	50S ribosomal subunit protein L7/L12	-2,47	6,3672E-22	1,18595E-20
VSAL_II0568	putative membrane protein	-2,47	3,01192E-07	1,58773E-06
VSAL_I0108	membrane protein	-2,47	0,001365713	0,003923688
VSAL_I0362	50S ribosomal protein L27	-2,47	5,53467E-19	8,54025E-18
VSAL_I1391	conserved hypothetical protein	-2,47	8,2187E-11	6,58061E-10
VSAL_I1988	membrane protein	-2,47	1,28461E-07	7,05116E-07
VSAL_I1691	tRNA-(ms[2]io[6]A)-hydroxylase (pseudogene)	-2,46	1,94118E-06	9,07313E-06
VSAL_I0110	hypothetical protein	-2,46	0,007354452	0,017711496
VSAL_I0887	D-methionine transport system permease protein MetI	-2,46	3,87095E-09	2,55143E-08
VSAL_II1030	binding-protein-dependent transport system, inner membrane	-2,46	2,63754E-13	2,60401E-12

VSAL_I2980	hypothetical protein	-2,45	1,92201E-05	7,69463E-05
VSAL_I3127s	srna	-2,45	1,11732E-15	1,33505E-14
VSAL_I1286	hypothetical protein	-2,45	8,77955E-11	7,01762E-10
VSAL_II1080	membrane protein	-2,45	7,12567E-09	4,56749E-08
VSAL_I0535	tRNA (guanine-n(7)-)-methyltransferase	-2,44	1,15122E-12	1,09039E-11
pVSAL840_03	conjugative transfer protein TraL	-2,44	8,04739E-05	0,000290704
VSAL_II0753	outer membrane protein, OmpA family	-2,44	8,99812E-09	5,66639E-08
VSAL_II0245	nitrite reductase large subunit	-2,43	4,91197E-10	3,59338E-09
VSAL_I2084	50S ribosomal protein L25	-2,42	2,78365E-20	4,6494E-19
VSAL_I0343	30S ribosomal protein S4	-2,42	3,07219E-21	5,549E-20
VSAL_I1822	methyl-accepting chemotaxis protein (fragment)	-2,42	1,96044E-06	9,14478E-06
VSAL_II0089	fructose repressor	-2,41	2,23735E-05	8,88078E-05
VSAL_I1573	conserved hypothetical protein	-2,41	1,75727E-10	1,36709E-09
VSAL_I0750	phosphoribosylformylglycinamidine synthase	-2,41	2,27142E-15	2,63304E-14
VSAL_I0650	16S rRNA processing protein RimM	-2,41	2,21032E-18	3,24924E-17
VSAL_I2897	putative flagellar basal body-associated protein FliL	-2,40	8,47926E-10	6,03257E-09
VSAL_I4003s	srna	-2,40	4,56124E-07	2,33063E-06
VSAL_I0688	putative membrane protein	-2,40	4,25489E-11	3,49696E-10
VSAL_I0601	30S ribosomal protein S15	-2,40	4,22613E-19	6,6309E-18
VSAL_I0649	30S ribosomal protein S16	-2,40	7,27965E-16	8,72061E-15
VSAL_II0146	ATP-independent RNA helicase (DEAD/DEAH box helicase)	-2,39	6,4146E-07	3,19701E-06
VSAL_II0675	methyl-accepting chemotaxis protein	-2,38	6,51723E-05	0,00023876
VSAL_II0999	branched-chain amino acid transport system II carrier protein	-2,37	6,56256E-11	5,30009E-10
VSAL_I1535	membrane protein	-2,37	3,1146E-07	1,63815E-06
VSAL_I0342	30S ribosomal protein S11	-2,37	9,149E-19	1,38423E-17
VSAL_I1409	transporter, BCCT family (pseudogene)	-2,36	4,82802E-09	3,14226E-08
VSAL_II1027	putative exported protein	-2,36	1,32401E-07	7,25014E-07
VSAL_I4022s	srna	-2,35	0,054307226	0,101188194
VSAL_I3105s	srna	-2,35	1,09218E-12	1,03657E-11
VSAL_I0334	30S ribosomal protein S8	-2,35	5,81748E-15	6,57997E-14
VSAL_I2236	conserved hypothetical protein	-2,34	3,91779E-18	5,65229E-17
pVSAL840_25	antirestriction protein ArdC	-2,34	3,40758E-08	2,01515E-07

VSAL_I1220	branched chain amino acid transport system II carrier protein	-2,34	3,3386E-11	2,7683E-10
VSAL_II1029	binding-protein-dependent transport system, inner membrane	-2,33	3,09693E-14	3,31002E-13
VSAL_I4140s	srna	-2,33	1,71418E-09	1,17299E-08
VSAL_I2329	hypothetical protein	-2,33	3,93972E-11	3,24366E-10
VSAL_I0578	virulence factor MviN homolog	-2,33	1,25531E-10	9,91482E-10
VSAL_I0344	RNA polymerase alpha-subunit	-2,33	2,4048E-20	4,04562E-19
VSAL_II0741	putative phage zinc-binding transcriptional activator	-2,32	0,000639595	0,001969937
VSAL_I1393	hypothetical protein	-2,32	3,66486E-09	2,42588E-08
VSAL_II0631	phage replication and integration protein	-2,32	3,46495E-09	2,30009E-08
VSAL_II0634	phage replication protein	-2,32	3,54474E-09	2,34972E-08
VSAL_I1678	Hypothetical protein	-2,31	2,86968E-05	0,000111999
VSAL_II0814	2-phosphonoacetaldehyde hydrolase	-2,31	3,22825E-08	1,91639E-07
VSAL_I0107	membrane protein	-2,31	0,00010179	0,00036237
VSAL_I4110s	srna	-2,31	0,000869777	0,002611572
VSAL_I2232	putative sulfate transporter	-2,31	4,50054E-06	2,0012E-05
VSAL_I1330	6-pyruvoyl tetrahydrobiopterin synthase	-2,31	2,48343E-11	2,08519E-10
VSAL_I0310	30S ribosomal protein S12	-2,31	4,38402E-12	3,97462E-11
VSAL_I4058s	srna	-2,31	0,02312364	0,048806532
pVSAL840_13	conjugative transfer protein TraN	-2,30	0,000220929	0,000744417
VSAL_I0335	50E ribosomal protein L6	-2,30	1,05974E-19	1,69705E-18
VSAL_I0853	exported peptidase	-2,30	6,83516E-10	4,93827E-09
VSAL_I2039	putative exported protein	-2,30	6,73516E-14	7,10087E-13
VSAL_I2338	flagellar basal-body rod protein FlgB	-2,29	1,27094E-09	8,83967E-09
VSAL_I2553	autonomous glycyl radical cofactor	-2,29	1,15147E-05	4,76963E-05
VSAL_II1032	conserved hypothetical protein	-2,29	2,94228E-13	2,89874E-12
VSAL_I0738	GMP synthase [glutamine-hydrolyzing]	-2,29	6,55273E-13	6,30903E-12
VSAL_I0232	putative exported protein	-2,28	2,63581E-09	1,77498E-08
VSAL_I2144	putative sodium/proton antiporter	-2,28	3,84235E-10	2,84212E-09
VSAL_I2859	minor curlin subunit, CsgB like (pseudogene)	-2,28	0,007375482	0,017752968
VSAL_I1919	membrane protein	-2,28	1,13355E-05	4,70797E-05
VSAL_I2302	polar flagellar protein FliL	-2,27	2,13555E-11	1,80611E-10
VSAL_I2311	histidine kinase	-2,27	1,26291E-13	1,28217E-12

VSAL_II0488	putative binding protein-dependent transport system, membrai	-2,27	2,8083E-06	1,28679E-05
VSAL_I0329	30S ribosomal protein S17	-2,26	8,29783E-18	1,13396E-16
VSAL_I0333	30S ribosomal protein S14	-2,26	6,74434E-19	1,03725E-17
VSAL_I0051	cold shock protein	-2,26	6,99127E-08	3,9538E-07
VSAL_I0785	peptidyl-tRNA hydrolase	-2,26	6,22939E-09	4,02621E-08
VSAL_I2117	methyl-accepting chemotaxis protein (fragment)	-2,26	9,7494E-07	4,73746E-06
VSAL_I4057s	srna	-2,26	7,09987E-09	4,5619E-08
VSAL_I2985	thiamine biosynthesis adenylyltransferase ThiF	-2,26	0,00017648	0,000603372
VSAL_I1755	heme transporter protein HuvC, transmembrane permease com	-2,26	1,46102E-08	9,01766E-08
VSAL_I1963	putative secretion protein, HlyD family	-2,26	1,79519E-06	8,45009E-06
VSAL_II1028	conserved hypothetical protein	-2,25	5,09958E-08	2,93082E-07
VSAL_II2024s	srna	-2,25	4,13572E-06	1,84602E-05
VSAL_I0111	hypothetical protein	-2,25	0,015161405	0,033595886
VSAL_I0134	L-2,4-diaminobutyrate decarboxylase	-2,25	2,60894E-07	1,3847E-06
VSAL_I1221	membrane protein	-2,25	7,58309E-11	6,10314E-10
VSAL_I1982	putative DNA transformation protein TfoX	-2,24	5,10064E-08	2,93082E-07
VSAL_II0489	putative exported protein	-2,24	1,86951E-09	1,27181E-08
VSAL_I0341	30S ribosomal protein S13	-2,24	2,87876E-18	4,17913E-17
VSAL_I2426	elongation factor TS	-2,24	1,14615E-14	1,26565E-13
VSAL_I2348	putative membrane associated GGDEF protein	-2,24	2,78576E-05	0,000109089
VSAL_I2295	polar flagellar assembly protein FlhB	-2,23	1,2172E-11	1,0662E-10
VSAL_I0773	putative bacteriophage terminase	-2,23	0,000717299	0,002191876
VSAL_I1686	phosphoribosylglycinamide formyltransferase 2	-2,23	0,00011189	0,000395307
pVSAL840_04	conjugative transfer protein TraE	-2,23	6,03744E-05	0,000222759
VSAL_I1168	putative type VI secretion protein VasV-1, PAAR domain protei	-2,22	0,02077292	0,044486124
VSAL_II2040s	srna	-2,22	3,97154E-08	2,33679E-07
pVSAL840_34	hypothetical protein	-2,21	4,47238E-05	0,000169166
VSAL_II0121	putative exported protein	-2,21	0,079657204	0,138819212
VSAL_I2328	flagellar hook-associated protein type 3 FlgL	-2,21	1,99756E-09	1,353E-08
VSAL_I2493	putative sodium/alanine symporter	-2,21	1,86376E-08	1,13978E-07
VSAL_II0209	hypothetical protein (fragment)	-2,21	3,33267E-06	1,50341E-05
VSAL_II0810	ABC transporter, ATP-binding protein	-2,21	1,31672E-06	6,30616E-06

VSAL_I1215	membrane protein	-2,21	1,10812E-07	6,1401E-07
VSAL_I2337	flagellar basal-body rod protein FlgC	-2,20	2,0727E-10	1,58341E-09
pVSAL840_18	conjugative transfer protein TraG	-2,20	5,04901E-06	2,23441E-05
VSAL_I1927	hypothetical protein, putative phage gene (fragment)	-2,20	0,007113665	0,01721167
VSAL_I0021	antirestriction protein	-2,20	3,31994E-10	2,46745E-09
VSAL_I2327	hypothetical protein	-2,20	2,87609E-06	1,31398E-05
VSAL_II1031	ABC transport system, ATP-binding protein	-2,20	2,55397E-10	1,93206E-09
VSAL_I2500	anaerobic C4-dicarboxylate transporter DcuB	-2,20	2,19453E-07	1,17008E-06
VSAL_II0715	putative cation efflux system protein	-2,19	0,000386172	0,001241934
VSAL_I1287	putative RNA methyltransferase	-2,19	5,18808E-09	3,36719E-08
VSAL_II2038s	srna	-2,19	1,89519E-06	8,86704E-06
VSAL_I2842	bifunctional purine biosynthesis protein PurH	-2,19	1,21952E-12	1,15273E-11
VSAL_II0486	phosphomethylpyrimidine kinase	-2,19	2,05236E-10	1,57044E-09
pVSAL840_02	conjugative transfer protein TraA, putative fimbrial protein pre	-2,19	0,003435158	0,008978035
VSAL_I1320	membrane protein	-2,18	6,15543E-06	2,66335E-05
VSAL_I4150s	srna	-2,18	0,000227585	0,000765184
VSAL_II0551	hypothetical protein, putative phage gene	-2,18	0,000201652	0,000682921
VSAL_I2293	polar flagellar assembly protein FlhA	-2,18	1,12585E-11	9,88031E-11
VSAL_I2299	polar flagellar assembly protein FliO	-2,18	1,13525E-10	9,01236E-10
VSAL_I0311	30S ribosomal protein S7	-2,17	2,69076E-16	3,35266E-15
VSAL_I2298	polar flagellar assembly protein FliP	-2,17	4,26159E-08	2,49799E-07
VSAL_II0821	putative exported protein	-2,16	6,72769E-06	2,90019E-05
VSAL_II0856	hypothetical protein	-2,16	0,043777716	0,084063767
VSAL_II0731	putative membrane protein	-2,16	1,02789E-12	9,79547E-12
VSAL_I0109	hypothetical protein	-2,16	0,184971649	0,275241301
VSAL_II0490	putative thiaminase (transcriptional activator TenA)	-2,16	1,40128E-06	6,69052E-06
VSAL_I4118s	srna	-2,16	4,38847E-08	2,56269E-07
VSAL_I2158	L-asparaginase I	-2,16	7,47951E-07	3,68052E-06
VSAL_I1165	putative sodium/sulfate symporter (fragment)	-2,16	9,76013E-07	4,73773E-06
VSAL_I0744	transposase	-2,15	0,6385204	0,737174978
VSAL_I1863	sodium-type flagellar protein MotY precursor	-2,15	3,21576E-08	1,91141E-07
VSAL_I0974	membrane permease	-2,15	2,77247E-07	1,46648E-06

VSAL_II0528	hemolysin secretion protein	-2,15	2,73874E-08	1,65104E-07
VSAL_I2112	acetate kinase	-2,15	4,10253E-16	5,031E-15
VSAL_I1452	putative membrane protein	-2,15	0,005272528	0,013195479
VSAL_I2304	polar flagellar assembly protein FliJ	-2,15	3,16154E-07	1,6591E-06
VSAL_II0557	transposase	-2,14	5,99055E-08	3,41271E-07
VSAL_II0511	superoxide dismutase [Cu-Zn] precursor	-2,14	3,80029E-11	3,13996E-10
VSAL_I2330	peptidoglycan hydrolase FlgJ	-2,14	7,04998E-10	5,07773E-09
VSAL_I1357	secreted protein Hcp-2 (haemolysin co-regulated protein)	-2,14	0,001805893	0,005030163
VSAL_II0149	MFS transporter	-2,13	2,97998E-08	1,78492E-07
VSAL_I1909	membrane protein	-2,13	1,23588E-09	8,62157E-09
VSAL_I0865	putative ABC transporter permease	-2,13	1,72941E-08	1,0618E-07
VSAL_II0543	putative plasmid stabilisation system protein	-2,13	4,31216E-07	2,21796E-06
VSAL_I2313	polar flagellar protein FliS (polar flagellar protein FlaJ)	-2,13	4,52032E-14	4,82029E-13
VSAL_I2336	flagellar basal-body rod protein FlgD	-2,13	1,60739E-11	1,38712E-10
VSAL_I2137	saccharopine dehydrogenase	-2,13	8,37918E-09	5,29092E-08
VSAL_I2983	thiamine biosynthesis protein ThiC	-2,12	3,12639E-08	1,86304E-07
VSAL_I4077s	srna	-2,12	7,50516E-06	3,21157E-05
VSAL_I2305	polar flagellum-specific ATP synthase FliI	-2,12	4,42477E-08	2,57981E-07
VSAL_I4056s	srna	-2,12	6,45503E-07	3,21372E-06
VSAL_I2891	multidrug efflux pump	-2,12	7,33085E-10	5,26376E-09
VSAL_I2345	putative exported protein	-2,12	1,60359E-05	6,49803E-05
VSAL_I2984	thiamine-phosphate pyrophosphorylase	-2,12	1,38402E-06	6,61488E-06
VSAL_I0930	autoinducer 2 sensor kinase/phosphatase LuxQ	-2,12	4,27336E-10	3,15592E-09
VSAL_I1861	sodium/proton antiporter	-2,12	7,45802E-07	3,67382E-06
VSAL_I1986	putative lipoprotein	-2,12	8,55323E-12	7,54888E-11
VSAL_I2017	MFS transporter	-2,12	0,021943501	0,046713894
VSAL_I2300	polar flagellar switch protein FliN	-2,11	5,30662E-10	3,86993E-09
VSAL_II0829	transposase	-2,11	0,51610593	0,627296201
VSAL_II0530	putative membrane protein	-2,11	1,40005E-09	9,63696E-09
VSAL_II0799	hypothetical protein	-2,11	0,001510585	0,004289657
VSAL_II0777	hypothetical protein	-2,11	1,91777E-05	7,68426E-05
VSAL_I2018	ribosomal small subunit pseudouridine synthase A (16S pseudo	-2,11	9,15218E-08	5,11995E-07

VSAL_I2029	putative transport protein	-2,10	1,13741E-09	7,97046E-09
VSAL_I1627	membrane protein	-2,10	0,044985636	0,086091607
VSAL_II0854	secretion protein, HlyD family	-2,10	0,000165141	0,000567939
VSAL_I2344	putative lipoprotein	-2,10	2,37952E-06	1,09791E-05
VSAL_II0356	putative exported protein	-2,10	0,00090939	0,002714771
VSAL_I1743	hypothetical protein	-2,10	0,0069341	0,016812126
VSAL_I4102s	srna	-2,09	0,003254546	0,008544328
VSAL_I2314	polar flagellar protein FlaI	-2,09	6,60284E-08	3,74322E-07
pVSAL840_10	conjugative transfer protein TraW	-2,08	0,006206891	0,015215209
VSAL_I0230	conserved hypothetical protein	-2,08	4,85465E-10	3,55702E-09
VSAL_II0432	membrane protein	-2,08	0,000438562	0,001401715
VSAL_II0677	putative glycosyl transferase	-2,08	2,21127E-06	1,02329E-05
VSAL_II0093	putative exported protein	-2,08	1,28464E-07	7,05116E-07
VSAL_I1147	probable intracellular septation protein	-2,07	8,85837E-06	3,75273E-05
VSAL_I1750	putative coproporphyrinogen oxidase PhuW	-2,07	2,39426E-06	1,10359E-05
VSAL_I4044s	srna	-2,07	0,000754431	0,002294809
VSAL_I4043s	srna	-2,06	7,48186E-09	4,76956E-08
VSAL_II0947	hypothetical protein	-2,06	0,000833176	0,002517898
VSAL_I2316	polar flagellar protein FlaG (pseudogene)	-2,06	6,5584E-07	3,25475E-06
VSAL_I4139s	srna	-2,06	2,56005E-13	2,53288E-12
VSAL_I2701	pyruvate kinase I	-2,06	2,97215E-10	2,22672E-09
VSAL_I2303	polar flagellar hook-length control protein FliK	-2,05	1,39124E-09	9,59048E-09
VSAL_I4129s	srna	-2,05	5,4387E-11	4,41539E-10
VSAL_I2136	carboxynorspermidine decarboxylase	-2,05	1,71923E-07	9,25127E-07
VSAL_I1634	hypothetical protein	-2,05	5,20886E-06	2,29861E-05
VSAL_I1338	tyrosine-specific transport protein (tyrosine permease) (pseudo	-2,05	3,61174E-07	1,87633E-06
VSAL_I0536	thermolabile glutaminase	-2,05	1,25111E-06	6,01047E-06
VSAL_I1450	putative ferredoxin	-2,05	2,70358E-07	1,43167E-06
VSAL_II0512	putative exported protein	-2,05	4,26068E-12	3,87032E-11
VSAL_II0535	transposase (pseudogene)	-2,04	5,41088E-07	2,72591E-06
VSAL_I4169s	srna	-2,04	4,55901E-07	2,33063E-06
VSAL_I2326	putative exported protein	-2,04	9,52991E-07	4,64048E-06

VSAL_I0971	alanine racemase (pseudogene)	-2,03	0,009934843	0,02310198
VSAL_II0111	putative exported protein	-2,03	0,002386723	0,006466353
VSAL_II1088	putative membrane protein	-2,03	0,001189442	0,003464248
VSAL_I1752	TonB system transport protein ExbB1	-2,03	0,000266547	0,000877816
VSAL_I0863	accessory colonization factor AcfD precursor (fragment)	-2,03	7,55315E-10	5,40671E-09
pVSAL320_06	membrane protein	-2,03	2,38791E-12	2,19914E-11
VSAL_II0541	hypothetical protein, putative phage gene	-2,03	3,08837E-06	1,39998E-05
VSAL_II0015	secretion protein, HlyD family	-2,03	4,6418E-05	0,000175148
VSAL_I0726	conserved hypothetical protein	-2,03	5,20876E-07	2,63835E-06
VSAL_II1026	putative tryptophanyl-tRNA synthetase	-2,03	9,39414E-08	5,249E-07
VSAL_I1185	putative type VI secretion protein VasX-1	-2,03	0,033925227	0,067879586
VSAL_II0373	bacterial type II secretion system protein F	-2,03	6,62312E-05	0,000242258
VSAL_I0231	conserved hypothetical protein	-2,02	7,47745E-08	4,21341E-07
VSAL_I2887	tRNA (uracil-5)-methyltransferase	-2,02	3,12056E-07	1,63944E-06
VSAL_II0203	hypothetical protein	-2,02	0,208048583	0,303102688
VSAL_II0293	conserved hypothetical protein	-2,02	1,11075E-07	6,14739E-07
VSAL_I2987	thiamine biosynthesis protein ThiG	-2,02	0,00044879	0,001427551
VSAL_I2335	flagellar hook protein FlgE	-2,02	2,87125E-06	1,31305E-05
VSAL_II0680	hypothetical protein	-2,02	0,060229216	0,110008378
VSAL_I4146s	srna	-2,02	3,48207E-07	1,81596E-06
VSAL_I2939	putative elongation factor Tu, GTP binding domain	-2,02	1,48303E-08	9,1414E-08
VSAL_I2558	response regulator, aerobic respiration control protein ArcA	-2,02	3,30738E-11	2,74942E-10
VSAL_II0253	putative 3-hydroxy-3-methylglutaryl coenzyme a reductase	-2,02	1,76745E-05	7,1064E-05
VSAL_I2301	polar flagellar switch protein FliM (flagellar motor switch prote	-2,02	3,22856E-09	2,15237E-08
VSAL_I2346	putative exported protein	-2,01	2,31145E-06	1,06859E-05
VSAL_I1847	inosine-guanosine kinase	-2,01	2,64527E-09	1,77878E-08
VSAL_I4182s	srna	-2,01	5,30542E-06	2,33018E-05
VSAL_I1451	putative cytoplasmic chaperone TorD	-2,01	0,000806641	0,00244564
VSAL_I2216	putative arginine-tRNA-protein transferase	-2,01	5,55819E-08	3,17806E-07
VSAL_I4187s	srna	-2,01	2,21038E-06	1,02329E-05
VSAL_I1629	glycosyl transferase, family 2 (pseudogene)	-2,01	5,32194E-05	0,000198085
VSAL_II0713	putative exported protein	-2,00	4,1236E-07	2,12566E-06

VSAL_I1026	terminase, ATPase subunit	-2,00	9,74858E-05	0,00034811
VSAL_I0610	putative exported protein	2,00	0,000452518	0,001437517
VSAL_I2211	putative lipoprotein	2,00	1,77412E-06	8,35935E-06
VSAL_I4031s	srna	2,01	0,041409943	0,080004285
VSAL_I2666	putative membrane protein	2,01	2,98581E-07	1,57575E-06
VSAL_II0844	hypothetical protein	2,01	3,12658E-06	1,41592E-05
VSAL_I2349	putative exported protein	2,02	0,005564876	0,013860141
VSAL_I0972	transposase	2,02	0,503300421	0,615145208
VSAL_I0608	putative acetyltransferase	2,02	1,58823E-07	8,58601E-07
VSAL_I0498	RNA polymerase sigma-54 factor (sigma-N)	2,02	2,98268E-15	3,42035E-14
VSAL_I1505	putative exported protein	2,02	1,68466E-07	9,07576E-07
VSAL_I0403	sulfite reductase [NADPH] hemoprotein beta-component	2,03	0,352927473	0,464588142
VSAL_II0127	hypothetical protein, putative phage gene	2,03	1,66916E-06	7,89672E-06
VSAL_I0594	phosphoglucosamine mutase	2,03	1,99785E-05	7,9914E-05
VSAL_II0422	membrane protein	2,04	1,09227E-08	6,83219E-08
VSAL_I1719	hypothetical protein (fragment)	2,05	5,78967E-06	2,52384E-05
VSAL_II0444	binding-protein-dependent transport system inner membrane c	2,05	5,48795E-07	2,75878E-06
VSAL_I0379	putative membrane protein	2,06	6,84707E-07	3,3944E-06
VSAL_I0822	DNA-binding protein HU-beta	2,06	1,16709E-09	8,16614E-09
VSAL_I1006	conserved hypothetical protein	2,07	1,70782E-06	8,07143E-06
VSAL_I2379	dihydrodipicolinate synthase	2,07	8,87771E-10	6,27772E-09
VSAL_I0924	3,4-dihydroxy-2-butanone 4-phosphate synthase (GTP cyclohydr	2,07	6,99329E-06	3,00357E-05
VSAL_I0402	sulfite reductase [NADPH] flavoprotein alpha-component	2,07	0,35930754	0,470197455
VSAL_I2674	ADP-ribose pyrophosphatase	2,07	3,19111E-13	3,13725E-12
VSAL_II0021	pyridoxamine 5'-phosphate oxidase	2,07	4,66315E-11	3,81233E-10
VSAL_I2714	transcriptional regulator OxyR, LysR family (hydrogen peroxide-	2,07	4,80767E-09	3,13778E-08
VSAL_I1005	hypothetical protein	2,08	1,37316E-05	5,62297E-05
VSAL_I4067s	srna	2,08	0,002724678	0,007301323
VSAL_II0010	conserved hypothetical protein	2,08	9,66926E-06	4,07827E-05
VSAL_I1341	putative lipoprotein	2,08	9,6183E-08	5,3614E-07
VSAL_I1011	probable phage regulatory protein	2,08	0,002377999	0,006455697
VSAL_I2223	inner membrane protein	2,08	1,4922E-09	1,02561E-08

VSAL_II0719	hypothetical protein	2,09	7,95821E-05	0,000287706
VSAL_I2818	glyceraldehyde 3-phosphate dehydrogenase	2,09	1,19933E-05	4,9503E-05
VSAL_I2751	transposase	2,09	0,000154432	0,000532289
VSAL_I2033	putative exported protein	2,09	6,48674E-05	0,00023783
VSAL_I1899	hypothetical protein	2,10	2,80912E-12	2,57181E-11
VSAL_I2351	putative lipoprotein	2,10	0,000579371	0,001802316
VSAL_I2050	membrane protein	2,10	2,33926E-11	1,96768E-10
pVSAL840_66	DNA-binding protein HU-alpha	2,10	1,03803E-05	4,35003E-05
VSAL_I1533	hypothetical protein	2,10	0,000252776	0,000838986
VSAL_I2128	putative exported protein	2,10	0,131859655	0,208505596
VSAL_II0796	putative membrane protein	2,10	2,99812E-08	1,79348E-07
VSAL_I1082	response regulator	2,11	6,74044E-10	4,8774E-09
VSAL_I1325	proton glutamate symport protein	2,11	4,28251E-11	3,51347E-10
VSAL_I1481	putative lipoprotein	2,12	2,16146E-05	8,59422E-05
VSAL_I2937	D-tyrosyl-tRNA(tyr) deacylase	2,12	7,10716E-09	4,5619E-08
VSAL_I2660	ubiquinol--cytochrome c reductase, cytochrome C1	2,13	1,89847E-12	1,76938E-11
VSAL_I2672	Calcineurin-like phosphoesterase	2,13	2,10018E-07	1,12106E-06
VSAL_I1795	putative membrane protein	2,13	1,68159E-10	1,3104E-09
VSAL_I2164	peptidase family M16 (fragment)	2,14	1,24101E-09	8,64441E-09
VSAL_I1798	amino acid transport protein, LysE type	2,14	4,33479E-09	2,84109E-08
VSAL_II0360	HTH-type transcriptional regulator, LysR-family	2,14	4,48778E-08	2,61087E-07
VSAL_II0421	membrane protein	2,14	1,12835E-08	7,04839E-08
VSAL_I1327	putative exported protein	2,14	1,34406E-07	7,3427E-07
VSAL_I0880	hypothetical protein	2,14	2,88927E-06	1,31871E-05
VSAL_I2817	hypothetical protein	2,14	1,88761E-06	8,84045E-06
VSAL_I2678	methyl-accepting chemotaxis protein	2,14	0,000140808	0,000489674
VSAL_I2569	integral membrane protein, putative multidrug resistance prote	2,15	1,13506E-10	9,01236E-10
VSAL_I2068	membrane protein	2,15	1,92421E-10	1,48457E-09
VSAL_I1111	hypothetical protein (fragment)	2,15	5,45923E-06	2,39548E-05
VSAL_I0430	putative exported protein	2,16	6,13782E-12	5,47936E-11
VSAL_I0373	exported protein	2,16	2,49053E-08	1,50726E-07
VSAL_I1956	putative formate transporter 1	2,16	2,34721E-07	1,25006E-06

VSAL_II0582	L-allo-threonine aldolase	2,17	1,31869E-09	9,1309E-09
VSAL_I1518	hypothetical protein	2,17	0,000267925	0,00088173
VSAL_I1355	cystathionine beta-lyase	2,17	1,25188E-14	1,37589E-13
VSAL_I1599	putative polysaccharide deacetylase	2,18	0,00041229	0,001319555
VSAL_I0219	uroporphyrinogen III synthase HemD	2,18	1,40024E-10	1,10408E-09
VSAL_I1833	transposase (pseudogene)	2,18	7,17725E-09	4,58793E-08
VSAL_II2048s	srna	2,19	4,42887E-08	2,57981E-07
VSAL_I1950	oligopeptide transport ATP-binding protein F	2,19	4,70169E-09	3,07723E-08
VSAL_I2849	putative D-isomer specific 2-hydroxyacid dehydrogenase, NAD b	2,19	1,28739E-08	7,98494E-08
VSAL_I0407	opacity-associated protein A	2,19	8,77678E-13	8,39832E-12
VSAL_II0789	amino acid biosynthesis aminotransferase	2,20	3,35451E-11	2,77656E-10
VSAL_II0656	conserved hypothetical protein	2,20	5,30657E-07	2,67626E-06
VSAL_I4153s	srna	2,20	3,44397E-07	1,80016E-06
VSAL_II0986	hypothetical protein	2,20	1,55061E-07	8,40214E-07
VSAL_I1485	conserved hypothetical protein	2,21	1,70797E-08	1,05002E-07
VSAL_I2742	HTH-type transcriptional repressor CytR	2,21	5,24797E-07	2,65244E-06
VSAL_I1521	putative arginase (fragment)	2,22	1,86246E-06	8,74023E-06
VSAL_II0159	protoheme IX farnesyltransferase (cytochrome o ubiquinol oxid	2,22	1,78438E-09	1,21567E-08
VSAL_II0818	hypothetical protein	2,23	7,35798E-09	4,69701E-08
pVSAL840_20	conjugative transfer protein TraD	2,23	1,07979E-07	5,99743E-07
VSAL_I1882	membrane protein	2,24	5,80589E-17	7,57856E-16
VSAL_II0579	pyruvate kinase II	2,24	4,33011E-08	2,53496E-07
VSAL_I2982	hypothetical protein	2,25	1,32827E-09	9,16999E-09
VSAL_I0968	hypothetical protein, putative phage gene	2,25	2,10474E-11	1,78329E-10
VSAL_I1499	putative exported protein	2,25	0,002138403	0,005882502
VSAL_I1368	ribokinase	2,25	0,000538976	0,001689058
VSAL_II0087	hypothetical protein	2,25	0,159230271	0,243282972
VSAL_I2713	hybrid peroxiredoxin (thioredoxin reductase)	2,26	2,96577E-11	2,48008E-10
VSAL_I2992	MFS transporter	2,26	2,99464E-15	3,42035E-14
VSAL_I0125	diaminopimelate decarboxylase	2,26	2,84315E-15	3,27138E-14
VSAL_II0344	putative HTH-type transcriptional regulator	2,26	5,76215E-06	2,5142E-05
VSAL_II0637	hypothetical protein, putative phage gene	2,27	3,27881E-09	2,17964E-08

VSAL_II0267	HTH-type transcriptional regulator, AraC family	2,27	1,02367E-09	7,19501E-09
VSAL_I1213	transporter, LysE family	2,27	1,02442E-05	4,29685E-05
VSAL_I1456	ribosomal-protein-serine acetyltransferase	2,28	1,49398E-12	1,39798E-11
VSAL_I2733	acetylornithine aminotransferase/succinylornithine transamina	2,28	7,47682E-08	4,21341E-07
VSAL_I0229	cytochrome c	2,28	2,47332E-20	4,14592E-19
VSAL_I1903	HTH-type transcriptional regulator, AraC family	2,28	8,257E-12	7,30126E-11
VSAL_I2627	AmpD protein (N-acetylmuramoyl-L-alanine amidase)	2,29	3,12296E-09	2,08496E-08
VSAL_II0072	hypothetical protein (fragment)	2,29	1,53506E-06	7,29935E-06
VSAL_I1191	HTH-type transcriptional regulator, AraC family	2,30	1,96614E-10	1,51191E-09
VSAL_II0889	hypothetical protein	2,30	1,25511E-11	1,09734E-10
VSAL_I0376	3-isopropylmalate dehydrogenase	2,30	1,00382E-09	7,06616E-09
VSAL_I4047s	srna	2,31	6,7535E-06	2,90608E-05
VSAL_I4079s	srna	2,33	3,99163E-05	0,000152592
VSAL_II1098	ABC transporter ATP-binding protein	2,33	6,13884E-15	6,9099E-14
VSAL_I0874	hypothetical protein	2,33	1,75946E-13	1,76705E-12
VSAL_I0374	3-isopropylmalate dehydratase small subunit	2,34	1,62143E-11	1,39665E-10
VSAL_I2734	arginine N-succinyltransferase	2,34	1,11866E-07	6,18381E-07
VSAL_I1375	membrane protein	2,34	0,001005667	0,002975499
VSAL_II0361	putative exported protein	2,35	9,58267E-12	8,42551E-11
VSAL_I0864	putative exported protein	2,36	9,58239E-14	9,9011E-13
VSAL_II0233	maltose/maltodextrin transport ATP-binding protein (fragment	2,36	6,16183E-07	3,07761E-06
VSAL_I0830	N-acetylglucosamine-6-phosphate deacetylase	2,37	1,36317E-08	8,42489E-08
VSAL_I0375	3-isopropylmalate dehydratase large subunit	2,37	2,33349E-17	3,10688E-16
VSAL_I1806	conserved hypothetical protein	2,37	2,05566E-08	1,24894E-07
VSAL_I1809	transposase	2,38	9,50918E-06	4,01748E-05
VSAL_I0757	endochitinase ChiA	2,38	2,67284E-12	2,45185E-11
VSAL_II1004	HTH-type transcriptional regulator, LacI family (fragment)	2,38	4,11029E-08	2,41538E-07
VSAL_I1615	PTS permease for glucose	2,39	3,30992E-11	2,74942E-10
VSAL_I2377	putative membrane protein	2,39	5,77497E-09	3,73769E-08
VSAL_I1319	membrane receptor, histidine kinase	2,39	1,21503E-15	1,44072E-14
VSAL_I1482	glucose 1-dehydrogenase	2,39	4,82704E-12	4,3593E-11
VSAL_II0704	histidine utilization repressor	2,39	3,10456E-08	1,8524E-07

VSAL_I0829	N-acetylglucosamine repressor	2,40	6,25579E-07	3,1212E-06
VSAL_I1881	hypothetical protein	2,40	4,14568E-23	8,47319E-22
VSAL_I2972	putative zinc-binding alcohol dehydrogenase	2,40	1,14175E-08	7,12258E-08
VSAL_II0615	hypothetical protein	2,40	3,69518E-09	2,44249E-08
VSAL_I0646	putative transport protein	2,40	5,3233E-14	5,6507E-13
VSAL_I2540	putative cell division protein ZapA	2,40	2,312E-13	2,29233E-12
VSAL_II0795	membrane protein	2,41	1,92774E-11	1,64529E-10
VSAL_II0232	putative alpha amylase	2,41	1,98202E-12	1,83258E-11
VSAL_I1771	hypothetical protein (pseudogene)	2,42	1,03042E-16	1,33013E-15
VSAL_I4141s	srna	2,43	1,26069E-12	1,18806E-11
VSAL_II0239	glycogen synthase	2,44	3,57802E-07	1,86089E-06
VSAL_I2124	hypothetical protein	2,45	0,00023445	0,000782621
VSAL_I0622	purine nucleoside phosphorylase (pseudogene)	2,45	1,29441E-12	1,21612E-11
VSAL_I0292	regulator of ribonuclease activity A	2,45	5,35706E-11	4,3567E-10
VSAL_I2085	heat shock protein	2,46	1,8727E-16	2,3714E-15
VSAL_I1710	putative hemolysin (pseudogene)	2,46	4,99347E-17	6,55481E-16
VSAL_I2945	conserved hypothetical protein	2,46	1,99755E-14	2,16478E-13
VSAL_II0078	putative aminotransferase	2,47	2,12639E-17	2,83924E-16
VSAL_I0637	carbon storage regulator	2,47	1,1022E-19	1,75899E-18
VSAL_I0843	succinate dehydrogenase hydrophobic membrane anchor protei	2,47	1,08431E-09	7,60976E-09
VSAL_I1949	oligopeptide transport ATP-binding protein D	2,47	5,46217E-12	4,92335E-11
VSAL_II0399	peptidase T	2,47	1,02382E-05	4,29685E-05
VSAL_I0992	apolipoprotein N-acyltransferase	2,49	1,41054E-13	1,42275E-12
VSAL_II0215	catalase	2,49	2,24831E-11	1,8946E-10
VSAL_I0445	aminotransferase class-V	2,49	2,11769E-05	8,44179E-05
VSAL_I0842	succinate dehydrogenase cytochrome b556 subunit	2,50	7,58455E-10	5,42086E-09
VSAL_I0100	putative cyclic nucleotide binding protein	2,50	4,50119E-10	3,31892E-09
VSAL_II0104	putative 6-phosphogluconate dehydrogenase	2,51	0,000278547	0,000914751
VSAL_I2201	ferredoxin--NADP reductase	2,51	1,92779E-09	1,30764E-08
VSAL_I1340	putative lipoprotein	2,51	1,40636E-07	7,65612E-07
VSAL_I0087	ketol-acid reductoisomerase	2,52	4,37598E-16	5,33823E-15
VSAL_I2536	hypothetical protein	2,52	1,92359E-07	1,0339E-06

VSAL_II0614	cold shock-like protein	2,53	4,80755E-16	5,83416E-15
VSAL_II1014	conserved hypothetical protein	2,53	5,05408E-11	4,1247E-10
VSAL_I2075	methyl-accepting chemotaxis protein	2,54	6,35961E-09	4,10468E-08
VSAL_I1310	conserved hypothetical protein	2,54	3,30599E-07	1,731E-06
VSAL_I0378	transcriptional regulator, AcrR/TetR family (pseudogene)	2,54	0,000249604	0,000829639
VSAL_I4028s	srna	2,54	3,77271E-08	2,22261E-07
VSAL_I2188	putative phospholipase	2,55	1,18205E-14	1,30221E-13
VSAL_II0817	proline permease	2,56	2,77076E-18	4,03492E-17
VSAL_I1348	transposase	2,56	1,77328E-10	1,37725E-09
VSAL_I0674	putative membrane protein	2,57	4,59898E-07	2,34734E-06
VSAL_II0386	glycerol-3-phosphate repressor protein	2,57	2,92036E-08	1,75372E-07
VSAL_I4185s	srna	2,57	6,95386E-09	4,47583E-08
VSAL_I4111s	srna	2,57	2,6228E-12	2,4107E-11
VSAL_I2825	integral membrane protein, MarC family	2,58	1,06551E-13	1,09609E-12
VSAL_I2948	universal stress protein B	2,58	2,64084E-15	3,04612E-14
VSAL_I0099	putative exonuclease	2,59	2,52808E-18	3,70467E-17
VSAL_I0871	inner membrane ABC transporter permease protein	2,60	8,60857E-10	6,11524E-09
VSAL_II0169	hypothetical protein	2,60	3,87827E-11	3,19871E-10
VSAL_I1545	putative exported protein	2,60	3,51928E-10	2,61144E-09
VSAL_I1294	methyl-accepting chemotaxis protein	2,61	4,62944E-08	2,68323E-07
VSAL_II2008s	srna	2,62	2,44451E-17	3,2362E-16
VSAL_II1100	hypothetical protein (pseudogene)	2,62	3,22534E-13	3,16423E-12
VSAL_II0574	conserved hypothetical protein	2,62	8,03529E-14	8,35813E-13
VSAL_II0307	response regulator, histidine kinase	2,63	1,00541E-14	1,11553E-13
VSAL_II0075	hypothetical protein	2,63	1,18642E-10	9,40261E-10
VSAL_I1519	putative membrane protein	2,63	3,31274E-08	1,96155E-07
VSAL_I2229	putative outer membrane assembly protein	2,64	1,00213E-13	1,03317E-12
VSAL_I2596	putative exported protein (pseudogene)	2,64	9,55318E-08	5,33148E-07
VSAL_I4048s	srna	2,64	1,75239E-05	7,05191E-05
VSAL_I2671	conserved hypothetical protein	2,65	2,30778E-09	1,55633E-08
VSAL_I1254	transporter, BCCT family	2,65	1,26634E-08	7,8682E-08
VSAL_I0866	putative lipoprotein	2,66	5,67819E-15	6,43804E-14

VSAL_II0878	putative cytochrome c-554	2,66	4,82561E-09	3,14226E-08
VSAL_II0455	HTH-type transcriptional regulator	2,66	3,06796E-08	1,83291E-07
VSAL_II0496	glycine cleavage system T protein	2,66	2,10183E-16	2,64003E-15
VSAL_I4090s	srna	2,66	1,91318E-05	7,67246E-05
VSAL_I1298	putative lipoprotein	2,66	2,49175E-28	6,41521E-27
VSAL_II1056	putative rhodanese-related sulfurtransferase	2,67	5,14656E-08	2,95357E-07
VSAL_I0969	hypothetical protein, putative phage gene	2,67	1,67993E-21	3,05799E-20
VSAL_II0794	DNA-3-methyladenine glycosylase I	2,68	1,46215E-15	1,72061E-14
VSAL_I0760	ribosomal protein S6 modification protein	2,68	1,18699E-15	1,41106E-14
VSAL_I2661	ubiquinol--cytochrome c reductase, cytochrome B	2,69	7,67693E-14	8,02119E-13
VSAL_I2269	hypothetical protein	2,69	0,005729982	0,014187948
VSAL_I0204	response regulator homolog OmpR	2,69	7,85865E-07	3,86301E-06
VSAL_I0619	deoxyribose-phosphate aldolase	2,69	6,47216E-07	3,21881E-06
VSAL_I0432	peptide methionine sulfoxide reductase MSRA	2,71	1,22041E-18	1,83455E-17
VSAL_II0165	membrane protein	2,71	1,19011E-10	9,41581E-10
VSAL_I4080s	srna	2,71	0,001024988	0,003030738
VSAL_II0346	putative nuclease	2,73	6,23875E-11	5,04732E-10
VSAL_I2451	phosphate transport system regulatory protein PhoU	2,73	1,77552E-13	1,77934E-12
VSAL_I4162s	srna	2,76	1,86194E-11	1,59497E-10
VSAL_I0294	phosphoribulokinase	2,77	1,86575E-13	1,86575E-12
VSAL_II0237	conserved hypothetical protein	2,77	1,92309E-10	1,48457E-09
VSAL_II0423	exported serine protease, trypsin elastase	2,78	1,39554E-15	1,64638E-14
VSAL_I0377	2-isopropylmalate synthase	2,79	7,15066E-14	7,52192E-13
VSAL_I1731	integration host factor alpha-subunit (IHF-alpha)	2,80	2,01958E-09	1,36593E-08
VSAL_I0831	PTS permease for N-acetylglucosamine and glucose	2,80	1,30468E-09	9,04732E-09
VSAL_I1548	NAD-dependent glutamate dehydrogenase (pseudogene)	2,81	3,08432E-11	2,57118E-10
VSAL_I2546	small-conductance mechanosensitive channel	2,81	5,93652E-18	8,32042E-17
VSAL_I0418	membrane protein	2,81	1,99383E-08	1,21454E-07
VSAL_I1840	leucine-responsive regulatory protein	2,82	1,97236E-20	3,39158E-19
VSAL_I1852	conserved hypothetical protein	2,83	5,00099E-06	2,21738E-05
VSAL_I0872	hypothetical protein	2,83	1,21167E-13	1,23284E-12
VSAL_II0238	glucose-1-phosphate adenylyltransferase	2,83	3,87961E-07	2,00655E-06

VSAL_I1512	membrane protein	2,83	1,91618E-12	1,78231E-11
VSAL_I0618	putative membrane protein	2,83	1,90767E-11	1,63114E-10
VSAL_I2130	methyl-accepting chemotaxis protein	2,84	4,08564E-21	7,35099E-20
VSAL_II0451	hypothetical protein	2,86	1,56267E-07	8,45767E-07
VSAL_II0819	proline dehydrogenase	2,86	4,77916E-08	2,76314E-07
VSAL_I4186s	srna	2,87	1,9987E-16	2,51728E-15
VSAL_I0735	conserved hypothetical protein	2,88	5,25687E-18	7,42333E-17
VSAL_I0218	putative uroporphyrin-III C-methyltransferase HemX	2,88	5,20986E-18	7,37932E-17
VSAL_I0870	inner membrane ABC transporter permease protein	2,89	9,26792E-12	8,16418E-11
VSAL_I0673	HTH-type transcriptional regulator, LysR family (pseudogene)	2,90	2,0136E-13	2,00928E-12
VSAL_I1876	conserved hypothetical protein	2,92	3,21898E-23	6,63736E-22
VSAL_I2673	conserved hypothetical protein	2,92	7,29732E-19	1,1186E-17
VSAL_I4019s	srna	2,92	0,000136223	0,000474439
VSAL_I2662	ubiquinol-cytochrome c reductase iron-sulfur subunit (rieske iro	2,92	7,59616E-19	1,16059E-17
VSAL_I1297	putative lipoprotein	2,93	2,94388E-20	4,86471E-19
VSAL_I0932	antibiotic biosynthesis monooxygenase	2,93	5,94571E-18	8,32042E-17
VSAL_I1679	type I restriction enzyme R protein (pseudogene)	2,95	4,8022E-15	5,45811E-14
VSAL_II0394	cytochrome c551 peroxidase	2,95	7,75991E-15	8,69259E-14
VSAL_I0395	hypothetical protein, putative phage gene (fragment)	2,96	7,30953E-14	7,67171E-13
VSAL_I1622	putative cell wall lytic enzyme	2,96	8,35443E-17	1,08445E-15
VSAL_I0620	thymidine phosphorylase	2,97	6,54411E-07	3,25112E-06
VSAL_I1334	putative thioesterase	2,98	7,70896E-18	1,0597E-16
VSAL_I0419	2',3'-cyclic-nucleotide 2'-phosphodiesterase precursor	2,98	1,93906E-07	1,04101E-06
VSAL_I0695	conserved hypothetical protein	3,00	1,28195E-16	1,63668E-15
VSAL_I1092	coniferyl aldehyde dehydrogenase	3,00	1,32531E-09	9,16316E-09
VSAL_I2408	nitrogen regulatory protein P-II	3,00	4,82449E-16	5,83952E-15
VSAL_II0912	putative exported protein	3,01	1,95522E-12	1,81501E-11
VSAL_I1831	uridine phosphorylase	3,01	0,018089362	0,039237439
VSAL_I1212	transcriptional regulator, AraC-family	3,02	3,03383E-10	2,26227E-09
VSAL_II0405	putative HTH-type transcriptional regulator	3,03	8,53234E-17	1,10446E-15
VSAL_II1099	membrane signal transduction protein	3,03	5,16544E-17	6,7615E-16
VSAL_I4055s	srna	3,04	9,46252E-18	1,28558E-16

VSAL_I0846	2-oxoglutarate dehydrogenase E1 component	3,04	4,99465E-24	1,07258E-22
VSAL_I2409	cytochrome c-552	3,04	4,40914E-13	4,29845E-12
VSAL_I0973	aminoacyl-histidine dipeptidase	3,04	6,11857E-16	7,36758E-15
VSAL_I1411	hypothetical protein	3,05	5,13482E-13	4,98506E-12
VSAL_I0800	5'-nucleotidase precursor	3,05	2,79123E-08	1,68051E-07
VSAL_II0840	putative Lon protease	3,06	8,34998E-08	4,69371E-07
VSAL_II0793	hypothetical protein	3,06	5,69492E-11	4,61536E-10
VSAL_I2890	soluble pyridine nucleotide transhydrogenase	3,07	9,14127E-21	1,60179E-19
VSAL_I2936	putative acyltransferase	3,07	3,31244E-22	6,3004E-21
VSAL_I0284	5-carboxymethyl-2-hydroxymuconate isomerase	3,08	3,45013E-16	4,26462E-15
VSAL_I1855	aldehyde-alcohol dehydrogenase	3,08	1,90681E-09	1,2953E-08
VSAL_I0217	protein HemY	3,09	1,21162E-24	2,66328E-23
VSAL_II0788	putative lipoprotein	3,09	1,01199E-18	1,52618E-17
VSAL_II0393	response regulator, histidine kinase	3,11	5,95835E-12	5,32935E-11
VSAL_II0654	HTH-type regulatory protein, AraC family	3,14	4,36756E-19	6,7931E-18
VSAL_II1101	secretion protein, HlyD family	3,14	2,12249E-20	3,60979E-19
VSAL_I0844	putative exported protein	3,14	1,06183E-14	1,17533E-13
VSAL_I2570	membrane protein, putative periplasmic component of a bacte	3,14	1,06719E-25	2,48656E-24
VSAL_I2361	putative exported protein	3,15	9,79735E-09	6,15305E-08
VSAL_II0162	cytochrome o ubiquinol oxidase subunit I (ubiquinol oxidase sub	3,15	2,03347E-20	3,47106E-19
VSAL_I4165s	srna	3,15	6,99384E-10	5,04509E-09
VSAL_I4084s	srna	3,16	1,43322E-12	1,34382E-11
VSAL_I4007s	srna	3,17	2,97157E-16	3,69268E-15
VSAL_II0772	trimethylamine-N-oxide reductase precursor	3,17	1,1402E-16	1,4597E-15
VSAL_II0595	putative exported oxidoreductase	3,18	1,29466E-29	3,4475E-28
VSAL_II0773	cytochrome c-type protein	3,19	1,08856E-22	2,14037E-21
VSAL_I4094s	srna	3,19	3,16944E-07	1,66137E-06
VSAL_I4098s	srna	3,19	3,17857E-25	7,26085E-24
VSAL_II0886	hypothetical protein	3,21	3,25589E-06	1,4702E-05
VSAL_II0978	peptidase E	3,22	1,54457E-07	8,37916E-07
VSAL_II0655	putative phosphate-binding protein (pseudogene)	3,22	7,69549E-18	1,0597E-16
VSAL_I4188s	srna	3,22	5,55975E-13	5,37519E-12

VSAL_I1318	transcriptional regulator, two-component response regulator	3,22	2,25028E-14	2,43302E-13
VSAL_I2855	curli production assembly/transport component, CsgG precurso	3,23	4,89004E-27	1,19307E-25
VSAL_II0965	transcriptional activator protein LuxR	3,23	1,14532E-13	1,16788E-12
VSAL_II0331	putative exported protein	3,23	3,73902E-13	3,6528E-12
VSAL_I1935	sodium-dependent transporter	3,24	1,8828E-16	2,37774E-15
VSAL_I4025s	srna	3,25	1,41513E-07	7,6949E-07
VSAL_I4112s	srna	3,27	3,0101E-10	2,25153E-09
VSAL_II2013s	srna	3,28	1,61835E-06	7,67192E-06
VSAL_I0995	PhoH-like protein	3,31	1,76721E-11	1,51661E-10
VSAL_I1511	conserved hypothetical protein	3,31	3,43837E-19	5,43146E-18
VSAL_I0621	phosphopentomutase	3,31	7,00405E-18	9,71395E-17
VSAL_I2111	membrane protein	3,31	2,47103E-37	9,13887E-36
VSAL_II0641	putative acetyltransferase	3,31	1,47314E-23	3,06466E-22
VSAL_II1069	HTH-type transcriptional regulator, LysR family (pseudogene)	3,32	2,36154E-12	2,17916E-11
VSAL_II0280	integral membrane protein	3,33	4,58705E-31	1,28769E-29
VSAL_I1520	hypothetical protein	3,35	4,79922E-12	4,3426E-11
VSAL_I2083	putative exported protein	3,35	1,60348E-24	3,49169E-23
VSAL_I2557	demethylmenaquinone methyltransferase	3,36	5,45116E-10	3,96913E-09
VSAL_II0787	putative transglycosylase protein	3,38	5,18012E-27	1,25726E-25
VSAL_II0281	membrane protein	3,38	2,15852E-22	4,1565E-21
VSAL_II1036	putative mechanosensitive ion channel protein	3,39	9,52217E-24	2,01697E-22
VSAL_I2562	glutamate synthase, large subunit	3,40	3,31546E-44	1,57654E-42
VSAL_II0161	cytochrome o ubiquinol oxidase subunit III	3,40	6,5463E-28	1,64896E-26
VSAL_I0913	putative hydrolytic enzyme	3,41	1,12046E-13	1,14503E-12
VSAL_I0847	dihydrolipoamide succinyltransferase component of 2-oxoglutar	3,41	4,45785E-41	1,95977E-39
VSAL_I0867	oligopeptide transport ATP-binding protein (pseudogene)	3,42	3,87001E-16	4,77097E-15
VSAL_II0160	cytochrome o ubiquinol oxidase subunit CyoD	3,42	5,84428E-18	8,22789E-17
VSAL_II0223	hypothetical protein	3,42	7,78526E-05	0,000281672
VSAL_I2619	HTH-type luminescence regulator LitR	3,43	2,38685E-29	6,28402E-28
VSAL_I4075s	srna	3,44	3,0038E-06	1,36563E-05
VSAL_I2973	fatty oxidation complex beta subunit, 3-ketoacyl-CoA thiolase	3,44	9,59803E-13	9,16533E-12
VSAL_II0774	putative periplasmic nitrate reductase protein NapE	3,45	5,35912E-25	1,21231E-23

VSAL_I1657	PTS system, cellobiose-specific EIIC membrane component (pse	3,45	1,17548E-15	1,40096E-14
VSAL_I2159	aspartate-semialdehyde dehydrogenase	3,49	1,92914E-39	7,68358E-38
VSAL_I2064	conserved hypothetical protein	3,50	4,70306E-21	8,33318E-20
VSAL_I1428	conserved hypothetical protein	3,50	2,17653E-16	2,72651E-15
VSAL_I2576	ABC transporter, periplasmic chitin oligosaccharide [(GlcNAc)n]	3,51	8,09014E-20	1,3045E-18
VSAL_I2362	inner membrane protein	3,51	1,487E-10	1,16854E-09
VSAL_I2036	putative genetic competence protein (fragment)	3,52	7,66407E-12	6,80278E-11
VSAL_I2620	transposase (pseudogene)	3,55	1,02088E-23	2,14293E-22
VSAL_II0497	conserved hypothetical protein	3,56	3,00129E-36	1,08419E-34
VSAL_I1438	putative allophanate hydrolase subunit 2	3,57	1,262E-12	1,18806E-11
VSAL_I1658	glycosylasparaginase	3,58	1,59428E-19	2,53561E-18
VSAL_I1586	HTH-type transcriptional regulator, LysR family	3,61	2,31932E-34	7,72001E-33
VSAL_II0163	cytochrome o ubiquinol oxidase subunit II (ubiquinol oxidase sul	3,62	6,22924E-23	1,2621E-21
VSAL_I2796	putative periplasmic protein CpxP	3,65	1,48512E-35	5,12642E-34
VSAL_I1510	conserved hypothetical protein	3,65	6,54473E-20	1,06266E-18
VSAL_I1231	extracellular solute-binding protein	3,70	1,0891E-08	6,82148E-08
VSAL_II0957	autoinducer synthesis protein LuxI	3,72	1,66648E-38	6,36542E-37
VSAL_I1947	oligopeptide transport system permease protein B (pseudogene	3,72	2,61388E-28	6,69268E-27
VSAL_I0346	fructose-1,6-bisphosphatase	3,72	6,16342E-26	1,45058E-24
VSAL_I1981	membrane protein	3,72	4,13301E-32	1,24257E-30
VSAL_I4192s	srna	3,73	7,30628E-25	1,6448E-23
VSAL_I0662	putative exported protein	3,76	8,47201E-14	8,79277E-13
VSAL_I0046	putative ferredoxin	3,78	4,8878E-28	1,23789E-26
VSAL_I2667	exported serine protease	3,79	4,33729E-30	1,1751E-28
VSAL_I0645	S-ribosylhomocysteine lyase	3,80	4,91793E-22	9,24095E-21
VSAL_I1729	oligopeptidase F	3,82	1,09784E-41	4,87232E-40
VSAL_I1371	ribose transport ATP-binding protein RbsA	3,83	1,21809E-06	5,86393E-06
VSAL_I1907	putative ion channel	3,83	4,19513E-15	4,77978E-14
VSAL_I2254	putative sodium-dependent transporter	3,83	8,55889E-24	1,82121E-22
VSAL_I1230	DctM-like transport protein	3,84	1,56173E-18	2,32514E-17
VSAL_I0355	integral membrane transport protein	3,85	3,40046E-32	1,02897E-30
VSAL_I2352	chitoporin (pseudogene)	3,87	0,000348576	0,001129599

VSAL_I1436	conserved hypothetical protein	3,87	5,97575E-20	9,73671E-19
VSAL_I0806	putative NAD dependent epimerase/dehydratase	3,89	1,05655E-39	4,28132E-38
VSAL_II0600	membrane protein	3,90	8,13367E-18	1,11479E-16
VSAL_I1435	conserved hypothetical protein	3,92	5,06203E-14	5,38563E-13
VSAL_I1808	hypothetical protein	3,93	1,23207E-31	3,63382E-30
VSAL_II0019	hypothetical protein	3,93	1,87735E-28	4,86025E-27
VSAL_I1712	glycerophosphoryl diester phosphodiesterase precursor	3,93	3,13733E-19	4,97277E-18
VSAL_I1713	glycerol-3-phosphate transporter	3,94	5,87085E-15	6,62426E-14
VSAL_I2170	putative MgtC/SapB transporter	3,94	1,82503E-14	1,98243E-13
VSAL_I0845	succinate dehydrogenase iron-sulfur protein	3,95	6,81361E-23	1,37452E-21
VSAL_II0837	L-threonine 3-dehydrogenase	3,95	9,33343E-15	1,03804E-13
VSAL_I2735	succinylglutamic semialdehyde dehydrogenase	3,96	5,30544E-24	1,1341E-22
VSAL_I4135s	srna	4,03	6,284E-08	3,57115E-07
VSAL_I0609	putative membrane protein	4,05	1,62086E-12	1,51367E-11
VSAL_I1589	hypothetical protein	4,08	2,94513E-27	7,30015E-26
VSAL_I0497	sigma-54 modulation protein	4,09	1,06999E-44	5,24858E-43
VSAL_I2563	glutamate synthase, small subunit	4,13	7,90582E-43	3,54242E-41
VSAL_I4193s	srna	4,14	1,72693E-31	5,02969E-30
VSAL_I1590	quinolone resistance determinant QnrC	4,14	3,13712E-29	8,21292E-28
VSAL_I1431	putative acetyltransferase	4,21	5,38442E-20	8,83501E-19
VSAL_II0797	putative exported protein	4,21	2,38127E-17	3,16145E-16
VSAL_II0836	2-amino-3-ketobutyrate coenzyme A ligase	4,21	5,84768E-14	6,19323E-13
VSAL_I2178	transposase	4,23	0,577197999	0,684643402
VSAL_II0434	secretion protein, HlyD family	4,23	2,92197E-25	6,70758E-24
VSAL_I2940	glutamine synthetase	4,23	2,09114E-33	6,72049E-32
VSAL_I1437	putative allophanate hydrolase subunit 1	4,25	1,77012E-20	3,0551E-19
VSAL_I1971	membrane protein	4,27	3,64724E-27	8,94534E-26
VSAL_I0638	oxaloacetate decarboxylase 1, subunit gamma	4,32	2,5669E-31	7,38381E-30
VSAL_I1384	hypothetical protein	4,33	7,45057E-14	7,80217E-13
VSAL_I1370	ribose transport system permease protein RbsC	4,37	3,81533E-12	3,47255E-11
VSAL_I0414	hypothetical protein	4,39	5,72586E-16	6,91257E-15
VSAL_I2564	putative lipoprotein	4,39	3,04925E-40	1,28014E-38

VSAL_I1427	hypothetical protein	4,40	2,0913E-22	4,05562E-21
VSAL_I1434	HTH-type transcriptional regulator, LysR family (pseudogene)	4,41	4,30526E-39	1,68593E-37
VSAL_I4051s	srna	4,43	4,01804E-19	6,3257E-18
VSAL_I2824	transcriptional regulator, LuxR response regulator receiver	4,46	1,08345E-12	1,03038E-11
VSAL_I1238	exported serine protease (pseudogene)	4,51	4,819E-21	8,50626E-20
VSAL_II0866	deoxyribodipyrimidine photo-lyase (photoreactivating enzyme)	4,54	1,36445E-39	5,48132E-38
VSAL_I2056	general L-amino acid ABC transporter permease protein	4,55	1,24437E-20	2,17145E-19
VSAL_I0048	putative sporulation-control protein	4,56	3,82558E-31	1,08044E-29
VSAL_II0317	putative membrane protein	4,57	7,81027E-17	1,01664E-15
VSAL_I4008s	srna	4,57	1,75681E-09	1,2004E-08
VSAL_I3216s	srna	4,58	8,44765E-32	2,50739E-30
VSAL_II0456	conserved hypothetical protein, putative transposase	4,60	1,30759E-13	1,32178E-12
VSAL_II0062	membrane protein	4,62	1,66149E-16	2,10968E-15
VSAL_I2255	putative exported protein	4,62	2,42553E-14	2,61643E-13
VSAL_I3142s	srna	4,63	1,39143E-14	1,52208E-13
VSAL_I0854	putative exported protein	4,64	6,17596E-14	6,52607E-13
VSAL_II0435	putative membrane protein	4,67	6,2959E-22	1,17827E-20
VSAL_I0873	hypothetical protein	4,69	8,01903E-22	1,48288E-20
VSAL_II0446	binding-protein-dependent transport system inner membrane c	4,72	1,69242E-53	1,06577E-51
VSAL_II0018	outer membrane protein OmpA family	4,75	6,26505E-38	2,33561E-36
VSAL_I0588	putative exported protein	4,77	7,84925E-51	4,75033E-49
VSAL_II0164	membrane protein	4,81	8,7543E-18	1,19284E-16
VSAL_II0437	hypothetical protein	4,84	3,76682E-12	3,4351E-11
VSAL_I0915	membrane protein	4,84	1,98902E-11	1,6914E-10
pVSAL840_19	putative exported protein	4,86	2,6805E-14	2,88479E-13
VSAL_II0884	glutaredoxin	4,90	1,31446E-24	2,87577E-23
VSAL_II0462	cytochrome c'	4,94	6,98044E-36	2,44578E-34
VSAL_I0868	dipeptide transport ATP-binding protein DppD	4,96	2,09759E-35	7,18732E-34
VSAL_I0416	hypothetical protein	4,96	2,0273E-47	1,08588E-45
VSAL_II0887	conserved hypothetical protein	4,97	2,73382E-50	1,57279E-48
VSAL_II0920	maltose transport system permease protein MalG	4,98	2,25441E-34	7,55796E-33
VSAL_I1054	putative acetyltransferase	5,00	1,25925E-22	2,46559E-21

VSAL_I1347	fumarate hydratase class I	5,03	3,94182E-16	4,84666E-15
VSAL_II0318	putative exported protein	5,03	9,14326E-21	1,60179E-19
VSAL_II0445	bacterial extracellular solute-binding protein	5,07	8,64305E-41	3,72932E-39
VSAL_II0067	hypothetical protein	5,09	1,26433E-08	7,8662E-08
VSAL_I1905	membrane protein	5,11	1,59135E-30	4,4141E-29
VSAL_I1623	putative sucrose-6F-phosphate phosphohydrolase	5,12	1,05967E-21	1,94411E-20
VSAL_I2069	putative ABC transporter, ATP-binding protein (fragment)	5,15	8,0788E-19	1,2303E-17
VSAL_I2967	putative membrane protein	5,16	2,68701E-17	3,54715E-16
VSAL_I2595	aconitate hydratase 2 (citrate hydro-lyase 2)	5,17	1,76823E-25	4,09947E-24
VSAL_II1003	putative tRNA-binding protein	5,21	7,65935E-25	1,71599E-23
pVSAL840_28	DNA-binding protein HU-alpha	5,22	2,68168E-28	6,82876E-27
VSAL_II0061	exported glycosyl hydrolase, family 16	5,24	1,63078E-11	1,40211E-10
VSAL_I0359	hypthetical product	5,25	2,48279E-33	7,92451E-32
VSAL_I0431	conserved hypothetical protein	5,29	1,48515E-46	7,68979E-45
VSAL_II0052	response regulator protein	5,32	3,13038E-55	2,11414E-53
VSAL_I3217s	srna	5,33	3,16403E-45	1,56855E-43
VSAL_I0417	membrane protein	5,38	3,84719E-37	1,41165E-35
VSAL_II0315	putative response regulator	5,39	1,3434E-17	1,80931E-16
VSAL_I1572	universal stress protein E	5,39	1,59558E-15	1,86351E-14
VSAL_I0869	extracellular solute-binding protein	5,50	9,91862E-46	5,024E-44
VSAL_I2736	hypothetical protein	5,50	5,35103E-44	2,49358E-42
VSAL_I0415	hypothetical protein	5,51	4,24554E-21	7,58371E-20
VSAL_I4086s	srna	5,51	4,76337E-18	6,80899E-17
VSAL_I2055	general L-amino acid ABC transporter permease protein	5,53	2,03301E-20	3,47106E-19
VSAL_I2214	ATP-dependent Clp protease ATP-binding subunit ClpA	5,54	2,39564E-47	1,2686E-45
VSAL_I1251	putative membrane protein	5,55	2,81527E-20	4,68541E-19
VSAL_I1659	PTS system, Lactose/Cellobiose specific IIB subunit	5,57	4,45227E-36	1,58379E-34
VSAL_II0065	membrane protein	5,60	6,10209E-13	5,88732E-12
VSAL_I2450	putative exported protein	5,62	9,38613E-20	1,50825E-18
VSAL_I0848	succinyl-CoA synthetase beta chain	5,67	7,53682E-62	6,05545E-60
VSAL_I2156	2,4-dienoyl-CoA reductase [NADPH]	5,67	7,87192E-23	1,56099E-21
VSAL_II0060	putative type I toxin secretion system, ATP-binding protein	5,67	7,11687E-23	1,42337E-21

VSAL_I0401	hypothetical protein	5,74	3,09165E-32	9,4164E-31
VSAL_I2928	phosphoenolpyruvate carboxykinase	5,85	1,9831E-64	1,74363E-62
VSAL_I1372	high affinity ribose transport protein RbsD	5,92	2,40395E-07	1,27881E-06
VSAL_I0841	citrate synthase	5,99	4,10321E-22	7,74128E-21
VSAL_I2213	ATP-dependent Clp protease adaptor protein ClpS	6,08	1,50698E-47	8,16572E-46
VSAL_II0865	conserved hypothetical protein	6,09	5,59352E-46	2,86437E-44
VSAL_II0020	hemolysin-type calcium-binding protein	6,16	1,88358E-85	3,13482E-83
VSAL_I2550	putative hemerythrin	6,21	2,73342E-50	1,57279E-48
VSAL_II0306	two-component response regulator, transcriptional regulatory p	6,21	1,03766E-49	5,82589E-48
VSAL_I0094	ABC transporter, ATP-binding protein (pseudogene)	6,21	1,64673E-38	6,34196E-37
VSAL_I2205	hypothetical protein	6,22	5,00798E-41	2,18105E-39
VSAL_I1904	secretion protein, HlyD family	6,24	7,26618E-35	2,47156E-33
VSAL_I1660	PTS system, lactose/cellobiose specific IIA subunit	6,27	2,31787E-64	2,00024E-62
VSAL_I1943	transposase	6,32	0,010084612	0,02343855
VSAL_II0449	conserved hypothetical protein	6,33	7,85952E-33	2,44169E-31
VSAL_I1661	hypothetical protein (fragment)	6,36	2,66342E-47	1,39455E-45
VSAL_I0411	hemolysin	6,37	3,14411E-43	1,43643E-41
VSAL_I0849	succinyl-CoA synthetase alpha chain	6,40	3,07306E-78	3,87039E-76
VSAL_I2946	universal stress protein A	6,45	1,41219E-18	2,11601E-17
VSAL_I0567	sigma-54 interacting regulatory protein	6,45	1,96543E-52	1,20512E-50
VSAL_I1906	membrane protein	6,47	6,12272E-40	2,52495E-38
VSAL_I4107s	srna	6,52	4,92185E-19	7,61987E-18
VSAL_I1730	succinylglutamate desuccinylase	6,58	1,49276E-64	1,33774E-62
VSAL_I2507	lipoprotein	6,61	6,77955E-82	9,57355E-80
VSAL_I1198	probable membrane permease	6,75	3,4199E-40	1,42292E-38
VSAL_I2974	fatty oxidation complex alpha subunit, enoyl-CoA hydratase	6,89	3,51062E-36	1,25842E-34
VSAL_II0166	hypothetical protein	6,92	3,26305E-31	9,27183E-30
VSAL_II0428	integral membrane protein, putative two-component signal tra	6,94	6,70766E-40	2,7419E-38
VSAL_II0963	acyl transferase LuxD	6,99	1,65072E-30	4,55168E-29
VSAL_I1585	NAD-dependent deacetylase	7,02	7,31479E-58	5,32608E-56
VSAL_I0412	membrane protein	7,02	1,21834E-34	4,11412E-33
VSAL_I2437	conserved hypothetical protein	7,07	3,97201E-18	5,71283E-17

VSAL_I2054	general L-amino acid transport ATP-binding subunit	7,22	1,79427E-27	4,49533E-26
pVSAL840_26	hypothetical protein	7,33	6,50244E-55	4,2678E-53
VSAL_II0879	NifS-related protein, putative aminotransferase	7,36	2,12365E-61	1,64937E-59
VSAL_II0059	putative type I toxin secretion system, membrane transport pro	7,37	3,04825E-40	1,28014E-38
VSAL_I1676	aquaporin Z (bacterial nodulin-like intrinsic protein)	7,46	8,12794E-27	1,95238E-25
VSAL_II0058	putative type I toxin secretion system, outer membrane efflux p	7,47	1,83154E-28	4,76813E-27
VSAL_I0413	hypothetical protein	7,48	7,10056E-39	2,75739E-37
VSAL_I0639	oxaloacetate decarboxylase 2, subunit alpha	7,57	7,58199E-56	5,35334E-54
VSAL_I0640	oxaloacetate decarboxylase, beta subunit	7,58	2,17431E-57	1,55881E-55
VSAL_I1385	conserved hypothetical protein	7,69	8,74761E-22	1,61122E-20
VSAL_I0991	conserved hypothetical protein	7,70	3,237E-27	7,98118E-26
VSAL_II2004s	srna	7,72	3,70469E-30	1,01552E-28
VSAL_II1012	response regulator, histidine kinase	7,79	7,52295E-34	2,43451E-32
VSAL_I1960	arginine/ornithine periplasmic binding protein-dependent trans	7,82	2,62764E-50	1,54997E-48
VSAL_I0860	transcriptional activator MetR	7,92	3,52819E-23	7,2429E-22
VSAL_I4059s	srna	7,95	5,33759E-37	1,94321E-35
VSAL_II0167	hypothetical protein	8,02	9,11145E-23	1,79913E-21
VSAL_I1197	glutamate decarboxylase beta	8,18	2,48266E-44	1,1927E-42
VSAL_I0809	transposase	8,43	0,285681111	0,391436042
VSAL_I2443	putative exported protein	8,44	3,18502E-61	2,43315E-59
VSAL_II0325	putative exported protein	8,48	1,27535E-66	1,18862E-64
VSAL_I1364	putative exported nuclease	8,51	5,31698E-34	1,73267E-32
VSAL_II0705	imidazolonepropionase	8,53	3,92961E-22	7,44389E-21
VSAL_II0053	membrane associated response regulator, histidine kinase	8,60	1,30769E-66	1,19487E-64
VSAL_II0880	cell aggregate formation protein, biofilm development BsmA	8,74	2,05266E-72	2,27748E-70
VSAL_I2854	Regulator of RNA polymerase sigma (70) subunit	8,74	5,89169E-55	3,92218E-53
VSAL_II0316	response regulator, histidine kinase	8,89	9,1926E-68	8,74235E-66
VSAL_II0404	conserved hypothetical protein	8,98	6,04553E-05	0,000222881
VSAL_I0827	asparagine synthetase B	9,03	1,25339E-83	1,94693E-81
VSAL_II0133	putative sodium/sulfate symporter (fragment)	9,05	3,49609E-33	1,1008E-31
VSAL_II0066	membrane protein	9,25	2,46435E-38	9,2612E-37
VSAL_I0405	putative membrane protein	9,34	9,55709E-63	7,95286E-61

VSAL_II0384	glycerol uptake facilitator protein	9,38	4,52493E-24	9,76212E-23
VSAL_II0324	putative lipoprotein	9,49	2,37364E-70	2,45803E-68
VSAL_II0509	hypothetical protein	9,59	1,76188E-31	5,09959E-30
VSAL_II0960	long-chain-fatty-acid ligase LuxE	9,85	9,27534E-30	2,48409E-28
VSAL_I4092s	srna	9,90	1,04629E-69	1,05994E-67
VSAL_I1957	arginine/ornithine periplasmic binding protein-dependent trans	10,05	4,88088E-74	5,83202E-72
VSAL_II0385	glycerol kinase	10,10	4,08856E-30	1,11419E-28
VSAL_II0959	probable flavin reductase LuxG	10,14	4,91005E-32	1,46672E-30
VSAL_II1013	putative heme binding protein	10,23	2,58423E-55	1,77095E-53
VSAL_II0333	transposase	10,31	2,70957E-62	2,21519E-60
VSAL_II0706	arginase	10,42	8,67577E-10	6,15359E-09
VSAL_II0057	putative membrane associated response regulator	10,88	2,71663E-34	8,97836E-33
VSAL_I0356	putative exported protein	10,88	6,71326E-97	1,42199E-94
VSAL_I1856	hypothetical protein	11,01	7,08487E-30	1,90841E-28
VSAL_II0319	RNA polymerase sigma factor	11,04	4,48026E-43	2,02699E-41
VSAL_I1959	arginine/ornithine periplasmic binding protein-dependent trans	11,17	1,52675E-72	1,77866E-70
VSAL_I2444	accessory colonization factor precursor AcfA	11,38	3,41101E-60	2,56376E-58
VSAL_II0056	putative type I secretion protein, HlyD family	11,39	6,75456E-44	3,11646E-42
VSAL_I2506	RNA polymerase sigma subunit RpoS (sigma-38)	11,49	8,03186E-88	1,43956E-85
VSAL_I2431	hypothetical protein	11,62	2,05187E-72	2,27748E-70
VSAL_I2267	fatty acid oxidation complex alpha subunit [includes: enoyl-co h	11,76	1,57797E-69	1,56454E-67
VSAL_I2698	hypothetical protein (pseudogene)	12,06	3,39307E-64	2,87485E-62
VSAL_I1317	carbon starvation protein (pseudogene)	12,09	1,83417E-55	1,27571E-53
VSAL_I1832	hypothetical protein (fragment)	12,13	7,68169E-82	1,02276E-79
VSAL_I1946	oligopeptide transport system permease protein B	12,18	3,39109E-75	4,15855E-73
VSAL_I1839	alanine dehydrogenase	12,18	1,03869E-87	1,7927E-85
VSAL_II0063	putative type I secretion system, ATP-binding protein	12,50	6,48867E-58	4,79955E-56
VSAL_II0763	putative DNA-binding protein	12,86	1,9801E-12	1,83258E-11
VSAL_I0631	putative AMP-binding acetyl-CoA synthetase	12,89	5,37189E-69	5,21521E-67
VSAL_II0064	putative type I secretion protein, HlyD family	12,99	2,1904E-54	1,41768E-52
VSAL_II0330	hypothetical protein	13,10	1,40543E-31	4,11907E-30
VSAL_I2268	3-ketoacyl-CoA thiolase (fatty acid oxidation complex subunit b	13,14	5,19152E-34	1,7037E-32

VSAL_I1229	putative immunogenic protein precursor	13,68	1,16709E-71	1,2648E-69
VSAL_II0073	hypothetical protein	13,84	1,09659E-35	3,8135E-34
VSAL_I1591	hypothetical protein	14,29	1,651E-123	5,9183E-121
VSAL_II0961	alkanal monooxygenase beta chain LuxB (bacterial luciferase be	15,13	1,17798E-30	3,28707E-29
VSAL_II0320	putative membrane associated signaling protein	15,20	9,0798E-116	2,4889E-113
VSAL_I1369	D-ribose-binding periplasmic protein precursor RbsB	15,41	1,95337E-27	4,86775E-26
VSAL_II0594	putative membrane protein	16,00	8,1275E-62	6,41934E-60
VSAL_I0755	membrane protein	16,00	5,7567E-124	2,2355E-121
VSAL_I0859	hypothetical protein	16,30	5,99077E-10	4,34168E-09
VSAL_II0055	hypothetical protein	16,67	5,21636E-79	6,75229E-77
VSAL_II0764	glycine cleavage system H protein	17,04	3,03416E-10	2,26227E-09
VSAL_II0964	acyl-CoA reductase LuxC	17,11	2,74501E-53	1,70557E-51
VSAL_I4078s	srna	17,64	3,1838E-17	4,19111E-16
VSAL_II0457	7 purine nucleoside phosphorylase	17,67	2,21436E-13	2,2002E-12
VSAL_II0962	alkanal monooxygenase alpha chain LuxA (bacterial luciferas al	17,97	4,51842E-49	2,50665E-47
VSAL_II0332	putative hemolysin-type calcium-binding protein (fragment)	18,17	5,45614E-89	1,0594E-86
VSAL_II0765	glycine dehydrogenase (decarboxylating)	18,36	2,31235E-10	1,75498E-09
VSAL_I2549	hypothetical protein	19,44	2,93796E-10	2,2072E-09
VSAL_II0326	hypothetical protein	19,45	6,54245E-84	1,0513E-81
VSAL_II0329	putative response regulator	19,90	7,17131E-82	9,82891E-80
VSAL_I2212	cold shock-like protein CspD	20,18	7,82433E-89	1,45846E-86
VSAL_II1002	sodium/proton-dependent alanine carrier protein	20,93	3,08457E-82	4,49191E-80
VSAL_I2827	putative membrane protein	22,68	4,15106E-39	1,63932E-37
VSAL_I2828	putative sodium/solute symporter	22,78	7,88283E-48	4,32164E-46
VSAL_II0323	putative lipoprotein	23,65	4,5928E-116	1,3376E-113
VSAL_I2395	acyl-coenzyme A dehydrogenase	23,68	7,4527E-118	2,4807E-115
VSAL_II2034s	srna	25,69	2,41869E-38	9,16348E-37
VSAL_I2206	putative sporulation protein	26,37	1,0129E-149	4,72E-147
VSAL_II0707	urocanate hydratase	26,65	1,83984E-18	2,73047E-17
VSAL_II0708	histidine ammonia-lyase	27,11	2,23076E-20	3,76643E-19
VSAL_II0321	putative glycosyl transferase	28,25	1,0373E-158	6,9055E-156
VSAL_II0322	putative membrane protein	28,74	1,8147E-153	1,0571E-150

VSAL_I2832	putative exonuclease	29,93	1,36485E-45	6,83894E-44
VSAL_I0315	transposase	29,98	0,004869556	0,012312604
VSAL_I4133s	srna	31,27	6,9307E-110	1,7943E-107
VSAL_I1958	arginine/ornithine periplasmic binding protein-dependent trans	32,83	3,8458E-104	9,4324E-102
VSAL_II2029s	srna	33,37	7,15219E-83	1,07513E-80
VSAL_II0054	hypothetical protein	33,61	9,4356E-174	8,794E-171
VSAL_I2207	conserved hypothetical protein	35,75	1,6298E-100	3,61658E-98
VSAL_I2831	putative nucleotidyltransferases	38,11	8,45211E-19	1,28296E-17
VSAL_II0327	putative nucleotidyl transferase	40,77	7,5614E-117	2,3491E-114
VSAL_I1555	ribosome modulation factor	44,83	5,9745E-163	4,6402E-160
VSAL_II0328	putative anti-sigma F factor antagonist	47,87	1,27435E-94	2,58194E-92
VSAL_I2057	general L-amino acid-binding periplasmic protein precursor	51,77	3,6494E-146	1,546E-143
VSAL_I2208	putative PrkA serine protein kinase	56,64	4,8091E-180	5,6026E-177
VSAL_I2438	isocitrate lyase	57,86	4,37324E-19	6,7931E-18
VSAL_I2439	malate synthase A	61,58	1,98043E-15	2,30144E-14
VSAL_II0389	transposase	101,29	0,088703691	0,151635803
VSAL_I1321	hypothetical protein	113,31	6,8765E-241	1,0682E-237
VSAL_I1339	transposase	129,70	0,07279675	0,128692282
VSAL_I1911	transposase	237,06	2,03499E-10	1,55971E-09
VSAL_I2833	acetyl-coenzyme A synthetase	290,53	0	0
VSAL_I0514	transposase (pseudogene)	529,36	9,53244E-14	9,87137E-13
VSAL_II0030	transposase (pseudogene)	1975,26	5,5138E-20	9,01555E-19

Additional file 3

Table S3 The functional distribution of one thousand and thirteen DEGs of wt1.2/wt0.3 The table represents the number of up (*n* = 597) and downregulated (*n* = 416) genes with their percentage distribution within the different functional groups.

Functional categories	**Upregulated genes (n=597)**		**Downregulated genes (n=416)**	
	Number of genes (n)	*Percentage (%)*	*Number of genes (n)*	*Percentage (%)*
Unknown function, no known homologues	94	15.7	40	9.6
Cell processes	4	0.6	37	8.8
Protection responses	3	0.5	3	0.7
Transport/binding proteins	73	12.2	57	13.7
Adaptation	8	1.3	2	0.4
Cell division	3	0.5	1	0.2
Macromolecule metabolism	20	3.3	6	1.4
Macromolecule synthesis, modification	13	2.1	21	5.0
Amino acid biosynthesis	14	2.1	3	0.7
Biosynthesis of cofactors, carriers	8	1.3	11	2.6
Central intermediary metabolism	29	4.8	6	1.4
Degradation of small molecules	29	4.8	9	2.1
Energy metabolism, carbon	34	5.6	11	2.6
Fatty acid biosynthesis	3	0.5	0	0
Nucleotide biosynthesis	0	0	8	1.9
Cell envelope	97	16.2	57	13.7
Ribosome constituents	2	0.3	47	11.2
Extrachromosomal / foreign DNA	28	4.6	48	11.5
Regulation	59	9.8	8	1.9
Not classified (included putative assignments)	31	5.1	8	1.9
sRNA	45	7.5	33	7.9

Additional file 4 **Table S4. The table lists the differentially expressed genes of *ΔlitR* mutant compared to wild-type at LCD.**

VSAL_nr	Function	Fold Change	p-value	p-adjusted
VSAL_II0366	fimbrial protein, Flp/Fap pilin component	12,21	7,7059E-78	7,54215E-75
VSAL_II0367	type IV leader peptidase	8,59	6,03254E-62	3,93623E-59
VSAL_II0721	PTS system permease for N-acetylglucosamine and glucose	5,86	3,33917E-51	1,86755E-48
VSAL_I1342	hypothetical protein	5,05	1,69568E-64	1,32772E-61
VSAL_II0370	putative lipoprotein	4,67	4,97159E-40	1,76943E-37
VSAL_II0368	putative Flp pilus assembly protein	4,30	2,73116E-41	1,06925E-38
VSAL_I2117	methyl-accepting chemotaxis protein (fragment)	3,84	1,01859E-28	2,65852E-26
VSAL_II0371	type II secretion system protein Z	3,73	5,34793E-27	1,30857E-24
VSAL_II0372	type II/IV secretion system protein, ATP binding domain	3,67	9,03283E-30	2,52597E-27
VSAL_II0369	type II/III secretion system protein	3,45	1,40469E-32	4,58279E-30
VSAL_II0252	hypothetical protein	2,81	1,0566E-18	1,42641E-16
VSAL_I1475	hypothetical protein	2,63	7,25141E-20	1,05145E-17
VSAL_II0753	outer membrane protein, OmpA family	2,62	1,09831E-18	1,43329E-16
VSAL_II0823	PTS system, lactose/cellobiose specific IIB subunit	2,53	9,27644E-16	1,03764E-13
VSAL_II0373	bacterial type II secretion system protein F	2,49	1,97834E-13	1,88908E-11
VSAL_II1062	membrane protein	2,47	1,40655E-18	1,72082E-16
VSAL_I2124	hypothetical protein	2,45	4,99088E-08	NA
VSAL_I2749	probable HTH-type transcriptional regulator LeuO	2,43	1,7563E-20	2,64458E-18
VSAL_II0312	hypothetical protein, putative anti-sigma factor antagonist	2,41	3,56556E-08	NA
VSAL_II1088	putative membrane protein	2,38	6,54613E-10	3,76884E-08
VSAL_II0722	hypothetical protein	2,34	1,67353E-07	NA
VSAL_II0824	putative sugar-specific permease, SgaT/UlaA	2,25	3,88442E-26	8,94559E-24
VSAL_II0362	hypothetical protein	2,19	1,34219E-10	8,90624E-09
VSAL_I1325	proton glutamate symport protein	2,15	1,25916E-14	1,33233E-12
VSAL_I1982	putative DNA transformation protein TfoX	2,11	9,23987E-10	5,16773E-08
VSAL_I4118s	srna	2,09	6,48697E-10	3,76884E-08
VSAL_I1012	phage regulatory protein CII	2,09	4,06334E-10	2,52508E-08
VSAL_II0825	putative phosphotransferase enzyme II, A component	2,06	9,23585E-17	1,09571E-14
VSAL_I2495	hypothetical protein	2,03	4,49817E-10	2,70928E-08
VSAL_I0550	endonuclease I precursor	2,02	9,73955E-12	7,1944E-10
VSAL_II0171	putative membrane protein	2,02	8,08102E-13	7,03049E-11

VSAL_I0880	hypothetical protein	-2,02	1,80784E-06	6,75535E-05
VSAL_II0914	MFS transporter	-2,06	2,9181E-05	0,00075658
VSAL_II0010	conserved hypothetical protein	-2,07	2,72207E-08	1,34897E-06
VSAL_I0137	TonB-dependent iron-siderophore receptor precursor	-2,15	3,77586E-13	3,51964E-11
VSAL_I0135	siderophore biosynthetis protein	-2,23	3,04269E-10	1,92131E-08
VSAL_II0238	glucose-1-phosphate adenylyltransferase	-2,28	4,32415E-06	0,0001485
VSAL_I0134	L-2,4-diaminobutyrate decarboxylase	-2,35	4,15283E-12	3,25167E-10
VSAL_I4020s	srna	-2,36	1,76152E-06	NA
VSAL_I0395	hypothetical protein, putative phage gene (fragment)	-2,42	7,66044E-13	6,81605E-11
VSAL_I1484	short chain dehydrogenase	-2,48	8,01594E-14	7,84561E-12
pVSAL840_57	hypothetical protein	-2,49	3,32766E-19	4,65279E-17
VSAL_II0322	putative membrane protein	-2,54	1,45053E-14	1,49443E-12
VSAL_I1395	membrane protein	-2,58	2,09759E-22	3,9105E-20
VSAL_II0968	putative exported protein	-2,63	4,81081E-31	1,44879E-28
VSAL_I1458	hypothetical protein	-2,63	4,361E-14	4,37777E-12
VSAL_I1198	probable membrane permease	-2,72	NA	NA
VSAL_I0136	siderophore biosynthesis protein	-2,76	1,06009E-22	2,07512E-20
VSAL_II0321	putative glycosyl transferase	-2,84	1,14656E-18	1,448E-16
VSAL_I1394	hypothetical protein	-3,00	1,79994E-44	7,82975E-42
VSAL_II0323	putative lipoprotein	-3,06	4,86763E-24	1,05871E-21
VSAL_I1197	glutamate decarboxylase beta	-3,08	8,36359E-23	1,72334E-20
VSAL_I1456	ribosomal-protein-serine acetyltransferase	-3,23	1,47877E-20	2,31576E-18
VSAL_I1457	hypothetical protein	-3,43	4,11961E-21	7,0123E-19
VSAL_I1493	microbial collagenase precursor (pseudogene)	-3,63	1,73163E-48	8,47418E-46
VSAL_II0320	putative membrane associated signaling protein	-3,83	6,00605E-21	9,79737E-19
VSAL_II0319	RNA polymerase sigma factor	-4,29	4,40214E-22	7,83381E-20
pVSAL840_56	hypothetical protein	-4,72	1,34624E-85	1,75685E-82
VSAL_I2620	transposase (pseudogene)	-6,17	8,4125E-106	1,6467E-102
VSAL_II0964	acyl-CoA reductase LuxC	-9,71	0,99987166	0,99987166
VSAL_II0130	transposase	-10,44	1,85609E-38	NA
VSAL_I2619	HTH-type luminescence regulator LitR	-141,22	8,2757E-298	3,2399E-294

Additional file 5 Table S5. The table lists the differentially expressed genes of *ΔlitR* mutant compared to wild-type at HCD.

VSAL_nr	Function	Fold Change	p-value	p-adjusted
VSAL_I2619	HTH-type luminescence regulator LitR	-588,49	4,4905E-258	1,7881E-254
VSAL_I2620	transposase (pseudogene)	-10,48	1,03742E-44	3,40013E-42
VSAL_II0327	putative nucleotidyl transferase	-9,74	1,14685E-65	9,13352E-63
VSAL_II0322	putative membrane protein	-9,29	6,50825E-78	1,29579E-74
VSAL_II0323	putative lipoprotein	-9,08	4,8567E-54	2,76277E-51
VSAL_II0321	putative glycosyl transferase	-9,00	6,23808E-66	6,21001E-63
VSAL_II0320	putative membrane associated signaling protein	-9,00	7,6314E-72	1,01294E-68
VSAL_II0328	putative anti-sigma F factor antagonist	-8,79	1,47729E-34	3,26809E-32
VSAL_II0330	hypothetical protein	-8,76	NA	NA
VSAL_I1197	glutamate decarboxylase beta	-8,50	NA	NA
VSAL_II0054	hypothetical protein	-8,46	1,3171E-53	6,55585E-51
VSAL_I1198	probable membrane permease	-8,38	1,72507E-58	1,14487E-55
pVSAL840_56	hypothetical protein	-7,66	1,21758E-47	5,3871E-45
VSAL_II0319	RNA polymerase sigma factor	-7,51	3,43733E-39	9,77675E-37
VSAL_II0332	putative hemolysin-type calcium-binding protein (fragment)	-7,38	1,59682E-38	4,23903E-36
VSAL_II0326	hypothetical protein	-7,34	2,24293E-38	5,58208E-36
VSAL_II0324	putative lipoprotein	-6,70	3,63773E-30	7,62392E-28
VSAL_I2057	general L-amino acid-binding periplasmic protein precursor	-6,60	1,46194E-27	2,91071E-25
VSAL_I0264	ADP-L-glycero-D-manno-heptose-6-epimerase	6,50	0,999906077	0,999906077
VSAL_I2208	putative PrkA serine protein kinase	-6,21	1,40249E-26	2,42814E-24
VSAL_II0329	putative response regulator	-6,14	NA	NA
VSAL_I2207	conserved hypothetical protein	-5,53	1,4033E-47	5,58793E-45
VSAL_II0325	putative exported protein	-5,38	1,14706E-16	1,34341E-14
VSAL_I1394	hypothetical protein	-5,34	9,70632E-45	3,40013E-42
VSAL_II0057	putative membrane associated response regulator	-4,95	7,10488E-16	7,44517E-14
VSAL_II0055	hypothetical protein	-4,93	9,90388E-24	1,57749E-21
VSAL_I1456	ribosomal-protein-serine acetyltransferase	-4,68	2,09505E-23	3,08981E-21
VSAL_II0333	transposase	-4,43	3,69029E-16	4,08188E-14
VSAL_I2206	putative sporulation protein	-4,41	1,54789E-35	3,62571E-33
VSAL_II0063	putative type I secretion system, ATP-binding protein	-4,38	1,17126E-12	8,96918E-11
VSAL_II0237	conserved hypothetical protein	-4,36	9,22041E-16	9,41428E-14

VSAL_II0064	putative type I secretion protein, HlyD family	-4,29	3,9934E-11	2,74167E-09
VSAL_II0058	putative type I toxin secretion system, outer membrane efflux prot	-4,26	1,08868E-09	6,66944E-08
VSAL_I1832	hypothetical protein (fragment)	-4,25	6,21313E-25	1,03086E-22
VSAL_II0066	membrane protein	-4,14	1,35632E-08	6,83655E-07
VSAL_I1676	aquaporin Z (bacterial nodulin-like intrinsic protein)	-4,11	5,73719E-12	4,23065E-10
VSAL_I0755	membrane protein	-4,08	9,34802E-17	1,12799E-14
VSAL_II0056	putative type I secretion protein, HlyD family	-3,93	3,54996E-13	2,94499E-11
VSAL_II0053	membrane associated response regulator, histidine kinase	-3,92	5,25966E-19	6,75612E-17
VSAL_I2698	hypothetical protein (pseudogene)	-3,62	2,26751E-18	2,82164E-16
VSAL_II0316	response regulator, histidine kinase	-3,62	4,69341E-13	3,81411E-11
pVSAL840_26	hypothetical protein	-3,62	4,4177E-16	4,7544E-14
pVSAL840_57	hypothetical protein	-3,60	3,66898E-27	6,95708E-25
VSAL_I1457	hypothetical protein	-3,45	1,51085E-07	6,26688E-06
VSAL_I4059s	srna	-3,40	2,61231E-10	1,67778E-08
VSAL_II0318	putative exported protein	-3,31	3,225E-09	1,83456E-07
VSAL_I1591	hypothetical protein	-3,30	5,37543E-11	3,62796E-09
VSAL_II0644	putative membrane protein	-3,28	2,52053E-07	1,02416E-05
VSAL_II0059	putative type I toxin secretion system, membrane transport protei	-3,24	2,73849E-06	9,5655E-05
VSAL_II0052	response regulator protein	-3,23	2,59291E-20	3,44166E-18
VSAL_I4092s	srna	-3,19	4,0299E-12	3,02775E-10
VSAL_I2054	general L-amino acid transport ATP-binding subunit	-3,17	NA	NA
VSAL_II0060	putative type I toxin secretion system, ATP-binding protein	-3,13	1,30357E-05	0,000403146
VSAL_I1395	membrane protein	-3,10	1,03637E-12	8,25367E-11
VSAL_II0331	putative exported protein	-2,85	6,2243E-08	2,75391E-06
VSAL_I2055	general L-amino acid ABC transporter permease protein	-2,83	3,624E-05	0,001038184
VSAL_I1904	secretion protein, HlyD family	-2,82	1,83496E-13	1,55464E-11
VSAL_I1589	hypothetical protein	-2,80	1,58771E-11	1,1495E-09
VSAL_I2069	putative ABC transporter, ATP-binding protein (fragment)	-2,77	1,15018E-07	4,87235E-06
VSAL_I2056	general L-amino acid ABC transporter permease protein	-2,74	3,46143E-07	1,37834E-05
VSAL_I1458	hypothetical protein	-2,73	5,09073E-06	0,000167531
VSAL_I2085	heat shock protein	-2,63	6,3719E-09	3,42877E-07
VSAL_II0067	hypothetical protein	-2,62	0,002259137	0,037026249

VSAL_I0476	type IV pilus, mannose-sensitive hemagglutinin A	-2,57	2,87826E-09	1,66105E-07
VSAL_I1590	quinolone resistance determinant QnrC	-2,53	1,43438E-08	7,05149E-07
VSAL_II0394	cytochrome c551 peroxidase	-2,52	8,53215E-05	0,002206169
VSAL_II1012	response regulator, histidine kinase	-2,52	3,4881E-09	1,95628E-07
VSAL_I1808	hypothetical protein	-2,51	6,47095E-10	4,09005E-08
VSAL_I0395	hypothetical protein, putative phage gene (fragment)	-2,51	4,14602E-09	2,29298E-07
VSAL_II0238	glucose-1-phosphate adenylyltransferase	-2,51	2,84858E-08	1,33448E-06
VSAL_I1906	membrane protein	-2,50	6,81119E-07	2,58306E-05
VSAL_I1484	short chain dehydrogenase	-2,48	2,63995E-07	1,06185E-05
VSAL_II1013	putative heme binding protein	-2,48	2,0558E-09	1,22182E-07
VSAL_I0588	putative exported protein	-2,46	1,35384E-07	5,67472E-06
VSAL_I2214	ATP-dependent Clp protease ATP-binding subunit ClpA	-2,43	5,2939E-07	2,08716E-05
VSAL_I2213	ATP-dependent Clp protease adaptor protein ClpS	-2,42	7,26904E-07	2,73069E-05
pVSAL840_28	DNA-binding protein HU-alpha	-2,42	5,7809E-07	2,25682E-05
VSAL_II0062	membrane protein	-2,42	0,00049668	0,010300945
VSAL_II0315	putative response regulator	-2,40	2,19135E-05	0,000651192
VSAL_II0920	maltose transport system permease protein MalG	-2,36	9,49398E-08	4,10924E-06
VSAL_II0040	1,4-alpha-glucan branching enzyme (fragment)	-2,35	2,40201E-09	1,40659E-07
VSAL_II0020	hemolysin-type calcium-binding protein	-2,29	1,71816E-11	1,22174E-09
VSAL_I0401	hypothetical protein	-2,28	8,92222E-07	3,3204E-05
VSAL_II0393	response regulator, histidine kinase	-2,26	0,00174971	0,030425095
VSAL_I0099	putative exonuclease	-2,24	9,64374E-10	6,00022E-08
VSAL_II0428	integral membrane protein, putative two-component signal transd	-2,23	1,43742E-06	5,2512E-05
VSAL_II0446	binding-protein-dependent transport system inner membrane com	-2,22	NA	NA
VSAL_II0280	integral membrane protein	-2,22	6,16649E-08	2,75391E-06
VSAL_II0281	membrane protein	-2,17	1,49182E-08	7,24443E-07
VSAL_I1238	exported serine protease (pseudogene)	-2,13	7,38263E-06	0,000239005
VSAL_I1555	ribosome modulation factor	-2,12	2,97903E-05	0,000872241
VSAL_I0631	putative AMP-binding acetyl-CoA synthetase	-2,11	2,44567E-06	8,6183E-05
VSAL_I1907	putative ion channel	-2,07	0,000935214	0,018077781
VSAL_II0424	putative fatty acid desaturase	-2,06	NA	NA
VSAL_II0239	glycogen synthase	-2,06	1,5389E-06	5,56336E-05

VSAL_II0061	exported glycosyl hydrolase, family 16	-2,02	NA	NA
VSAL_II0445	bacterial extracellular solute-binding protein	-2,02	NA	NA
VSAL_II0065	membrane protein	-2,02	0,026925276	0,23307924
VSAL_I2068	membrane protein	-2,01	3,03662E-05	0,000882614
VSAL_I4075s	srna	-2,01	0,032281634	0,256066669
VSAL_I1325	proton glutamate symport protein	12,00	1,11004E-44	3,40013E-42
VSAL_II0366	fimbrial protein, Flp/Fap pilin component	10,24	3,24653E-15	2,93811E-13
VSAL_II1088	putative membrane protein	7,16	6,51407E-27	1,17905E-24
VSAL_II0721	PTS system permease for N-acetylglucosamine and glucose	6,78	2,20112E-21	3,02236E-19
VSAL_II0367	type IV leader peptidase	6,44	1,38951E-14	1,20283E-12
VSAL_I1608	HTH-type transcriptional regulator GalR	5,24	1,10699E-23	1,6954E-21
VSAL_I2820	hypothetical protein	4,07	2,12365E-15	2,06253E-13
VSAL_II0102	hypothetical protein	4,02	1,79491E-10	1,17169E-08
VSAL_I1610	putative aminotransferase class I and II	3,95	1,97882E-15	1,96992E-13
VSAL_II0825	putative phosphotransferase enzyme II, A component	3,84	3,22749E-22	4,58995E-20
VSAL_II0134	hypothetical protein	3,65	4,30851E-15	3,81255E-13
VSAL_I1018	hypothetical protein, putative phage gene	3,65	5,22731E-05	0,001406428
VSAL_II0662	putative signaling protein	3,58	1,53728E-16	1,74898E-14
VSAL_I2117	methyl-accepting chemotaxis protein (fragment)	3,46	4,5447E-09	2,47904E-07
VSAL_II0362	hypothetical protein	3,41	1,05928E-12	8,27067E-11
VSAL_II0824	putative sugar-specific permease, SgaT/UlaA	3,40	2,50547E-11	1,75031E-09
VSAL_I2124	hypothetical protein	3,38	1,1288E-08	5,78291E-07
VSAL_II0823	PTS system, lactose/cellobiose specific IIB subunit	3,35	6,26367E-07	2,42155E-05
VSAL_II0338	MFS transporter	3,34	2,17639E-15	2,06342E-13
VSAL_II0337	glycerophosphoryl diester phosphodiesterase	3,21	3,67458E-08	1,70142E-06
VSAL_II0369	type II/III secretion system protein	3,10	1,72728E-06	6,14109E-05
VSAL_I0103	HTH-type transcriptional regulator	2,94	1,39992E-08	6,96813E-07
VSAL_I1982	putative DNA transformation protein TfoX	2,88	9,60475E-11	6,37435E-09
VSAL_I1609	sodium/proton antiporter	2,88	9,75432E-09	5,11075E-07
VSAL_I2950	putative signaling protein (pseudogene)	2,86	2,50191E-15	2,31688E-13
VSAL_II1079	NADPH-flavin oxidoreductase	2,85	6,9023E-08	3,02032E-06
VSAL_II0370	putative lipoprotein	2,74	0,000470016	0,009798979

VSAL_I4118s	rna	2,72	1,55081E-06	5,56336E-05
VSAL_I1927	hypothetical protein, putative phage gene (fragment)	2,71	NA	NA
VSAL_II0384	glycerol uptake facilitator protein	2,71	1,6865E-09	1,01752E-07
VSAL_I1974	ABC transporter, ATP-binding component	2,68	NA	NA
VSAL_I2319	hypothetical protein	2,64	6,0259E-08	2,72672E-06
VSAL_I0550	endonuclease I precursor	2,62	1,0612E-07	4,54376E-06
VSAL_I1029	phage terminase, endonuclease subunit	2,61	0,001503921	0,026975734
VSAL_I1015	hypothetical protein, putative phage gene	2,61	NA	NA
VSAL_I2017	MFS transporter	2,60	NA	NA
VSAL_II0138	hypothetical protein	2,59	1,13276E-08	5,78291E-07
VSAL_I0560	branched chain amino acid transport system II carrier protein	2,57	9,2064E-09	4,88799E-07
VSAL_II0139	PilA-like type-IV pilus protein	2,55	3,1311E-06	0,000108418
VSAL_II0363	putative response regulator	2,55	0,000124546	0,003042585
VSAL_I0007	putative amino-acid ABC transporter, permease protein	2,53	NA	NA
VSAL_II0373	bacterial type II secretion system protein F	2,53	NA	NA
VSAL_II0385	glycerol kinase	2,52	1,79841E-08	8,62802E-07
VSAL_I1037	hypothetical protein, putative phage gene	2,50	NA	NA
VSAL_I1043	hypothetical protein, putative phage gene	2,50	NA	NA
VSAL_I1038	hypothetical protein, putative phage gene	2,44	0,009086747	NA
VSAL_II0372	type II/IV secretion system protein, ATP binding domain	2,43	3,19642E-06	0,000108788
VSAL_I1035	probable tail tube protein	2,42	0,004628046	0,063245338
pVSAL840_11	conjugative transfer protein TraU	2,42	NA	NA
VSAL_II0368	putative Flp pilus assembly protein	2,42	NA	NA
VSAL_I2173	hypothetical protein, GGDEF domain	2,38	4,40979E-08	2,01837E-06
VSAL_II0371	type II secretion system protein Z	2,38	0,000180569	0,004220895
VSAL_I0773	putative bacteriophage terminase	2,37	NA	NA
pVSAL54_02	putative mobilization protein	2,36	NA	NA
VSAL_I0679	putative C4-dicarboxylate/malic acid transport protein	2,31	6,52661E-07	2,49894E-05
VSAL_I1020	phage replication protein	2,30	0,000593957	0,012005771
VSAL_I1813	sodium/dicarboxylate symporter	2,29	0,000710865	0,014224444
VSAL_I1028	major capsid protein	2,28	0,000149907	0,003574427
VSAL_II0914	MFS transporter	2,26	0,012617374	0,139555461

VSAL_II0310	polysaccharide biosynthesis/export protein	2,26	0,001319543	0,024326018
VSAL_I2631	type IV pilus assembly protein PilC (pseudogene)	2,25	0,01169986	0,133110982
VSAL_I2577	ABC-type [(GlcNAc)2] transporter, permease protein	2,25	0,007504674	0,09397362
VSAL_I1026	terminase, ATPase subunit	2,24	0,004159346	0,059792481
VSAL_II0381	response regulator, histidine kinase	2,24	0,003570828	0,053656749
VSAL_I2348	putative membrane associated GGDEF protein	2,23	0,006824619	0,088232573
VSAL_I2192	hypothetical protein	2,22	0,000534257	0,011022865
VSAL_II0899	putative exported protein (pseudogene)	2,21	NA	NA
pVSAL840_12	hypothetical protein, putative conjugative transfer protein TrbC	2,21	NA	NA
VSAL_I0008	putative amino acid ABC transporter, substrate-binding protein	2,21	0,023265466	0,213272622
VSAL_II0252	hypothetical protein	2,21	1,89394E-05	0,0005757
VSAL_II0275	siderophore biosynthesis protein IucC (Pseudogene)	2,20	NA	NA
VSAL_II0715	putative cation efflux system protein	2,20	0,014556875	0,157944078
VSAL_I0423	adenylylsulfate kinase	2,19	0,024408347	0,218905494
VSAL_II0312	hypothetical protein, putative anti-sigma factor antagonist	2,19	0,003803603	0,055889105
VSAL_II0265	hypothetical protein	2,19	NA	NA
VSAL_II0109	cytochrome C-type protein (pseudogene)	2,18	0,004314299	0,061137153
VSAL_I1342	hypothetical protein	2,18	3,68642E-06	0,000123704
VSAL_II0821	putative exported protein	2,18	4,08896E-05	0,001138618
VSAL_I1012	phage regulatory protein CII	2,16	9,29953E-05	0,002389079
VSAL_I1041	probable tail length determinator	2,15	0,009778363	0,116154974
VSAL_I1328	putative membrane associated peptidase	2,15	5,29607E-05	0,001415365
VSAL_I2717	fimbrial assembly protein PilN	2,15	NA	NA
VSAL_II0663	integral membrane protein, putative transmembrane transporter	2,14	1,22851E-05	0,000385192
VSAL_II0119	putative exported protein	2,14	NA	NA
VSAL_II0685	6-phosphogluconate dehydrogenase	2,13	6,28133E-06	0,000205018
VSAL_I1259	HTH-type transcription regulator, RpiR family	2,12	0,000251528	0,005690811
VSAL_II1089	hypothetical protein (fragment)	2,12	0,00034635	0,007375226
VSAL_I1044	hypothetical protein, putative phage gene	2,12	0,028693348	0,243618147
VSAL_I1998	cytochrome c-type protein NrfB precursor	2,11	5,10342E-05	0,001382437
VSAL_II0687	glucose-6-phosphate 1-dehydrogenase	2,10	1,57571E-05	0,000482652
VSAL_I1019	hypothetical protein, putative phage gene	2,10	0,005200341	0,070195796

VSAL_I2963	valine--pyruvate aminotransferase (alanine--valine transaminase)	2,10	1,2043E-05	0,000380597
VSAL_II0135	putative cytochrome b561	2,10	0,000221884	0,005077838
VSAL_I1036	probable rRNA transcription initiatior protein, putative phage gene	2,10	0,030573838	NA
pVSAL54_01	acyltransferase	2,09	NA	NA
VSAL_II0919	maltose transport system permease protein MalF (fragment)	2,09	0,012124405	0,136382431
VSAL_I1502	putative acyltransferase	2,08	0,000110431	0,002783142
VSAL_II0273	siderophore biosynthesis protein IucA (fragment)	2,07	NA	NA
VSAL_I0703	PTS system, cellobiose permease IIC component	2,07	NA	NA
VSAL_I0108	membrane protein	2,06	NA	NA
pVSAL320_01	hypothetical protein	2,06	0,018624319	0,185869769
VSAL_I2190	integral membrane protein	2,06	0,018495082	0,185061562
VSAL_I1027	phage capsid scaffolding protein	2,06	0,000344808	0,007375226
VSAL_I1033	hypothetical protein, putative phage gene (pseudogene)	2,05	0,019888364	0,195062726
VSAL_II0125	ABC-3 transporter protein, membrane component	2,04	0,026449542	0,229960862
VSAL_I1030	membrane protein, putative phage gene	2,04	0,042199911	NA
VSAL_I4159s	srna	2,03	0,0148031	0,15931336
VSAL_I1014	hypothetical protein, putative phage gene	2,03	0,003691763	0,054649075
VSAL_I2352	chitoporin (pseudogene)	2,02	1,93121E-05	0,000582583
VSAL_I0422	ion transporter superfamily protein	2,01	0,045062469	0,309210606
VSAL_I1017	hypothetical protein, putative phage gene	2,01	0,008972271	0,109258665
VSAL_I0203	sensor outer membrane protein EnvZ	2,00	NA	NA

Additional file 6

Table S6 The functional distribution of sixty-two DEGs of *ΔlitR*/wt at LCD. The table represents the number of up- (n = 31) and downregulated (n = 31) genes with their percentage distribution within the different functional groups.

Functional categories	**Upregulated genes (n=31)**		**Downregulated genes (n=31)**	
	Number of genes (n)	*Percentage (%)*	*Number of genes (n)*	*Percentage (%)*
Unknown function, no known homologues	5	16.1	7	16.1
Cell processes	1	3.2	0	0
Transport/binding proteins	5	16.1	3	9.6
Macromolecule metabolism	1	3.2	1	3.2
Macromolecule synthesis, modification	0	0	1	3.2
Amino acid biosynthesis	0	0	1	3.2
Biosynthesis of cofactors, carriers	0	0	2	6.4
Central intermediary metabolism	0	0	1	3.2
Fatty acid biosynthesis	0	0	1	3.2
Cell envelope	10	32.2	5	16.1
Extrachromosomal / foreign DNA	5	16.1	3	9.6
Regulation	1	3.2	4	12.9
Not classified (included putative assignments)	2	6.4	1	3.2
sRNA	1	3.2	1	3.2

Table S7 The functional distribution of two-hundred and twelve DEGs of *ΔlitR*/wt at HCD. The table represents the number of up (n = 112) and down regulated (n = 100) genes with the percentage of transcripts within the different functional groups.

Functional categories	**Upregulated genes (*n*=112)**		**Downregulated genes (*n*=100)**	
	Number of genes (n)	*Percentage (%)*	*Number of genes (n)*	*Percentage (%)*
Unknown function, no known homologues	9	8.0	19	19
Cell processes	2	1.7	0	0
Protection responses	0	0	1	1
Transport/binding proteins	23	20.5	18	18
Adaptation	0	0	1	1
Cell division	0	0	1	1
Macromolecule metabolism	2	1.7	5	5
Macromolecule synthesis, modification	2	1.7	5	5
Amino acid biosynthesis	1	0.8	0	0
Biosynthesis of cofactors, carriers	2	1.7	0	0
Central intermediary metabolism	5	4.4	2	2
Energy metabolism, carbon	6	5.3	1	1
Fatty acid biosynthesis	0	0	2	2
Cell envelope	17	15.1	19	19
Ribosome constituents	0	0	1	1
Extrachromosomal / foreign DNA	28	25	1	1
Regulation	6	5.3	12	12
Not classified (included putative assignments)	7	6.2	7	7
sRNA	2	1.7	3	3

Additional file 7 **Table S8. The table lists the differentially expressed genes of *ΔrpoQ* mutant compared to wild-type at LCD.**

VSAL_nr	Function	Fold Change	p-value	p-adjusted
pVSAL43_02	acetyltransferase	-64,42	3,3119E-111	1,0529E-108
VSAL_I2327	hypothetical protein	-61,99	0	0
pVSAL43_01	replication initiation protein	-51,33	3,66747E-98	8,91627E-96
VSAL_I2329	hypothetical protein	-37,84	4,6076E-264	6,3478E-261
VSAL_I2328	flagellar hook-associated protein type 3 FlgL	-19,88	8,2385E-164	6,8099E-161
VSAL_I2337	flagellar basal-body rod protein FlgC	-18,63	NA	NA
VSAL_I2338	flagellar basal-body rod protein FlgB	-18,14	1,9497E-296	4,029E-293
VSAL_I2336	flagellar basal-body rod protein FlgD	-18,12	7,7898E-195	8,0488E-192
VSAL_I2335	flagellar hook protein FlgE	-15,86	2,3319E-145	1,6063E-142
VSAL_I2334	flagellar basal-body rod protein FlgF	-11,96	4,5296E-116	1,7019E-113
VSAL_I4140s	srna	-11,79	2,00161E-50	3,06395E-48
VSAL_I2333	flagellar basal-body rod protein FlgG (distal rod protein)	-10,23	3,2651E-93	7,10244E-91
VSAL_I2332	flagellar L-ring protein 1 precursor (basal body L-ring protein 1)	-10,01	4,312E-109	1,1881E-106
VSAL_II0130	transposase	-9,44	2,60892E-25	2,24638E-23
VSAL_II1022	methyl-accepting chemotaxis protein	-9,07	6,2551E-133	3,6932E-130
VSAL_I2330	peptidoglycan hydrolase FlgJ	-6,52	5,02715E-46	6,49288E-44
VSAL_I2319	hypothetical protein	-6,29	2,86711E-69	5,15207E-67
VSAL_II0319	RNA polymerase sigma factor	-5,92	2,7537E-23	2,32266E-21
VSAL_II0785	putative exported protein	-5,59	1,68644E-53	2,68079E-51
VSAL_II1023	hypothetical protein	-4,80	4,62901E-18	3,35644E-16
VSAL_I2061	hypothetical protein	-4,34	1,78631E-47	2,5458E-45
VSAL_II0643	transposase	-3,86	1,59779E-09	NA
VSAL_I0799	methyl-accepting chemotaxis protein	-3,62	1,41333E-46	1,88429E-44
VSAL_II2038s	srna	-3,36	5,28776E-16	3,46894E-14
VSAL_II0168	putative exported protein	-3,29	8,47987E-21	6,87202E-19
VSAL_I2331	flagellar P-ring protein 2 precursor (basal body P-ring protein 2)	-3,16	6,86725E-31	6,92252E-29
VSAL_I2193	methyl-accepting chemotaxis protein	-3,13	1,40293E-42	1,75707E-40
VSAL_I2326	putative exported protein	-3,06	3,39339E-19	2,54998E-17
VSAL_I1699	outer membrane protein, OmpA-like	-3,02	3,98735E-30	3,92374E-28
VSAL_I4139s	srna	-2,77	9,64853E-29	9,06304E-27
VSAL_II0238	glucose-1-phosphate adenylyltransferase	-2,72	4,96507E-09	2,28007E-07

VSAL_I2317	hypothetical protein	-2,70	1,00079E-31	1,06059E-29
VSAL_I2345	putative exported protein	-2,58	1,04548E-17	7,32367E-16
VSAL_I2346	putative exported protein	-2,38	1,22438E-21	1,01207E-19
VSAL_I2897	putative flagellar basal body-associated protein FliL	-2,34	5,10443E-11	2,57276E-09
VSAL_I2316	polar flagellar protein FlaG (pseudogene)	-2,34	4,60876E-17	3,12262E-15
VSAL_II2008s	srna	-2,20	8,05326E-16	5,12064E-14
VSAL_I2315	polar flagellar hook-associated protein 2 (HAP2) (flagellar cap prot	-2,12	2,84089E-16	1,89377E-14
VSAL_I1863	sodium-type flagellar protein MotY precursor	-2,09	7,25664E-09	3,22491E-07
VSAL_I2325	flagellin subunit B	-2,05	1,62473E-14	9,59288E-13
VSAL_I0863	accessory colonization factor AcfD precursor (fragment)	-2,04	1,01555E-13	5,91165E-12
VSAL_II0311	outer membrane protein, OmpA family	2,03	3,56365E-05	0,001197444
VSAL_II0379	outer membrane protein, OmpA family (pseudogene)	2,15	1,7599E-17	1,21228E-15
VSAL_II0382	hypothetical protein	2,15	2,13715E-06	8,33288E-05
VSAL_II0134	hypothetical protein	2,34	8,80826E-13	4,85394E-11
VSAL_II0935	hypothetical protein	2,40	1,27385E-19	9,93362E-18
VSAL_I0132	putative lipoprotein	2,42	4,0182E-05	0,001328015
VSAL_II0170	methyl-accepting chemotaxis protein	2,54	5,17481E-13	2,8902E-11
VSAL_II0381	response regulator, histidine kinase	2,62	5,88866E-15	3,57909E-13
VSAL_II0135	putative cytochrome b561	2,62	7,22418E-18	5,14785E-16
VSAL_II0932	cellulose synthase catalytic subunit	2,63	1,76343E-19	1,34968E-17
VSAL_I0133	hypothetical protein	2,71	8,5353E-10	4,00868E-08
VSAL_II0947	hypothetical protein	2,76	5,86757E-12	3,10906E-10
VSAL_II0172	hypothetical protein	2,76	3,89513E-11	1,98748E-09
VSAL_II0171	putative membrane protein	2,84	2,56554E-15	1,5826E-13
VSAL_II0375	putative secretion system protein	2,94	1,12501E-31	1,16241E-29
VSAL_I1056	carbonic anhydrase precursor	2,99	1,62335E-15	1,01656E-13
VSAL_II0378	membrane associated secretion system protein	3,04	1,50343E-32	1,67937E-30
VSAL_II0377	membrane associated secretion system protein	3,11	8,61909E-32	9,37439E-30
VSAL_II0931	membrane protein (fragment)	3,15	7,8878E-16	5,09379E-14
VSAL_II0376	membrane associated secretion system protein	3,17	1,17023E-33	1,38188E-31
VSAL_II0933	putative exported protein	3,21	1,18667E-26	1,0662E-24
VSAL_I1820	putative lipoprotein	3,24	3,06244E-49	4,52038E-47

VSAL_II0934	hypothetical protein	3,37	1,02922E-12	5,59709E-11
VSAL_I1819	outer membrane protein A	3,79	3,73956E-47	5,15186E-45
VSAL_II1062	membrane protein	3,81	5,17101E-27	4,74928E-25
VSAL_I2749	probable HTH-type transcriptional regulator LeuO	3,97	9,97706E-30	9,58958E-28
VSAL_I1486	cold-shock protein	4,17	1,53374E-26	1,34872E-24
VSAL_II0364	hypothetical protein	4,55	2,39515E-18	1,7677E-16
VSAL_II0374	bacterial type II secretion system protein F	4,65	5,71955E-66	9,45556E-64
VSAL_II0722	hypothetical protein	5,08	1,50838E-20	1,19888E-18
VSAL_II0363	putative response regulator	5,34	1,9304E-37	2,34657E-35
VSAL_I1476	membrane protein	6,49	1,84531E-33	2,11852E-31
VSAL_II0362	hypothetical protein	9,54	1,1758E-72	2,20891E-70
VSAL_I1475	hypothetical protein	9,59	3,38005E-79	6,65227E-77
VSAL_II0373	bacterial type II secretion system protein F	10,33	5,59472E-89	1,15615E-86
VSAL_II0369	type II/III secretion system protein	10,94	2,0028E-100	5,17355E-98
VSAL_II0372	type II/IV secretion system protein, ATP binding domain	12,73	1,4614E-120	6,0398E-118
VSAL_II0371	type II secretion system protein Z	13,54	7,2752E-111	2,1477E-108
VSAL_II0368	putative Flp pilus assembly protein	14,23	3,5943E-126	1,8569E-123
VSAL_II0370	putative lipoprotein	14,26	1,1551E-115	3,9783E-113
VSAL_II0252	hypothetical protein	16,12	5,96985E-68	1,02806E-65
VSAL_II0367	type IV leader peptidase	24,82	1,5536E-121	7,1347E-119
VSAL_II0366	fimbrial protein, Flp/Fap pilin component	25,55	6,88757E-98	1,58146E-95

Additional file 8 **Table S9. The table lists the differentially expressed genes of *ΔrpoQ* mutant compared to wild-type at HCD.**

VSAL_nr	Function	Fold Change	p-value	p-adjusted
pVSAL43_01	replication initiation protein	-147,74	9,50003E-65	3,92541E-61
pVSAL43_02	acetyltransferase	-131,84	1,97629E-60	4,08301E-57
VSAL_II0054	hypothetical protein	-22,36	3,68698E-38	5,0782E-35
VSAL_II0328	putative anti-sigma F factor antagonist	-21,06	NA	NA
VSAL_I2057	general L-amino acid-binding periplasmic protein precursor	-17,95	6,04144E-38	6,24081E-35
VSAL_I2327	hypothetical protein	-17,36	2,44215E-29	1,68183E-26
VSAL_II0327	putative nucleotidyl transferase	-17,07	1,34917E-25	6,96848E-23
VSAL_I2329	hypothetical protein	-11,69	7,38028E-20	2,34579E-17
VSAL_II0329	putative response regulator	-9,44	NA	NA
VSAL_II0326	hypothetical protein	-9,05	4,90521E-27	2,89548E-24
VSAL_II0319	RNA polymerase sigma factor	-8,98	7,22721E-19	2,13306E-16
VSAL_I2337	flagellar basal-body rod protein FlgC	-8,57	4,20203E-23	1,73628E-20
VSAL_I2338	flagellar basal-body rod protein FlgB	-7,76	1,17486E-20	4,04545E-18
VSAL_II0332	putative hemolysin-type calcium-binding protein (fragment)	-7,50	5,3891E-12	8,24732E-10
VSAL_I2336	flagellar basal-body rod protein FlgD	-7,21	NA	NA
VSAL_II0330	hypothetical protein	-6,91	NA	NA
VSAL_I2333	flagellar basal-body rod protein FlgG (distal rod protein)	-6,87	3,71604E-25	1,70607E-22
VSAL_I2328	flagellar hook-associated protein type 3 FlgL	-6,65	6,84376E-11	9,42614E-09
VSAL_I2334	flagellar basal-body rod protein FlgF	-5,90	2,08372E-10	2,75236E-08
VSAL_II0333	transposase	-5,19	3,91538E-10	4,75834E-08
VSAL_I2335	flagellar hook protein FlgE	-4,94	4,02495E-09	4,49489E-07
VSAL_I2698	hypothetical protein (pseudogene)	-4,63	2,60727E-12	4,48884E-10
VSAL_I4140s	srna	-4,40	5,47556E-06	0,000348077
VSAL_I1832	hypothetical protein (fragment)	-4,23	3,95841E-07	3,40753E-05
VSAL_II0055	hypothetical protein	-4,19	1,61482E-06	0,00011706
VSAL_I2054	general L-amino acid transport ATP-binding subunit	-4,17	NA	NA
VSAL_II0053	membrane associated response regulator, histidine kinase	-4,07	8,48832E-10	1,00211E-07
VSAL_I2332	flagellar L-ring protein 1 precursor (basal body L-ring protein 1)	-4,00	1,23308E-07	1,15798E-05
VSAL_II0057	putative membrane associated response regulator	-3,66	1,16961E-05	0,00064438
VSAL_II1022	methyl-accepting chemotaxis protein	-3,64	1,35007E-05	0,000734011
VSAL_II0322	putative membrane protein	-3,63	6,80488E-09	7,39941E-07

VSAL_I0755	membrane protein	-3,61	3,19223E-05	0,001551798
VSAL_I2330	peptidoglycan hydrolase FlgJ	-3,53	5,92869E-06	0,000360255
VSAL_II0321	putative glycosyl transferase	-3,51	9,33864E-08	8,97378E-06
VSAL_II0323	putative lipoprotein	-3,34	1,16849E-06	9,1098E-05
VSAL_II0063	putative type I secretion system, ATP-binding protein	-3,28	NA	NA
VSAL_II0064	putative type I secretion protein, HlyD family	-3,26	0,000459776	0,015077719
VSAL_II0058	putative type I toxin secretion system, outer membrane efflux p	-3,24	1,49429E-05	0,000791589
VSAL_II0052	response regulator protein	-3,23	7,93976E-14	1,56224E-11
VSAL_I1676	aquaporin Z (bacterial nodulin-like intrinsic protein)	-3,20	2,72758E-05	0,00134171
VSAL_I2438	isocitrate lyase	-3,18	0,00081801	0,024671647
VSAL_I4059s	srna	-3,14	6,84427E-06	0,000404008
VSAL_I2208	putative PrkA serine protein kinase	-3,03	0,000283461	0,010274205
VSAL_II0316	response regulator, histidine kinase	-3,03	0,000166131	0,006600522
pVSAL840_26	hypothetical protein	-2,99	2,83374E-06	0,000188855
VSAL_II0066	membrane protein	-2,97	0,001166727	0,033247702
VSAL_I1808	hypothetical protein	-2,96	4,96755E-13	8,92431E-11
VSAL_II0056	putative type I secretion protein, HlyD family	-2,94	NA	NA
VSAL_I2056	general L-amino acid ABC transporter permease protein	-2,90	0,000113893	0,004753582
VSAL_II0785	putative exported protein	-2,90	1,1631E-05	0,00064438
VSAL_II0331	putative exported protein	-2,85	2,46654E-05	0,001273966
VSAL_I2439	malate synthase A	-2,84	0,003640861	0,067160876
VSAL_II0920	maltose transport system permease protein MalG	-2,82	5,18262E-08	5,22307E-06
VSAL_I2269	hypothetical protein	-2,79	0,000724632	0,022344633
VSAL_II0318	putative exported protein	-2,79	0,000169607	0,00667445
VSAL_II0324	putative lipoprotein	-2,74	1,30138E-06	9,95795E-05
VSAL_I2069	putative ABC transporter, ATP-binding protein (fragment)	-2,71	4,43647E-05	0,002036831
VSAL_I4098s	srna	-2,67	7,41756E-05	0,003260572
VSAL_I0588	putative exported protein	-2,65	3,50807E-05	0,001666132
VSAL_II0059	putative type I toxin secretion system, membrane transport pro	-2,64	0,001144338	0,032836151
VSAL_I0761	conserved hypothetical protein	-2,55	2,56017E-05	0,001306001
VSAL_I2061	hypothetical protein	-2,53	0,000268859	0,009922307
VSAL_II0325	putative exported protein	-2,46	3,03671E-06	0,000199169

VSAL_II0445	bacterial extracellular solute-binding protein	-2,44	0,000109519	0,00461767
VSAL_I2331	flagellar P-ring protein 2 precursor (basal body P-ring protein 2)	-2,44	8,17328E-06	0,000469055
VSAL_II1012	response regulator, histidine kinase	-2,43	7,36523E-06	0,000428636
VSAL_II0712	methyl-accepting chemotaxis citrate transducer	-2,39	1,13352E-05	0,000641605
VSAL_II0067	hypothetical protein	-2,39	0,0092456	0,120513627
VSAL_II0060	putative type I toxin secretion system, ATP-binding protein	-2,37	0,005503994	0,084544628
VSAL_I2207	conserved hypothetical protein	-2,36	0,011242869	0,13992631
VSAL_II0446	binding-protein-dependent transport system inner membrane c	-2,35	0,000331709	0,011714713
VSAL_II0765	glycine dehydrogenase (decarboxylating)	-2,34	0,007073483	0,099413713
VSAL_I1517	conserved hypothetical protein	-2,32	0,000107001	0,004558014
VSAL_II1013	putative heme binding protein	-2,32	6,29802E-05	0,002828635
VSAL_I0631	putative AMP-binding acetyl-CoA synthetase	-2,29	2,70637E-05	0,00134171
VSAL_I2206	putative sporulation protein	-2,29	0,011902102	0,145933194
VSAL_I2973	fatty oxidation complex beta subunit, 3-ketoacyl-CoA thiolase	-2,28	0,001348935	0,037128731
VSAL_II0764	glycine cleavage system H protein	-2,27	0,009185252	0,120487176
VSAL_II0320	putative membrane associated signaling protein	-2,26	5,28261E-05	0,002398652
VSAL_II0020	hemolysin-type calcium-binding protein	-2,22	1,91762E-06	0,000134298
VSAL_I2974	fatty oxidation complex alpha subunit, enoyl-CoA hydratase	-2,22	0,000160184	0,006426026
VSAL_II0964	acyl-CoA reductase LuxC	-2,19	0,002571375	0,054574947
VSAL_II0962	alkanal monooxygenase alpha chain LuxA (bacterial luciferas al	-2,18	0,008093847	0,111852089
VSAL_I2130	methyl-accepting chemotaxis protein	-2,16	0,000702555	0,021931048
VSAL_I1555	ribosome modulation factor	-2,16	0,008629238	0,116143366
VSAL_I1589	hypothetical protein	-2,12	0,000486052	0,015813927
VSAL_II0315	putative response regulator	-2,08	0,015021673	0,177341576
VSAL_I1699	outer membrane protein, OmpA-like	-2,07	NA	NA
VSAL_II1002	sodium/proton-dependent alanine carrier protein	-2,07	0,003531558	0,06573153
VSAL_I1198	probable membrane permease	-2,07	0,005432009	0,083967648
VSAL_I2319	hypothetical protein	-2,04	0,002183254	0,049893839
VSAL_I1904	secretion protein, HlyD family	-2,02	5,9257E-06	0,000360255
VSAL_II2008s	srna	-2,01	0,011415575	0,141336369
VSAL_I0620	thymidine phosphorylase	-2,01	0,009034616	0,119650745
pVSAL320_19	putative antirestriction protein	2,00	NA	NA

VSAL_II0124	ABC transporter, ATP binding protein	2,00	0,05505911	0,401950957
VSAL_II0112	biopolymer transport protein TolR	2,01	0,03202097	0,299345354
VSAL_I1228	putative exported protein	2,01	NA	NA
VSAL_II1047	putative transcriptional regulator, LysR family (fragment)	2,01	0,039369424	0,340616165
VSAL_II0525	putative membrane protein	2,01	0,004387669	0,074681458
VSAL_II0116	putative exported protein	2,01	NA	NA
pVSAL320_20	putative membrane protein	2,01	NA	NA
VSAL_II0110	TonB dependent receptor	2,01	0,008324252	0,114271788
VSAL_II0118	membrane protein	2,01	NA	NA
VSAL_II0356	putative exported protein	2,01	NA	NA
VSAL_I0894	sodium/solute symporter (fragment)	2,02	NA	NA
VSAL_I2862	transposase (fragment)	2,02	NA	NA
VSAL_I1253	X-Pro dipeptidyl-peptidase	2,02	NA	NA
VSAL_II0170	methyl-accepting chemotaxis protein	2,03	0,02520466	0,25778627
pVSAL320_24	transposase	2,03	NA	NA
VSAL_II0074	membrane protein	2,04	0,016962841	0,192028659
VSAL_I2472	putative membrane protein	2,04	2,52568E-06	0,000171084
pVSAL840_43	hypothetical protein	2,04	0,041413984	0,350661025
pVSAL840_38	putative cell wall degradation protein	2,04	NA	NA
pVSAL320_02	putative exported protein	2,04	0,0103531	0,130811619
VSAL_II0873	conserved hypothetical protein	2,04	NA	NA
VSAL_I2005	anaerobic C4-dicarboxylate transporter	2,05	NA	NA
VSAL_I1812	putative methyl-accepting chemotaxis protein (fragment)	2,05	0,022376232	0,236736086
VSAL_I1028	major capsid protein	2,05	0,011424576	0,141336369
pVSAL320_10	hypothetical protein	2,05	NA	NA
VSAL_I0266	hypothetical protein	2,05	NA	NA
VSAL_I0138	iron-siderophore ABC transporter, periplasmic binding protein	2,06	NA	NA
pVSAL840_09	conjugative transfer protein TrbI trbi	2,06	NA	NA
VSAL_II0755	membrane protein	2,07	0,003444119	0,064394108
VSAL_I1034	hypothetical protein, putative phage gene	2,07	0,025857412	0,261869673
VSAL_I2064	conserved hypothetical protein	2,08	0,035173686	0,316639803
VSAL_I2717	fimbrial assembly protein PilN	2,08	NA	NA

VSAL_I0770	hypothetical protein, putative phage gene	2,08	0,040296601	0,343310426
VSAL_II0759	putative suppressor for copper-sensitivity D	2,08	0,033308938	0,30790276
VSAL_II0989	putative exported protein (fragment)	2,08	0,001239559	0,034842565
VSAL_I1490	hypothetical protein	2,08	0,048057416	0,374666493
VSAL_I0703	PTS system, cellobiose permease IIC component	2,09	NA	NA
VSAL_I0137	TonB-dependent iron-siderophore receptor precursor	2,09	0,00960223	0,124705244
VSAL_II0568	putative membrane protein	2,10	0,010261565	0,130768584
VSAL_II0245	nitrite reductase large subunit	2,10	NA	NA
VSAL_I0203	sensor outer membrane protein EnvZ	2,10	NA	NA
VSAL_I0134	L-2,4-diaminobutyrate decarboxylase	2,11	0,002879724	0,057130137
VSAL_I1686	phosphoribosylglycinamide formyltransferase 2	2,12	0,032931901	0,305785647
VSAL_I0107	membrane protein	2,12	0,028018891	0,277867798
VSAL_II0752	putative exported protein	2,12	0,002485162	0,053482757
VSAL_II0274	siderophore biosynthesis protein IucB (N6-hydroxylysine acetyl t	2,12	NA	NA
VSAL_II0936	membrane protein	2,13	0,00144539	0,038372806
VSAL_I2348	putative membrane associated GGDEF protein	2,13	NA	NA
VSAL_II0881	drug resistance translocator protein	2,13	NA	NA
VSAL_I1234	sodium-dependent nucleoside transport protein	2,14	0,013802777	0,164360445
pVSAL840_25	antirestriction protein ArdC	2,14	NA	NA
VSAL_II0338	MFS transporter	2,14	NA	NA
VSAL_II0150	ferrichrome transport ATP-binding protein FhuC	2,14	0,00999677	0,127884372
VSAL_I1033	hypothetical protein, putative phage gene (pseudogene)	2,14	0,036269328	0,325793177
VSAL_II0015	secretion protein, HlyD family	2,14	0,021683979	0,231905261
VSAL_I2704	membrane associated GGDEF protein	2,14	NA	NA
VSAL_II0123	periplasmic solute binding protein	2,15	NA	NA
VSAL_I1742	hypothetical protein (pseudogene)	2,15	NA	NA
VSAL_I2117	methyl-accepting chemotaxis protein (fragment)	2,15	NA	NA
VSAL_I2492	probable cadaverine/lysine antiporter	2,16	NA	NA
pVSAL840_10	conjugative transfer protein TraW	2,16	NA	NA
VSAL_II0687	glucose-6-phosphate 1-dehydrogenase	2,16	0,001419344	0,038331555
pVSAL840_34	hypothetical protein	2,17	NA	NA
VSAL_I1116	putative type VI secretion protein VasD	2,17	0,02090334	0,227296318

VSAL_II0382	hypothetical protein	2,18	0,005251052	0,082767139
pVSAL320_04	hypothetical protein	2,19	NA	NA
VSAL_II0299	putative glycosyl transferases	2,19	0,008083503	0,111852089
VSAL_I2577	ABC-type [(GlcNAc)2] transporter, permease protein	2,19	0,028311882	0,278534996
VSAL_II0295	sugar transferase	2,19	0,004401132	0,074681458
VSAL_II0279	ferric aerobactin receptor precursor	2,19	0,023038068	0,241797708
pVSAL840_36	VgrG protein, VgrG-2	2,19	NA	NA
pVSAL840_06	conjugative transfer protein TraB	2,19	0,024425715	0,251062323
VSAL_II0309	putative capsular polysaccharide synthesis protein	2,19	0,006170099	0,089455615
VSAL_II0396	anaerobic glycerol-3-phosphate dehydrogenase subunit B	2,19	0,006850447	0,09727164
VSAL_I2004	aspartate racemase	2,20	0,020777027	0,227118194
VSAL_II0120	putative membrane protein	2,20	NA	NA
VSAL_I0453	membrane protein	2,20	NA	NA
VSAL_II0313	putative exported protein	2,21	0,002453201	0,053350657
VSAL_I1119	chaperone ClpB	2,22	NA	NA
VSAL_I4022s	srna	2,22		
VSAL_II0086	putative membrane protein	2,23	0,030436069	0,291115364
VSAL_I1750	putative coproporphyrinogen oxidase PhuW	2,24	NA	NA
VSAL_I1042	hypothetical protein, putative phage gene	2,24	0,031002649	0,293814099
pVSAL54_01	acyltransferase	2,24	NA	NA
VSAL_I1041	probable tail length determinator	2,25	NA	NA
VSAL_I1026	terminase, ATPase subunit	2,25	NA	NA
VSAL_II0215	catalase	2,25	0,006444728	0,09278612
VSAL_I2852	NADH pyrophosphatase (pseudogene)	2,25	0,017534451	0,196881394
VSAL_I0136	siderophore biosynthesis protein	2,26	0,010327703	0,130811619
VSAL_I2630	type IV pilus assembly protein PilB	2,26	NA	NA
VSAL_I1219	hypothetical protein (fragment)	2,26	0,028103029	0,277867798
VSAL_I0202	membrane permease (pseudogene)	2,26	NA	NA
pVSAL840_17	conjugative transfer protein TraH	2,27	NA	NA
VSAL_I2631	type IV pilus assembly protein PilC (pseudogene)	2,28	NA	NA
VSAL_II0688	putative membrane protein	2,29	0,004500407	0,074681458
VSAL_I1056	carbonic anhydrase precursor	2,30	0,00251524	0,053849586

VSAL_I2985	thiamine biosynthesis adenylyltransferase ThiF	2,30	NA	NA
VSAL_II0125	ABC-3 transporter protein, membrane component	2,30	NA	NA
pVSAL54_02	putative mobilization protein	2,31	NA	NA
VSAL_I0135	siderophore biosynthetis protein	2,31	0,009245596	0,120513627
VSAL_II0715	putative cation efflux system protein	2,32	NA	NA
VSAL_I1124	putative type VI secretion protein VasQ	2,32	0,017046302	0,192446234
VSAL_II0430	hypothetical protein (pseudogene)	2,33	NA	NA
VSAL_I2190	integral membrane protein	2,33	0,016341861	0,186531963
VSAL_I1029	phage terminase, endonuclease subunit	2,34	0,013412569	0,160639811
VSAL_I2192	hypothetical protein	2,35	0,002675783	0,055692574
VSAL_II0273	siderophore biosynthesis protein IucA (fragment)	2,35	NA	NA
pVSAL840_08	conjugative transfer protein TraC	2,35	NA	NA
pVSAL840_37	hypothetical protein	2,35	NA	NA
pVSAL320_11	putative DNA-damage-inducible protein	2,36	NA	NA
VSAL_II0171	putative membrane protein	2,36	0,002575536	0,054574947
VSAL_I1822	methyl-accepting chemotaxis protein (fragment)	2,38	NA	NA
VSAL_I1526	membrane protein	2,38	NA	NA
VSAL_II0189	transposase (fragment)	2,40	0,000451811	0,014935071
VSAL_II0261	hypothetical protein	2,40	0,009011319	0,119650745
VSAL_I1339	transposase	2,40	NA	NA
VSAL_II0432	membrane protein	2,41	0,004847363	0,077935038
VSAL_I1038	hypothetical protein, putative phage gene	2,41	0,017096983	0,192492459
pVSAL840_23	transglycosylase PilT	2,41	NA	NA
VSAL_II0937	membrane protein	2,44	4,97611E-07	4,19618E-05
VSAL_II0899	putative exported protein (pseudogene)	2,46	0,012888141	0,155712858
VSAL_II1063	putative HTH-type transcriptional regulator (fragment)	2,46	0,011937479	0,145933919
VSAL_I2126	putative membrane protein	2,46	0,005731383	0,086019507
pVSAL320_01	hypothetical protein	2,46	NA	NA
VSAL_II0298	putative membrane protein	2,47	0,001650555	0,04236082
VSAL_II0914	MFS transporter	2,48	NA	NA
VSAL_I1115	putative type VI secretion protein VasE	2,50	NA	NA
VSAL_I1030	membrane protein, putative phage gene	2,54	NA	NA

VSAL_II0296	putative transmembrane glycosyl transferase	2,59	9,90004E-05	0,004261143
VSAL_I0774	putative portal vertex protein (pseudogene)	2,63	0,006637839	0,095028786
VSAL_II0387	aerobic glycerol-3-phosphate dehydrogenase	2,63	0,005144739	0,081670505
VSAL_II0115	TonB protein	2,63	NA	NA
pVSAL320_31	putative phage intergrase	2,64	NA	NA
VSAL_I1043	hypothetical protein, putative phage gene	2,65	NA	NA
VSAL_I2127	hypothetical protein	2,66	NA	NA
VSAL_I2017	MFS transporter	2,67	NA	NA
VSAL_II0853	membrane protein	2,67	0,001484204	0,038785149
VSAL_II0265	hypothetical protein	2,67	NA	NA
VSAL_I2016	secretion protein, HlyD family (fragment)	2,68	NA	NA
VSAL_I1743	hypothetical protein	2,70	NA	NA
VSAL_I0773	putative bacteriophage terminase	2,70	NA	NA
VSAL_II0302	putative polysaccharide biosynthesis protein	2,71	0,001575864	0,040696689
VSAL_II0364	hypothetical protein	2,71	0,002682193	0,055692574
VSAL_II0381	response regulator, histidine kinase	2,71	0,00034069	0,011929916
VSAL_I1044	hypothetical protein, putative phage gene	2,72	0,005792477	0,086019507
VSAL_I0108	membrane protein	2,72	NA	NA
pVSAL840_18	conjugative transfer protein TraG	2,72	NA	NA
VSAL_II0275	siderophore biosynthesis protein IucC (Pseudogene)	2,73	NA	NA
VSAL_II0119	putative exported protein	2,75	0,005091011	0,081220295
VSAL_I1037	hypothetical protein, putative phage gene	2,76	NA	NA
pVSAL840_13	conjugative transfer protein TraN	2,77	NA	NA
VSAL_I2030	glutaredoxin 1	2,78	6,56344E-05	0,002916146
pVSAL840_11	conjugative transfer protein TraU	2,80	0,005405821	0,083967648
pVSAL840_12	hypothetical protein, putative conjugative transfer protein TrbC	2,81	NA	NA
VSAL_I1035	probable tail tube protein	2,81	0,002266495	0,050897605
VSAL_II0988	hypothetical protein	2,86	NA	NA
VSAL_II0304	putative glycosyl transferase	2,86	4,03719E-05	0,001874346
VSAL_I1015	hypothetical protein, putative phage gene	2,89	NA	NA
VSAL_II0365	hypothetical protein	2,91	0,004083717	0,071808708
VSAL_II0303	putative glycosyl transferase	2,93	0,000263149	0,00991193

VSAL_II0931	membrane protein (fragment)	2,94	6,48618E-06	0,000388419
VSAL_II0986	hypothetical protein	2,95	2,13154E-10	2,75236E-08
VSAL_II0214	patatin-like phospholipase	2,98	0,000375488	0,012929306
VSAL_II0135	putative cytochrome b561	3,00	0,000156638	0,00640819
VSAL_II0987	hypothetical protein	3,01	0,000188041	0,007330062
VSAL_I1018	hypothetical protein, putative phage gene	3,03	0,002351641	0,052241832
VSAL_II0947	hypothetical protein	3,15	5,61081E-06	0,000351271
VSAL_II0300	hypothetical protein	3,17	0,000158765	0,006426026
VSAL_I1974	ABC transporter, ATP-binding component	3,18	NA	NA
VSAL_II0297	putative glycosyl transferase	3,18	1,38962E-06	0,000104399
VSAL_I1036	probable rRNA transcription initiatior protein, putative phage ge	3,20	NA	NA
VSAL_I1927	hypothetical protein, putative phage gene (fragment)	3,22	0,001356834	0,037128731
VSAL_I0902	chitinase A (fragment)	3,26	3,44407E-12	5,47342E-10
VSAL_II0854	secretion protein, HlyD family	3,34	0,000439413	0,014642381
VSAL_II0935	hypothetical protein	3,36	1,20447E-14	2,48843E-12
VSAL_II0722	hypothetical protein	3,42	7,11212E-07	5,76222E-05
VSAL_I1475	hypothetical protein	3,43	1,90294E-07	1,74732E-05
VSAL_I4109s	rnas	3,54	1,5584E-06	0,000114988
VSAL_I2713	hybrid peroxiredoxin (thioredoxin reductase)	3,56	0,000130144	0,005377566
VSAL_I1820	putative lipoprotein	3,64	2,22457E-13	4,17815E-11
VSAL_I1476	membrane protein	3,64	1,03888E-06	8,25507E-05
VSAL_II0933	putative exported protein	3,69	3,27159E-10	4,09643E-08
VSAL_I0133	hypothetical protein	3,72	6,91011E-07	5,71051E-05
VSAL_II0310	polysaccharide biosynthesis/export protein	3,81	2,4072E-06	0,000165776
VSAL_I1486	cold-shock protein	3,94	3,43482E-07	3,01972E-05
VSAL_I0132	putative lipoprotein	3,97	3,19019E-06	0,000205967
VSAL_II0932	cellulose synthase catalytic subunit	4,02	3,80745E-17	8,76068E-15
VSAL_II0934	hypothetical protein	4,14	3,02162E-08	3,12134E-06
VSAL_I2712	dihydrolipoyl dehydrogenase (dihydrolipoamide dehydrogenase)	4,35	2,72746E-05	0,00134171
VSAL_II0134	hypothetical protein	4,37	2,455E-07	2,20523E-05
VSAL_II0311	outer membrane protein, OmpA family	4,38	1,78587E-06	0,000127228
VSAL_II0128	hypothetical protein, putative phage gene	4,43	3,89686E-05	0,001829755

VSAL_II0363	putative response regulator	4,75	8,54868E-09	9,05721E-07
VSAL_I1819	outer membrane protein A	4,86	3,81637E-17	8,76068E-15
VSAL_II0372	type II/IV secretion system protein, ATP binding domain	5,63	1,53067E-09	1,75686E-07
VSAL_II0312	hypothetical protein, putative anti-sigma factor antagonist	6,05	5,50146E-08	5,41239E-06
VSAL_II0371	type II secretion system protein Z	6,16	NA	NA
VSAL_II0368	putative Flp pilus assembly protein	6,78	1,54986E-16	3,37053E-14
VSAL_II0373	bacterial type II secretion system protein F	6,99	1,75707E-18	4,53762E-16
VSAL_II0369	type II/III secretion system protein	7,24	1,59471E-18	4,39289E-16
VSAL_II0370	putative lipoprotein	7,42	3,11133E-12	5,1424E-10
VSAL_II0362	hypothetical protein	7,59	1,4531E-21	5,45835E-19
VSAL_II0367	type IV leader peptidase	10,45	5,76732E-12	8,51092E-10
VSAL_II0366	fimbrial protein, Flp/Fap pilin component	11,91	8,14849E-12	1,16102E-09
VSAL_II0252	hypothetical protein	23,04	4,90373E-31	4,05244E-28

Additional file 9

Table S10 The functional distribution of eighty four DEGs of *ΔrpoQ*/wt at LCD. The table represents the number of up (n = 43) and downregulated (n = 41) genes with their percentage distribution within the different functional groups

Functional categories	**Upregulated genes (n=43)**		**Downregulated genes (n=41)**	
	Number of genes (n)	*Percentage (%)*	*Number of genes (n)*	*Percentage (%)*
Unknown function, no known homologues	9	20.9	2	4.8
Cell processes	1	2.3	22	53.6
Adaptation	1	2.3	0	0
Macromolecule synthesis, modification	0	0	2	4.8
Cell envelope	18	41.8	6	14.6
Extrachromosomal / foreign DNA	9	20.9	4	9.7
Regulation	3	6.9	1	2.4
sRNA	0	0	4	9.7

Table S11 The functional distribution of three hundred DEGs of *ΔrpoQ*/wt at HCD. The table represents the number of up (n = 206) and down regulated (n = 94) genes with their percentage distribution within the different functional groups.

Functional categories	**Upregulated genes (n=206)**		**Downregulated genes (n=94)**	
	Number of genes (n)	*Percentage (%)*	*Number of genes (n)*	*Percentage (%)*
Unknown function, no known homologues	30	14.5	14	14.8
Cell processes	5	2.4	16	17
Protection responses	3	1.4	0	0
Transport/binding proteins	28	13.5	18	19
Adaptation	1	0.4	0	0
Cell division	0	0	1	1
Macromolecule metabolism	2	0.9	0	0
Macromolecule synthesis, modification	11	5.0	1	1
Amino acid biosynthesis	1	0.4	0	0
Biosynthesis of cofactors, carriers	9	4.3	0	0
Central intermediary metabolism	2	0.9	4	4.2
Degradation of small molecules	0	0	4	4.2
Energy metabolism, carbon	5	2.4	0	0
Fatty acid biosynthesis	1	0.4	0	0
Nucleotide biosynthesis	1	0.4	0	0
Cell envelope	53	25.7	12	12.7
Ribosome constituents	0	0	1	1
Extrachromosomal / foreign DNA	42	20	2	0
Regulation	4	1.9	11	11.7
Not classified (included putative assignments)	6	2.9	6	6.3
sRNA	2	0.9	4	4.2

Additional file 10

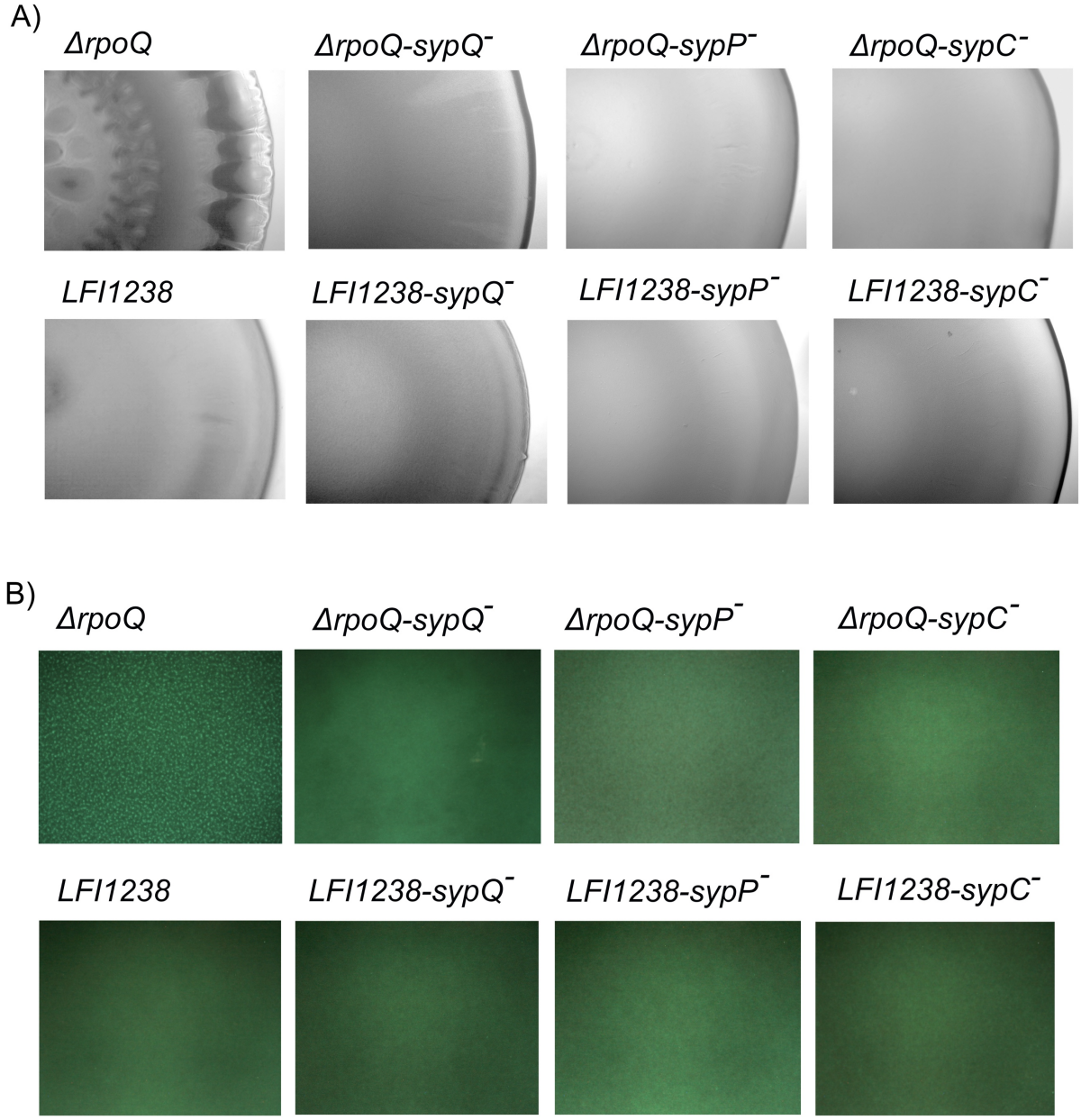

Additional file 10: Figure S1. **Colony morphology and biofilm formation of *ΔrpoQ* and LFI1238 *syp* mutants. A)** The colonies of *A. salmonicida* mutant strains (*ΔrpoQ-sypQ*$^-$, *ΔrpoQ-sypP*$^-$, *ΔrpoQ-sypC*$^-$, LFI1238-*sypQ*$^-$, LFI1238-*sypP*$^-$ and LFI1238-*sypC*$^-$) were allowed to form on SWT plates for 12 days at 8°C. The colonies were viewed microscopically with Zeiss Primo Vert and photographed with AxioCam ERc5s at x4 magnification. **B)** The GFP tagged strains (*ΔrpoQ-sypQ*$^-$-pVSV102, *ΔrpoQ-sypP*$^-$-pVSV102, *ΔrpoQ-sypC*$^-$-pVSV102, LFI1238-*sypQ*$^-$-pVSV102, LFI1238-*sypP*$^-$-pVSV102 and LFI1238-*sypC*$^-$-pVSV102) were allowed to form biofilms in SWT media at 8°C for 72 hours. The biofilms were viewed, in a Nikon Eclipse TS100 microscope at x10 magnification and photographed with Nikon DS-5Mc.

Additional file 11 Table S12. The table lists the differentially expressed genes of *ΔrpoQ* compared to *ΔlitR* at LCD.

VSAL_nr	Function	Fold Change	p-value	p-adjusted
VSAL_I2619	HTH-type luminescence regulator LitR	197,53	6,14E-201	4,79E-198
VSAL_I0386	putative chemotaxis protein	18,77	0,99981198	0,99981198
VSAL_II0252	hypothetical protein	5,89	4,89E-17	2,58E-15
VSAL_I2620	transposase (pseudogene)	5,63	2,22E-53	3,62E-51
VSAL_II0934	hypothetical protein	4,66	6,13E-17	3,19E-15
VSAL_II0362	hypothetical protein	4,61	1,89E-51	2,95E-49
VSAL_I1486	cold-shock protein	4,52	6,70E-32	6,23E-30
VSAL_I1819	outer membrane protein A	4,46	1,50E-48	2,09E-46
VSAL_I1476	membrane protein	4,40	9,63E-29	8,00E-27
VSAL_II0373	bacterial type II secretion system protein F	4,20	1,03E-49	1,54E-47
VSAL_I1394	hypothetical protein	4,13	2,72E-61	4,62E-59
VSAL_II0320	putative membrane associated signaling protein	3,90	1,25E-16	6,27E-15
pVSAL840_56	hypothetical protein	3,89	1,53E-71	3,31E-69
VSAL_I1475	hypothetical protein	3,84	4,13E-38	4,75E-36
VSAL_II0371	type II secretion system protein Z	3,57	2,20E-36	2,39E-34
VSAL_II0372	type II/IV secretion system protein, ATP binding domain	3,43	7,93E-40	9,38E-38
VSAL_I1395	membrane protein	3,40	3,56E-36	3,75E-34
VSAL_II0933	putative exported protein	3,37	4,56E-24	3,36E-22
VSAL_II0947	hypothetical protein	3,37	8,84E-15	4,31E-13
VSAL_II0368	putative Flp pilus assembly protein	3,31	5,03E-32	4,79E-30
VSAL_II0363	putative response regulator	3,28	1,75E-32	1,71E-30
VSAL_II0369	type II/III secretion system protein	3,26	1,00E-35	1,03E-33
VSAL_II0364	hypothetical protein	3,18	7,44E-12	3,12E-10
VSAL_I1493	microbial collagenase precursor (pseudogene)	3,14	1,81E-40	2,21E-38
VSAL_II0370	putative lipoprotein	3,04	1,63E-34	1,63E-32
VSAL_II0935	hypothetical protein	3,04	1,84E-31	1,63E-29
VSAL_I1820	putative lipoprotein	3,02	6,18E-44	8,04E-42
VSAL_II0931	membrane protein (fragment)	2,98	1,47E-13	6,45E-12
VSAL_II0932	cellulose synthase catalytic subunit	2,97	6,46E-25	4,85E-23
VSAL_I0133	hypothetical protein	2,95	NA	NA
VSAL_I0132	putative lipoprotein	2,90	2,84E-06	6,40E-05

VSAL_II0367	type IV leader peptidase	2,89	5,45E-30	4,73E-28
VSAL_I1943	transposase	2,78	0,000170542	NA
VSAL_II0946	integral membrane protein	2,61	1,02E-18	5,63E-17
VSAL_I4109s	srna	2,59	1,65E-06	NA
VSAL_I1458	hypothetical protein	2,51	1,47E-10	5,59E-09
VSAL_II0374	bacterial type II secretion system protein F	2,47	1,81E-25	1,39E-23
VSAL_I1056	carbonic anhydrase precursor	2,45	5,32E-14	2,47E-12
VSAL_I1457	hypothetical protein	2,41	2,83E-07	7,79E-06
VSAL_I2712	dihydrolipoyl dehydrogenase (dihydrolipoamide dehydrogenase)	2,39	5,32E-14	2,47E-12
VSAL_I1484	short chain dehydrogenase	2,37	7,91E-11	3,09E-09
VSAL_II0215	catalase	2,37	2,32E-23	1,64E-21
VSAL_II0936	membrane protein	2,36	2,95E-06	6,57E-05
VSAL_II0937	membrane protein	2,30	6,24E-20	3,69E-18
pVSAL840_57	hypothetical protein	2,30	2,25E-23	1,63E-21
VSAL_II0378	membrane associated secretion system protein	2,30	1,07E-20	6,62E-19
VSAL_II0323	putative lipoprotein	2,29	6,57E-12	2,79E-10
VSAL_I0136	siderophore biosynthesis protein	2,26	1,60E-11	6,36E-10
VSAL_II0375	putative secretion system protein	2,25	2,41E-21	1,57E-19
VSAL_I1456	ribosomal-protein-serine acetyltransferase	2,24	1,47E-07	4,23E-06
VSAL_II0968	putative exported protein	2,23	4,90E-20	2,94E-18
VSAL_II0321	putative glycosyl transferase	2,23	2,68E-10	9,86E-09
VSAL_II0376	membrane associated secretion system protein	2,21	3,98E-19	2,25E-17
VSAL_II0366	fimbrial protein, Flp/Fap pilin component	2,21	6,64E-17	3,41E-15
VSAL_II0722	hypothetical protein	2,21	4,58E-07	1,18E-05
VSAL_I0134	L-2,4-diaminobutyrate decarboxylase	2,17	6,65E-10	2,34E-08
VSAL_II0280	integral membrane protein	2,17	1,07E-08	3,49E-07
VSAL_I2713	hybrid peroxiredoxin (thioredoxin reductase)	2,11	1,68E-14	8,00E-13
VSAL_II0377	membrane associated secretion system protein	2,05	9,57E-14	4,25E-12
VSAL_II0322	putative membrane protein	2,04	1,63E-08	5,20E-07
VSAL_I0135	siderophore biosynthetis protein	2,03	5,19E-07	1,32E-05
VSAL_I1197	glutamate decarboxylase beta	2,03	4,35E-09	1,49E-07
VSAL_II0086	putative membrane protein	2,03	0,007127847	NA

VSAL_II0823	PTS system, lactose/cellobiose specific IIB subunit	-2,03	6,78E-08	2,10E-06
VSAL_II0824	putative sugar-specific permease, SgaT/UlaA	-2,05	1,01E-19	5,88E-18
VSAL_II0051	inner membrane protein	-2,11	0,001236134	0,010355015
VSAL_I1405	hypothetical protein	-2,11	0,000389354	0,003958429
VSAL_I2820	hypothetical protein	-2,11	2,10E-07	5,94E-06
VSAL_I2325	flagellin subunit B	-2,17	8,53E-22	5,84E-20
VSAL_I2339	chemotaxis protein methyltransferase CheR	-2,17	4,60E-18	2,50E-16
VSAL_I1608	HTH-type transcriptional regulator GalR	-2,19	4,37E-06	9,18E-05
VSAL_I1995	phospholipase A1 precursor	-2,23	1,02E-18	5,63E-17
VSAL_I2315	polar flagellar hook-associated protein 2 (HAP2) (flagellar cap protein)	-2,26	6,28E-21	4,02E-19
VSAL_II1068	putative exported protein	-2,31	9,40E-11	3,60E-09
VSAL_II2008s	srna	-2,32	1,78E-20	1,09E-18
VSAL_I4127s	srna	-2,33	0,002091567	NA
VSAL_I2318	hypothetical protein	-2,34	1,54E-25	1,20E-23
VSAL_II0231	chemotaxis protein CheV	-2,39	5,57E-27	4,44E-25
VSAL_I1325	proton glutamate symport protein	-2,39	6,08E-15	3,00E-13
VSAL_I2316	polar flagellar protein FlaG (pseudogene)	-2,46	1,87E-21	1,24E-19
VSAL_I2517	hypothetical protein	-2,51	9,39E-22	6,32E-20
VSAL_I2495	hypothetical protein	-2,56	1,07E-11	4,39E-10
VSAL_I1863	sodium-type flagellar protein MotY precursor	-2,57	2,14E-17	1,15E-15
VSAL_I2346	putative exported protein	-2,59	7,27E-29	6,17E-27
VSAL_I2897	putative flagellar basal body-associated protein FliL	-2,72	2,41E-19	1,38E-17
VSAL_II1088	putative membrane protein	-2,89	7,54E-14	3,46E-12
VSAL_I2345	putative exported protein	-3,15	9,75E-32	8,85E-30
VSAL_I2326	putative exported protein	-3,22	6,75E-22	4,71E-20
VSAL_I2331	flagellar P-ring protein 2 precursor (basal body P-ring protein 2)	-3,36	7,47E-42	9,40E-40
VSAL_I2317	hypothetical protein	-3,48	6,41E-72	1,47E-69
VSAL_I4139s	srna	-3,77	2,01E-68	4,13E-66
VSAL_I2193	methyl-accepting chemotaxis protein	-3,82	NA	NA
VSAL_I2061	hypothetical protein	-3,83	4,71E-38	5,26E-36
VSAL_II2038s	srna	-3,87	1,05E-20	6,62E-19
VSAL_II0721	PTS system permease for N-acetylglucosamine and glucose	-4,13	1,85E-27	1,50E-25

VSAL_I1699	outer membrane protein, OmpA-like	-4,32	2,96E-78	8,25E-76
VSAL_II1023	hypothetical protein	-4,37	8,17E-14	3,71E-12
VSAL_II0168	putative exported protein	-4,45	5,98E-49	8,64E-47
VSAL_I0799	methyl-accepting chemotaxis protein	-4,56	9,05E-80	2,72E-77
VSAL_I1342	hypothetical protein	-5,05	5,52E-63	9,80E-61
VSAL_I2117	methyl-accepting chemotaxis protein (fragment)	-5,10	6,08E-46	8,19E-44
VSAL_II0785	putative exported protein	-6,36	1,37E-64	2,55E-62
VSAL_II1022	methyl-accepting chemotaxis protein	-6,40	2,81E-77	7,32E-75
VSAL_I2330	peptidoglycan hydrolase FlgJ	-9,03	3,12E-75	7,62E-73
VSAL_I2319	hypothetical protein	-9,63	4,59E-130	2,56E-127
VSAL_I2332	flagellar L-ring protein 1 precursor (basal body L-ring protein 1)	-10,69	2,11E-108	8,22E-106
VSAL_I2333	flagellar basal-body rod protein FlgG (distal rod protein)	-12,33	1,32E-126	5,73E-124
VSAL_I2334	flagellar basal-body rod protein FlgF	-12,79	1,11E-129	5,40E-127
VSAL_I4140s	srna	-19,46	2,49E-68	4,85E-66
VSAL_I2335	flagellar hook protein FlgE	-19,67	NA	NA
VSAL_I2328	flagellar hook-associated protein type 3 FlgL	-23,22	7,61E-188	4,95E-185
VSAL_I2338	flagellar basal-body rod protein FlgB	-24,11	0	0
VSAL_I2337	flagellar basal-body rod protein FlgC	-26,34	NA	NA
VSAL_I2336	flagellar basal-body rod protein FlgD	-27,52	1,50E-305	1,46E-302
VSAL_I2329	hypothetical protein	-55,72	0	0
VSAL_I2327	hypothetical protein	-75,41	0	0
pVSAL43_01	replication initiation protein	-81,69	2,61E-84	8,49E-82
pVSAL43_02	acetyltransferase	-109,92	2,17E-99	7,69E-97

Additional file 12 **Table S13. The table lists the differentially expressed genes of *ΔrpoQ* compared to *ΔlitR* at HCD.**

VSAL_nr	Function	Fold Change	p-value	p-adjusted
VSAL_I2619	HTH-type luminescence regulator LitR	69,2	NA	NA
VSAL_II0252	hypothetical protein	7,76	8,51E-17	4,93E-14
VSAL_I2620	transposase (pseudogene)	5,82	2,07E-15	1,05E-12
pVSAL840_56	hypothetical protein	4,14	1,07E-10	3,55E-08
VSAL_I1394	hypothetical protein	3,47	8,53E-07	0,00011532
VSAL_II0934	hypothetical protein	3,45	4,78E-07	6,69E-05
VSAL_II0320	putative membrane associated signaling protein	3,22	2,93E-09	7,91E-07
VSAL_II0237	conserved hypothetical protein	3,08	1,61E-07	2,84E-05
VSAL_I0132	putative lipoprotein	3,05	1,26E-05	0,001242334
VSAL_I1197	glutamate decarboxylase beta	2,98	2,01E-05	0,001743222
VSAL_I1819	outer membrane protein A	2,91	4,58E-09	1,16E-06
VSAL_I2712	dihydrolipoyl dehydrogenase (dihydrolipoamide dehydrogenase	2,81	0,000168004	0,011954845
VSAL_II0986	hypothetical protein	2,79	1,55E-05	0,001457661
VSAL_I2713	hybrid peroxiredoxin (thioredoxin reductase)	2,75	0,0001994	0,013944275
VSAL_I0133	hypothetical protein	2,75	2,76E-05	0,002330297
VSAL_II0933	putative exported protein	2,74	2,02E-05	0,001743222
VSAL_I1198	probable membrane permease	2,71	3,66E-05	0,003031247
pVSAL840_57	hypothetical protein	2,67	3,73E-08	7,97E-06
VSAL_II0935	hypothetical protein	2,66	3,86E-06	0,000447603
VSAL_I1395	membrane protein	2,54	0,000116605	0,008728101
VSAL_II0312	hypothetical protein, putative anti-sigma factor antagonist	2,43	0,001037071	0,056842697
VSAL_I1820	putative lipoprotein	2,37	1,96E-06	0,000240323
VSAL_II0311	outer membrane protein, OmpA family	2,35	0,000964688	0,054344118
VSAL_I1456	ribosomal-protein-serine acetyltransferase	2,33	4,76E-06	0,00051492
VSAL_II0370	putative lipoprotein	2,33	0,000614238	0,03774772
VSAL_II0368	putative Flp pilus assembly protein	2,27	0,000745731	0,044480662
VSAL_I2472	putative membrane protein	2,27	9,37E-06	0,00095045
VSAL_I1484	short chain dehydrogenase	2,25	0,000409127	0,026339956
VSAL_II0128	hypothetical protein, putative phage gene	2,22	0,0037199	0,153958291
VSAL_II0371	type II secretion system protein Z	2,21	NA	NA
VSAL_II0372	type II/IV secretion system protein, ATP binding domain	2,2	0,00195389	0,096646076

VSAL_II0947	hypothetical protein	2,19	0,00175157	0,088804587
VSAL_I1493	microbial collagenase precursor (pseudogene)	2,16	0,001724005	0,088513491
VSAL_I1486	cold-shock protein	2,16	0,004993773	0,180845928
VSAL_II0362	hypothetical protein	2,16	0,000105488	0,008228079
VSAL_II0946	integral membrane protein	2,14	0,000101584	0,008078876
VSAL_II0214	patatin-like phospholipase	2,12	0,004627447	0,174638179
VSAL_II0297	putative glycosyl transferase	2,12	0,000860843	0,049177175
VSAL_II0324	putative lipoprotein	2,12	0,000454958	0,028832946
VSAL_I3080t	null	2,09	0,006686105	0,214752741
VSAL_I2064	conserved hypothetical protein	2,09	0,007300978	0,225328083
VSAL_I2857	assembly/transport component in curli production, CsgE precu	2,09	0,002451804	0,115606384
VSAL_I1457	hypothetical protein	2,08	0,002778704	0,128072987
VSAL_II0323	putative lipoprotein	2,07	NA	NA
VSAL_I1818	phosphoesterase (pseudogene)	2,06	NA	NA
VSAL_II0644	putative membrane protein	2,06	0,003881255	0,155865072
VSAL_II0367	type IV leader peptidase	2,06	0,007863317	0,234511872
VSAL_II0074	membrane protein	2,05	0,005881559	0,197153735
VSAL_II0854	secretion protein, HlyD family	2,05	0,008990486	0,253232018
VSAL_II0932	cellulose synthase catalytic subunit	2,05	NA	NA
VSAL_II0215	catalase	2,05	0,006830154	0,214752741
VSAL_II0931	membrane protein (fragment)	2,04	0,005561039	0,192008306
VSAL_II0373	bacterial type II secretion system protein F	2,03	0,00558604	0,192008306
VSAL_I2547	conserved hypothetical protein	2,02	0,002977441	0,132708802
VSAL_II0322	putative membrane protein	2,02	NA	NA
VSAL_II0366	fimbrial protein, Flp/Fap pilin component	2,01	0,010974208	0,298734145
VSAL_II0300	hypothetical protein	2,01	0,008294642	0,243790342
VSAL_I1475	hypothetical protein	2	0,003873117	0,155865072
VSAL_I2124	hypothetical protein	-2,01	0,004752504	0,174638179
VSAL_I2061	hypothetical protein	-2,02	0,00039866	0,026080109
VSAL_I4118s	null	-2,02	0,003460818	0,14954986
VSAL_I1609	sodium/proton antiporter	-2,04	0,005220765	0,187393114
VSAL_I1610	putative aminotransferase class I and II	-2,06	0,002864243	0,130532239

VSAL_I2820	hypothetical protein	-2,08	0,003465899	0,14954986
VSAL_I1982	putative DNA transformation protein TfoX	-2,1	0,000118354	0,008728101
VSAL_I0560	branched chain amino acid transport system II carrier protein	-2,1	NA	NA
VSAL_II0327	putative nucleotidyl transferase	-2,11	NA	NA
VSAL_I2346	putative exported protein	-2,14	5,54E-06	0,000576025
VSAL_II0817	proline permease	-2,17	NA	NA
VSAL_I2331	flagellar P-ring protein 2 precursor (basal body P-ring protein 2	-2,2	0,000207894	0,014291846
VSAL_I1344	serine transporter	-2,23	0,002347293	0,112007307
VSAL_I1608	HTH-type transcriptional regulator GalR	-2,26	0,002081612	0,100512126
VSAL_II0662	putative signaling protein	-2,27	1,88E-05	0,001698539
VSAL_I2269	hypothetical protein	-2,28	0,000776259	0,045630552
VSAL_I0799	methyl-accepting chemotaxis protein	-2,31	0,000577455	0,036033202
VSAL_I2495	hypothetical protein	-2,31	1,46E-05	0,001411011
VSAL_I1317	carbon starvation protein (pseudogene)	-2,36	0,000343908	0,022867049
VSAL_I2345	putative exported protein	-2,39	1,94E-06	0,000240323
VSAL_I1343	L-serine dehydratase 1	-2,56	2,52E-06	0,000300421
VSAL_I1951	methyl-accepting chemotaxis protein	-2,57	3,27E-08	7,37E-06
VSAL_II0328	putative anti-sigma F factor antagonist	-2,59	0,000116216	0,008728101
VSAL_I2057	general L-amino acid-binding periplasmic protein precursor	-2,59	1,82E-05	0,001673827
VSAL_II1079	NADPH-flavin oxidoreductase	-2,66	4,13E-06	0,000464873
VSAL_II0054	hypothetical protein	-2,8	4,82E-06	0,00051492
VSAL_II0721	PTS system permease for N-acetylglucosamine and glucose	-2,98	5,46E-08	1,01E-05
VSAL_II0824	putative sugar-specific permease, SgaT/UlaA	-3,18	1,73E-07	2,92E-05
VSAL_II0785	putative exported protein	-3,27	5,18E-08	1,00E-05
VSAL_II0823	PTS system, lactose/cellobiose specific IIB subunit	-3,29	3,36E-07	5,05E-05
VSAL_I1342	hypothetical protein	-3,32	4,79E-08	9,71E-06
VSAL_II1022	methyl-accepting chemotaxis protein	-3,33	2,94E-07	4,58E-05
VSAL_I2330	peptidoglycan hydrolase FlgJ	-3,34	1,17E-06	0,000152928
VSAL_I2332	flagellar L-ring protein 1 precursor (basal body L-ring protein 1	-3,38	2,64E-07	4,28E-05
VSAL_II0825	putative phosphotransferase enzyme II, A component	-3,6	7,15E-12	3,22E-09
VSAL_II1088	putative membrane protein	-3,85	8,13E-11	3,00E-08
VSAL_I4140s	null	-3,96	3,99E-07	5,78E-05

VSAL_I2319	hypothetical protein	-4	4,94E-09	1,18E-06
VSAL_I2334	flagellar basal-body rod protein FlgF	-4,77	2,26E-10	6,56E-08
VSAL_I2335	flagellar hook protein FlgE	-4,83	1,14E-10	3,55E-08
VSAL_I2328	flagellar hook-associated protein type 3 FlgL	-5,6	1,47E-11	5,96E-09
VSAL_I2333	flagellar basal-body rod protein FlgG (distal rod protein)	-5,69	NA	NA
VSAL_I2336	flagellar basal-body rod protein FlgD	-7,28	6,55E-19	4,43E-16
VSAL_I1325	proton glutamate symport protein	-8,52	1,35E-20	1,10E-17
VSAL_I2337	flagellar basal-body rod protein FlgC	-8,85	2,37E-22	3,20E-19
VSAL_I2338	flagellar basal-body rod protein FlgB	-8,93	4,77E-26	9,67E-23
VSAL_I2329	hypothetical protein	-10,14	5,63E-21	5,70E-18
VSAL_I2327	hypothetical protein	-12,51	1,52E-26	6,17E-23
pVSAL43_02	acetyltransferase	-15,79	NA	NA
pVSAL43_01	replication initiation protein	-38,82	NA	NA

Paper III

Exploring the transcriptome of *luxI*$^{-}$ and *ΔainS* mutants and the impact of N-3-oxo-hexanoyl-L- and N-3-hydroxy-decanoyl-L-homoserine lactones on biofilm formation in *Aliivibrio salmonicida*

Miriam Khider, Hilde Hansen, Jostein A. Johansen, Erik Hjerde and Nils Peder Willassen // PeerJ., 30 April 2019., 7:e6845

Exploring the transcriptome of *luxI*$^-$ and Δ*ainS* mutants and the impact of N-3-oxo-hexanoyl-L- and N-3-hydroxy-decanoyl-L-homoserine lactones on biofilm formation in *Aliivibrio salmonicida*

Miriam Khider[1], Hilde Hansen[1], Erik Hjerde[1,2], Jostein A. Johansen[1] and Nils Peder Willassen[1,2]

[1] Norwegian Structural Biology Centre, Department of Chemistry, Faculty of Science and Technology, UiT—The Arctic University of Norway, Tromsø, Norway
[2] Centre for Bioinformatics, Department of Chemistry, Faculty of Science and Technology, UiT—The Arctic University of Norway, Tromsø, Norway

ABSTRACT

Background: Bacterial communication through quorum sensing (QS) systems has been reported to be important in coordinating several traits such as biofilm formation. In *Aliivibrio salmonicida* two QS systems the LuxI/R and AinS/R, have been shown to be responsible for the production of eight acyl-homoserine lactones (AHLs) in a cell density dependent manner. We have previously demonstrated that inactivation of LitR, the master regulator of the QS system resulted in biofilm formation, similar to the biofilm formed by the AHL deficient mutant Δ*ainSluxI*$^-$. In this study, we aimed to investigate the global gene expression patterns of *luxI* and *ainS* autoinducer synthases mutants using transcriptomic profiling. In addition, we examined the influence of the different AHLs on biofilm formation.
Results: The transcriptome profiling of Δ*ainS* and *luxI*$^-$ mutants allowed us to identify genes and gene clusters regulated by QS in *A. salmonicida*. Relative to the wild type, the Δ*ainS* and *luxI*$^-$ mutants revealed 29 and 500 differentially expressed genes (DEGs), respectively. The functional analysis demonstrated that the most pronounced DEGs were involved in bacterial motility and chemotaxis, exopolysaccharide production, and surface structures related to adhesion. Inactivation of *luxI*, but not *ainS* genes resulted in wrinkled colony morphology. While inactivation of both genes (Δ*ainSluxI*$^-$) resulted in strains able to form wrinkled colonies and mushroom structured biofilm. Moreover, when the Δ*ainSluxI*$^-$ mutant was supplemented with N-3-oxo-hexanoyl-L-homoserine lactone (3OC6-HSL) or N-3-hydroxy-decanoyl-L-homoserine lactone (3OHC10-HSL), the biofilm did not develop. We also show that LuxI is needed for motility and for repression of EPS production, where repression of EPS is likely operated through the RpoQ-sigma factor.
Conclusion: These findings imply that the LuxI and AinS autoinducer synthases play a critical role in the regulation of biofilm formation, EPS production, and motility.

Submitted 21 December 2018
Accepted 18 March 2019
Published 30 April 2019

Corresponding author
Miriam Khider,
miriam.khider@uit.no

Academic editor
Fabiano Thompson

Additional Information and Declarations can be found on page 24

DOI 10.7717/peerj.6845

How to cite this article Khider M, Hansen H, Hjerde E, Johansen JA, Willassen NP. 2019. Exploring the transcriptome of *luxI*$^-$ and Δ*ainS* mutants and the impact of N-3-oxo-hexanoyl-L- and N-3-hydroxy-decanoyl-L-homoserine lactones on biofilm formation in *Aliivibrio salmonicida*. **PeerJ 7:e6845 DOI 10.7717/peerj.6845**

Subjects Bioinformatics, Microbiology, Molecular Biology
Keywords Quorum sensing, Acyl homoserine lactone, *Aliivibrio salmonicida*, Biofilm, Exopolysccharides

INTRODUCTION

Quorum sensing (QS) is a widespread mechanism in bacteria that employs autoinducing chemical signals in response to cell density. A variety of classes of QS chemical signals have been identified in different bacteria. Gram-negative bacteria usually employ N-acyl homoserine lactones (AHLs) which contain a conserved homoserine lactone (HSL) ring and an amide (N)-linked acyl side chain. The acyl groups identified to date range from 4 to 18 carbons in length (*Fuqua, Parsek & Greenberg, 2001*; *Swift et al., 2001*; *Whitehead et al., 2001*). AHL-mediated QS was originally discovered in the marine bacterium *Aliivibrio fischeri*, which was found to regulate bioluminescence through the *lux* operon in a cell-density dependent manner (*Nealson & Hastings, 1979*). The bacterium *A. fischeri* controls luminescence via the QS systems LuxS/LuxPQ, LuxI/LuxR, and AinS/AinR, where LuxS, LuxI, and AinS are the AHL autoinducer synthases (*Lupp & Ruby, 2004*, *2005*; *Lupp et al., 2003*).

The marine bacterium *Aliivibrio salmonicida*, is known to cause cold-water vibriosis in Atlantic salmon (*Salmo salar*), rainbow trout (*Oncorhynchus mykiss*), and captive Atlantic cod (*Gadus morhua*) (*Egidius et al., 1981*, *1986*; *Holm et al., 1985*). The genome sequence of *A. salmonicida* revealed five QS systems of which three are similar to those of *A. fischeri*, the LuxS/PQ, LuxI/R, and AinS/R (*Hjerde et al., 2008*). In *A. salmonicida* the LuxS/PQ and AinS/R systems transduce the information from the autoinducers AI-2 and 3OHC10-HSL to the histidine phosphotransferase protein LuxU and finally to the response regulator LuxO. The level of phosphorylated LuxO depends on the autoinducer concentrations. The phosphorylated LuxO controls the expression of small regulatory RNAs Qrr that together with the RNA chaperon Hfq, destabilize the transcript of the master regulator LitR.

A. salmonicida produces eight AHLs, where the LuxI is responsible for production of seven autoinducers (3OC4-HSL, C4-HSL, 3OC6-HSL, C6-HSL, C8-HSL, 3OC8-HSL, and 3OC10-HSL), and AinS only one autoinducer, 3OHC10-HSL (*Hansen et al., 2015*). Although, *A. salmonicida* encodes the *lux* operon (*luxCDABEG*) (*Nelson et al., 2007*), the bacteria is only able to produce bioluminescence after addition of decyl aldehyde (*Fidopiastis, Sørum & Ruby, 1999*). LitR, the master regulator of QS is a positive regulator of AHL production and hence, cryptic bioluminescence in *A. salmonicida* (*Bjelland et al., 2012*).

In addition to regulating bioluminescence, AHLs are also involved in several physiological processes in bacteria such as production of virulence factors, drug resistance, motility, and biofilm formation (*Abisado et al., 2018*; *Whitehead et al., 2001*). AHL-mediated QS is involved in all stages of biofilm formation from attachment to maturation and dispersal in a number of bacterial species (*Emerenini et al., 2015*; *Fazli et al., 2014*; *Guvener & McCarter, 2003*; *Hmelo, 2017*; *Huber et al., 2001*; *Pratt & Kolter, 1998*; *Whitehead et al., 2001*; *Yildiz & Visick, 2009*). In many *Vibrio* species

development of biofilm and rugose colony morphology dependent on exopolysaccharide (EPS) production (*Yildiz & Visick, 2009*). In *A. salmonicida* the EPS is produced by an operon known as the *symbiosis polysaccharide (syp)* operon, which is regulated by LitR via RpoQ sigma factor (*Hansen et al., 2014*; *Khider, Willassen & Hansen, 2018*). Mutation in LitR of *A. salmonicida* resulted in strains with wrinkled colonies and three-dimensional biofilm formation (*Bjelland et al., 2012*). Similar to *A. salmonicida*, inactivation of HapR, the master regulator of *Vibrio cholerae*, resulted in a regulatory state mimicking low cell density (LCD) conditions, where the mutant produced more EPS compared to wild type (*Zhu & Mekalanos, 2003*). In contrast to the two species mentioned above, *Vibrio parahaemolyticus* and *Vibrio vulnificus*, form biofilm and opaque colonies at high cell density (HCD). The inactivation of the master QS regulators, OpaR and SmcR, resulted in translucent colonies with decreased EPS production (*Lee et al., 2013*; *McCarter, 1998*).

We have previously shown that AinS and LuxI in *A. salmonicida* are responsible for the production of eight AHLs that are involved in regulation of biofilm formation (*Hansen et al., 2015*). When both *luxI* and *ainS* synthases genes were inactivated, no AHL production was observed in *A. salmonicida* and the double mutant (Δ*ainSluxI*$^{-}$) produced a biofilm similar to the biofilm of Δ*litR* mutant (*Hansen et al., 2015*). In the present work, we aimed to understand the complex regulation of biofilm formation, EPS production and motility using transcriptomic profiling on the Δ*ainS* and *luxI*$^{-}$ mutants. At HCD, inactivation of *luxI* had a global effect on the transcriptome and resulted in nearly 500 differentially expressed genes (DEGs), whereas deletion of *ainS* only resulted in 29 DEGs under the same conditions. Genes involved in motility and EPS production were among the DEGs in the *luxI*$^{-}$ mutant, which may explain the observations that this mutant lacks flagella, is non-motile and produces rugose colonies. The Δ*ainS* mutant showed DEGs associated with phosphorylation and was not involved in regulating colony rugosity. Exposing the Δ*ainSluxI*$^{-}$ double mutant to 3OC6-HSL (LuxI product) or 3OHC10-HSL (AinS product), resulted in restoration of wild type traits and no biofilm formation was observed indicating that both LuxI/R and AinS/R systems are important in the regulation of biofilm formation.

MATERIALS AND METHODS

Bacterial strains and supplements

Bacterial strains used in this study are listed in Table 1. *A. salmonicida* LFI1238 strain and the *A. salmonicida* mutants were grown from a frozen glycerol stock on blood agar base no. 2 (Oxoid, Basingstoke, UK) with a total concentration of 5% blood and 2.5% NaCl (BA2.5) or in Luria Bertani broth (Difco; BD Diagnostics, Berkshire, UK) with a total concentration of 2.5% NaCl (LB2.5).

A seawater-based medium (SWT) used for all assays consists of five g/L of bacto peptone (BD, Biosciences, San Jose, CA, USA), three g/L of yeast extract (Sigma-Aldrich, Darmstadt, Germany), and 28 g/L of a synthetic sea salt (Instant Ocean, Aquarium Systems, Blacksburg, VA, USA).

The green fluorescence protein (GFP) constitutive plasmid pVSV102 and helper plasmid pEVS104 propagated in *Escherichia coli*, DH5αλpir and CC118λpir, respectively.

Table 1 Bacterial strains and plasmids used in this study.

Bacterial strains or plasmids	Description	Source
A. salmonicida		
LFI1238	Wild type, isolated from Atlantic cod	*Hjerde et al. (2008)*
Δ*litR*	LFI1238 containing an in-frame deletion in *litR*	*Bjelland et al. (2012)*
Δ*ainS*	LFI1238 containing an in-frame deletion in *ainS*	*Hansen et al. (2015)*
luxI$^-$	LFI1238 containing an insertional disruption in *luxI*, Cm^r	*Hansen et al. (2015)*
Δ*ainSluxI*$^-$	Δ*ainS* containing an insertional disruption in *luxI*, Cm^r	*Hansen et al. (2015)*
LFI1238-pVSV102	*A. salmonicida* LFI238 carrying pVSV102, Kn^r	*Khider, Willassen & Hansen (2018)*
Δ*litR*-pVSV102	Δ*litR* carrying pVSV102, Kn^r	*Khider, Willassen & Hansen (2018)*
Δ*ainS*-pVSV102	Δ*ainS* carrying pVSV102, Kn^r	This study
luxI$^-$-pVSV102	*luxI*$^-$ carrying pVSV102, Kn^r	This study
Δ*ainSluxI*$^-$-pVSV102	Δ*ainS luxI*$^-$ carrying pVSV102, Kn^r	This study
E. coli		
C118λpir	Helper strain containing pEVS104	*Dunn et al. (2006)*
DH5αλpir	*E. coli* strain containing GFP plasmid pVSV102	*Dunn et al. (2006)*
Plasmids		
pVSV102	pES213, constitutive GFP, Kn^r	*Dunn et al. (2006)*
pEVS104	R6Korigin, RP4, *oriT, trb tra*, and Kn^r	*Stabb & Ruby (2002)*

Culture conditions

A. salmonicida strains were cultivated from single colonies in two ml (LB2.5) at 12 °C, 220 rpm for 2 days (primary culture). The primary cultures were diluted 1:20 and grown at 12 °C, 220 rpm for an additional day (secondary cultures). GFP tagged strains were selected on BA2.5 supplemented with 150 µl/ml kanamycin.

The *E. coli* strains were cultivated in LB or LA (Luria Agar) containing 1% NaCl (LB1 and LA1, respectively) and incubated at 37 °C and 220 rpm.

Transcriptomics

Sample collection

The overnight secondary cultures of Δ*ainS*, *luxI*$^-$, and *A. salmonicida* LFI1238 wild type were diluted to $OD_{600} = 0.05$ (optical density measured at 600 nm) in a total volume of 70 ml SWT media supplemented with 2.5% sea salt. The cultures were grown further at 8 °C and 220 rpm in 250 ml baffled flasks. A total of 10 ml of the grown cultures were collected at LCD $OD_{600} = 0.30$ (early logarithmic phase) and 2.5 ml was collected at HCD $OD_{600} = 1.20$ (late exponential phase). The collected samples were harvested by centrifugation at 13,000×*g* for 2 min at 4 °C (Heraeus 3XR; Thermo Scientific, Waltham, MA, USA) and preserved in RNA*later* (Invitrogen, Carlsbad, CA, USA). The preserved cultures were stored at −80 °C until RNA extraction.

Total RNA isolation and rRNA depletion

The total RNA was extracted from the cell pellets following the standard protocols provided by the manufacturer (Epicenter, Madison, WI, USA). Ribosomal rRNA was removed from the samples using Ribo-Zero rRNA Removal kit for bacteria (Illumina, San Diego, CA, USA) following the manufacturer's instructions. The quality of total RNA before and after depletion was determined using the Agilent 2100 Bioanalyzer with the RNA 600 Nano and RNA 600 Pico chips, respectively (Agilent Technologies, Santa Clara, CA, USA).

RNA sequencing and data analysis

The RNA-sequencing libraries were constructed using the TruSeq Stranded mRNA Library Prep Kit (Illumina, San Diego, CA, USA), and sequenced at the Norwegian Sequencing Center with the Illumina NextSeq 500 system using Mid-Output Kit v2 for a 75-cycle sequencing run.

The sequencing quality of FASTQ files was assessed using FastQC (http://www.bioinformatics.babraham.ac.uk/projects/fastqc). Further analysis of the RNA-Seq data was performed using EDGE-pro v1.0.1 (*Magoc, Wood & Salzberg, 2013*) and DESeq2 (*Love, Huber & Anders, 2014*). EDGE-pro was used to align the reads to the *A. salmonicida* LFI1238 genome (*Hjerde et al., 2008*) and to estimate gene expression levels. Differences in gene expression between wild type and *luxI*$^-$, and wild type and Δ*ainS* mutants were determined using DESeq2. DESeq2 first estimates size factors for each gene, then estimate the dispersion by fitting this to a model using the negative binomial distribution. Finally, DESeq2 performs a statistical test to see whether there is evidence for the observed differential expression between wild type and mutant genes, which is reported as a *p*-value. Log2 fold changes of the genes were recalculated to x differential expression values (i.e., Δ*ainS*/wt) and genes were defined as significantly DEGs based on a p-value ≤ 0.05 and fold change values of ≥ 2 and ≤ -2 equal to $\log_2$ fold 1 and −1. tRNA and rRNA reads were filtered out before analysis.

PCA plots are automatically generated by DESeq2 and were used for quality control of the biological replicates. DESeq2 normalize differences in gene expression patterns to compute a distance matrix. The *X*- and *Y*-axes in the PCA plot correspond to a mathematical transformation of these distances so that data can be displayed in two dimensions (*Love, Huber & Anders, 2014*).

The RNA sequence data presented in this study have been deposited in the European Nucleotide Archive (www.ebi.ac.uk/ena) under study accession number PRJEB29457 for Δ*ainS* and *luxI*$^-$ and accession number PRJEB28385 for *A. salmoncida* wild type.

High-performance liquid chromatography tandem mass spectrometry assay

AHL standards

The following AHL standards, purchased from University of Nottingham, UK were: N-3-oxo-butyryl-L-homoserine lactone (3OC4-HSL), N-3-hydroxy-butyryl-L-homoserine lactone (3OHC4-HSL), N-3-hydroxy-hexanoyl-L-homoserine lactone

(3OHC6-HSL), N-3-hydroxy-octanoyl-L-homoserine lactone (3OHC8-HSL), N-3-hydroxy-decanoyl-L-homoserine lactone (3OHC10-HSL). In addition, N-butyryl-DL-homoserine lactone (C4-HSL), N-hexanoyl-L-homoserine lactone (C6-HSL), N-3-oxo-hexanoyl-L-homoserine lactone (3OC6-HSL), N-octanoyl-L-homoserine lactone (C8-HSL), N-3-oxo-octanoyl-L-homoserine lactone (3OC8-HSL), N-decanoyl-DL-homoserine lactone (C10-HSL), N-3-oxo-decanoyl-L-homoserine lactone (3OC10-HSL), N-dodecanoyl-DL-homoserine lactone (C12-HSL), N-3-oxo-dodecanoyl-L-homoserine lactone (3OC12-HSL), N-3-hydroxy-dodecanoyl-DL-homoserine lactone (3OHC12-HSL), acetonitrile, and formic acid for HPLC were obtained from Sigma-Aldrich (St. Louis, MO, USA).

Preparation of bacterial supernatants for AHL measurements

Two biological replicates were used for all *A. salmonicida* strains. The overnight secondary cultures were diluted to an $OD_{600} = 0.05$ in a total volume of 60 ml SWT media supplemented with 2.5% sea salt. The cultures were grown further at 8 °C and 220 rpm in 250 ml baffled flasks for 50 h. Cells from one ml were harvested from each culture using 13,000×*g* (Heraeus Fresco 21; Thermo Scientific, Waltham, MA, USA) for 2 min at 4 °C. The supernatants were acidified with 1M HCl before threefold ethyl acetate extraction as previously described (*Purohit et al., 2013*). The ethyl acetate phase was dried using a rotary vacuum centrifuge (CentriVap; Labconco, Kansas City, MO, USA) for 15 min at 40 °C and then redissolved in 150 µl of 20% acetonitrile containing 0.1% formic acid and 775 nM of the internal standard 3OC12-HSL.

Detection of AHL profiles using a mix of HPLC-MS/MS and full scan HR-MS analysis

The detection of AHL was adapted from the methods described previously (*Hansen et al., 2015*). Briefly, the samples (20 µl) were injected into an Ascentis Express C18 5 cm × 2.1 mm, 2.7 µm reverse phase column (Supelco, Sigma-Adrich, Darmstadt, Germany) using an Accela autosampler (Thermo Scientific, Waltham, MA, USA). The elution was performed using an Accela pump (Thermo Scientific, Waltham, MA, USA) with an acetonitrile gradient in 0.1% formic acid and consisted of 5% acetonitrile for 18 s, followed by a linear gradient up to 90% acetonitrile over 222 s, and finally 90% acetonitrile for 60 s. The column was re-equilibrated for 60 s with 5% acetonitrile in 0.1% formic acid before the next sample was injected. Flow rate was 500 µl/min for all steps.

The separated compounds were ionized in positive ion electrospray using the following settings: sheath gas flow rate 70, auxiliary gas flow rate 10, sweep gas flow rate 10, spray voltage +4.50 kV, capillary temperature 330 °C, capillary voltage 37 V, and tube lens 80 V.

The ionized components where detected using an LTQ Orbitrap XL (Thermo Scientific, Waltham, MA, USA) run in either MS/MS low resolution mode or full scan HRMS mode. C4 AHLs are difficult to detect using full scan HR-MS analysis due to co-eluting isobaric compounds seen in some samples, so these components together with 3OC6 and 3OHC6 where measured using high-performance liquid chromatography tandem mass

spectrometry (HPLC-MS/MS) using the LTQ part of the LTQ orbitrap XL. The rest of the compounds were measured using Full Scan HR-MS analysis. The C4's, 3OHC6, and 3OC6 elute early in the chromatogram and where measured in two segments each with three scan events. Segment 1 ran from 0 to 0.88 min, with the following scan events. m/z 172.10-> (101.2–103.2) (C4-HSL), m/z 186.10-> (101.2–103.2) (3OC4-HSL), and 188.10-> (101.2–103.2) (3OHC4-HSL). Segment 2 ran from 0.88 to 1.76 min with the following scan events: 172.10-> (101.2–102.3) (C4-HSL), 214.10-> (101.2–102.3) (3OC6-HSL), 216.12-> (101.2–102.3) (3OHC6-HSL). Segment 3 ran from 1.76 to 5 min in which the rest of the compounds where measured using only one scan event, FTMS (165–450) resolution 15,000. Target setting was 5×10^5 ions per scan and the maximum injection time was 250 ms. Lock mass was enabled for correction of background ions from caffeine (m/z 195.0877) and diisooctyl phthalate (m/z 391.2843 and m/z 413.2662). The system was calibrated with a mixture of 15 AHLs including the internal standard 3OC12-HSL. The ion chromatograms were analyzed using the Xcalibur v. 2.1.0 software package (Thermo Scientific, Waltham, MA, USA). The mass window was set to eight parts per million. The limit of detection and the limit of quantification for the different AHLs were calculated as previously described (*Purohit et al., 2013*).

Construction of GFP tagged *A. salmonicida* strains

A. salmonicida mutants used in this study were constructed previously (*Bjelland et al., 2012*; *Hansen et al., 2015*). The Δ*ainS* mutant is a complete deletion of the *ainS* gene resulting from a double cross-over event, *luxI*$^-$ is an insertional mutant constructed by cloning an internal part of the *luxI* gene into a suicide vector pNQ705. The insertional mutant is a result of a single cross-over event and is chloramphenicol resistant, Δ*ainSluxI*$^-$ is the Δ*ainS* complete deletion mutant with an insertional mutation in the *luxI* gene using a *luxI*-pNQ705 plasmid (chloramphenicol resistant) and Δ*litR* is a complete deletion of the *litR* gene using a suicide plasmid and a double cross-over event. All mutants were tagged with GFP using tri-parental mating as described previously (*Khider, Willassen & Hansen, 2018*). Briefly, the pVSV102 plasmid carrying the gene coding for GFP and kanamycin was transferred from *E. coli* DH5αλpir to the mutant strains using the conjugative helper strain CC118λpir harboring pEVS104 helper plasmid. Donor and helper cells were grown to mid-log phase ($OD_{600} = 0.7$) in LB1. Recipient strains (*A. salmonicida*) were grown to early stationary phase ($OD_{600} = 1.2$) in LB2.5. The donor, helper, and recipient strains were harvested (13,000×*g* for 1 min) and washed twice with LB1 before they were mixed in 1:1 ratio and spotted onto BA2.5 plates, followed by overnight incubation at 16 °C. The spotted cells were re-suspended in LB2.5 and incubated for 24 h at 12 °C with agitation (220 rpm). The potential tagged strains were selected on BA2.5 supplemented with 150 µl/ml kanamycin after 5 days. The tagged strains were confirmed using Nikon Eclipse TS100 Inverted Fluorescence Microscope (Nikon, Melville, NY, USA).

Static biofilm assay

The biofilm assay was performed as described previously (*Hansen et al., 2014*; *Khider, Willassen & Hansen, 2018*). Briefly, the overnight secondary cultures were grown to an

OD_{600} of 1.3. The secondary cultures were further diluted 1:10 in SWT and a total volume of 300 µl of culture was added to each well of flat-bottomed, non-tissue culture-treated Falcon 24-well plates (BD, Biosciences). For each mutant and the wild type, final concentrations of 1,400 ng/ml of 3OC6-HSL, 100 ng/ml of 3OHC10-HSL, 197 ng/ml of 3OC8, 100 ng/ml of C8, or 400 ng/ml of C6 were added separately to each well. The concentrations of the AHLs were selected based on those *A. salmonicida* produced in "in vitro" experiments (*Hansen et al., 2015*). The plates were incubated statically at 8 °C, for 72 h and the biofilm was visualized using a Nikon Eclipse TS100 Inverted Fluorescence Microscope (Nikon) at 10× magnification and photographed with Nikon DS-5Mc (Nikon) camera. The biomasses of the biofilms were indirectly quantified using crystal violet. The medium was removed and 300 µl of 0.1% (wt/vol) crystal violet in H_2O was added. The plates were incubated at room temperature for 30 min. The crystal violet stain was removed by flipping the plates gently. The wells were then washed twice with 0.5 ml of H_2O. The plates were air dried overnight and the biofilm was dissolved in 0.5 ml of 96% ethanol with agitation (250 rpm) overnight. The dissolved biofilm was diluted 1:10 in 96% ethanol and transferred to a 96-well plate (100 µl/well). The absorbance was measured at 590 nm (Vmax kinetic microplate reader; Molecular Devices, LabX, Midland, ON, Canada).

Soft agar motility assay

The motility assay was performed using SWT soft agar plates containing 0.25% agar as previously described (*Khider, Willassen & Hansen, 2018*). Briefly, the secondary overnight cultures were diluted to an OD_{600} of 0.4 and three µl of each culture was spotted onto the soft agar plates and incubated at 8 °C for 5 days. The degree of motility for each strain was monitored every 24 h for 5 days by measuring the diameters of spreading halos on the soft agar plate.

Colony morphology and adhesion assay

The colony morphology assay was carried out as described previously (*Hansen et al., 2014*; *Khider, Willassen & Hansen, 2018*). In short, a 250 µl aliquot was harvested from each secondary overnight culture by centrifugation and the pellet was re-suspended in 250 µl SWT. Two microliters of each culture was then spotted onto SWT agar plates and incubated at 8 °C for 14 days. The colonies were viewed microscopically with Zeiss Primo Vert and photographed with AxioCam ERc5s (Zeiss, Berlin, Germany) at 4× magnification. Adhesion was examined by using the same 14 day old colonies to test their ability to adhere to the SWT agar plates. The assay was performed by touching the colonies using a sterile plastic loop as previously described (*Bjelland et al., 2012*; *Khider, Willassen & Hansen, 2018*). The adherence grading was only recorded as "Non adhesive" for smooth and non adherent colonies, "Weak" for slightly adherent and "Strong" for colonies that were impossible to separate from the SWT agar plate.

Scanning electron microscopy

The overnight secondary cultures of *A. salmonicida* strains were fixed with 2.5% (wt/vol) glutaraldehyde and 4% formaldehyde in PHEM-buffer and incubated for one day at 4 °C.

Table 2 AHL production in *A. salmonicida* LFI1238, Δ*litR*, *luxI*⁻, Δ*ainS*, and Δ*ainSluxI*⁻.

Strains	3OC6 (nM)	C6 (nM)	3OC8 (nM)	3OC10 (nM)	3OHC10 (nM)	C8 (nM)
LFI1238	8,403 ± 279.3	606 ± 3.5	366 ± 27	67 ± 5.9	161 ± 2.1	28 ± 3.0
Δ*litR*	5,173 ± 113.6	593 ± 82.3	330 ± 42.1	72 ± 4.7	11 ± 1.70	25 ± 3.4
luxI⁻	NF	NF	NF	NF	105 ± 6.7	NF
Δ*ainS*	8,691 ± 0.0	709 ± 54.6	382 ± 42.5	89 ± 16.9	NF	30 ± 0.0
Δ*ainSluxI*⁻	NF	NF	NF	NF	NF	NF

Notes:
The values represent the mean of two biological replicates ± standard deviation.
C4-HSL and 3OC4-HSL were not detected in this analysis.
NF, not found.

A total of 100 microliters of each sample was mounted on a poly-L-lysine coated coverslip for 5 min. Coverslips were washed three times with PHEM buffer before they were postfixed in 1% (wt/vol) Osmium tetroxide (OsO_4). Samples were washed an additional three times with PHEM buffer. All samples were dehydrated with a graded series of ethanol solutions at room temperature for 5 min. The samples were dried using hexamethyldisilazane as a drying agent and left to dry in a desiccator overnight before being mounted on aluminum stubs using carbon tape and silver paint. The samples were coated with gold-palladium using a Polaron Range Sputter Coater (Polaron, Quorum Technologies Ltd, East Sussex, UK). Pictures were obtained with Ziess Zigma Scanning Electron Microscopy (Ziess, Berlin, Germany).

All biological assays were carried out in biological triplicates, unless otherwise indicated. The assays were performed in two to three independent experiments to validate the results. The difference between the mutants relative to the wild type in AHL production, biofilm formation, and motility migration zones were calculated using student's *t*-test. A p-value ≤ 0.05 was regarded as significant.

RESULTS

AHL profiling of *A. salmonicida* in SWT medium

In our previous studies, AHL profiling of *A. salmonicida* LFI1238 and mutants thereof were performed after growth in LB2.5 medium. However, since SWT medium is required for biofilm formation we first wanted to know whether a change of medium would affect the AHL profiles of *A. salmonicida* wild type and the mutants.

The different *A. salmonicida* strains (LFI1238, Δ*litR*, Δ*ainS*, *luxI*⁻, and Δ*ainSluxI*⁻) were grown in SWT medium at 8 °C for 50 h (OD_{600} ~ 2.0) before samples were harvested and analyzed using HPLC-MS/MS. The *A. salmonicida* wild type and mutants showed AHL profiles (Table 2) that were similar to the profiles after growth in LB (*Hansen et al., 2015*) with the exception of C4 and 3OC4. Thus, the wild type and the Δ*litR* AHL profiles consisted of six AHLs, where the 3OC6-HSL was the most abundant. No AHLs were detected in the Δ*ainSluxI*⁻ supernatant. The *luxI*⁻ mutant produced only 3OHC10-HSL, and the Δ*ainS* mutant produced the remaining five AHLs. Compared to the wild type, the Δ*litR* mutant produced lower concentrations of the 3OC6-HSL and 3OHC10-HSL confirming that LitR is a positive regulator of these two AHLs also after growth in SWT medium.

N-acyl homoserine 3OHC10 and 3OC6 downregulate biofilm formation in *A. salmonicida*

Our previously reported results (*Hansen et al., 2015*) and the AHL profiling presented above, have shown that *litR* deletion significantly influenced the production of 3OC6-HSL (LuxI product) and 3OHC10-HSL (AinS product) compared to the wild type. Therefore, we wished to investigate the possible effects of 3OC6-HSL and 3OHC10-HSL on biofilm formation. The different AHLs were added separately to the SWT medium and *A. salmonicida* strains were allowed to form biofilm at 8 °C for 72 h. As shown in Fig. 1A, the biofilm formation of Δ*ainSluxI*$^-$ was totally inhibited when supplemented with either 3OHC10-HSL or 3OC6-HSL. The Δ*ainS, luxI*$^-$ and the wild type do not form a biofilm (*Hansen et al., 2015*), and no clear morphological differences in the biofilm formation was observed when treated with 3OHC10-HSL or 3OC6-HSL (Fig. 1A). The mushroom structured Δ*litR* biofilm remained unchanged after the addition of AHLs. This shows that LuxI-3OC6-HSL and AinS-3OHC10-HSL functions through LitR, and downregulation of biofilm formation cannot be achieved when *litR* is inactivated (Fig. 1A). Next, the biomasses of treated and untreated biofilms were quantified using crystal violet. Relative to the untreated control samples, the addition of either 3OHC10-HSL or 3OC6-HSL significantly decreased the biomass of Δ*ainSluxI*$^-$ biofilm (p-value ≤ 0.05). Quantitation of treated and untreated Δ*litR*, LFI1238, Δ*ainS*, and *luxI*$^-$ showed no significant changes (Fig. 1B). The treatment of *A. salmonicida* wild type and the mutant strains with other AHLs (C6, C8, and 3OC8) did not interfere with the biofilm formation (data not shown). This may indicate that these AHLs are not involved in the regulation of biofilm and have other functions in *A. salmonicida*.

luxI$^-$ mutant forms adherent wrinkled colonies in *A. salmonicida*

To determine whether any of the *A. salmonicida* QS systems (*lux* and/or *ain*) are involved in the formation of wrinkled colony morphology, the *luxI*$^-$, Δ*ainS*, and the double mutant Δ*ainSluxI*$^-$ were allowed to form colonies on SWT plates at 8 °C. As shown in Fig. 2, the Δ*ainS* mutant formed smooth colonies indistinguishable from those formed by the wild type. This may indicate that *ainS* is not required for formation of rugosity. The *luxI*$^-$ and Δ*ainSluxI*$^-$ mutants formed wrinkled colonies after 14 days of incubation similar to the colonies formed by Δ*litR*. The wrinkled colonies formed by the *luxI*$^-$, Δ*ainSluxI*$^-$, and Δ*litR* mutants were found to be adhesive on the SWT agar at 8 °C. The Δ*ainS* mutant behaved similarly to the wild type and produced non-adhesive smooth colonies under the same conditions (Table S1).

Expression profiles of *A. salmonicida luxI*$^-$ and Δ*ainS* mutants revealed differentially expressed genes related to QS

Transcriptome data of A. salmonicida wild type, luxI$^-$ *and* Δ*ainS mutants*

In order to gain a better understanding of the roles of LuxI and AinS work in the QS system, samples from *A. salmonicida* LFI1238 wild type, *luxI*$^-$ and Δ*ainS* mutants were

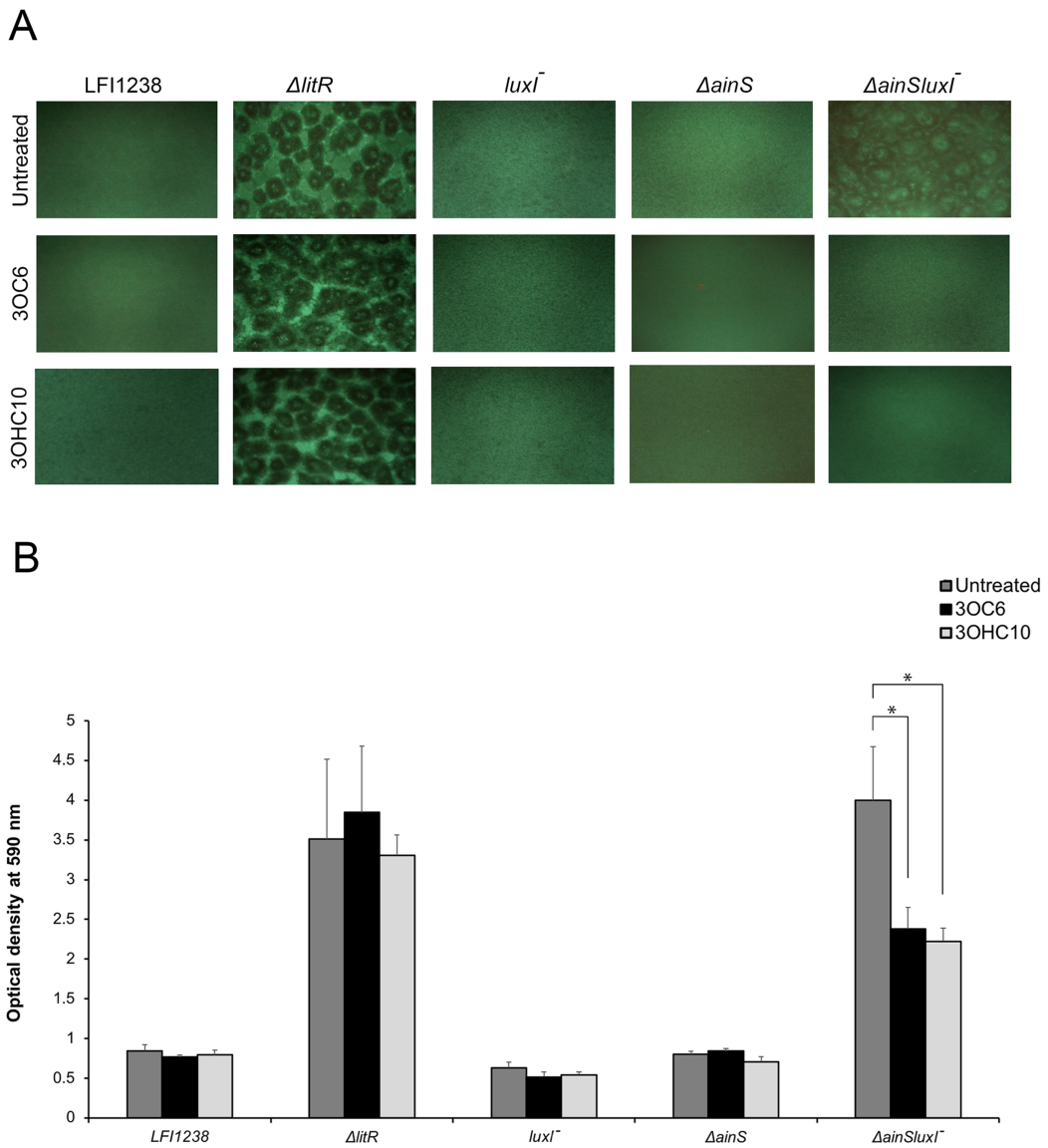

Figure 1 The effect of 3OC6-HSL and 3OHC10-HSL on biofilm formation of LFI1238, Δ*litR*, *luxI*⁻, Δ*ainS*, and Δ*ainSluxI*⁻. (A) The strains (LFI1238, Δ*litR*, *luxI*⁻, Δ*ainS*, and Δ*ainSluxI*⁻) were allowed to form biofilm in SWT media supplemented with 1,400 ng/ml 3OC6-HSL or 100 ng/ml 3OHC10-HSL at 8 °C for 72 h. The biofilms were viewed in Inverted Fluorescence Microscope Nikon Eclipse TS100 at 10× magnification and photographed with Nikon DS-5Mc camera. (B) The formed biofilms were staining with crystal violet and quantified by measuring the absorbance at 590 nm. The error bars represent the standard deviation of biological triplicates. *Represents p-value ≤ 0.05.

Full-size DOI: 10.7717/peerj.6845/fig-1

extracted at early logarithmic ($OD_{600} = 0.3$) and late exponential ($OD_{600} = 1.2$) phases from three independent cultures. The transcriptome expression profiles (*luxI*⁻ and Δ*ainS*) of these cultures were compared to the *A. salmonicida* LFI1238 wild type. The total assembled transcriptome of *A. salmonicida* wild type LFI1238 generated an average of 9.87 million reads at LCD and 9.56 million at HCD. The average of mapped reads to the reference genome (*A. salmonicida* LFI1238) was 88.7% at LCD and 91.4% at HCD,

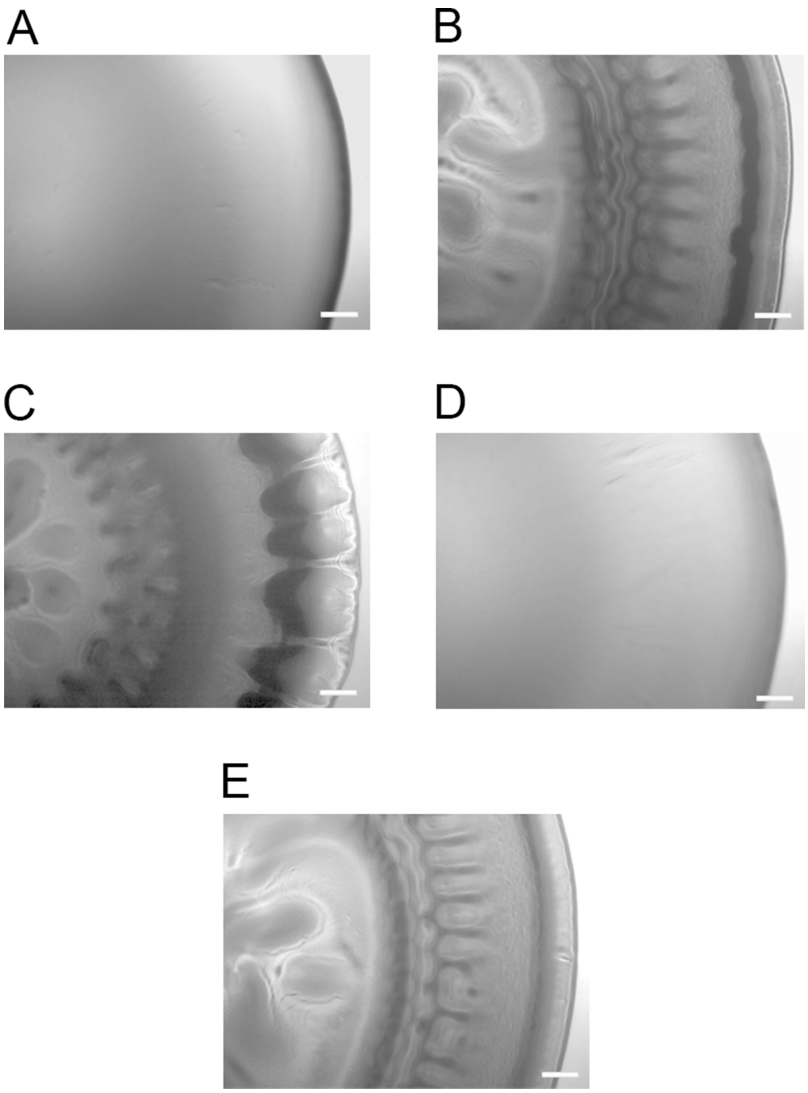

Figure 2 Colony morphology on SWT agar. (A) LFI1238, (B) Δ*litR*, (C) *luxI*⁻, (D) Δ*ainS*, and (E) Δ*ainSluxI*⁻. The colonies of different strains were allowed to form on SWT plates at 8 °C for 14 days. The colonies were viewed in a Zeiss Primo Vert microscope at 4× magnification and photographed with AxioCam ERc5s. Scale bars represent 0.5 mm. Full-size DOI: 10.7717/peerj.6845/fig-2

with an average mapping coverage of 140.6 and 141.0, respectively. The total assembled transcriptome of *luxI*⁻ generated an average of 11.5 million reads at LCD and 9.18 million at HCD. The average of mapped reads to the reference genome (*A. salmonicida* LFI1238) was 94.5% at LCD and 92.9% at HCD, with an average mapping coverage of 109.5 and 85.2, respectively. The detailed transcriptome data of Δ*ainS* also showed average of mapped reads to the reference genome of 93.9% and 92.8% at LCD and HCD, respectively, with average mapping coverage of 88 at LCD and 100.8 at HCD (Table S2). To control for technical variations between biological replicates PCA analysis on the expression data from HCD vs. LCD was performed using DESeq2. The biological replicates clustered together well and were distinct between HCD and LCD.

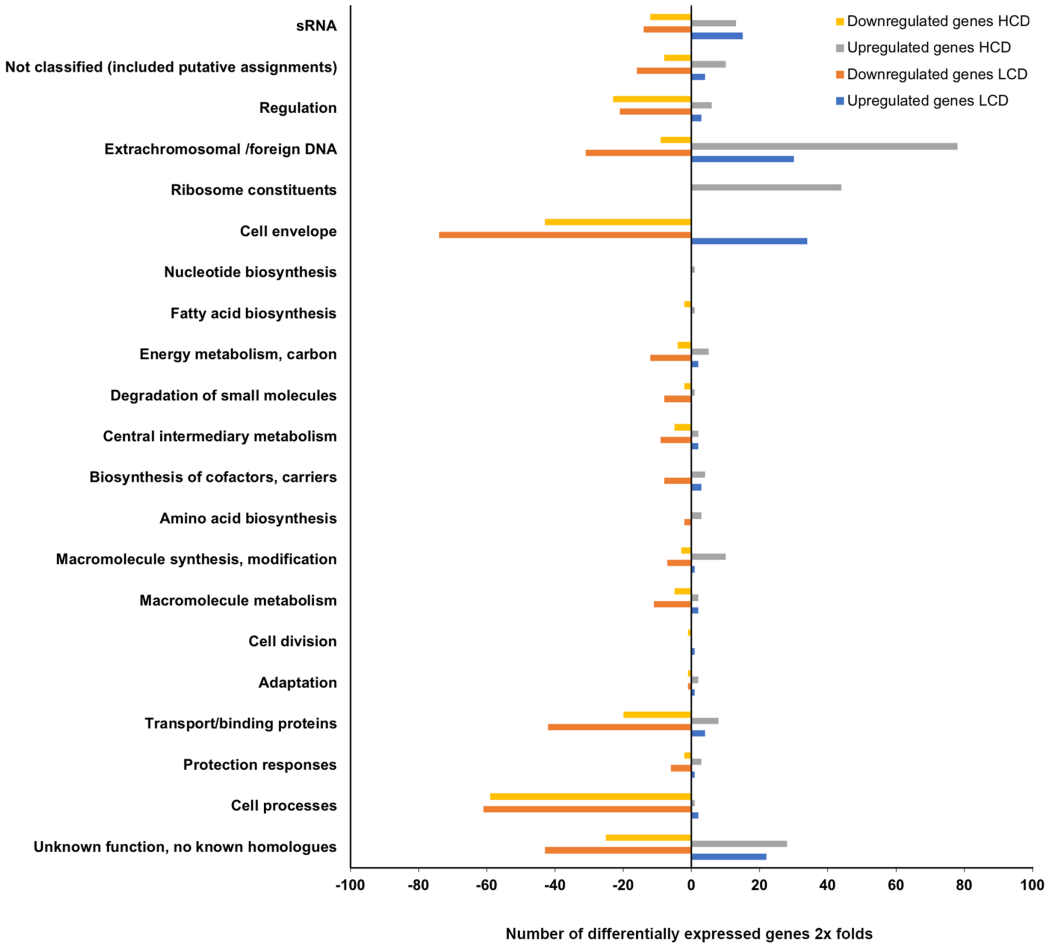

Figure 3 Functional distribution of genes between *A. salmonicida* wild type and *luxI*⁻ mutant at HCD and LCD that are ≥2 × differentially expressed. The *x*-axis represents the number of upregulated and downregulated differentially expressed genes of the *luxI*⁻/*wt* at high and low cell densities (filled bars), that fell into various functional groups represented at the *y*-axis.

Full-size DOI: 10.7717/peerj.6845/fig-3

The transcriptome profile of A. salmonicida luxI⁻ mutant relative to the wild type

The expression profiling of *luxI*⁻ mutant relative to the wild type LFI1238 revealed 494 and 446 DEGs at LCDs and HCDs, respectively, that fell into various functional gene classes adapted from MultiFun (*Serres & Riley, 2000*) (Fig. 3). The *luxI*⁻ DEGs were distributed almost equally between the large and small *A. salmonicida* chromosomes with 292 DEGs at LCD (59%) and 259 DEGs at HCD (55%). Among the DEGs at LCD 366 were downregulated and 128 were upregulated (Table S3). While at HCD 224 genes were downregulated and 222 genes were upregulated (Table S4). Many of the DEGs we discovered were genes organized in operons. One of the significantly downregulated genes is the *rpoQ* sigma factor (*VSAL_II0319*), organized in an operon of seven genes (*VSAL_II0319–VSAL_II0325*). The whole operon was differentially expressed at HCD and five genes of the operon were differentially expressed at LCD with fold change values

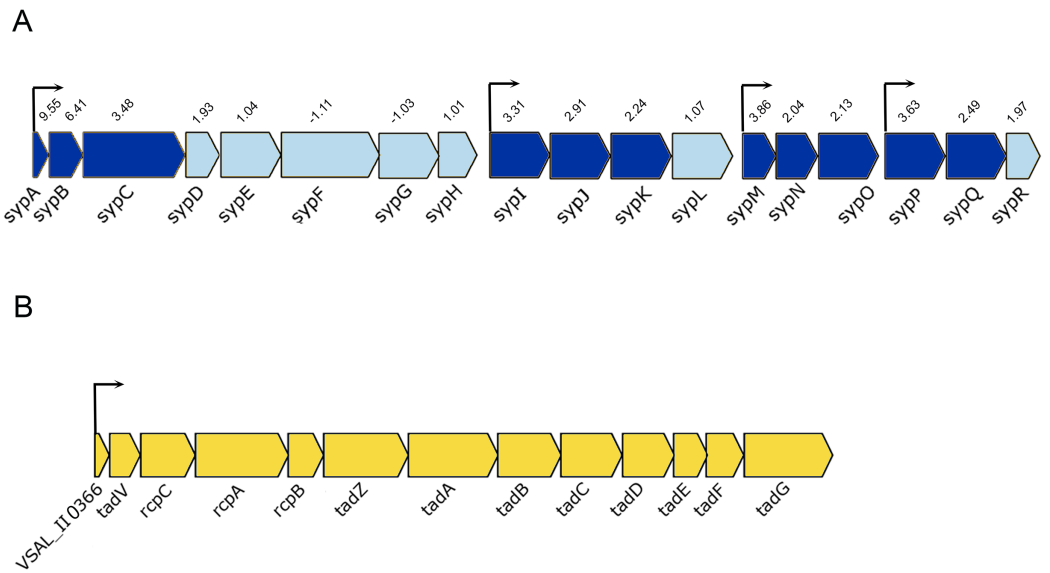

Figure 4 Schematic representation of the genetic organization of *A. salmonicida syp* and *tad* operons. (A) The *syp* operon (*VSAL_II0312–VSAL_II0296*) consists of four transcriptional units. Arrows indicate genes and their direction of transcription. The dark blue arrows represent genes with significantly expressed *p*-values, whereas the arrows in light blue are gene with no significant expression values. Number above the arrows indicate the expression level in 2× fold change. (B) The *tad* operon (*VSAL_II0366–VSAL_II0378*), arrows indicate the genes and their direction of transcription.

Full-size DOI: 10.7717/peerj.6845/fig-4

ranging from −8.15 to −3.43. The remaining genes of the operon (*VSAL_II0324* and *VSAL_II0325*) were expressed with fold change values −1.74 and −1.93, respectively (Table 3).

The *luxI*$^{-}$ mutant formed wrinkled colony morphology on SWT plates. The rugosity is associated with the enhanced production of EPSs, which requires the expression of *syp* operon (18 genes) in *A. salmonicida* (*Hansen et al., 2014*; *Khider, Willassen & Hansen, 2018*). The *syp* operon (*VSAL_II0295–VSAL_II0312*) is located on chromosome II and organized in four transcription units (Fig. 4A). Our data at HCD demonstrated that 11 genes in the *syp* operon were significantly upregulated with fold change values ranging from 9.55 to 2.04, the remaining genes of the *syp* operon with fold change values ranging from 1.01 to 1.97 were filtered out due to the predominant criteria for identifying DEGs (fold change $\geq$2 and $\leq$−2, *p*-value $\leq$ 0.05) (Table 3).

Among the upregulated genes that fell into the *cell envelope* (*surface structures*) functional group were genes associated with the tight adherence (Tad) loci also known as *tad* operon, that consists of 13 genes located on chromosome II of *A. salmonicida* genome (Fig. 4B). Among the genes of the *tad* operon with highest level of expression were *VSAL_II0366* (83.8-fold change at LCD and 151.5-fold change at HCD) and *VSAL_II0377* (57.3-fold change at LCD and 39.5-fold change at HCD) coding for fimbrial proteins, Flp/Fap pilin component and type IV leader peptidase, respectively. The remaining genes of the *tad* operon were also upregulated in the *luxI*$^{-}$ mutant relative to the wild type at both cell densities, and are listed in detail in Table 3. Within the same functional group (*cell envelope*), we were able to identify four downregulated DEGs (*VSAL_I0471*,

Table 3 Genes of the *rpoQ*, *tad*, and *syp* operons at low and high cell densities in the *luxI*⁻/wt transcriptome.

VSAL_ID	LCD		HCD		Gene	Function
	FC	*p*-value	FC	*p*-value		
rpoQ genes						
VSAL_II0319	−8.15	1.78*E*-25	−5.08	9.15*E*-28	*rpoQ*	RNA polymerase sigma factor
VSAL_II0320	−5.33	2.33*E*-19	−6.69	6.19*E*-24		Putative membrane associated signaling protein
VSAL_II0321	−4.82	1.20*E*-23	−6.54	2.38*E*-32		Putative glycosyl transferase
VSAL_II0322	−3.43	3.88*E*-15	−6.52	7.94*E*-33		Putative membrane protein
VSAL_II0323	−3.67	1.22*E*-20	−5.67	5.44*E*-24		Putative lipoprotein
VSAL_II0324	**−1.74**	0.0001	−4.25	8.65*E*-26		Putative lipoprotein
VSAL_II0325	**−1.93**	2.26*E*-05	−4.20	3.29*E*-23		Putative exported protein
tad genes						
VSAL_II0366	83.84	3.32*E*-45	151.51	2.68*E*-33	?	Fimbrial protein. Flp/Fap pilin component
VSAL_II0367	57.37	3.31*E*-157	39.53	7.92*E*-39	*tadV*	Type IV leader peptidase
VSAL_II0368	22.97	7.63*E*-96	8.23	4.51*E*-32	*rcpC*	Putative Flp pilus assembly protein
VSAL_II0369	18.78	5.99*E*-121	10.82	1.54*E*-38	*rcpA*	Type II/III secretion system protein
VSAL_II0370	24.63	7.18*E*-155	18.12	4.12*E*-24	*rcpB*	Putative lipoprotein
VSAL_II0371	24.11	4.75*E*-138	9.57	1.62*E*-27	*tadZ*	Type II secretion system protein Z
VSAL_II0372	20.25	3.92*E*-140	10.26	3.51*E*-33	*tadA*	Type II/IV secretion system protein. ATP binding domain
VSAL_II0373	15.02	6.78*E*-77	7.32	2.97*E*-33	*tadB*	Bacterial type II secretion system protein F
VSAL_II0374	6.75	4.86*E*-59	2.17	7.26*E*-09	*tadC*	Bacterial type II secretion system protein F
VSAL_II0375	3.63	6.47*E*-32	**1.31**	**0.0135**	*tadD*	Putative secretion system protein
VSAL_II0376	3.85	3.98*E*-32	**1.23**	**0.1109**	*tadE*	Membrane associated secretion system protein
VSAL_II0377	3.97	6.25*E*-43	**1.37**	**0.0301**	*tadF*	Membrane associated secretion system protein
VSAL_II0378	3.58	1.99*E*-41	**1.09**	**0.5780**	*tadG*	Membrane associated secretion system protein
syp genes						
VSAL_II0295			**1.97**	0.001811	***sypR***	Sugar transferase
VSAL_II0296			2.49	3.35*E*-09	*sypQ*	Putative transmembrane glycosyl transferase
VSAL_II0297			3.63	1.34*E*-15	*sypP*	Putative glycosyl transferase
VSAL_II0298			2.13	2.02*E*-07	*sypO*	Putative membrane protein
VSAL_II0299			2.04	0.003254	*sypN*	Putative glycosyl transferases
VSAL_II0300			3.86	4.63*E*-08	*sypM*	Hypothetical protein
VSAL_II0301			**1.07**	0.742157	***sypL***	O-antigen polymerase
VSAL_II0302			2.24	8.25*E*-07	*sypK*	Putative polysaccharide biosynthesis protein

(Continued)

Table 3 (continued).

VSAL_ID	LCD		HCD		Gene	Function
	FC	*p*-value	FC	*p*-value		
VSAL_II0303			2.91	3.04*E*-08	*sypJ*	Putative glycosyl transferase
VSAL_II0304			3.31	5.28*E*-08	*sypI*	Putative glycosyl transferase
VSAL_II0305			**1.01**	0.937840	***sypH***	Putative glycosyl transferase
VSAL_II0306			**−1.03**	0.001601	***sypG***	Two-component response regulator. transcriptional regulatory protein LuxO
VSAL_II0307			**−1.11**	0.294485	***sypF***	Response regulator. histidine kinase
VSAL_II0308			**1.04**	0.691913	***sypE***	Putative response regulator
VSAL_II0309			**1.93**	0.001993	***sypD***	Putative capsular polysaccharide synthesis protein
VSAL_II0310			3.48	4.60*E*-12	*sypC*	Polysaccharide biosynthesis/export protein
VSAL_II0311			6.41	3.45*E*-15	*sypB*	Outer membrane protein. OmpA family
VSAL_II0312			9.55	4.70*E*-26	*sypA*	Hypothetical protein. putative anti-sigma factor antagonist

Note:
Values indicated in bold are genes filtered out from the analysis due to fold change values (FC) below ≤2 and ≥−2 (not significantly expressed).

VSAL_I0473, and *VSAL_I0479*) at LCD and one at HCD (*VSAL_I0476*) associated with type IV pilus.

In several bacteria, QS has been shown to regulate motility and flagellar synthesis (*Kim et al., 2007*; *Ng & Bassler, 2009*). The expression profile of the *luxI*$^-$ mutant revealed genes associated with motility and chemotaxis (59 DEGs at LCD and 57 DEGs at HCD) (Tables S3 and S4). The greatest transcript abundance at LCD and HCD were regulatory genes *flrA* (*VSAL_I2312*) encoding sigma 54-dependent transcription regulator, *flrB* (*VSAL_I2311*) coding for two-component system, sensor histidine kinase and *flrC* (*VSAL_I2310*) coding for response regulator. Other genes coding for flagellin subunits and flagellar basal body rod, ring, hook, and cap proteins, were also downregulated in the *luxI*$^-$ mutant relative to the wild type at both cell densities. Additionally, genes coding for methyl-accepting chemotaxis proteins and motor proteins as MotA and MotB were downregulated in the *luxI*$^-$ mutant (Fig. 5).

The transcriptome of *luxI*$^-$ (*luxI*$^-$/wt) showed a downregulation of the *lux* operon, *luxCDABEG* (*VSAL_I0964–VSAL_I0959*). Among the downregulated genes at LCD were *luxC* (−3.53-fold change), *luxD* (−2.09-fold change), *luxA* (−2.14-fold change), and *luxB* (−2.07-fold change) the remaining genes of the operon were not differentially expressed. At HCD the whole operon was significantly downregulated with a fold change values ranging from −51.44 (*luxC*) to −8.21-fold change (*luxG*).

The remaining DEGs of the *luxI*$^-$/wt transcriptome were mostly genes with *unknown functions*, *transport/binding proteins, extrachromosomal/foreign DNA*, and *small RNAs* functional groups (Fig. 3).

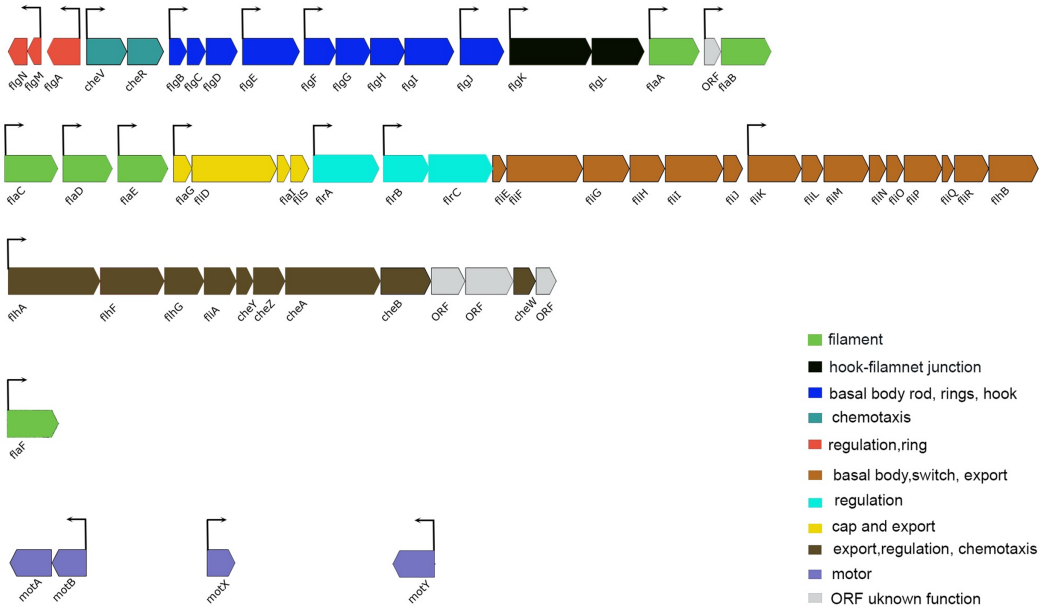

Figure 5 Schematic representation of the genetic organization of *A. salmonicida* flagellar gene system. Flagellar genes of *A. salmonicida* are located in chromosome I and are organized in different chromosomal regions. *flgN* to *flaB* (*VSAL_I2343–VSAL_I2325*) are found in nucleotides (2516889–2499860). *flaC* to *flhB* (*VSAL_I2319–VSAL_I2295*) are found in nucleotides (2492863–2470553). *flhA* to ORF coding for putative membrane protein (*VSAL_I2293–VSAL_I2282*) are found in nucleotides (2466352–2456322). The *flaF* (*VSAL_2517*) is located distinct from the other five filament coding genes (*flaA-flaE*) and is found in nucleotides (2696413–2697570). Motor genes *motA* and *motB* (*VSAL_I0936* and *VSAL_I0937*) are located in an operon and are found in nucleotides (1033690–1035398). *motX* (*VSAL_2771*) is found in nucleotides (3000998–3001630) and *motY* (*VSAL_I1863*) is found in nucleotides (1998701–1999579). In *Vibrios* flagellar genes fall into four different hierarchical classes; Class I encode the regulatory protein FlrA, which together with sigma factor 54 controls expression of Class II genes. Class II proteins FlrB and FlrC are important for controlling transcription of Class III genes necessary for synthesis of hook, basal body, and filaments. Class II sigma factor 28 (FliA) regulates transcription of Class IV genes associated with the production of motor components (*Brennan et al., 2013*; *Norsworthy & Visick, 2013*; *Millikan & Ruby, 2003*, *2004*; *Stewart & McCarter, 2003*). Arrows indicate the direction of transcription. The color code provided in the image represent the different functions of each group in the flagellar apparatus. Full-size DOI: 10.7717/peerj.6845/fig-5

The transcriptome profile of A. salmonicida ΔainS relative to the wild type

The transcriptome of Δ*ainS* relative to the wild type revealed fewer DEGs compared to the *luxI*⁻. At LCD, a total of 20 DEGs (8 up- and 12 downregulated) were identified. At HCD we were able to identify 29 DEGs where 8 were upregulated and 21 genes were downregulated (Tables S5 and S6). The DEGs fell into 10 functional groups (Fig. S1). At LCD and in the absence of AHLs, the *ain* system of *V. harveyi* act as kinase and serve as phosphoryl-donors to LuxU, which in turn phosphorylates LuxO (*Freeman & Bassler, 1999*). The Δ*ainS* transcriptome demonstrates an upregulation in genes responsible for phosphorylation. The DEGs with significant expression level relative to the wild type was phosphorelay protein LuxU (*VSAL_I1875*) with a fold change values of 2.22 and 2.37 at LCD and HCD, respectively. Whereas the *luxO* gene (*VSAL_I1874*) was not differentially expressed (1.14-fold change at LCD and 1.62-fold change at HCD) and thus not considered further.

Among the upregulated genes that fell into the *surface structures* functional group was the *tad* operon (*VSAL_II0366–VSAL_II0378*). The *VSAL_II0366* gene coding for fimbrial protein showed a fold change values of 2.82 and 4.24 at LCD and HCD, respectively. *VSAL_II0367* coding for Flp/Fap pilin component and type IV leader peptidase was identified among upregulated genes at LCD only (Table S5). Among the 21 genes that were downregulated at HCD, the DEGs with highest fold change values were assigned to *amino acid biosynthesis* functional group including the sulfate adenyltransferase subunit 1 and 2 encoded by *VSAL_I0421* and *VSAL_I0420*, respectively (Table S6).

LuxI controls motility in *A. salmonicida* LFI1238

The flagellum is required for motility of bacteria, mediating their movements toward favorable environments and avoiding unfavorable conditions (*Utada et al., 2014*; *Zhu, Kojima & Homma, 2013*). Since the expression profile demonstrated that a large group of flagellar biosynthesis and assembly genes are regulated by the *lux* system, we wished to analyse the motility behavior of the QS mutants (*luxI*$^-$, Δ*ainS*, and Δ*ainSluxI*$^-$), using a soft motility assay.

Our results showed that inactivation of *luxI* resulted in a non-motile strain, where the size of the spotted colony (2.0 mm) did not change, indicating no migration from the site of inoculation (Figs. 6A and 6B). AinS was shown to negatively regulate motility in *A. fischeri* (*Lupp & Ruby, 2004*), and similarly, we assessed the impact of *ainS* deletion on motility of *A. salmonicida*. Compared to the wild type, which showed motility zones of 26.6 ± 0.57 mm, the Δ*ainS* showed an increased motility, where migration through the soft agar resulted in motility zones of 30.3 ± 0.57 mm. Similarly, the Δ*ainSluxI*$^-$ double mutant also demonstrated an increased motility compared to the wild type with motility zones of 31.3 ± 1.15 mm (Table S7). In order to determine whether the strains analyzed by soft motility assay possess or lack flagella, the wild type and the constructed mutants were visualized by scanning electron microscopy. The Δ*ainS* and Δ*ainSluxI*$^-$ mutants produced several flagella similar to the wild type. As expected the *luxI*$^-$ mutant is non-motile and lacks flagella (Fig. 6C).

DISCUSSION

Acyl-homoserine lactones have been identified in many vibrio and aliivibrio species including *A. salmonicida* (*Buchholtz et al., 2006*; *García-Aljaro et al., 2008*; *Purohit et al., 2013*; *Valiente et al., 2009*), which showed to produce a broad range of AHLs through LuxI and AinS synthases (*Hansen et al., 2015*). However, there is still limited understanding of the biological advantages of this AHL diversity in the QS mechanism. In this study, we have demonstrated the influence of *luxI* and *ainS* on the global gene regulation and the impact of AHLs on several phenotypic traits related to QS in order to understand the complex network of signal production and regulation in *A. salmonicida*.

The ability to form rugose colonies and biofilm are often correlated features in vibrios (*Casper-Lindley & Yildiz, 2004*; *Yildiz & Schoolnik, 1999*; *Yildiz et al., 2004*), where wrinkled colony phenotype is generally associated with enhanced EPS production (*Yildiz & Schoolnik, 1999*). Likewise, in *A. salmonicida* colony wrinkling (rugosity) and

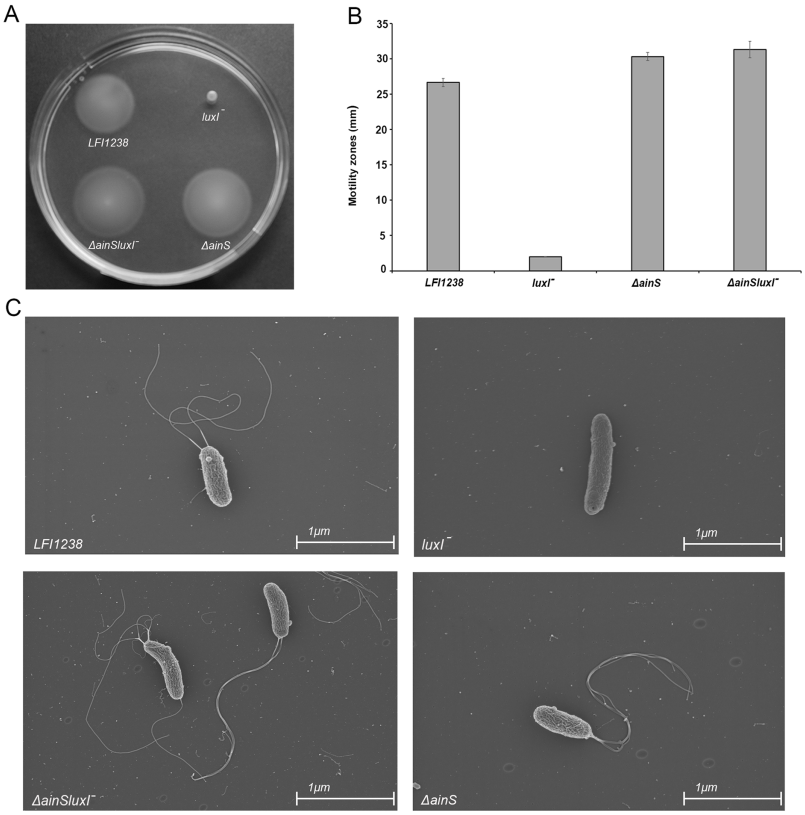

Figure 6 Motility of LFI1238, *luxI*⁻, Δ*ainS*, and Δ*ainSluxI*⁻. (A) Motility zones on soft agar plates after 5 days on incubation at 8 °C. (B) Measurement of motility zones (mm) of LFI1238, *luxI*⁻, Δ*ainS*, and Δ*ainSluxI*⁻ after 5 days, error bars are standard deviation of biological triplicates. (C) scanning electron microscopy images for flagellum observation of LFI1238, *luxI*⁻, Δ*ainS*, and Δ*ainSluxI*⁻ taken with Ziess Zigma at two kV with an in-lens detector. Scale bars represent one μm.

Full-size DOI: 10.7717/peerj.6845/fig-6

biofilm formation requires the expression of *syp* genes responsible for the production of EPS (*Hansen et al., 2014*; *Khider, Willassen & Hansen, 2018*). In the study presented here, we show that *luxI*⁻ mutant exhibited a strong wrinkling colony morphology, indicating an enhanced polysaccharide production. Earlier studies demonstrated that inactivation of the AHL synthase (*luxI* homologous) in several bacteria caused a reduction in both AHL and EPS production (*Koutsoudis et al., 2006*; *Molina et al., 2005*; *Von Bodman, Bauer & Coplin, 2003*). However, here we show that inactivation of *luxI* in *A. salmonicida* enhanced the EPS production and resulted in wrinkled colonies. Unlike the *luxI*⁻ mutants, the Δ*ainS* mutant formed smooth colonies, similar to the wild type. These findings are further confirmed by the transcription analysis, which revealed upregulation of 11 *syp* genes and downregulation in the *rpoQ* gene in the *luxI*⁻ mutant relative to the wild type. Whereas no DEGs associated with EPS production or *rpoQ* were found in the Δ*ainS* transcriptome. The sigma factor RpoQ functions downstream of LitR and is known to be a strong repressor of *syp* in *A. salmonicida* (*Khider, Willassen & Hansen, 2018*). Although LitR was shown to be a positive regulator of *rpoQ* (*Khider, Willassen & Hansen, 2018*), the gene (*litR*) was not found among the DEGs of the *luxI*⁻ or Δ*ainS* transcriptome.

We have previously proposed that the expression of *rpoQ* may be independent of LitR and that its regulatory function can be altered by environmental conditions (*Khider, Willassen & Hansen, 2018*). Hence, our results indicate that the negative regulation of EPS through *rpoQ* is controlled directly or indirectly by LuxI, where this regulation may involve other genes and transcription factors independent of LitR, AinS or the 3OHC10-HSL production. Interestingly, the active AinS and thereby the production of 3OHC10-HSL did not downregulate the rugosity of the *luxI*$^-$ mutant through the LitR-RpoQ pathway. This can be explained by the late production of the 3OHC10-HSL in *A. salmonicida* (*Hansen et al., 2015*). We have reported previously that the concentration of 3OHC10-HSL is very low at $OD_{600} = 1.2$ (the OD_{600} of transcriptomics analysis and morphology assay), which may not be strong enough to induce the LitR-RpoQ cascade involved in the repression of *syp* genes. On the other hand, the Δ*ainS* mutant appeared to have wild type colony morphology, indicating a stronger regulatory effect of the LuxI on the RpoQ leading to repression of EPS (via *syp*) and downregulation of rugosity. These results suggest that the *luxI*$^-$ mutant is locked into a regulatory state in the bacterial life cycle that requires the EPS production, whereas the Δ*ainS* is locked into a different regulatory state, where the EPS production is not necessary.

LitR is suggested to link AinS/R and LuxS/PQ systems to LuxI/R systems in *A. salmonicida*, where its deletion influenced the production of AinS and LuxI AHLs. When both *luxI* and *ainS* were inactivated simultaneously, biofilm and colony morphology similar to Δ*litR* mutant was formed (*Hansen et al., 2015*). A simple explanation for this observation is the deficiency in AHL production, leading to *litR* inactivation (*Bjelland et al., 2012*; *Hansen et al., 2014*), and thereby no repression of biofilm or colony rugosity is achieved. Furthermore, the exogenous addition of either 3OHC10-HSL (AinS signal) or 3OC6-HSL (LuxI signal) to Δ*ainSluxI*$^-$, completely inhibited biofilm formation. We have previously shown that the disruption of either EPS or other matrix components (e.g., proteins, lipoproteins, and eDNA), disrupts the mature biofilm formation in *A. salmonicida* (*Hansen et al., 2014*; *Khider, Willassen & Hansen, 2018*).

While the Δ*ainS* mutant did not produce neither mature biofilm nor wrinkled colonies, introduction of *luxI* mutation to a Δ*ainS* background, resulted in strains (Δ*ainSluxI*$^-$) with three-dimensional biofilm architecture and wrinkled colonies. These data suggest that these two systems regulate biofilm formation synergistically, where the effect of AinS and LuxI AHLs is operated through a common pathway as previously reported (*Hansen et al., 2015*). The results presented here show that both systems function to either promote or repress production of EPS and other matrix components. However, the *lux* system is believed to be essential for the production of EPS rather than the *ain* system (as discussed above). Studies showed that one key function of EPS involves the attachment of cells to different substratum, which is the initial step in biofilm formation (*Vu et al., 2009*). For example in *V. cholerae*, the EPS production is the first step in biofilm formation as cells switch from motile planktonic state to being non-motile and surface attached (*Silva & Benitez, 2016*). Likewise, we suggest that the non-motile *luxI*$^-$ mutant, increases EPS production to mediate the initial steps in biofilm formation, whereas *ainS* is neither fully activated nor required at this time. This suggests that *lux* system may operate

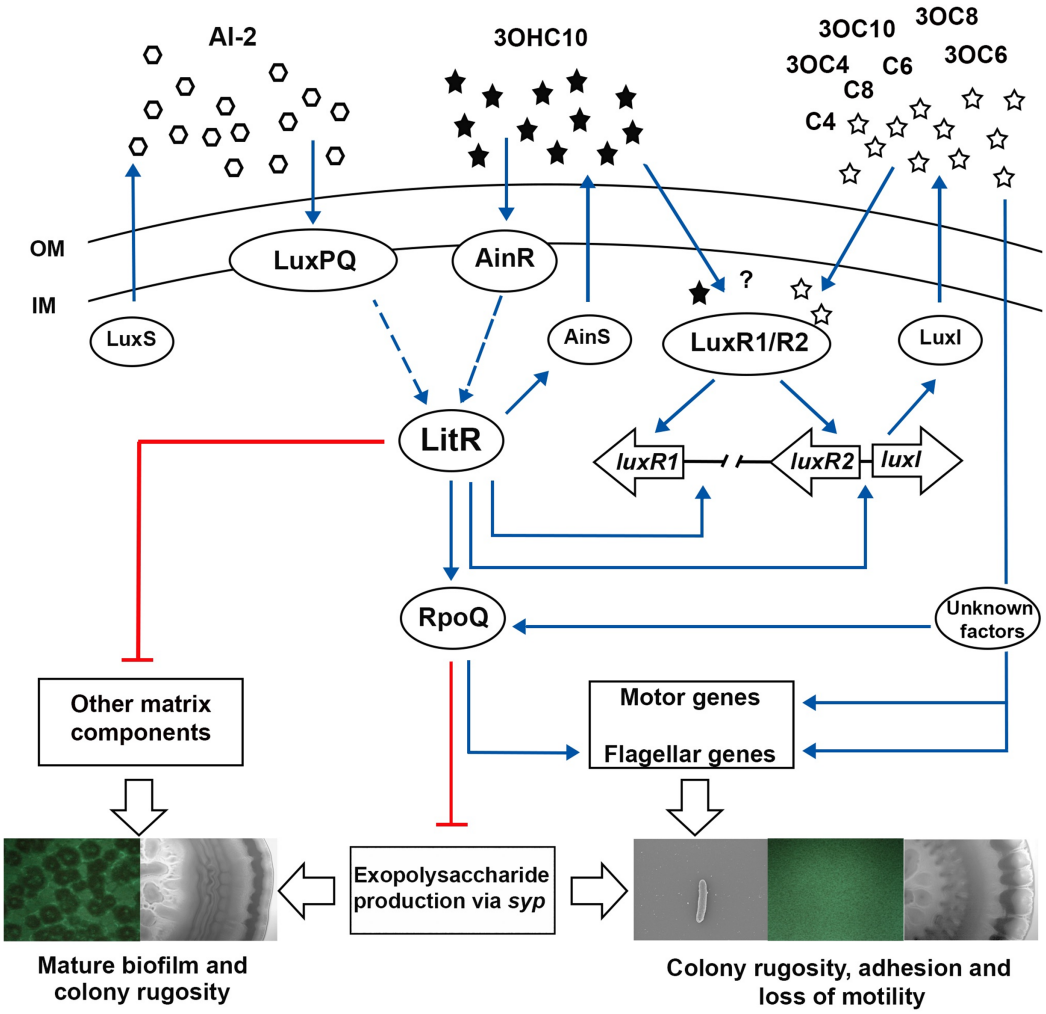

Figure 7 The proposed model of QS system in *A. salmonicida* LFI1238. The autoinducers synthases LuxS, LuxI, and AinS produces AI-2 and eight AHLs that are transported across the outer (OM) and inner membrane (IM) (*Hansen et al., 2015*). At high cell density AHLs and AI-2 are accumulated to reach a critical concentration to be sensed by their receptors LuxPQ, AinR, or LuxRs. It is still unknown which AHLs bind the LuxRs and is illustrated with a question mark. The Al-2 binds LuxPQ and 3OHC10-HSL binds AinR, which in turn induces a dephosphorylation cascade, resulting in LitR activation. Although due to a frame shift mutation within *luxP*, the LuxS/PQ pathway may not be active. The expressed LitR, activates the production of the AinS AHL (3OHC10-HSL) and the expression of downstream *rpoQ* gene. The increased RpoQ levels represses *syp* operon leading to biofilm disruption and inhibition of colony rugosity. Moreover, LitR represses other matrix components, through a pathway that remain unknown (*Khider, Willassen & Hansen 2018*). LitR together with LuxRs are proposed to regulate *luxI*. The expressed LuxI mediate the production of seven AHLs and represses *syp* genes via RpoQ either directly or indirectly through unknown factors. Blue arrows and red lines with bar end indicate pathways of positive and negative regulation, respectively, and may consist of several steps. The thicker, empty arrows indicate the resulting phenotypes. Full-size DOI: 10.7717/peerj.6845/fig-7

at a lower threshold cell density than *ain* system, which is more essential at later stages of biofilm development, mainly the maturation into three-dimensional mushroom structure. With our results, we expand the previously suggested model, to include *luxI* and *ainS* and their proposed role in regulating biofilm formation and colony rugosity. In the model

presented in Fig. 7, we propose that as cell density rises 3OHC10-HSL binds AinR receptor, resulting in activation of LitR, which in turn regulates the production of AinS AHL. The activated LitR leads to a repression on other matrix components required for building a mature biofilm through a mechanism that remain unknown. The activated LitR also leads to increased levels of RpoQ, resulting in repression of EPS through *syp* genes. It has been proposed that *luxI* is activated by both LitR and LuxRs. The active LuxI synthesizes seven AHLs and represses *syp* operon via RpoQ most probably independently of the AinS-LitR pathway. Hence, the production of EPS (via LuxI) and other matrix components (via AinS) appears to play an important role in building the three-dimensional architecture of the biofilm. In summary, our results further support the hypothesis that biofilm formation is a LCD dependent phenotype, when neither LuxI nor AinS AHLs are present. As AHLs accumulate at HCDs, the biofilm is dispersed, indicating that AHL-mediated QS in *A. salmonicida* is involved in the dispersal step of the biofilm cycle. Although further investigations are needed to support this hypothesis.

The deletion of *luxI* was shown to influence expression of 500 genes in the *A. salmonicida*. A similar global regulation of QS regulon has also been observed in *Pseudomonas aeruginosa*, where around 600 genes were believed to be regulated by *las* and *rhI* QS systems (*Wagner et al., 2003*). The most pronounced regulation in the *luxI*$^-$ mutant was observed for genes involved in motility and chemotaxis, exhibiting a significantly low expression level. The regulatory mechanism of motility in *A. salmonicida* remain poorly understood, however, the motility genes are organized in a similar fashion to *A. fischeri* (*Karlsen et al., 2008*), where flagellar genes are often grouped into different hierarchical classes (Fig. 5). We propose that the loss of motility and flagellation is associated with the elevated level of EPS production by the *luxI*$^-$ mutant. Inverse regulation of EPS production and flagellum has been observed in several other microorganisms (*Burdman et al., 1998*; *Garrett, Perlegas & Wozniak, 1999*; *Prigent-Combaret et al., 1999*). In *V. cholerae* O139, strains with inactivated flagellar genes (e.g., *fliK, flhB, fliF, fliE*, and *fliR*) exhibited rugose colony morphology, while mutations in genes coding for motor proteins (*motB* and *motY*) did not display *V. cholerae* strains with a rugose colony morphology (*Watnick et al., 2001*). We also recently showed that RpoQ in *A. salmonicida* regulates motility and EPS production inversely, where the Δ*rpoQ* mutant exhibited a strong colony rugosity and reduced motility. The transcriptome of Δ*rpoQ* revealed a downregulation in a number of flagellar biosynthesis genes mainly *flaA* (*Khider, Willassen & Hansen, 2018*; *Khider et al., 2019*). Our *luxI*$^-$ transcriptomics results demonstrated DEGs that fell into all hierarchical classes (Fig. 5) including flagellar and motor genes. Thus, it is unclear at which regulatory level LuxI affects motility genes and which motility genes may be associated with the rugose phenotype. Nevertheless, our lack of ability to complement the *luxI*$^-$ mutant makes it difficult to exclude other factors influencing flagellar synthesis and/or motility and a question remains to be investigated is *whether there is a relationship between the loss of motility and the rugose colony morphology in A. salmonicida*. LitR, is a positive regulator of *ainS* in *A. salmonicida* (*Hansen et al., 2015*). Thus, not surprisingly, we found that Δ*ainS* displayed an increased motility compared to the wild type, similar to that reported for Δ*litR* (*Bjelland et al., 2012*). The defect

or increase in motility cannot be explained by differences in growth rate, as cultures for different mutants reached the stationary phase at the same rate as the wild type (Fig. S2). However, the regulation of motility in *A. salmonicida* and the target of these regulators still remains to be determined.

Our transcriptome analysis revealed additional genes that are regulated by the *lux* system and might play an important role in adhesion and virulence. Tad loci is a widespread colonization island found in several vibrios and known to play an essential role in motility, biofilm formation, and adhesion (*Tomich, Planet & Figurski, 2007*). Recent studies in *V. vulnificus* showed a correlation between *tad* genes and the biofilm formation, auto-aggregation, and initiation of attachment to the host (*Pu & Rowe-Magnus, 2018*). Information regarding the role of *tad* operon in *A. salmonicida* is scant, and the inactivation of *tadV* (*VSAL_II0367*) and *rcpC* (*VSAL_II0368*) did not affect biofilm formation (*Hansen et al., 2014*). However, our recent transcriptome analysis of the Δ*litR* and Δ*rpoQ* mutants revealed an upregulation in the *tad* genes, moreover, the functional analysis also showed a strong adhesion of the mutants to the agar plates (*Khider, Willassen & Hansen, 2018*). Furthermore, the comparison transcriptome of *A. salmonicida* wild type at HCD relative to low, showed a downregulation in *tad* genes at HCD when both LitR and RpoQ were upregulated. This led us to suggest that *tad* genes are essential at LCD and are downregulated by LitR-RpoQ when cell density rises. The *luxI*$^-$ transcriptome demonstrated an upregulation in *tad* genes with significant fold change values. We have earlier suggested in this work that the *luxI*$^-$ mutant is locked into the initial steps of biofilm formation, when cells are non-motile, produce high amount of EPS and are adhesive. This suggests further that *tad* genes are important at early stages of the life cycle (e.g., LCD) to mediate attachment and micro-colony formation, which is consistent with previous observations in other bacteria (*Nika et al., 2002*; *Pu & Rowe-Magnus, 2018*; *Pu et al., 2018*; *Watnick & Kolter, 1999*).

We have previously shown that changes in media composition altered biological traits such as biofilm formation and colony rugosity in *A. salmonicida* (*Hansen et al., 2014*). Contrary to what was previously reported (*Purohit et al., 2013*; *Hansen et al., 2015*) neither C4-HSL nor 3OC4-HSL were detected in the present work, suggesting that the concentration of these AHLs are either below the detectable limit or not produced due to different culturing temperatures and/or media. However, the profiles for the remaining six AHLs were unaffected.

CONCLUSION

In this study, we have shown that *luxI*, but not *ainS* is essential for formation of wrinkled colonies at LCD, whereas both systems are required to form a three-dimensional mature biofilm in *A. salmonicida* LFI1238. We also demonstrated that addition of either LuxI-3OC6-HSL or AinS-3OHC10-HSL is able to inhibit biofilm formation. Our results show that *lux* and *ain* systems regulate biofilm formation through a common pathway, where LuxI acts mainly as a repressor of EPS production (*syp* operon) via RpoQ. While AinS is probably involved in the repression of other matrix components required to

build the mature biofilm. Furthermore, we identified DEGs associated with motility were regulated by LuxI. These results add a new knowledge to the nature of the QS mechanism of *A. salmonicida*, however further investigations are needed to understand the regulation and complexity of this mechanism.

ABBREVIATIONS

AHL	acyl homoserine lactone
GFP	green fluorescent protein
rpm	rounds per minute
RNA	ribonucleic acid
tRNA	transfer RNA
rRNA	ribosomal RNA
h	hours
OD	optical density
RNA-Seq	RNA sequencing
s	seconds
min	minutes

ACKNOWLEDGEMENTS

We would like to thank Augusta Hlin Aspar Sundbø from advanced microscopy core facility (AMCF) at UiT- the Arctic University of Tromsø for helping us with Scanning Electron Microscopy. We thank Marie Cooper, researcher Adele Kim Willamson and Prof. Richard Engh (UiT The Arctic University of Norway) for proofreading the manuscript. We also thank Dr. Eric V. Stabb (University of Georgia) for the pVSV102 and pEVS104 plasmids.

ADDITIONAL INFORMATION AND DECLARATIONS

Funding

This work was funded by UiT, The Arctic University of Norway. The publication charges for this article have been funded by a grant from the publication fund of UiT, The Arctic University of Norway. The funders had no role in study design, data collection and analysis, decision to publish, or preparation of the manuscript.

Grant Disclosure

The following grant information was disclosed by the authors:
UiT, The Arctic University of Norway.

Competing Interests

The authors declare that they have no competing interests.

Author Contributions

- Miriam Khider conceived and designed the experiments, performed the experiments, analyzed the data, contributed reagents/materials/analysis tools, prepared figures and/or tables, authored or reviewed drafts of the paper, approved the final draft, wrote the paper.
- Hilde Hansen conceived and designed the experiments, performed the experiments, analyzed the data, contributed reagents/materials/analysis tools, approved the final draft.
- Erik Hjerde contributed reagents/materials/analysis tools, approved the final draft, analyzed the transcriptomics data.
- Jostein A. Johansen contributed reagents/materials/analysis tools, approved the final draft, performed HPLC analysis.
- Nils Peder Willassen conceived and designed the experiments, analyzed the data, contributed reagents/materials/analysis tools, authored or reviewed drafts of the paper, approved the final draft, coordinated the project.

Data Availability

The following information was supplied regarding data availability:

RNA sequencing data are accessible in the European Nucleotide Archive (ENA) under accession numbers PRJEB29457 and PRJEB28385.

Supplemental Information

Supplemental information for this article can be found online at http://dx.doi.org/10.7717/peerj.6845#supplemental-information.

REFERENCES

Abisado RG, Benomar S, Klaus JR, Dandekar AA, Chandler JR. 2018. Bacterial quorum sensing and microbial community interactions. *MBio* **9(3)**:e02331-17 DOI 10.1128/mBio.02331-17.

Bjelland AM, Sørum H, Tegegne DA, Winther-Larsen HC, Willassen NP, Hansen H. 2012. LitR of *Vibrio salmonicida* is a salinity-sensitive quorum-sensing regulator of phenotypes involved in host interactions and virulence. *Infection and Immunity* **80(5)**:1681–1689 DOI 10.1128/IAI.06038-11.

Brennan CA, Mandel MJ, Gyllborg MC, Thomasgard KA, Ruby EG. 2013. Genetic determinants of swimming motility in the squid light-organ symbiont *Vibrio fischeri*. *MicrobiologyOpen* **2(4)**:576–594 DOI 10.1002/mbo3.96.

Buchholtz C, Nielsen KF, Milton DL, Larsen JL, Gram L. 2006. Profiling of acylated homoserine lactones of *Vibrio anguillarum* in vitro and in vivo: Influence of growth conditions and serotype. *Systematic and Applied Microbiology* **29(6)**:433–445 DOI 10.1016/j.syapm.2005.12.007.

Burdman S, Jurkevitch E, Schwartsburd B, Hampel M, Okon Y. 1998. Aggregation in *Azospirillum brasilense*: effects of chemical and physical factors and involvement of extracellular components. *Microbiology* **144(7)**:1989–1999 DOI 10.1099/00221287-144-7-1989.

Casper-Lindley C, Yildiz FH. 2004. VpsT is a transcriptional regulator required for expression of vps biosynthesis genes and the development of rugose colonial morphology in

Vibrio cholerae O1 El Tor. *Journal of Bacteriology* **186(5)**:1574–1578 DOI 10.1128/JB.186.5.1574-1578.2004.

Dunn AK, Millikan DS, Adin DM, Bose JL, Stabb EV. 2006. New *rfp*- and pES213-derived tools for analyzing symbiotic *Vibrio fischeri* reveal patterns of infection and *lux* expression in *situ*. *Applied and Environmental Microbiology* **72(1)**:802–810 DOI 10.1128/AEM.72.1.802-810.2006.

Egidius E, Andersen K, Clausen E, Raa J. 1981. Cold-water vibriosis or "Hitra disease" in Norwegian salmonid farming. *Journal of Fish Diseases* **4(4)**:353–354 DOI 10.1111/j.1365-2761.1981.tb01143.x.

Egidius E, Wiik R, Andersen K, Hoff KA, Hjeltnes B. 1986. *Vibrio salmonicida* sp. nov., a new fish pathogen. *International Journal of Systematic Bacteriology* **36(4)**:518–520 DOI 10.1099/00207713-36-4-518.

Emerenini BO, Hense BA, Kuttler C, Eberl HJ. 2015. A mathematical model of quorum sensing induced biofilm detachment. *PLOS ONE* **10(7)**:e0132385 DOI 10.1371/journal.pone.0132385.

Fazli M, Almblad H, Rybtke ML, Givskov M, Eberl L, Tolker-Nielsen T. 2014. Regulation of biofilm formation in *Pseudomonas* and *Burkholderia* species. *Environmental Microbiology* **16(7)**:1961–1981 DOI 10.1111/1462-2920.12448.

Fidopiastis PM, Sørum H, Ruby EG. 1999. Cryptic luminescence in the cold-water fish pathogen *Vibrio salmonicida*. *Archives of Microbiology* **171(3)**:205–209 DOI 10.1007/s002030050700.

Freeman JA, Bassler BL. 1999. A genetic analysis of the function of LuxO, a two-component response regulator involved in quorum sensing in *Vibrio harveyi*. *Molecular Microbiology* **31(2)**:665–677 DOI 10.1046/j.1365-2958.1999.01208.x.

Fuqua C, Parsek MR, Greenberg EP. 2001. Regulation of gene expression by cell-to-cell communication: acyl-homoserine lactone quorum sensing'. *Annual Review of Genetics* **35(1)**:439–468 DOI 10.1146/annurev.genet.35.102401.090913.

García-Aljaro C, Eberl L, Riedel K, Blanch AR. 2008. Detection of quorum-sensing-related molecules in *Vibrio scophthalmi*. *BMC Microbiology* **8(1)**:138 DOI 10.1186/1471-2180-8-138.

Garrett ES, Perlegas D, Wozniak DJ. 1999. Negative control of flagellum synthesis in *Pseudomonas aeruginosa* is modulated by the alternative sigma factor AlgT (AlgU). *Journal of Bacteriology* **181**:7401–7404.

Guvener ZT, McCarter LL. 2003. Multiple regulators control capsular polysaccharide production in *Vibrio parahaemolyticus*. *Journal of Bacteriology* **185(18)**:5431–5441 DOI 10.1128/JB.185.18.5431-5441.2003.

Hansen H, Bjelland AM, Ronessen M, Robertsen E, Willassen NP. 2014. LitR is a repressor of *syp* genes and has a temperature-sensitive regulatory effect on biofilm formation and colony morphology in *Vibrio* (*Aliivibrio*) *salmonicida*. *Applied and Environmental Microbiology* **80(17)**:5530–5541 DOI 10.1128/AEM.01239-14.

Hansen H, Purohit AA, Leiros H-KS, Johansen JA, Kellermann SJ, Bjelland AM, Willassen NP. 2015. The autoinducer synthases LuxI and AinS are responsible for temperature-dependent AHL production in the fish pathogen *Aliivibrio salmonicida*. *BMC Microbiology* **15(1)**:69 DOI 10.1186/s12866-015-0402-z.

Hjerde E, Lorentzen MS, Holden MT, Seeger K, Paulsen S, Bason N, Churcher C, Harris D, Norbertczak H, Quail MA, Sanders S, Thurston S, Parkhill J, Willassen NP, Thomson NR. 2008. The genome sequence of the fish pathogen *Aliivibrio salmonicida* strain

LFI1238 shows extensive evidence of gene decay. *BMC Genomics* **9(1)**:616 DOI 10.1186/1471-2164-9-616.

Hmelo LR. 2017. Quorum sensing in marine microbial environments. *Annual Review of Marine Science* **9(1)**:257–281 DOI 10.1146/annurev-marine-010816-060656.

Holm KO, Strøm E, Stensvaag K, Raa J, Jorgensen T. 1985. Characteristics of a Vibrio sp. associated with the "Hitra disease" of Atlantic salmon in Norwegian fish farms. *Fish Pathology* **20(2/3)**:125–129 DOI 10.3147/jsfp.20.125.

Huber B, Riedel K, Hentzer M, Heydorn A, Gotschlich A, Givskov M, Molin S, Eberl L. 2001. The cep quorum-sensing system of *Burkholderia cepacia* H111 controls biofilm formation and swarming motility. *Microbiology* **147(9)**:2517–2528 DOI 10.1099/00221287-147-9-2517.

Karlsen C, Paulsen SM, Tunsjø HS, Krinner S, Sørum H, Haugen P, Willassen N-P. 2008. Motility and flagellin gene expression in the fish pathogen *Vibrio salmonicida*: effects of salinity and temperature. *Microbial Pathogenesis* **45(4)**:258–264 DOI 10.1016/j.micpath.2008.06.002.

Khider M, Hjerde E, Hansen H, Willassen NP. 2019. Differential expression profiling of Δ*litR* and Δ*rpoQ* mutants reveals insight into QS regulation of motility, adhesion and biofilm formation in *Aliivibrio salmonicida*. *BMC Genomics* **20**:200 DOI 10.1186/s12864-019-5594-4.

Khider M, Willassen NP, Hansen H. 2018. The alternative sigma factor RpoQ regulates colony morphology, biofilm formation and motility in the fish pathogen *Aliivibrio salmonicida*. *BMC Microbiology* **18(1)**:116 DOI 10.1186/s12866-018-1258-9.

Kim J, Kang Y, Choi O, Jeong Y, Jeong J-E, Lim JY, Kim M, Moon JS, Suga H, Hwang I. 2007. Regulation of polar flagellum genes is mediated by quorum sensing and FlhDC in *Burkholderia glumae*. *Molecular Microbiology* **64(1)**:165–179 DOI 10.1111/j.1365-2958.2007.05646.x.

Koutsoudis MD, Tsaltas D, Minogue TD, Von Bodman SB. 2006. Quorum-sensing regulation governs bacterial adhesion, biofilm development, and host colonization in *Pantoea stewartii* subspecies stewartii. *Proceedings of the National Academy of Sciences of the United States of America* **103(15)**:5983–5988 DOI 10.1073/pnas.0509860103.

Lee KJ, Kim JA, Hwang W, Park SJ, Lee KH. 2013. Role of capsular polysaccharide (CPS) in biofilm formation and regulation of CPS production by quorum-sensing in *Vibrio vulnificus*. *Molecular Microbiology* **90(4)**:841–857 DOI 10.1111/mmi.12401.

Love MI, Huber W, Anders S. 2014. Moderated estimation of fold change and dispersion for RNA-seq data with DESeq2. *Genome Biology* **15(12)**:550 DOI 10.1186/s13059-014-0550-8.

Lupp C, Ruby EG. 2004. *Vibrio fischeri* LuxS and AinS: comparative study of two signal synthases. *Journal of Bacteriology* **186(12)**:3873–3881 DOI 10.1128/JB.186.12.3873-3881.2004.

Lupp C, Ruby EG. 2005. *Vibrio fischeri* uses two quorum-sensing systems for the regulation of early and late colonization factors. *Journal of Bacteriology* **187(11)**:3620–3629 DOI 10.1128/JB.187.11.3620-3629.2005.

Lupp C, Urbanowski M, Greenberg EP, Ruby EG. 2003. The *Vibrio fischeri* quorum-sensing systems *ain* and *lux* sequentially induce luminescence gene expression and are important for persistence in the squid host. *Molecular Microbiology* **50(1)**:319–331 DOI 10.1046/j.1365-2958.2003.t01-1-03585.x.

Magoc T, Wood D, Salzberg SL. 2013. EDGE-pro: estimated degree of gene expression in prokaryotic genomes. *Evolutionary Bioinformatics Online* **9**:127–136.

McCarter LL. 1998. OpaR, a homolog of *Vibrio harveyi* LuxR, controls opacity of *Vibrio parahaemolyticus*. *Journal of Bacteriology* **180**:3166–3173.

Millikan DS, Ruby EG. 2003. FlrA, a σ^{54}-dependent transcriptional activator in *Vibrio fischeri*, is required for motility and symbiotic light-organ colonization. *Journal of Bacteriology* **185(12)**:3547–3557 DOI 10.1128/JB.185.12.3547-3557.2003.

Millikan DS, Ruby EG. 2004. *Vibrio fischeri* flagellin A is essential for normal motility and for symbiotic competence during initial squid light organ colonization. *Journal of Bacteriology* **186(13)**:4315–4325 DOI 10.1128/JB.186.13.4315-4325.2004.

Molina L, Rezzonico F, Defago G, Duffy B. 2005. Autoinduction in *Erwinia amylovora*: evidence of an acyl-homoserine lactone signal in the fire blight pathogen. *Journal of Bacteriology* **187(9)**:3206–3213 DOI 10.1128/JB.187.9.3206-3213.2005.

Nealson KH, Hastings JW. 1979. Bacterial bioluminescence: its control and ecological significance. *Microbiology Review* **43**:496–518.

Nelson EJ, Tunsjo HS, Fidopiastis PM, Sørum H, Ruby EG. 2007. A novel *lux* operon in the cryptically bioluminescent fish pathogen *Vibrio salmonicida* is associated with virulence. *Applied and Environmental Microbiology* **73(6)**:1825–1833 DOI 10.1128/AEM.02255-06.

Ng WL, Bassler BL. 2009. Bacterial quorum-sensing network architectures. *Annual Review of Genetics* **43(1)**:197–222 DOI 10.1146/annurev-genet-102108-134304.

Nika JR, Latimer JL, Ward CK, Blick RJ, Wagner NJ, Cope LD, Mahairas Munson RS Jr, Hansen EJ. 2002. Haemophilus ducreyi requires the *flp* gene cluster for microcolony formation in vitro. *Infection and Immunity* **70(6)**:2965–2975 DOI 10.1128/IAI.70.6.2965-2975.2002.

Norsworthy AN, Visick KL. 2013. Gimme shelter: how *Vibrio fischeri* successfully navigates an animal's multiple environments. *Frontiers in Microbiology* **4**:356 DOI 10.3389/fmicb.2013.00356.

Pratt LA, Kolter R. 1998. Genetic analysis of *Escherichia coli* biofilm formation: roles of flagella, motility, chemotaxis and type I pili. *Molecular Microbiology* **30(2)**:285–293 DOI 10.1046/j.1365-2958.1998.01061.x.

Prigent-Combaret C, Vidal O, Dorel C, Lejeune P. 1999. Abiotic surface sensing and biofilm-dependent regulation of gene expression in *Escherichia coli*. *Journal of Bacteriology* **181**:5993–6002.

Pu M, Duriez P, Arazi M, Rowe-Magnus DA. 2018. A conserved *tad* pilus promotes *Vibrio vulnificus* oyster colonization. *Environmental Microbiology* **20(2)**:828–841 DOI 10.1111/1462-2920.14025.

Pu M, Rowe-Magnus DA. 2018. A Tad pilus promotes the establishment and resistance of *Vibrio vulnificus* biofilms to mechanical clearance. *NPJ Biofilms and Microbiomes* **4(1)**:10 DOI 10.1038/s41522-018-0052-7.

Purohit AA, Johansen JA, Hansen H, Leiros HK, Kashulin A, Karlsen C, Smalås A, Haugen P, Willassen NP. 2013. Presence of acyl-homoserine lactones in 57 members of the *Vibrionaceae* family. *Journal of Applied Microbiology* **115(3)**:835–847 DOI 10.1111/jam.12264.

Serres MH, Riley M. 2000. MultiFun, a multifunctional classification scheme for *Escherichia coli* K-12 gene products. *Microbial & Comparative Genomics* **5(4)**:205–222 DOI 10.1089/mcg.2000.5.205.

Silva AJ, Benitez JA. 2016. *Vibrio cholerae* biofilms and cholera pathogenesis. *PLOS Neglected Tropical Diseases* **10(2)**:e0004330 DOI 10.1371/journal.pntd.0004330.

Stabb EV, Ruby EG. 2002. RP4-based plasmids for conjugation between *Escherichia coli* and members of the *Vibrionaceae*. *Methods in Enzymology* **358**:413–426.

Stewart BJ, McCarter LL. 2003. Lateral flagellar gene system of *Vibrio parahaemolyticus*. *Journal of Bacteriology* **185(15)**:4508–4518 DOI 10.1128/JB.185.15.4508-4518.2003.

Swift S, Downie JA, Whitehead NA, Barnard AM, Salmond GP, Williams P. 2001. Quorum sensing as a population-density-dependent determinant of bacterial physiology. *Advanced in Microbial Physiology* **45**:199–270.

Tomich M, Planet PJ, Figurski DH. 2007. The *tad* locus: postcards from the widespread colonization island. *Nature Reviews Microbiology* **5(5)**:363–375 DOI 10.1038/nrmicro1636.

Utada AS, Bennett RR, Fong JCN, Gibiansky ML, Yildiz FH, Golestanian R, Wong GCL. 2014. *Vibrio cholerae* use pili and flagella synergistically to effect motility switching and conditional surface attachment. *Nature Communications* **5(1)**:4913 DOI 10.1038/ncomms5913.

Valiente E, Bruhn JB, Nielsen KF, Larsen JL, Roig FJ, Gram L, Amaro C. 2009. *Vibrio vulnificus* produces quorum sensing signals of the AHL-class. *FEMS Microbiology Ecology* **69(1)**:16–26 DOI 10.1111/j.1574-6941.2009.00691.x.

Von Bodman SB, Bauer WD, Coplin DL. 2003. Quorum sensing in plant-pathogenic bacteria. *Annual Review of Phytopathology* **41(1)**:455–482 DOI 10.1146/annurev.phyto.41.052002.095652.

Vu B, Chen M, Crawford RJ, Ivanova EP. 2009. Bacterial extracellular polysaccharides involved in biofilm formation. *Molecules* **14(7)**:2535–2554 DOI 10.3390/molecules14072535.

Wagner VE, Bushnell D, Passador L, Al Brooks, Iglewski BH. 2003. Microarray analysis of *Pseudomonas aeruginosa* quorum-sensing regulons: effects of growth phase and environment. *Journal of Bacteriology* **185(7)**:2080–2095 DOI 10.1128/JB.185.7.2080-2095.2003.

Watnick PI, Kolter R. 1999. Steps in the development of a *Vibrio cholerae* El Tor biofilm. *Molecular Microbiology* **34(3)**:586–595 DOI 10.1046/j.1365-2958.1999.01624.x.

Watnick PI, Lauriano CM, Klose KE, Croal L, Kolter R. 2001. The absence of a flagellum leads to altered colony morphology, biofilm development and virulence in *Vibrio cholerae* O139. *Molecular Microbiology* **39(2)**:223–235 DOI 10.1046/j.1365-2958.2001.02195.x.

Whitehead NA, Barnard AM, Slater H, Simpson NJ, Salmond GP. 2001. Quorum-sensing in Gram-negative bacteria. *FEMS Microbiology Reviews* **25(4)**:365–404 DOI 10.1111/j.1574-6976.2001.tb00583.x.

Yildiz FH, Liu XS, Heydorn A, Schoolnik GK. 2004. Molecular analysis of rugosity in a *Vibrio cholerae* O1 El Tor phase variant. *Molecular Microbiology* **53(2)**:497–515 DOI 10.1111/j.1365-2958.2004.04154.x.

Yildiz FH, Schoolnik GK. 1999. *Vibrio cholerae* O1 El Tor: identification of a gene cluster required for the rugose colony type, exopolysaccharide production, chlorine resistance, and biofilm formation. *Proceedings of the National Academy of Sciences of the United States of America* **96(7)**:4028–4033 DOI 10.1073/pnas.96.7.4028.

Yildiz FH, Visick KL. 2009. *Vibrio* biofilms: so much the same yet so different. *Trends in Microbiology* **17(3)**:109–118 DOI 10.1016/j.tim.2008.12.004.

Zhu S, Kojima S, Homma M. 2013. Structure, gene regulation and environmental response of flagella in *Vibrio*. *Frontiers in Microbiology* **4**:410 DOI 10.3389/fmicb.2013.00410.

Zhu J, Mekalanos JJ. 2003. Quorum sensing-dependent biofilms enhance colonization in *Vibrio cholerae*. *Developmental Cell* **5(4)**:647–656 DOI 10.1016/S1534-5807(03)00295-8.

Additional file 1

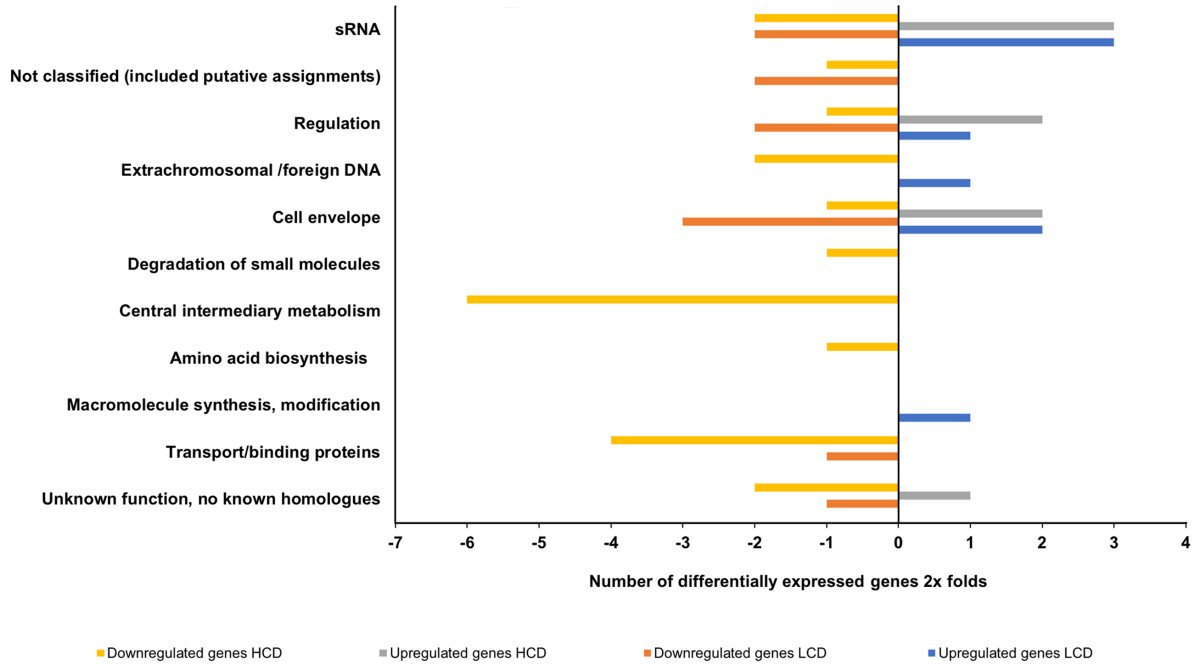

Figure S1. Functional distribution of genes between *A. salmonicida* wild type and *ΔainS* mutant at HCD compared to LCD that are ≥2× differentially expressed.
The number of upregulated and downregulated differentially expressed genes of the *ΔainS*/wt at high and low cell densities (filled bars), that are distributed into various functional groups.

Additional file 2

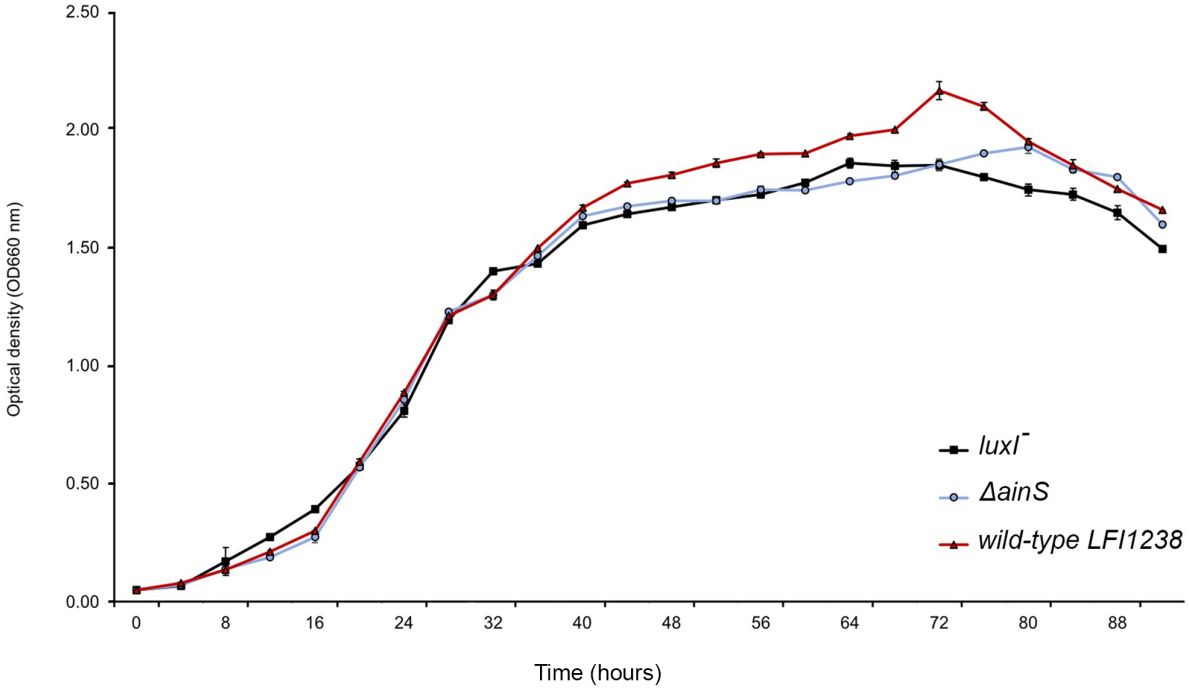

Figure S2. Growth curve of LFI1238, *luxI⁻*, *ΔainS*, and *ΔainSluxI⁻*.
The overnight secondary cultures were diluted to a starting OD_{600} of 0.05 in a total volume of 60 ml SWT. The cultures were grown further in 250 ml baffled flasks at 8°C and 220 rpm. The optical density was measured every 4 h using Ultrospec 10 cell density meter (Amersham Biosciences). The error bars represent the standard deviation of biological triplicates.

Additional file 3

Table S1. **Grading of adherence of LFI1238, *luxI⁻*, *ΔainS,* and *ΔlitR* to SWT agar.** The adherence of the colonies was analysed on SWT agar plates after 14 days of incubation at 8°C.

Bacterial strains	**8°C**
LFI1238	Non adhesive
luxI⁻	Strong
ΔainS	Non adhesive
ΔainSluxI⁻	Strong
ΔlitR	Strong

Additional file 4: Table S2. Summary of RNA seqeucing data.

	ΔluxI						*ΔainS*						WT					
	LCD OD_{600} = 0.3			HCD OD_{600} = 1.2			LCD OD_{600} = 0.3			HCD OD_{600} = 1.2			LCD OD_{600} = 0.3			HCD OD_{600} = 1.2		
	Replicate 1	Replicate 2	Replicate 3	Replicate 1	Replicate 2	Replicate 3	Replicate 1	Replicate 2	Replicate 3	Replicate 1	Replicate 2	Replicate 3	Replicate 1	Replicate 2	Replicate 3	Replicate 1	Replicate 2	Replicate 3
Total no. of reads	8956996	14568244	11191922	7908220	10603548	9029938	8941212	9293650	9873580	11791364	9958000	10724354	10069440	9175370	10357454	8998582	9383042	10313296
Total no. of reads mapped to *A. salmonicida* LFI1238	8428644	13835768	10598246	7458468	9811204	8298810	8396780	8716350	9294588	11046226	9235320	9978962	9145064	8622094	8440288	8493760	8547012	9154082
Percent mapped reads to *A. salmonicida* LFI1238	94.10%	94.97%	94.69%	94.31%	92.52%	91.90%	93.91%	93.79%	94.13%	92.68%	92.74%	93.04%	90.82%	93.97%	81.49%	94.39%	91.09%	88.76%

Additional file 5: Table S3. The differentially expressed genes of *luxI*⁻ mutant compared to wild type at LCD.

VSAL ID	Product	Fold Change	p-value	Functional classes
VSAL_II0030	transposase (pseudogene)	3206,05	2,37E-22	sRNA
VSAL_II0389	transposase	1226,55	2,13E-17	Extrachromosomal /foreign DNA
VSAL_I0514	transposase (pseudogene)	386,51	0,027905397	Extrachromosomal /foreign DNA
VSAL_I3102s	srna	259,74	3,80E-10	sRNA
VSAL_I1708	transposase	187,94	0,053440518	Extrachromosomal /foreign DNA
VSAL_II0515	transposase	147,44	0,065585986	Extrachromosomal /foreign DNA
VSAL_II0252	hypothetical protein	84,60	1,93E-231	Cell envelope
VSAL_II0366	fimbrial protein. Flp/Fap pilin component	83,84	3,32E-45	Cell envelope
VSAL_II0367	type IV leader peptidase	57,37	3,31E-157	Cell envelope
VSAL_I0809	transposase	50,33	0,149634538	Extrachromosomal /foreign DNA
VSAL_I1911	transposase	33,05	0,199375615	Extrachromosomal /foreign DNA
VSAL_II0128	hypothetical protein. putative phage gene	25,62	7,98082E-05	Extrachromosomal /foreign DNA
VSAL_II0370	putative lipoprotein	24,63	7,18E-155	Cell envelope
VSAL_II0371	type II secretion system protein Z	24,11	4,75E-138	Extrachromosomal /foreign DNA
VSAL_II0368	putative Flp pilus assembly protein	22,97	7,63E-96	Cell envelope
VSAL_I1475	hypothetical protein	22,80	2,20E-181	Cell envelope
VSAL_II0372	type II/IV secretion system protein. ATP binding domain	20,25	3,92E-140	Extrachromosomal /foreign DNA
VSAL_II0369	type II/III secretion system protein	18,78	5,99E-121	Extrachromosomal /foreign DNA
VSAL_II0362	hypothetical protein	16,94	2,59E-117	Unknown function
VSAL_I0315	transposase	16,25	0,137954023	Extrachromosomal /foreign DNA
VSAL_II0722	hypothetical protein	15,33	1,86E-58	Unknown function
VSAL_II0373	bacterial type II secretion system protein F	15,02	6,78E-77	Extrachromosomal /foreign DNA
VSAL_I1486	cold-shock protein	13,89	1,07E-95	Adaptation
VSAL_I2178	transposase	13,79	NA	Extrachromosomal /foreign DNA
VSAL_I1476	membrane protein	12,91	7,68E-51	Cell envelope
VSAL_II0364	hypothetical protein	11,09	7,18E-36	Unknown function
VSAL_I2749	probable HTH-type transcriptional regulator LeuO	11,02	8,01E-72	Regulation
VSAL_II0599	membrane protein	9,73	2,74E-144	Cell envelope
VSAL_II1062	membrane protein	9,49	1,60E-69	Cell envelope
VSAL_II0363	putative response regulator	8,84	4,08E-58	Regulation
VSAL_I1943	transposase	7,96	0,004837196	Extrachromosomal /foreign DNA

VSAL_I0132	putative lipoprotein	7,09	3,69E-39	Cell envelope
VSAL_II0374	bacterial type II secretion system protein F	6,75	4,86E-59	Extrachromosomal /foreign DNA
VSAL_I1056	carbonic anhydrase precursor	5,48	6,49E-49	Central intermediary metabolism
VSAL_I0133	hypothetical protein	5,36	4,83E-32	Unknown function
VSAL_II0171	putative membrane protein	5,21	3,09E-58	Cell envelope
VSAL_II0135	putative cytochrome b561	5,19	4,35E-52	Energy metabolism. carbon
VSAL_II0947	hypothetical protein	5,17	6,53E-28	Unknown function
VSAL_II0134	hypothetical protein	4,68	7,31E-44	Cell envelope
VSAL_II0170	methyl-accepting chemotaxis protein	4,65	7,87E-65	Cell processes
VSAL_I0460	colanic biosynthesis UDP-glucose lipid carrier transferase (ps	4,63	4,06E-31	Macromolecule synthesis. modificatior
VSAL_II0381	response regulator. histidine kinase	4,46	6,37E-19	Regulation
VSAL_I1685	putative amidase	4,38	3,07E-20	Not classified
VSAL_I1487	conserved hypothetical protein	4,30	1,57E-43	Unknown function
VSAL_I2124	hypothetical protein	4,16	3,59E-09	Unknown function
VSAL_II0172	hypothetical protein	4,12	1,09E-24	Unknown function
VSAL_II0931	membrane protein (fragment)	3,98	1,25E-15	Cell envelope
VSAL_II0377	membrane associated secretion system protein	3,97	6,25E-43	Extrachromosomal /foreign DNA
VSAL_I0902	chitinase A (fragment)	3,87	9,49E-18	Macromolecule metabolism
VSAL_II0376	membrane associated secretion system protein	3,85	3,98E-32	Extrachromosomal /foreign DNA
VSAL_II0934	hypothetical protein	3,75	3,77E-09	Unknown function
VSAL_II0375	putative secretion system protein	3,63	6,47E-32	Extrachromosomal /foreign DNA
VSAL_I4031s	srna	3,61	4,775E-05	sRNA
VSAL_II0378	membrane associated secretion system protein	3,58	1,99E-41	Extrachromosomal /foreign DNA
VSAL_I1819	outer membrane protein A	3,55	2,28E-28	Cell envelope
VSAL_II0382	hypothetical protein	3,32	6,36E-13	Unknown function
VSAL_I1820	putative lipoprotein	3,12	1,92E-35	Cell envelope
VSAL_II0933	putative exported protein	3,05	1,25E-21	Cell envelope
VSAL_II0169	hypothetical protein	3,04	1,91E-15	Unknown function
VSAL_I1625	hypothetical protein	2,92	0,000399532	Unknown function
VSAL_I1624	enhancing lycopene biosynthesis protein 2	2,79	9,10E-08	Biosynthesis of cofactors. carriers
VSAL_I0459	putative exported protein	2,75	6,49E-18	Cell envelope
VSAL_I0903	transposase	2,74	1,33641E-05	Extrachromosomal /foreign DNA

VSAL_I2075	methyl-accepting chemotaxis protein	2,73	3,41E-13	Cell processes
VSAL_I2323	transposase	2,70	0,679079083	Extrachromosomal /foreign DNA
VSAL_I4096s	srna	2,64	0,012231414	sRNA
VSAL_I1060	putative exported protein	2,63	1,11E-18	Cell envelope
VSAL_I1627	membrane protein	2,62	0,026511885	Cell envelope
VSAL_I2796	putative periplasmic protein CpxP	2,59	1,96E-17	Cell envelope
VSAL_I0820	transposase	2,58	0,059332114	Extrachromosomal /foreign DNA
VSAL_I2546	small-conductance mechanosensitive channel	2,56	2,49E-23	Transport/binding proteins
VSAL_I2269	hypothetical protein	2,53	1,45E-09	Transport/binding proteins
VSAL_I1300	putative membrane protein	2,52	2,82E-11	Cell envelope
VSAL_I2921	general secretion pathway protein G	2,48	3,79E-14	Transport/binding proteins
VSAL_I2536	hypothetical protein	2,48	1,11E-06	Unknown function
VSAL_II0932	cellulose synthase catalytic subunit	2,47	2,99E-15	Cell envelope
VSAL_I4042s	srna	2,46	0,749233072	sRNA
VSAL_I2741	putative cell division protein FtsN	2,45	5,94E-20	Cell division
VSAL_I1190	putative fumarylacetoacetate hydrolase	2,41	3,41E-09	Not classified
VSAL_I0458	polysaccharide biosynthesis/export protein	2,39	1,63E-08	Cell envelope
VSAL_II0365	hypothetical protein	2,36	0,264003707	Unknown function
VSAL_I2712	dihydrolipoyl dehydrogenase (dihydrolipoamide dehydrogenas	2,36	0,009100732	Not classified
VSAL_I2223	inner membrane protein	2,36	0,08844403	Cell envelope
VSAL_I1626	MltA-interacting protein MipA	2,35	0,002698698	Cell envelope
VSAL_I0853	exported peptidase	2,34	1,21E-13	Macromolecule metabolism
VSAL_I2773	putative membrane protein	2,32	0,206289899	Cell envelope
VSAL_I2713	hybrid peroxiredoxin (thioredoxin reductase)	2,27	3,59226E-06	Biosynthesis of cofactors. carriers
VSAL_I1547	hypothetical protein	2,26	4,48325E-05	Unknown function
VSAL_II0935	hypothetical protein	2,24	2,42E-13	Unknown function
VSAL_II0834	hypothetical protein	2,22	0,170611702	Unknown function
VSAL_I1687	aspartate aminotransferase	2,22	8,55E-06	Amino acid biosynthesis
VSAL_II0379	outer membrane protein. OmpA family (pseudogene)	2,20	4,12E-18	Cell envelope
VSAL_I0101	putative membrane protein	2,17	6,50E-10	Cell envelope
VSAL_I1394	hypothetical protein	2,17	8,64E-21	Unknown function
VSAL_I4118s	srna	2,16	6,71E-11	sRNA

VSAL_I1677	putative membrane protein	2,16	0,000719814	Cell envelope
VSAL_I4109s	srna	2,15	0,008769364	sRNA
VSAL_I1982	putative DNA transformation protein TfoX	2,15	8,04E-09	Not classified
VSAL_I4043s	srna	2,14	4,95541E-05	sRNA
VSAL_I0066	transposase	2,14	1,31663E-05	Extrachromosomal /foreign DNA
VSAL_I4094s	srna	2,13	0,013996228	sRNA
VSAL_I4160s	srna	2,13	1,2132E-05	sRNA
VSAL_II0044	transposase (fragment)	2,13	2,42529E-05	sRNA
VSAL_II0215	catalase	2,12	0,049088159	Protection responses
VSAL_I2030	glutaredoxin 1	2,12	1,02121E-05	Biosynthesis of cofactors. carriers
VSAL_II0523	putative membrane protein	2,10	2,54E-15	Cell envelope
VSAL_I0866	putative lipoprotein	2,10	6,97E-11	Cell envelope
VSAL_II0522	putative membrane protein	2,08	3,51E-14	Cell envelope
VSAL_I1781	putative exported protein	2,08	3,23E-11	Cell envelope
VSAL_I3179s	srna	2,07	1,10E-08	sRNA
VSAL_I0852	high-affinity zinc uptake system protein ZnuA precursor	2,07	6,54E-07	Transport/binding proteins
VSAL_I4105s	srna	2,05	0,005771036	sRNA
VSAL_I2665	conserved hypothetical protein	2,05	0,270418737	Unknown function
VSAL_I4095s	srna	2,05	0,032291216	sRNA
VSAL_II0527	conserved hypothetical protein. putative ATPase	2,04	7,84E-15	Unknown function
VSAL_II0992	transposase (fragment)	2,03	1,03E-09	Extrachromosomal /foreign DNA
VSAL_I1477	transposase	2,03	3,35502E-05	Extrachromosomal /foreign DNA
VSAL_I4145s	srna	2,03	3,14055E-05	sRNA
VSAL_I1716	transposase (pseudogene)	2,02	2,48E-09	Extrachromosomal /foreign DNA
VSAL_II0189	transposase (fragment)	2,02	9,58E-08	Extrachromosomal /foreign DNA
VSAL_I1672	transposase	2,02	3,03E-11	Extrachromosomal /foreign DNA
VSAL_II0685	6-phosphogluconate dehydrogenase	2,01	2,33E-07	Energy metabolism. carbon
VSAL_I2541	putative 5-formyltetrahydrofolate cyclo-ligase	2,01	4,22E-12	Central intermediary metabolism
VSAL_II0663	integral membrane protein. putative transmembrane transpc	2,01	8,90E-07	Cell envelope
VSAL_I1258	transposase (pseudogene)	2,00	2,38E-10	Extrachromosomal /foreign DNA
VSAL_I0628	hypothetical protein	2,00	0,000258029	Unknown function
VSAL_I2396	hypothetical protein	2,00	2,11E-07	Unknown function

VSAL_I1268	transposase (pseudogene)	2,00	6,05E-10	Extrachromosomal /foreign DNA
pVSAL840_05	conjugative transfer protein TraK	-2,00	0,000467974	Extrachromosomal /foreign DNA
VSAL_II0296	putative transmembrane glycosyl transferase	-2,00	1,29658E-05	Macromolecule synthesis. modificatior
VSAL_I0880	hypothetical protein	-2,01	0,000110579	Unknown function
VSAL_II0512	putative exported protein	-2,01	2,32E-07	Cell envelope
VSAL_II0249	putative exported protein	-2,01	1,77E-07	Cell envelope
VSAL_I2464	hypothetical protein	-2,01	0,022496807	Unknown function
VSAL_II0275	siderophore biosynthesis protein IucC (Pseudogene)	-2,01	0,007295087	Biosynthesis of cofactors. carriers
VSAL_I1855	aldehyde-alcohol dehydrogenase	-2,01	0,000108767	Degradation of small molecules
VSAL_I0479	type IV pilus. prepilin-like protein (MSHD)	-2,02	0,003970429	Cell envelope
VSAL_I1997	cytochrome c-552 precursor (ammonia-forming cytochrome r	-2,02	3,12E-06	Energy metabolism. carbon
VSAL_I1222	hypothetical protein	-2,02	3,44E-08	Cell envelope
VSAL_I2138	putative diaminobutyrate--2-oxoglutarate aminotransferase	-2,03	6,65E-07	Biosynthesis of cofactors. carriers
VSAL_I0743	inner membrane transport protein (pseudogene)	-2,03	1,8982E-05	Transport/binding proteins
VSAL_I2585	phosphoglucomutase/phosphomannomutase	-2,03	6,06E-06	Central intermediary metabolism
pVSAL840_29	hypothetical protein	-2,03	3,42352E-05	Unknown function
VSAL_I2001	cytochrome c-type biogenesis protein CcmF	-2,04	8,20E-08	Energy metabolism. carbon
VSAL_II0015	secretion protein. HlyD family	-2,04	8,52645E-05	Transport/binding proteins
VSAL_I4044s	srna	-2,05	0,006468058	sRNA
VSAL_II0791	anaerobic ribonucleoside-triphosphate reductase	-2,05	0,000564847	Central intermediary metabolism
VSAL_II0054	hypothetical protein	-2,06	1,13E-10	Unknown function
VSAL_II0677	putative glycosyl transferase	-2,06	0,000126612	Macromolecule synthesis. modificatior
VSAL_II0301	O-antigen polymerase	-2,06	9,88137E-05	Macromolecule synthesis. modificatior
VSAL_I1193	zinc metallopeptidase	-2,06	1,03101E-05	Macromolecule metabolism
VSAL_II0924	hypothetical protein (fragment)	-2,07	0,000178356	Unknown function
VSAL_II0254	biosynthetic arginine decarboxylase	-2,07	0,003775005	Central intermediary metabolism
VSAL_II0961	alkanal monooxygenase beta chain LuxB (bacterial luciferase	-2,07	0,000639448	Regulation
VSAL_II0642	putative membrane associated signal transducer (pseudogen	-2,07	1,11E-08	Regulation
VSAL_I0107	membrane protein	-2,07	0,002086229	Cell envelope
VSAL_I2631	type IV pilus assembly protein PilC (pseudogene)	-2,08	0,023475877	Cell envelope
pVSAL840_20	conjugative transfer protein TraD	-2,09	8,34E-09	Extrachromosomal /foreign DNA
VSAL_II0635	hypothetical protein. putative phage integrase (fragment)	-2,09	0,002281066	Extrachromosomal /foreign DNA

VSAL_II0963	acyl transferase LuxD	-2,09	0,000400306	Regulation
VSAL_II0857	dethiobiotin synthetase	-2,10	7,74209E-05	Biosynthesis of cofactors. carriers
VSAL_II0029	transporter. acriflavin resistance protein (pseudogene)	-2,10	6,67E-13	Protection responses
VSAL_II0181	ABC-type glycine betaine transport system. substrate binding	-2,10	0,006487674	Transport/binding proteins
VSAL_I3036	methyl-accepting chemotaxis protein (fragment)	-2,10	7,95E-12	Cell processes
VSAL_I1208	putative exported protein (fragment)	-2,10	0,000155061	Cell envelope
VSAL_I1755	heme transporter protein HuvC. transmembrane permease cc	-2,11	1,93E-07	Transport/binding proteins
VSAL_II2022s	srna	-2,11	0,038506746	sRNA
VSAL_I2438	isocitrate lyase	-2,12	0,000346705	Central intermediary metabolism
VSAL_II0746	conserved hypothetical protein (pseudogene)	-2,12	0,026994549	Unknown function
VSAL_II0063	putative type I secretion system. ATP-binding protein	-2,12	0,000298727	Transport/binding proteins
VSAL_II0462	cytochrome c'	-2,12	4,99E-08	Energy metabolism. carbon
VSAL_I2630	type IV pilus assembly protein PilB	-2,13	0,001291276	Cell envelope
VSAL_I1822	methyl-accepting chemotaxis protein (fragment)	-2,13	0,000406825	Cell processes
VSAL_I1927	hypothetical protein. putative phage gene (fragment)	-2,13	0,013486402	Extrachromosomal /foreign DNA
VSAL_I0424	hypothetical protein	-2,13	1,28E-10	Unknown function
VSAL_II0039	4-alpha-glucanotransferase	-2,14	5,76E-11	Macromolecule metabolism
VSAL_II0962	alkanal monooxygenase alpha chain LuxA (bacterial luciferas	-2,14	3,72617E-05	Regulation
pVSAL840_23	transglycosylase PilT	-2,14	8,06556E-05	Cell envelope
VSAL_II0247	nitrate transporter	-2,14	1,84E-07	Transport/binding proteins
VSAL_I1572	universal stress protein E	-2,14	0,026609139	Adaptation
VSAL_I2584	chitobiose phosphorylase (glycosyl transferase)	-2,15	1,35E-06	Central intermediary metabolism
VSAL_II0714	cation efflux system protein	-2,15	4,95E-08	Transport/binding proteins
VSAL_II0511	superoxide dismutase [Cu-Zn] precursor	-2,15	1,25E-09	Protection responses
VSAL_II0716	putative exported protein	-2,15	0,003230532	Cell envelope
pVSAL840_35	secreted protein Hcp-2 (haemolysin co-regulated protein)	-2,15	0,000429777	Cell envelope
VSAL_II0399	peptidase T	-2,16	2,77E-06	Macromolecule metabolism
VSAL_I0414	hypothetical protein	-2,16	0,001493854	Unknown function
pVSAL840_15	membrane protein	-2,17	7,11942E-05	Cell envelope
VSAL_I0920	nitrate and nitrite sensing methyl-accepting chemotaxis prote	-2,17	6,15E-13	Cell processes
VSAL_I1227	anaerobic C4-dicarboxylate transporter	-2,17	5,49E-06	Transport/binding proteins
VSAL_I1742	hypothetical protein (pseudogene)	-2,17	0,000516372	Unknown function

VSAL_I1973	ABC transporter. membrane protein	-2,17	0,000234828	Transport/binding proteins
pVSAL840_10	conjugative transfer protein TraW	-2,17	0,007571794	Extrachromosomal /foreign DNA
VSAL_I4178s	srna	-2,17	0,003528874	sRNA
VSAL_II1066	ornithine decarboxylase. inducible	-2,18	1,54123E-05	Central intermediary metabolism
VSAL_I0471	type IV pilus. mannose-sensitive hemagglutinin D (MSHN)	-2,18	1,53E-11	Cell envelope
VSAL_I0875	glycine betaine transporter OpuD	-2,18	4,94E-09	Transport/binding proteins
VSAL_II0859	8-amino-7-oxononanoate synthase	-2,18	0,000124671	Biosynthesis of cofactors. carriers
VSAL_II0331	putative exported protein	-2,18	0,000171067	Cell envelope
VSAL_II0101	peptidase	-2,19	3,43E-06	Macromolecule metabolism
VSAL_I0198	hypothetical protein	-2,19	5,10E-09	Unknown function
VSAL_I0474	type IV pilus. mannose-sensitive hemagglutinin protein MshF	-2,20	1,56051E-05	Cell envelope
VSAL_II1096	membrane protein (fragment)	-2,20	4,65E-13	Cell envelope
VSAL_I1427	hypothetical protein	-2,20	0,000731616	Unknown function
VSAL_I1599	putative polysaccharide deacetylase	-2,20	0,000384825	Not classified
pVSAL840_27	hypothetical protein	-2,20	7,84704E-05	Unknown function
VSAL_II0612	HTH-type transcriptional regulator. LysR family (pseudogene)	-2,21	7,89E-09	Regulation
VSAL_II0327	putative nucleotidyl transferase	-2,22	3,40414E-05	Central intermediary metabolism
VSAL_I0473	type IV pilus. mannose-sensitive hemagglutinin protein	-2,23	8,91E-08	Cell envelope
VSAL_II0690	putative glucosyl transferase	-2,23	7,53421E-05	Macromolecule synthesis. modificatior
VSAL_II0298	putative membrane protein	-2,23	2,23809E-05	Cell envelope
VSAL_I2117	methyl-accepting chemotaxis protein (fragment)	-2,23	1,63E-06	Cell processes
VSAL_II0209	hypothetical protein (fragment)	-2,23	1,43862E-05	Unknown function
VSAL_I1453	formate dehydrogenase	-2,23	2,07E-09	Energy metabolism. carbon
VSAL_I1448	putative formate dehydrogenase accessory protein	-2,24	7,14E-09	Not classified
VSAL_I0265	putative metallo-beta-lactamase	-2,24	3,08E-06	Not classified
VSAL_I2831	putative nucleotidyltransferases	-2,24	0,005643907	Not classified
VSAL_II0064	putative type I secretion protein. HlyD family	-2,24	0,000211084	Transport/binding proteins
VSAL_II0988	hypothetical protein	-2,25	0,006289964	Unknown function
VSAL_II0814	2-phosphonoacetaldehyde hydrolase	-2,25	7,24E-09	Degradation of small molecules
VSAL_II0016	putative plasmid-encoded multidrug efflux pump (fragment)	-2,25	0,000249299	Protection responses
VSAL_I2039	putative exported protein	-2,26	8,86E-17	Cell envelope
pVSAL840_03	conjugative transfer protein TraL	-2,26	0,000442626	Extrachromosomal /foreign DNA

VSAL_II0706	arginase	-2,26	0,000162761	Degradation of small molecules
VSAL_I0413	hypothetical protein	-2,26	0,002306598	Unknown function
VSAL_II1047	putative transcriptional regulator. LysR family (fragment)	-2,27	0,001029967	Regulation
VSAL_II0315	putative response regulator	-2,27	0,000472791	Regulation
VSAL_I1986	putative lipoprotein	-2,27	6,89E-13	Cell envelope
VSAL_II1037	hypothetical protein	-2,27	0,004113205	Unknown function
VSAL_I1523	putative membrane protein (fragment)	-2,27	2,70E-07	Cell envelope
VSAL_II0395	anaerobic glycerol-3-phosphate dehydrogenase subunit C	-2,28	0,000724702	Energy metabolism. carbon
VSAL_I2577	ABC-type [(GlcNAc)2] transporter. permease protein	-2,28	0,006859042	Transport/binding proteins
VSAL_I1194	anaerobic C4-dicarboxylate transporter DcuC	-2,29	0,000640789	Transport/binding proteins
VSAL_II0718	membrane protein	-2,29	4,86E-06	Cell envelope
VSAL_II0060	putative type I toxin secretion system. ATP-binding protein	-2,29	0,000105656	Transport/binding proteins
VSAL_II1025	HTH-type transcriptional regulator. LysR family	-2,30	1,91E-08	Regulation
VSAL_I1455	putative formate dehydrogenase	-2,30	1,37756E-05	Energy metabolism. carbon
VSAL_I2985	thiamine biosynthesis adenylyltransferase ThiF	-2,31	0,000150651	Biosynthesis of cofactors. carriers
VSAL_I2057	general L-amino acid-binding periplasmic protein precursor	-2,31	8,44484E-05	Transport/binding proteins
VSAL_I2056	general L-amino acid ABC transporter permease protein	-2,31	1,7189E-05	Transport/binding proteins
VSAL_I0798	nitrite reductase (NAD(P)H) large subunit	-2,31	0,032416725	Energy metabolism. carbon
VSAL_I0796	formate/nitrite transporter	-2,31	6,14E-06	Transport/binding proteins
VSAL_II0787	putative transglycosylase protein	-2,32	2,14E-08	Macromolecule metabolism
VSAL_II0691	hypothetical protein	-2,32	0,000399711	Unknown function
VSAL_II0939	hypothetical protein	-2,32	0,0089474	Unknown function
pVSAL840_11	conjugative transfer protein TraU	-2,33	1,4279E-05	Extrachromosomal /foreign DNA
VSAL_I2005	anaerobic C4-dicarboxylate transporter	-2,33	0,000104823	Transport/binding proteins
VSAL_I0606	putative signaling protein	-2,33	1,81E-16	Not classified
VSAL_I1413	putative membrane protein	-2,34	0,000160654	Cell envelope
VSAL_I1271	putative response regulator	-2,34	9,61E-06	Regulation
VSAL_I0771	phage major capsid protein	-2,34	0,002944583	Extrachromosomal /foreign DNA
VSAL_I2444	accessory colonization factor precursor AcfA	-2,35	0,000150193	Extrachromosomal /foreign DNA
pVSAL840_04	conjugative transfer protein TraE	-2,35	1,97438E-05	Extrachromosomal /foreign DNA
VSAL_II0745	major capsid protein	-2,35	0,00174582	Extrachromosomal /foreign DNA
VSAL_II0155	zinc-binding dehydrogenase	-2,36	4,06E-06	Not classified

VSAL_II0810	ABC transporter. ATP-binding protein	-2,37	1,33029E-05	Transport/binding proteins
VSAL_I0203	sensor outer membrane protein EnvZ	-2,37	0,003571282	Regulation
VSAL_I1054	putative acetyltransferase	-2,38	0,000303971	Not classified
VSAL_I1518	hypothetical protein	-2,38	0,008425781	Unknown function
VSAL_I2373	conserved hypothetical protein	-2,38	0,002609528	Unknown function
VSAL_II0245	nitrite reductase large subunit	-2,38	1,33E-09	Energy metabolism. carbon
VSAL_II1030	binding-protein-dependent transport system. inner membran	-2,39	2,68E-11	Transport/binding proteins
VSAL_I0797	nitrite reductase (NAD(P)H) small subunit	-2,39	0,002838126	Energy metabolism. carbon
VSAL_II0066	membrane protein	-2,39	0,00052283	Cell envelope
VSAL_II1027	putative exported protein	-2,40	1,80E-07	Cell envelope
VSAL_I0916	5-methyltetrahydropteroyltriglutamate--homocyst eine meth	-2,40	0,053158412	Amino acid biosynthesis
VSAL_II0813	aminotransferase class III	-2,41	7,40E-10	Degradation of small molecules
VSAL_I2828	putative sodium/solute symporter	-2,41	0,000200835	Transport/binding proteins
VSAL_I2974	fatty oxidation complex alpha subunit. enoyl-CoA hydratase	-2,41	2,03E-07	Degradation of small molecules
VSAL_I0266	hypothetical protein	-2,42	0,017613121	Unknown function
VSAL_I4003s	srna	-2,42	2,77E-06	sRNA
VSAL_II0166	hypothetical protein	-2,43	0,000714052	Unknown function
VSAL_I1289	alkaline-resistant alpha-amylase precursor	-2,43	1,08E-09	Macromolecule metabolism
VSAL_I4079s	srna	-2,43	0,005499365	sRNA
VSAL_II0350	putative exported protein	-2,44	2,44209E-06	Cell envelope
VSAL_II0212	gluconate permease	-2,44	4,15E-07	Transport/binding proteins
VSAL_II0955	putative multidrug transport protein (pseudogene)	-2,45	8,57E-08	Protection responses
VSAL_II0396	anaerobic glycerol-3-phosphate dehydrogenase subunit B	-2,46	0,001287792	Energy metabolism. carbon
VSAL_I2125	putative membrane protein	-2,46	0,015850805	Cell envelope
VSAL_II0065	membrane protein	-2,46	0,017960068	Cell envelope
VSAL_II0352	membrane associated sultatease	-2,46	8,35077E-05	Cell envelope
VSAL_I0774	putative portal vertex protein (pseudogene)	-2,47	0,000860475	Extrachromosomal /foreign DNA
VSAL_I1074	putative membrane protein	-2,47	3,18E-20	Cell envelope
VSAL_II0167	hypothetical protein	-2,47	0,000994253	Unknown function
VSAL_I1400	permease component of tungstate ABC transporter	-2,48	1,05E-13	Transport/binding proteins
VSAL_II0211	hydroxypyruvate isomerase	-2,48	3,16E-06	Central intermediary metabolism
VSAL_I0111	hypothetical protein	-2,48	0,007696175	Unknown function

pVSAL840_21	protein TraI (DNA helicase I)	-2,49	3,16E-11	Macromolecule synthesis. modificatior
VSAL_II1028	conserved hypothetical protein	-2,50	0,007734336	Unknown function
VSAL_II0812	putative aminotransferase class-V	-2,50	3,00E-06	Degradation of small molecules
VSAL_I1303	membrane protein	-2,51	2,35E-07	Cell envelope
VSAL_I2717	fimbrial assembly protein PilN	-2,52	0,002666288	Cell envelope
VSAL_II0056	putative type I secretion protein. HlyD family	-2,53	0,000286457	Transport/binding proteins
VSAL_I1043	hypothetical protein. putative phage gene	-2,53	0,00378988	Extrachromosomal /foreign DNA
VSAL_I2120	phosphate ABC transporter. permease protein	-2,53	0,017570618	Transport/binding proteins
pVSAL840_02	conjugative transfer protein TraA. putative fimbrial protein pr	-2,53	0,000534969	Extrachromosomal /foreign DNA
VSAL_II0811	extracellular solute-binding protein	-2,54	6,67E-11	Transport/binding proteins
VSAL_I1519	putative membrane protein	-2,54	1,72563E-05	Cell envelope
VSAL_II0210	putative class II aldolase	-2,54	0,000111489	Not classified
VSAL_I2988	thiamine biosynthesis protein ThiH	-2,56	5,94E-08	Biosynthesis of cofactors. carriers
VSAL_I2207	conserved hypothetical protein	-2,56	0,000725781	Unknown function
VSAL_I1358	VgrG preotein. VgrG-2	-2,56	3,94E-08	Cell envelope
pVSAL840_06	conjugative transfer protein TraB	-2,56	2,89652E-07	Extrachromosomal /foreign DNA
VSAL_I1359	hypothetical protein	-2,56	9,04479E-05	Unknown function
VSAL_II0273	siderophore biosynthesis protein IucA (fragment)	-2,57	4,92487E-05	Biosynthesis of cofactors. carriers
VSAL_II2051s	srna	-2,58	1,60516E-05	sRNA
pVSAL840_12	hypothetical protein. putative conjugative transfer protein Trb	-2,58	4,33472E-05	Unknown function
VSAL_II0278	siderophore biosynthesis protein IucD	-2,58	0,000354671	Biosynthesis of cofactors. carriers
VSAL_I2446	putative exported protein	-2,60	0,003117488	Cell envelope
VSAL_II0265	hypothetical protein	-2,60	0,001671401	Unknown function
VSAL_I0894	sodium/solute symporter (fragment)	-2,61	4,15E-07	Transport/binding proteins
VSAL_I1228	putative exported protein	-2,61	5,31E-06	Cell envelope
VSAL_I0416	hypothetical protein	-2,61	1,82E-10	Unknown function
VSAL_II0744	putative phage zinc-binding transcriptional activator	-2,63	0,052630248	Extrachromosomal /foreign DNA
VSAL_I2840	hypothetical protein	-2,64	9,57E-14	Unknown function
VSAL_I2126	putative membrane protein	-2,66	0,001307544	Cell envelope
VSAL_II0397	anaerobic glycerol-3-phosphate dehydrogenase subunit A	-2,66	0,000145167	Energy metabolism. carbon
VSAL_II0055	hypothetical protein	-2,67	0,00028792	Unknown function
VSAL_II1024	putative 6-phospho-beta-glucosidase	-2,69	1,73E-09	Degradation of small molecules

VSAL_I0270	putative lipoprotein	-2,70	4,39E-12	Cell envelope
VSAL_I1037	hypothetical protein. putative phage gene	-2,70	0,004550544	Extrachromosomal /foreign DNA
VSAL_II1029	binding-protein-dependent transport system. inner membran	-2,71	1,21E-09	Transport/binding proteins
VSAL_I1974	ABC transporter. ATP-binding component	-2,71	0,001120189	Transport/binding proteins
VSAL_I0703	PTS system. cellobiose permease IIC component	-2,71	0,000524411	Transport/binding proteins
VSAL_I1525	putative lipoprotein (pseudogene)	-2,71	1,95E-11	Cell envelope
VSAL_I0704	PTS system. cellobiose-specific component IIB	-2,72	0,008394656	Transport/binding proteins
pVSAL840_18	conjugative transfer protein TraG	-2,72	1,07E-09	Extrachromosomal /foreign DNA
VSAL_I2447	putative exported protein (pseudogene)	-2,72	0,000781386	Cell envelope
VSAL_I1493	microbial collagenase precursor (pseudogene)	-2,73	1,20E-14	Macromolecule metabolism
VSAL_I1520	hypothetical protein	-2,73	2,49E-06	Unknown function
VSAL_I1294	methyl-accepting chemotaxis protein	-2,73	8,40E-09	Cell processes
VSAL_I2200	nitric oxide reductase flrd-nad(+) reductase	-2,74	4,07526E-05	Protection responses
VSAL_I2192	hypothetical protein	-2,74	6,66E-07	Cell envelope
pVSAL840_37	hypothetical protein	-2,75	0,000186494	Unknown function
VSAL_I2352	chitoporin (pseudogene)	-2,76	0,009616022	Transport/binding proteins
VSAL_I2128	putative exported protein	-2,76	0,000146629	Cell envelope
VSAL_I1201	putative IMP dehydrogenase/GMP reductase	-2,77	1,67E-08	Not classified
VSAL_II0168	putative exported protein	-2,78	2,50E-15	Cell envelope
VSAL_II0232	putative alpha amylase	-2,79	1,38E-18	Macromolecule metabolism
VSAL_I1449	hypothetical protein	-2,80	7,14E-11	Unknown function
VSAL_I1200	putative pirin	-2,80	6,77E-06	Not classified
VSAL_I1401	extracellular tungstate binding protein precursor	-2,81	3,93E-11	Transport/binding proteins
VSAL_II0038	maltodextrin phosphorylase	-2,84	4,21E-10	Degradation of small molecules
VSAL_II0351	outer membrane protein transport protein	-2,85	4,78E-07	Cell envelope
VSAL_II0165	membrane protein	-2,86	3,32E-07	Cell envelope
pVSAL840_17	conjugative transfer protein TraH	-2,87	2,57E-08	Extrachromosomal /foreign DNA
VSAL_I2036	putative genetic competence protein (fragment)	-2,88	7,00E-09	Not classified
pVSAL840_25	antirestriction protein ArdC	-2,88	2,12E-09	Extrachromosomal /foreign DNA
VSAL_I2601	methyl-accepting chemotaxis protein (pseudogene)	-2,88	3,72E-16	Cell processes
pVSAL840_09	conjugative transfer protein TrbI trbi	-2,88	0,003197726	Extrachromosomal /foreign DNA
VSAL_II0631	phage replication and integration protein	-2,88	2,49E-08	Extrachromosomal /foreign DNA

VSAL_II0634	phage replication protein	-2,89	2,25E-08	Extrachromosomal /foreign DNA
VSAL_II0914	MFS transporter	-2,91	0,000127992	Transport/binding proteins
VSAL_II0332	putative hemolysin-type calcium-binding protein (fragment)	-2,92	5,06E-06	Not classified
VSAL_I1743	hypothetical protein	-2,92	0,000600477	Unknown function
pVSAL840_13	conjugative transfer protein TraN	-2,92	1,94E-06	Extrachromosomal /foreign DNA
VSAL_I1517	conserved hypothetical protein	-2,94	3,37E-19	Unknown function
VSAL_I0412	membrane protein	-2,95	2,14E-07	Cell envelope
VSAL_II2011s	srna	-2,96	0,007292556	sRNA
pVSAL840_38	putative cell wall degradation protein	-2,99	1,48E-08	Not classified
VSAL_I2590	nitrogen regulatory protein P-II	-2,99	0,000579321	Regulation
VSAL_II0104	putative 6-phosphogluconate dehydrogenase	-3,03	0,001491532	Not classified
VSAL_I0773	putative bacteriophage terminase	-3,07	8,25957E-05	Extrachromosomal /foreign DNA
VSAL_I1976	putative nickel transporter	-3,08	5,49E-12	Transport/binding proteins
VSAL_II1026	putative tryptophanyl-tRNA synthetase	-3,09	4,80E-14	Macromolecule synthesis. modificatior
pVSAL840_36	VgrG protein. VgrG-2	-3,11	3,34E-11	Cell envelope
VSAL_II0050	N.N'-diacetylchitobiase precursor (chitobiase)	-3,14	0,002185206	Macromolecule metabolism
pVSAL840_07	putative lipoprotein. putative TraV protein	-3,16	0,000473919	Extrachromosomal /foreign DNA
VSAL_I2199	anaerobic nitric oxide reductase flavorubredoxin	-3,17	8,25E-08	Protection responses
VSAL_I1168	putative type VI secretion protein VasV-1. PAAR domain prote	-3,21	0,006058183	Transport/binding proteins
VSAL_I2190	integral membrane protein	-3,25	6,37E-07	Cell envelope
VSAL_I0418	membrane protein	-3,26	0,000205893	Cell envelope
VSAL_I2017	MFS transporter	-3,27	0,000467469	Transport/binding proteins
VSAL_I2897	putative flagellar basal body-associated protein FliL	-3,27	5,11E-24	Cell processes
VSAL_I0202	membrane permease (pseudogene)	-3,27	6,21025E-05	Transport/binding proteins
VSAL_II0613	putative membrane protein	-3,28	1,33E-18	Cell envelope
VSAL_I1202	secreted protein Hcp-1 (haemolysin co-regulated protein)	-3,29	4,69E-09	Transport/binding proteins
VSAL_I2347	putative exported protein	-3,34	4,61E-17	Cell envelope
VSAL_I2191	membrane protein	-3,40	0,000189183	Cell envelope
VSAL_II0322	putative membrane protein	-3,43	3,88E-15	Cell envelope
VSAL_I1452	putative membrane protein	-3,44	2,10448E-05	Cell envelope
pVSAL840_16	conjugative transfer protein TrbB	-3,44	1,06505E-06	Extrachromosomal /foreign DNA
VSAL_I1851	putative membrane protein	-3,47	4,25E-19	Cell envelope

VSAL_I0863	accessory colonization factor AcfD precursor (fragment)	-3,48	4,57E-29	Extrachromosomal /foreign DNA
VSAL_I2827	putative membrane protein	-3,50	0,003326085	Cell envelope
VSAL_I1699	outer membrane protein. OmpA-like	-3,51	4,60E-31	Cell envelope
VSAL_II0964	acyl-CoA reductase LuxC	-3,53	2,61E-12	Regulation
VSAL_I2055	general L-amino acid ABC transporter permease protein	-3,58	1,81E-06	Transport/binding proteins
VSAL_II0786	transglycosylase protein	-3,59	7,19E-18	Macromolecule metabolism
VSAL_I0108	membrane protein	-3,59	2,30706E-05	Cell envelope
VSAL_I2349	putative exported protein	-3,64	0,004869098	Cell envelope
VSAL_I1450	putative ferredoxin	-3,66	3,37E-15	Energy metabolism. carbon
VSAL_II0731	putative membrane protein	-3,67	7,52E-34	Cell envelope
VSAL_II0323	putative lipoprotein	-3,67	1,22E-20	Cell envelope
VSAL_II0028	putative membrane protein	-3,71	1,19E-36	Cell envelope
VSAL_II1095	putative membrane protein	-3,71	1,19E-36	sRNA
VSAL_II2048s	srna	-3,71	4,42E-07	sRNA
VSAL_II0715	putative cation efflux system protein	-3,75	6,22E-08	Transport/binding proteins
VSAL_II0061	exported glycosyl hydrolase. family 16	-3,80	0,000226017	Macromolecule metabolism
VSAL_I2283	chemotaxis protein CheW	-3,80	2,18E-42	Cell processes
VSAL_I2397	putative exported protein	-3,82	1,16E-34	Cell envelope
VSAL_I2348	putative membrane associated GGDEF protein	-3,84	2,87E-09	Not classified
VSAL_I2340	chemotaxis protein methyltransferase CheV	-3,85	2,48E-44	Cell processes
VSAL_I2339	chemotaxis protein methyltransferase CheR	-3,85	9,31E-37	Cell processes
VSAL_I1451	putative cytoplasmic chaperone TorD	-3,92	3,56E-07	Cell processes
VSAL_I2282	putative membrane protein	-4,01	1,24E-36	Cell envelope
pVSAL840_14	conjugative transfer protein TraF	-4,07	2,36E-07	Extrachromosomal /foreign DNA
VSAL_II0644	putative membrane protein	-4,31	4,07E-08	Cell envelope
VSAL_I0861	5-methyltetrahydropteroyltriglutamate--homocyst eine meth	-4,51	1,79E-16	Amino acid biosynthesis
VSAL_II0238	glucose-1-phosphate adenylyltransferase	-4,77	5,21E-17	Macromolecule synthesis. modificatior
VSAL_I2295	polar flagellar assembly protein FlhB	-4,78	5,39E-37	Cell processes
VSAL_II0321	putative glycosyl transferase	-4,82	1,20E-23	Cell envelope
VSAL_I2127	hypothetical protein	-4,85	0,03349533	Unknown function
VSAL_II2008s	srna	-4,87	5,23E-32	sRNA
VSAL_II0320	putative membrane associated signaling protein	-5,33	2,33E-19	Regulation

VSAL_II0231	chemotaxis protein CheV	-5,60	3,62E-48	Cell processes
VSAL_I1977	membrane associated GGDEF protein	-5,60	2,60E-31	Cell envelope
VSAL_I2343	polar flagellar FlgN. putative chaperone	-5,67	1,70E-59	Cell processes
VSAL_I2061	hypothetical protein	-5,67	5,15E-40	Unknown function
VSAL_II0587	outer membrane protein. OmpA family	-5,94	1,52E-44	Cell envelope
VSAL_I2344	putative lipoprotein	-6,12	3,53E-34	Cell envelope
VSAL_I1357	secreted protein Hcp-2 (haemolysin co-regulated protein)	-6,60	8,91E-09	Transport/binding proteins
VSAL_I2342	negative regulator of flagellin synthesis FlgM. anti-sigma28 f	-7,92	4,80E-72	Regulation
VSAL_II0319	RNA polymerase sigma factor	-8,15	1,78E-25	Regulation
VSAL_I2300	polar flagellar switch protein FliN	-8,31	5,46E-59	Cell processes
VSAL_I2284	cheW-like protein	-8,36	3,86E-69	Not classified
VSAL_I1863	sodium-type flagellar protein MotY precursor	-9,01	2,25E-41	Cell processes
VSAL_I2346	putative exported protein	-9,36	1,08E-89	Cell envelope
VSAL_I2299	polar flagellar assembly protein FliO	-10,93	1,04E-53	Cell processes
VSAL_II2038s	srna	-11,03	4,98E-32	sRNA
VSAL_I2301	polar flagellar switch protein FliM (flagellar motor switch pro	-11,11	3,70E-93	Cell processes
VSAL_I2296	polar flagellar assembly protein FliR	-11,25	7,33E-57	Cell processes
VSAL_I1856	hypothetical protein	-11,41	3,10E-06	Unknown function
VSAL_I2304	polar flagellar assembly protein FliJ	-11,71	7,71E-47	Cell processes
VSAL_I2286	chemotaxis response regulator protein-glutamate methyleste	-12,06	8,27E-119	Cell processes
VSAL_I2289	chemotaxis protein CheY	-12,09	2,98E-100	Cell processes
VSAL_I2288	chemotaxis protein CheZ	-12,10	2,53E-126	Cell processes
VSAL_I2297	polar flagellar assembly protein FliR	-12,40	6,68E-44	Cell processes
VSAL_I2290	RNA polymerase sigma factor for flagellar regulon FliA	-12,55	1,08E-138	Regulation
VSAL_I2298	polar flagellar assembly protein FliP	-13,02	4,54E-87	Cell processes
VSAL_I2287	chemotaxis protein CheA	-14,08	1,52E-186	Cell processes
VSAL_I2285	putative chromosome segregation protein	-14,25	3,78E-115	Cell processes
VSAL_I2302	polar flagellar protein FliL	-14,57	1,01E-74	Cell processes
VSAL_I2291	flagellar biosynthesis protein FlhG (flagellar number regulato	-15,05	1,93E-117	Regulation
VSAL_II0647	hypothetical protein (pseudogene)	-15,42	3,61E-112	Unknown function
VSAL_I2305	polar flagellum-specific ATP synthase FliI	-15,67	1,68E-105	Cell processes
VSAL_I2771	sodium-type polar flagellar protein MotX	-15,88	3,95E-102	Cell processes

VSAL_I1995	phospholipase A1 precursor	-16,68	5,02E-94	Central intermediary metabolism
VSAL_II1023	hypothetical protein	-18,25	3,45E-25	Unknown function
VSAL_I1857	hypothetical protein	-18,83	7,74E-72	Unknown function
VSAL_I1951	methyl-accepting chemotaxis protein	-26,10	7,79E-141	Cell processes
VSAL_I2292	flagellar biosynthesis protein FlhF	-26,25	5,70E-171	Cell processes
VSAL_I2345	putative exported protein	-26,72	1,92E-133	Cell envelope
VSAL_II0785	putative exported protein	-28,54	8,16E-105	Cell envelope
VSAL_II1022	methyl-accepting chemotaxis protein	-29,30	5,69E-120	Cell processes
VSAL_II0957	autoinducer synthesis protein LuxI	-30,14	1,65E-213	Regulation
VSAL_I2293	polar flagellar assembly protein FlhA	-36,51	7,02E-188	Cell processes
VSAL_I2332	flagellar L-ring protein 1 precursor (basal body L-ring protein	-36,73	2,68E-121	Cell processes
VSAL_I2303	polar flagellar hook-length control protein FliK	-38,32	2,67E-181	Cell processes
VSAL_I0937	sodium-driven polar flagellar protein MotB	-41,79	5,97E-165	Cell processes
VSAL_II0528	hemolysin secretion protein	-42,50	4,43E-115	Extrachromosomal /foreign DNA
VSAL_I0936	sodium-driven polar flagellar protein MotA	-43,67	1,38E-134	Cell processes
VSAL_I2333	flagellar basal-body rod protein FlgG (distal rod protein)	-43,74	3,76E-166	Cell processes
VSAL_I2517	hypothetical protein flaF; flagellin subunit F	-45,83	2,10E-204	Cell processes
VSAL_I2328	flagellar hook-associated protein type 3 FlgL	-52,93	9,82E-218	Cell processes
VSAL_I4140s	srna	-60,59	1,55E-48	sRNA
VSAL_I2331	flagellar P-ring protein 2 precursor (basal body P-ring protein	-61,65	7,02E-182	Cell processes
VSAL_I0799	methyl-accepting chemotaxis protein	-69,74	4,54E-204	Cell processes
VSAL_I2330	peptidoglycan hydrolase FlgJ	-82,93	4,92E-134	Cell processes
VSAL_I2334	flagellar basal-body rod protein FlgF	-97,16	1,13E-179	Cell processes
VSAL_I2193	methyl-accepting chemotaxis protein	-100,17	9,46E-276	Cell processes
VSAL_II0821	putative exported protein	-110,51	1,61E-283	Cell envelope
VSAL_I2306	polar flagellar assembly protein FliH	-146,88	1,13E-103	Cell processes
VSAL_I2335	flagellar hook protein FlgE	-148,34	3,28E-249	Cell processes
VSAL_I1001	transposase	-242,87	0,042608997	sRNA
VSAL_I2336	flagellar basal-body rod protein FlgD	-313,43	8,79E-275	Cell processes
VSAL_II0130	transposase	-481,25	3,16E-13	Extrachromosomal /foreign DNA
VSAL_I2307	polar flagellar motor switch protein FliG	-1014,08	8,66E-08	Cell processes
VSAL_I2325	flagellin subunit B	-1060,19	1,01E-69	Cell processes

VSAL_I2326	putative exported protein	-1673,44	2,82E-19	Cell envelope
VSAL_I2308	polar flagellar M-ring protein FliF (pseudogene)	-2355,16	2,05E-09	Cell processes
VSAL_I2316	polar flagellar protein FlaG (pseudogene)	-2667,55	3,55E-24	Cell processes
VSAL_I2317	hypothetical protein flaE; flagellin subunit E	-2985,72	1,85E-07	Cell processes
VSAL_I2311	histidine kinase(maybe FlrB)	-4428,00	3,22E-27	Regulation
VSAL_I2315	polar flagellar hook-associated protein 2 (HAP2) (flagellar ca	-4899,86	2,46E-39	Cell processes
VSAL_I2318	hypothetical protein flaD; flagellin subunit D	-5395,49	2,23E-21	Cell processes
VSAL_I2309	flagellar hook-basal body complex protein FliE	-5407,49	2,07E-25	Cell processes
VSAL_I4139s	srna	-5537,86	1,95E-40	sRNA
VSAL_I2314	polar flagellar protein FlaI	-6749,11	9,63E-27	Cell processes
VSAL_I2310	sigma-54 dependent response regulator (maybe flrC)	-6760,47	7,75E-30	Regulation
VSAL_I2313	polar flagellar protein FliS (polar flagellar protein FlaJ)	-7588,93	1,85E-27	Cell processes
VSAL_I2327	hypothetical protein flaA; flagellin subunit A	-13134,08	1,28E-19	Cell processes
VSAL_I2312	sigma 54 dependent transcription regulator (FlrA)	-17298,29	2,62E-32	Regulation
VSAL_I2319	hypothetical protein flaC; flagellin subunit C	-39026,56	7,18E-38	Cell processes

Additional file 6: Table S4. The differentially expressed genes of *luxI*⁻ mutant compared to wild type at HCD.

VSAL ID	Product	Fold Change	p-value	Functional classes
VSAL_I3102s	srna	456,36	2,76448E-07	sRNA
VSAL_II0366	fimbrial protein, Flp/Fap pilin component	151,51	2,685E-33	Cell envelope
VSAL_II0252	hypothetical protein	90,72	8,8059E-155	Cell envelope
VSAL_II0367	type IV leader peptidase	39,53	7,92446E-39	Cell envelope
VSAL_II0134	hypothetical protein	38,73	2,4271E-192	Cell envelope
VSAL_II0128	hypothetical protein, putative phage gene	35,63	2,41009E-05	Extrachromosomal /foreign DNA
VSAL_I2712	dihydrolipoyl dehydrogenase (dihydrolipoamide dehydrogena	27,22	1,13967E-05	Not classified
VSAL_II0362	hypothetical protein	25,37	1,2355E-106	Unknown function
VSAL_II0135	putative cytochrome b561	19,03	1,06564E-50	Energy metabolism, carbon
VSAL_II0370	putative lipoprotein	18,12	4,11846E-24	Cell envelope
VSAL_II0986	hypothetical protein	17,01	2,88145E-74	Unknown function
VSAL_I2713	hybrid peroxiredoxin (thioredoxin reductase)	16,36	0,000172196	Biosynthesis of cofactors, carriers
VSAL_II0074	membrane protein	13,12	0,000976942	Cell envelope
VSAL_I2749	probable HTH-type transcriptional regulator LeuO	12,60	1,29552E-45	Regulation
VSAL_II0363	putative response regulator	12,34	1,495E-28	Regulation
VSAL_II0369	type II/III secretion system protein	10,82	1,53696E-38	Extrachromosomal /foreign DNA
VSAL_II0947	hypothetical protein	10,48	3,83583E-30	Unknown function
VSAL_II0372	type II/IV secretion system protein, ATP binding domain	10,26	3,50577E-33	Extrachromosomal /foreign DNA
VSAL_II0987	hypothetical protein	9,81	5,09656E-48	Unknown function
VSAL_II0722	hypothetical protein	9,62	9,87571E-33	Unknown function
VSAL_II0364	hypothetical protein	9,58	2,23328E-12	Unknown function
VSAL_II0371	type II secretion system protein Z	9,57	1,61514E-27	Extrachromosomal /foreign DNA
VSAL_II0312	hypothetical protein, putative anti-sigma factor antagonist	9,55	4,70059E-26	Not classified
VSAL_I2064	conserved hypothetical protein	9,37	0,001134015	Unknown function
VSAL_II0214	patatin-like phospholipase	9,34	3,88049E-05	Fatty acid biosynthesis
VSAL_I2030	glutaredoxin 1	9,00	1,38956E-15	Biosynthesis of cofactors, carriers
VSAL_I0902	chitinase A (fragment)	8,58	2,16194E-31	Macromolecule metabolism
VSAL_I0132	putative lipoprotein	8,48	3,68661E-21	Cell envelope
VSAL_I1475	hypothetical protein	8,42	7,17109E-23	Cell envelope
VSAL_I1625	hypothetical protein	8,33	0,003185864	Unknown function
VSAL_II0368	putative Flp pilus assembly protein	8,23	4,50769E-32	Cell envelope

VSAL_II0934	hypothetical protein	7,43	7,36457E-17	Unknown function
VSAL_II0373	bacterial type II secretion system protein F	7,32	2,97451E-33	Extrachromosomal /foreign DNA
VSAL_II0381	response regulator, histidine kinase	7,28	7,48374E-25	Regulation
VSAL_I1627	membrane protein	7,21	0,000110014	Cell envelope
VSAL_I1486	cold-shock protein	7,20	6,12208E-19	Adaptation
VSAL_II0215	catalase	7,20	0,000213899	Protection responses
VSAL_I0133	hypothetical protein	6,75	2,80854E-18	Unknown function
VSAL_II0311	outer membrane protein, OmpA family	6,41	3,45389E-15	Cell envelope
VSAL_I1603	putative exported protein	5,83	0,010115497	Cell envelope
VSAL_II0988	hypothetical protein	5,78	6,44735E-19	Unknown function
VSAL_II0687	glucose-6-phosphate 1-dehydrogenase	5,75	1,70291E-29	Energy metabolism, carbon
VSAL_II0382	hypothetical protein	5,08	1,92734E-13	Unknown function
VSAL_II0171	putative membrane protein	5,07	4,30288E-27	Cell envelope
VSAL_II0685	6-phosphogluconate dehydrogenase	4,85	1,65209E-22	Energy metabolism, carbon
VSAL_I1476	membrane protein	4,84	1,99349E-11	Cell envelope
VSAL_I1604	putative exported protein (fragment)	4,72	0,015864994	Cell envelope
VSAL_I1056	carbonic anhydrase precursor	4,61	8,56709E-14	Central intermediary metabolism
VSAL_II0686	6-phosphogluconolactonase	4,46	3,59378E-23	Energy metabolism, carbon
VSAL_I1685	putative amidase	4,39	1,06113E-18	Not classified
VSAL_II0102	hypothetical protein	4,25	2,66129E-08	Central intermediary metabolism
VSAL_II0933	putative exported protein	4,21	4,13051E-19	Cell envelope
VSAL_I1820	putative lipoprotein	4,16	1,55338E-46	Cell envelope
VSAL_II0989	putative exported protein (fragment)	4,11	3,8279E-15	Cell envelope
VSAL_I1819	outer membrane protein A	4,09	1,90448E-21	Cell envelope
VSAL_II0170	methyl-accepting chemotaxis protein	3,92	1,13941E-11	Cell processes
VSAL_I0134	L-2,4-diaminobutyrate decarboxylase	3,91	1,30507E-05	Amino acid biosynthesis
VSAL_II0599	membrane protein	3,89	1,46758E-11	Cell envelope
VSAL_II0300	hypothetical protein	3,86	4,63447E-08	Unknown function
VSAL_I1629	glycosyl transferase, family 2 (pseudogene)	3,83	0,000381753	Not classified
VSAL_I1526	membrane protein	3,74	0,000560119	Cell envelope
VSAL_I4160s	null	3,73	7,43286E-09	sRNA
VSAL_II0297	putative glycosyl transferase	3,63	1,34381E-15	Macromolecule synthesis, modification

VSAL_II0932	cellulose synthase catalytic subunit	3,60	8,42732E-21	Cell envelope
VSAL_I1687	aspartate aminotransferase	3,57	1,96918E-10	Amino acid biosynthesis
VSAL_I1626	MltA-interacting protein MipA	3,54	0,001387542	Cell envelope
VSAL_I2124	hypothetical protein	3,50	2,92623E-06	Unknown function
VSAL_II0310	polysaccharide biosynthesis/export protein	3,48	4,60149E-12	Macromolecule synthesis, modification
VSAL_II0935	hypothetical protein	3,45	2,81208E-18	Unknown function
VSAL_I0025	putative exported protein	3,44	1,48692E-20	Cell envelope
VSAL_II0931	membrane protein (fragment)	3,43	3,86822E-10	Cell envelope
VSAL_I2547	conserved hypothetical protein	3,33	0,036840948	Unknown function
VSAL_II0304	putative glycosyl transferase	3,31	5,27995E-08	Macromolecule synthesis, modification
VSAL_I0514	transposase (pseudogene)	3,28	3,9364E-12	Extrachromosomal /foreign DNA
VSAL_I4118s	srna	3,20	4,32816E-11	sRNA
VSAL_I0135	siderophore biosynthetis protein	3,18	3,14555E-05	Biosynthesis of cofactors, carriers
VSAL_I0903	transposase	3,13	4,04113E-09	Extrachromosomal /foreign DNA
VSAL_II0721	PTS system permease for N-acetylglucosamine and glucose	3,07	1,49912E-07	Transport/binding proteins
VSAL_II0172	hypothetical protein	3,04	5,33148E-08	Unknown function
VSAL_I1628	putative radical SAM superfamily protein	2,97	0,005591404	Not classified
VSAL_II1062	membrane protein	2,93	5,52399E-11	Cell envelope
VSAL_I0460	colanic biosynthesis UDP-glucose lipid carrier transferase (ps	2,93	9,61945E-13	Macromolecule synthesis, modification
VSAL_II0303	putative glycosyl transferase	2,91	3,04328E-08	Macromolecule synthesis, modification
VSAL_I2588	iron(III) ABC transporter, periplasmic iron-compound-binding	2,91	6,58032E-10	Transport/binding proteins
VSAL_I4109s	srna	2,87	8,69503E-07	sRNA
VSAL_I1686	phosphoribosylglycinamide formyltransferase 2	2,86	0,000169729	Nucleotide biosynthesis
VSAL_I1982	putative DNA transformation protein TfoX	2,84	9,49943E-11	Not classified
VSAL_I4145s	null	2,77	4,56011E-08	sRNA
VSAL_I1677	putative membrane protein	2,76	0,000482156	Cell envelope
VSAL_II0050	N,N'-diacetylchitobiase precursor (chitobiase)	2,75	3,27142E-11	Macromolecule metabolism
VSAL_I4031s	srna	2,72	9,17599E-05	sRNA
VSAL_I1018	hypothetical protein, putative phage gene	2,64	0,014176212	Extrachromosomal /foreign DNA
VSAL_II0189	transposase (fragment)	2,62	3,21154E-11	Extrachromosomal /foreign DNA
VSAL_II0512	putative exported protein	2,61	1,32213E-11	Cell envelope
VSAL_I1682	hypothetical protein (fragment)	2,60	0,019391837	Unknown function

VSAL_II2036s	srna	2,59	0,007393045	sRNA
VSAL_II0511	superoxide dismutase [Cu-Zn] precursor	2,58	1,0191E-12	Protection responses
VSAL_I2441	hypothetical protein	2,57	5,05561E-08	Protection responses
VSAL_I1036	probable rRNA transcription initiatior protein, putative phage	2,53	0,044688579	Extrachromosomal /foreign DNA
VSAL_I4105s	srna	2,52	0,001558042	sRNA
VSAL_II0946	integral membrane protein	2,52	3,44112E-10	Cell envelope
VSAL_II0296	putative transmembrane glycosyl transferase	2,49	3,34857E-09	Macromolecule synthesis, modification
VSAL_I0884	putative exported protein	2,49	1,99277E-07	Cell envelope
VSAL_I1751	TonB protein (pseudogene)	2,47	0,023640509	Transport/binding proteins
VSAL_I1547	hypothetical protein	2,46	7,84358E-06	Unknown function
VSAL_I1681	inner membrane protein, LrgA family	2,46	0,002852746	Cell envelope
VSAL_I4095s	srna	2,44	0,009730333	sRNA
VSAL_II0688	putative membrane protein	2,42	0,000846869	Cell envelope
VSAL_I3163s	null	2,42	0,001279358	sRNA
VSAL_II0663	integral membrane protein, putative transmembrane transp	2,41	1,46173E-07	Cell envelope
VSAL_I4144s	srna	2,40	5,21212E-08	sRNA
VSAL_I1667	putative exported protein	2,40	0,000482295	Cell envelope
VSAL_II0717	putative membrane protein	2,39	0,000132068	Cell envelope
VSAL_I1300	putative membrane protein	2,36	0,000108941	Cell envelope
VSAL_I1269	hypothetical protein	2,36	2,17809E-05	Unknown function
VSAL_I1666	hypothetical protein	2,36	0,00184758	Unknown function
VSAL_I1029	phage terminase, endonuclease subunit	2,35	0,011514963	Extrachromosomal /foreign DNA
VSAL_I4077s	srna	2,33	6,29023E-06	sRNA
VSAL_I1673	DNA repair protein	2,30	0,001283985	Macromolecule synthesis, modification
VSAL_II0992	transposase (fragment)	2,29	1,33696E-12	Extrachromosomal /foreign DNA
VSAL_I0026	hypothetical protein	2,29	9,14476E-12	Unknown function
VSAL_I1035	probable tail tube protein	2,27	0,019473234	Extrachromosomal /foreign DNA
VSAL_II0138	hypothetical protein	2,25	6,27581E-13	Unknown function
VSAL_I1465	hypothetical protein	2,25	0,023416617	Unknown function
VSAL_II0302	putative polysaccharide biosynthesis protein	2,24	8,24834E-07	Macromolecule synthesis, modification
VSAL_I1644	hypothetical protein, putative phage gene	2,23	3,4632E-06	Extrachromosomal /foreign DNA
VSAL_I0284	5-carboxymethyl-2-hydroxymuconate isomerase	2,22	1,06598E-10	Degradation of small molecules

VSAL_I1647	putative membrane protein, putative phage gene	2,22	0,000510771	Extrachromosomal /foreign DNA
VSAL_I1624	enhancing lycopene biosynthesis protein 2	2,22	0,001516672	Biosynthesis of cofactors, carriers
VSAL_I2963	valine--pyruvate aminotransferase (alanine--valine transami	2,21	3,86246E-07	Amino acid biosynthesis
VSAL_I1060	putative exported protein	2,20	8,98009E-10	Cell envelope
VSAL_I1325	proton glutamate symport protein	2,20	5,89763E-06	Transport/binding proteins
VSAL_I1909	membrane protein	2,19	0,000303912	Cell envelope
VSAL_I2989	putative beta-N-acetylhexosaminidase	2,19	3,55235E-08	Not classified
VSAL_I1668	small heat shock protein IbpA (16 kDa heat shock protein A)	2,19	0,001323247	Adaptation
VSAL_II0937	membrane protein	2,18	4,89008E-10	Cell envelope
VSAL_I2858	probable CsgAB operon transcriptional regulatory protein	2,18	3,26537E-05	Regulation
VSAL_II0098	transposase	2,18	5,1687E-10	Extrachromosomal /foreign DNA
VSAL_I2950	putative signaling protein (pseudogene)	2,17	1,64151E-07	Not classified
VSAL_II0374	bacterial type II secretion system protein F	2,17	7,26124E-09	Extrachromosomal /foreign DNA
VSAL_I1716	transposase (pseudogene)	2,16	4,90044E-10	Extrachromosomal /foreign DNA
VSAL_I1678	Hypothetical protein	2,16	0,011900347	Unknown function
VSAL_II0150	ferrichrome transport ATP-binding protein FhuC	2,15	0,00214349	Transport/binding proteins
VSAL_II0846	putative acetyltransferase	2,15	1,12331E-07	Not classified
VSAL_I1927	hypothetical protein, putative phage gene (fragment)	2,15	0,038086848	Extrachromosomal /foreign DNA
VSAL_II0257	transposase (pseudogene)	2,15	2,92438E-11	Extrachromosomal /foreign DNA
pVSAL320_11	putative DNA-damage-inducible protein	2,14	1,76236E-05	Not classified
VSAL_II0298	putative membrane protein	2,13	2,01584E-07	Cell envelope
VSAL_I0115	transposase	2,13	1,11972E-11	Extrachromosomal /foreign DNA
VSAL_II0928	transposase	2,13	3,30321E-11	Extrachromosomal /foreign DNA
VSAL_I1258	transposase (pseudogene)	2,12	6,8404E-11	Extrachromosomal /foreign DNA
VSAL_I1061	transposase	2,12	6,33534E-11	Extrachromosomal /foreign DNA
VSAL_I1747	transposase	2,12	9,16932E-11	Extrachromosomal /foreign DNA
VSAL_I1672	transposase	2,12	1,68214E-10	Extrachromosomal /foreign DNA
VSAL_II1089	hypothetical protein (fragment)	2,12	1,04363E-05	Unknown function
VSAL_I1656	transposase	2,12	4,9342E-10	Extrachromosomal /foreign DNA
VSAL_I2250	transposase	2,12	7,98059E-10	Extrachromosomal /foreign DNA
VSAL_I2611	transposase	2,11	2,98096E-12	Extrachromosomal /foreign DNA
VSAL_I0872	hypothetical protein	2,11	4,28348E-06	Unknown function

VSAL_II0985	membrane transport protein, putative auxin efflux carrier	2,11	6,01368E-07	Transport/binding proteins
VSAL_II0044	transposase (fragment)	2,11	2,30563E-05	Extrachromosomal /foreign DNA
VSAL_I2707	transposase	2,10	4,65529E-11	Extrachromosomal /foreign DNA
VSAL_I1780	transposase	2,10	9,05501E-11	Extrachromosomal /foreign DNA
VSAL_II0973	transposase	2,10	1,50421E-09	Extrachromosomal /foreign DNA
VSAL_I2953	transposase	2,10	2,06925E-10	Extrachromosomal /foreign DNA
VSAL_I0066	transposase	2,10	0,000605326	Extrachromosomal /foreign DNA
VSAL_I1998	cytochrome c-type protein NrfB precursor	2,10	0,000232479	Energy metabolism, carbon
VSAL_II0069	transposase	2,10	1,88876E-09	Extrachromosomal /foreign DNA
VSAL_II0175	transposase	2,09	4,66775E-11	Extrachromosomal /foreign DNA
VSAL_II0313	putative exported protein	2,09	7,43572E-09	Cell envelope
VSAL_II0243	transposase	2,09	3,69574E-10	Extrachromosomal /foreign DNA
VSAL_I2753	transposase	2,08	3,8098E-10	Extrachromosomal /foreign DNA
VSAL_I2263	hypothetical protein, putative phage gene (fragment)	2,08	4,65985E-05	Extrachromosomal /foreign DNA
VSAL_I1316	transposase (pseudogene)	2,08	2,52282E-09	Extrachromosomal /foreign DNA
VSAL_I1442	transposase	2,08	5,9732E-10	Extrachromosomal /foreign DNA
VSAL_II0768	transposase (pseudogene)	2,08	7,20304E-10	Extrachromosomal /foreign DNA
VSAL_I2943	transposase	2,08	1,44343E-10	Extrachromosomal /foreign DNA
VSAL_II1018	transposase	2,08	1,0083E-09	Extrachromosomal /foreign DNA
VSAL_II0068	hypothetical protein	2,07	0,014026951	Unknown function
VSAL_II0270	transposase	2,07	4,29473E-09	Extrachromosomal /foreign DNA
VSAL_I2462	transposase (pseudogene)	2,07	4,52971E-10	Extrachromosomal /foreign DNA
VSAL_II0219	transposase	2,07	5,20728E-10	Extrachromosomal /foreign DNA
VSAL_II0991	transposase	2,06	1,91848E-10	Extrachromosomal /foreign DNA
VSAL_I1241	transposase (pseudogene)	2,06	2,03725E-10	Extrachromosomal /foreign DNA
VSAL_I0971	alanine racemase (pseudogene)	2,06	0,011646089	Cell envelope
VSAL_II0197	transcriptional activator protein, response regulator	2,06	8,48894E-05	Regulation
VSAL_II0229	transposase	2,06	4,40849E-10	Extrachromosomal /foreign DNA
VSAL_I2163	transposase	2,06	2,75679E-10	Extrachromosomal /foreign DNA
VSAL_I2192	hypothetical protein	2,05	0,000683138	Cell envelope
VSAL_I0811	transposase	2,05	6,10099E-10	Extrachromosomal /foreign DNA
VSAL_I2114	transposase	2,05	3,50301E-09	Extrachromosomal /foreign DNA

VSAL_I0764	transposase (pseudogene)	2,05	8,97277E-10	Extrachromosomal /foreign DNA
VSAL_II0876	transposase	2,05	3,49213E-10	Extrachromosomal /foreign DNA
VSAL_I2320	transposase (pseudogene)	2,05	6,14305E-09	Extrachromosomal /foreign DNA
VSAL_I4189s	srna	2,05	4,68227E-06	sRNA
VSAL_II0335	transposase	2,05	4,2509E-10	Extrachromosomal /foreign DNA
VSAL_I2882	transposase	2,05	3,69758E-10	Extrachromosomal /foreign DNA
VSAL_I0857	anaerobic C4-dicarboxylate transporter DcuC	2,05	2,15504E-05	Transport/binding proteins
VSAL_I2257	ferrous iron transport protein FeoA	2,04	0,000233796	Transport/binding proteins
VSAL_I0318	transposase (pseudogene)	2,04	3,56177E-09	Extrachromosomal /foreign DNA
VSAL_II0299	putative glycosyl transferases	2,04	0,003254264	Macromolecule synthesis, modification
VSAL_II0080	transposase	2,04	5,07825E-10	Extrachromosomal /foreign DNA
VSAL_II1007	transposase	2,04	2,60948E-09	Extrachromosomal /foreign DNA
VSAL_I1270	ribonucleotide reductase	2,04	0,000129643	Macromolecule synthesis, modification
VSAL_I1268	transposase (pseudogene)	2,04	5,64967E-10	Extrachromosomal /foreign DNA
VSAL_II1090	transposase	2,04	2,86777E-10	Extrachromosomal /foreign DNA
VSAL_I0281	transposase (pseudogene)	2,04	3,4234E-09	Extrachromosomal /foreign DNA
VSAL_I2486	transposase	2,03	6,9756E-10	Extrachromosomal /foreign DNA
VSAL_I1107	transposase	2,03	6,34462E-08	Extrachromosomal /foreign DNA
VSAL_II0009	transposase (pseudogene)	2,03	3,79357E-09	Extrachromosomal /foreign DNA
VSAL_I1576	transposase	2,02	7,55243E-10	Extrachromosomal /foreign DNA
VSAL_II0833	transposase	2,02	4,20084E-10	Extrachromosomal /foreign DNA
VSAL_I1608	HTH-type transcriptional regulator GalR	2,02	0,000842525	Regulation
VSAL_I1811	transposase (pseudogene)	2,02	8,43713E-10	Extrachromosomal /foreign DNA
VSAL_I0291	transposase	2,02	1,39454E-09	Extrachromosomal /foreign DNA
VSAL_I2264	transposase	2,02	4,09837E-08	Extrachromosomal /foreign DNA
VSAL_II1050	transposase	2,02	1,61232E-09	Extrachromosomal /foreign DNA
VSAL_I0144	transposase	2,01	5,66312E-10	Extrachromosomal /foreign DNA
VSAL_I0883	putative exported protein	2,01	2,64148E-06	Cell envelope
VSAL_I1945	transposase (pseudogene)	2,01	3,61527E-09	Extrachromosomal /foreign DNA
VSAL_II0470	transposase	2,01	1,12263E-08	Extrachromosomal /foreign DNA
VSAL_II0046	transposase	2,00	6,4486E-10	Extrachromosomal /foreign DNA
VSAL_I1771	hypothetical protein (pseudogene)	-2,03	1,08511E-08	Unknown function

VSAL_II0445	bacterial extracellular solute-binding protein	-2,03	0,000171133	Transport/binding proteins
VSAL_II0147	membrane associated GGDEF protein	-2,04	2,11318E-07	Cell envelope
VSAL_I2620	transposase (pseudogene)	-2,04	4,60176E-07	Extrachromosomal /foreign DNA
VSAL_I1238	exported serine protease (pseudogene)	-2,05	0,000309728	Macromolecule metabolism
pVSAL840_67	hypothetical protein	-2,05	7,06394E-09	Unknown function
VSAL_I1590	quinolone resistance determinant QnrC	-2,06	1,15524E-06	Protection responses
VSAL_I4107s	srna	-2,06	0,001022235	sRNA
VSAL_I2170	putative MgtC/SapB transporter	-2,06	0,000438209	Transport/binding proteins
VSAL_I1271	putative response regulator	-2,07	0,002452707	Regulation
VSAL_II0955	putative multidrug transport protein (pseudogene)	-2,07	0,008498766	Protection responses
VSAL_I2156	2,4-dienoyl-CoA reductase [NADPH]	-2,07	8,08099E-10	Fatty acid biosynthesis
VSAL_I1589	hypothetical protein	-2,07	5,84934E-06	Unknown function
VSAL_I4092s	srna	-2,08	1,02257E-05	sRNA
VSAL_I1343	L-serine dehydratase 1	-2,10	9,66363E-09	Degradation of small molecules
VSAL_II0346	putative nuclease	-2,12	8,39976E-05	Macromolecule metabolism
VSAL_II0104	putative 6-phosphogluconate dehydrogenase	-2,12	0,000128284	Not classified
VSAL_I1344	serine transporter	-2,13	5,79567E-06	Transport/binding proteins
VSAL_II1020	membrane protein	-2,13	1,8632E-05	Cell envelope
VSAL_I0588	putative exported protein	-2,14	3,3486E-09	Cell envelope
pVSAL840_25	antirestriction protein ArdC	-2,17	0,000462972	Extrachromosomal /foreign DNA
VSAL_II0428	integral membrane protein, putative two-component signal t	-2,18	4,7877E-06	Regulation
VSAL_I1504	maltose O-acetyltransferase	-2,18	5,42282E-06	Degradation of small molecules
VSAL_II0969	putative exported protein	-2,18	0,003051726	Cell envelope
VSAL_I2773	putative membrane protein	-2,19	0,026476902	Cell envelope
VSAL_I0476	type IV pilus, mannose-sensitive hemagglutinin A	-2,19	4,20791E-06	Cell envelope
VSAL_II0424	putative fatty acid desaturase	-2,19	0,005457818	Fatty acid biosynthesis
VSAL_I1713	glycerol-3-phosphate transporter	-2,19	1,67574E-07	Transport/binding proteins
VSAL_I1851	putative membrane protein	-2,19	3,91279E-11	Cell envelope
VSAL_I0401	hypothetical protein	-2,19	3,25104E-05	Unknown function
pVSAL840_28	DNA-binding protein HU-alpha	-2,20	5,68665E-05	Macromolecule synthesis, modification
VSAL_II0446	binding-protein-dependent transport system inner membran	-2,20	2,45529E-06	Transport/binding proteins
VSAL_I0620	thymidine phosphorylase	-2,21	1,49405E-05	Central intermediary metabolism

VSAL_II1013	putative heme binding protein	-2,23	1,33531E-07	Not classified
VSAL_I1357	secreted protein Hcp-2 (haemolysin co-regulated protein)	-2,24	0,024249133	Transport/binding proteins
VSAL_I2283	chemotaxis protein CheW	-2,25	2,86288E-13	Cell processes
VSAL_II0731	putative membrane protein	-2,26	1,90145E-09	Cell envelope
VSAL_II0166	hypothetical protein	-2,28	9,31894E-09	Unknown function
VSAL_I2349	putative exported protein	-2,28	0,004447043	Cell envelope
VSAL_II0920	maltose transport system permease protein MalG	-2,29	6,7397E-06	Transport/binding proteins
VSAL_II0059	putative type I toxin secretion system, membrane transport p	-2,31	3,30042E-07	Transport/binding proteins
VSAL_II0239	glycogen synthase	-2,31	4,30802E-08	Macromolecule synthesis, modification
VSAL_I1907	putative ion channel	-2,31	9,91113E-06	Transport/binding proteins
VSAL_II0223	hypothetical protein	-2,35	0,005607129	Unknown function
VSAL_I1498	putative membrane protein	-2,35	0,001081873	Cell envelope
VSAL_I2282	putative membrane protein	-2,36	7,89179E-15	Cell envelope
VSAL_I1198	probable membrane permease	-2,37	6,56396E-08	Transport/binding proteins
VSAL_I1699	outer membrane protein, OmpA-like	-2,41	5,05801E-09	Cell envelope
VSAL_I2128	putative exported protein	-2,41	0,02128124	Cell envelope
VSAL_I2343	polar flagellar FlgN, putative chaperone	-2,41	5,24521E-08	Cell processes
VSAL_I2206	putative sporulation protein	-2,41	1,40818E-06	Cell division
VSAL_II1012	response regulator, histidine kinase	-2,41	3,82265E-09	Regulation
VSAL_I2304	polar flagellar assembly protein FliJ	-2,43	5,05574E-07	Cell processes
VSAL_I4178s	srna	-2,44	0,003980003	sRNA
VSAL_I4081s	srna	-2,45	0,002253892	sRNA
VSAL_II0394	cytochrome c551 peroxidase	-2,48	1,06061E-08	Energy metabolism, carbon
VSAL_II0060	putative type I toxin secretion system, ATP-binding protein	-2,49	7,67546E-10	Transport/binding proteins
VSAL_I1808	hypothetical protein	-2,52	2,15274E-16	Unknown function
VSAL_I2207	conserved hypothetical protein	-2,54	5,87626E-06	Unknown function
VSAL_I1449	hypothetical protein	-2,60	1,30683E-06	Unknown function
VSAL_II0052	response regulator protein	-2,63	2,53806E-15	Regulation
VSAL_I1451	putative cytoplasmic chaperone TorD	-2,66	0,002800726	Cell processes
VSAL_I0761	conserved hypothetical protein	-2,67	3,07295E-07	Unknown function
VSAL_II0232	putative alpha amylase	-2,68	5,57759E-10	Macromolecule metabolism
VSAL_I1450	putative ferredoxin	-2,70	3,2344E-05	Energy metabolism, carbon

VSAL_II0246	nitrite reductase [NAD(P)H] small subunit	-2,70	0,00998543	Energy metabolism, carbon
VSAL_I1977	membrane associated GGDEF protein	-2,71	3,23275E-10	Cell envelope
VSAL_I0824	putative exported protein	-2,72	0,00037412	Cell envelope
VSAL_II0057	putative membrane associated response regulator	-2,74	6,48776E-11	Regulation
VSAL_II0062	membrane protein	-2,76	1,47455E-07	Cell envelope
VSAL_II0238	glucose-1-phosphate adenylyltransferase	-2,76	2,03265E-08	Macromolecule synthesis, modification
VSAL_I1906	membrane protein	-2,76	3,04608E-06	Cell envelope
VSAL_I2340	chemotaxis protein methyltransferase CheV	-2,77	8,32824E-16	Cell processes
VSAL_II0315	putative response regulator	-2,79	3,08475E-10	Regulation
VSAL_II0712	methyl-accepting chemotaxis citrate transducer	-2,81	1,6846E-15	Cell processes
VSAL_II0644	putative membrane protein	-2,81	2,09575E-08	Cell envelope
VSAL_I2056	general L-amino acid ABC transporter permease protein	-2,92	5,40431E-10	Transport/binding proteins
VSAL_I2342	negative regulator of flagellin synthesis FlgM, anti-sigma28	-2,93	5,95666E-10	Regulation
VSAL_I1905	membrane protein	-2,94	1,74372E-08	Cell envelope
VSAL_II0058	putative type I toxin secretion system, outer membrane efflu	-2,95	2,17783E-10	Transport/binding proteins
VSAL_I1904	secretion protein, HlyD family	-2,98	1,40576E-16	Transport/binding proteins
VSAL_II0101	peptidase	-2,98	5,99086E-14	Macromolecule metabolism
VSAL_II0061	exported glycosyl hydrolase, family 16	-2,99	1,08598E-09	Macromolecule metabolism
VSAL_I1599	putative polysaccharide deacetylase	-2,99	0,000366386	Not classified
VSAL_II0317	putative membrane protein	-3,01	1,21517E-09	Cell envelope
VSAL_I2208	putative PrkA serine protein kinase	-3,03	3,16959E-09	Not classified
VSAL_II0028	putative membrane protein	-3,07	1,05957E-10	Cell envelope
VSAL_II1095	putative membrane protein	-3,07	1,05957E-10	Cell envelope
VSAL_I2295	polar flagellar assembly protein FlhB	-3,08	5,4745E-14	Cell processes
VSAL_II0055	hypothetical protein	-3,08	2,10265E-16	Unknown function
VSAL_I2054	general L-amino acid transport ATP-binding subunit	-3,13	1,11133E-09	Transport/binding proteins
VSAL_II0231	chemotaxis protein CheV	-3,13	6,05708E-17	Cell processes
VSAL_I2061	hypothetical protein	-3,20	8,99811E-07	Unknown function
VSAL_I2344	putative lipoprotein	-3,27	9,61491E-10	Cell envelope
VSAL_I1832	hypothetical protein (fragment)	-3,29	1,32193E-17	Unknown function
VSAL_II2019s	srna	-3,30	0,000937933	sRNA
VSAL_I0755	membrane protein	-3,30	6,80271E-22	Cell envelope

VSAL_II0065	membrane protein	-3,32	4,31018E-08	Cell envelope
VSAL_II2038s	srna	-3,33	9,87358E-07	sRNA
VSAL_II0718	membrane protein	-3,37	6,37366E-13	Cell envelope
VSAL_I4059s	srna	-3,37	1,72272E-13	sRNA
VSAL_II0067	hypothetical protein	-3,38	2,36208E-05	Unknown function
VSAL_I2055	general L-amino acid ABC transporter permease protein	-3,46	1,28615E-14	Transport/binding proteins
VSAL_I2339	chemotaxis protein methyltransferase CheR	-3,47	3,53902E-20	Cell processes
VSAL_II0968	putative exported protein	-3,48	0,007933275	Cell envelope
VSAL_II0316	response regulator, histidine kinase	-3,52	1,37027E-21	Regulation
VSAL_I2397	putative exported protein	-3,54	1,80927E-30	Cell envelope
VSAL_II0331	putative exported protein	-3,54	3,67349E-11	Cell envelope
VSAL_I2438	isocitrate lyase	-3,55	6,09198E-05	Central intermediary metabolism
VSAL_I1863	sodium-type flagellar protein MotY precursor	-3,59	5,05057E-12	Cell processes
VSAL_II0587	outer membrane protein, OmpA family	-3,60	2,55367E-22	Cell envelope
VSAL_II0056	putative type I secretion protein, HlyD family	-3,68	8,16614E-18	Transport/binding proteins
VSAL_II0318	putative exported protein	-3,72	2,15247E-11	Cell envelope
VSAL_I2299	polar flagellar assembly protein FliO	-3,74	1,91855E-14	Cell processes
VSAL_II0064	putative type I secretion protein, HlyD family	-3,80	9,23154E-26	Transport/binding proteins
VSAL_I2300	polar flagellar switch protein FliN	-3,80	9,96836E-18	Cell processes
VSAL_II0066	membrane protein	-3,81	5,9165E-30	Cell envelope
pVSAL840_26	hypothetical protein	-3,84	4,97626E-14	Unknown function
VSAL_I2439	malate synthase A	-3,86	0,011586201	Central intermediary metabolism
VSAL_II1023	hypothetical protein	-3,91	3,58248E-05	Unknown function
VSAL_I2130	methyl-accepting chemotaxis protein	-3,92	3,25158E-26	Cell processes
VSAL_I2698	hypothetical protein (pseudogene)	-4,00	3,88036E-22	Unknown function
VSAL_II0020	hemolysin-type calcium-binding protein	-4,01	3,07283E-31	Not classified
VSAL_II0053	membrane associated response regulator, histidine kinase	-4,07	6,81523E-30	Regulation
VSAL_II2008s	srna	-4,15	3,93935E-16	sRNA
VSAL_I4098s	srna	-4,16	2,66944E-29	sRNA
VSAL_I1856	hypothetical protein	-4,16	2,71941E-30	Unknown function
VSAL_I1317	carbon starvation protein (pseudogene)	-4,18	5,68076E-10	Adaptation
VSAL_II0325	putative exported protein	-4,20	3,28812E-23	Cell envelope

VSAL_I2302	polar flagellar protein FliL	-4,23	7,83168E-19	Cell processes
VSAL_II0324	putative lipoprotein	-4,25	8,64822E-26	Cell envelope
VSAL_I2305	polar flagellum-specific ATP synthase FliI	-4,33	3,83584E-16	Cell processes
VSAL_II0063	putative type I secretion system, ATP-binding protein	-4,46	1,02128E-23	Transport/binding proteins
VSAL_I2284	cheW-like protein	-4,50	1,14499E-32	Not classified
VSAL_I2346	putative exported protein	-4,54	5,3487E-18	Cell envelope
VSAL_II0329	putative response regulator	-4,74	1,7163E-21	Regulation
VSAL_I1428	conserved hypothetical protein	-4,82	1,25634E-17	Unknown function
VSAL_II0158	transposase	-4,84	0,000594602	Extrachromosomal /foreign DNA
VSAL_II0333	transposase	-4,92	8,40716E-28	Extrachromosomal /foreign DNA
VSAL_II0319	RNA polymerase sigma factor	-5,08	9,1462E-28	Regulation
VSAL_I2301	polar flagellar switch protein FliM (flagellar motor switch pr	-5,10	4,2377E-31	Cell processes
VSAL_I2057	general L-amino acid-binding periplasmic protein precursor	-5,14	1,88814E-30	Transport/binding proteins
VSAL_II0326	hypothetical protein	-5,22	2,98273E-22	Unknown function
VSAL_II0332	putative hemolysin-type calcium-binding protein (fragment)	-5,29	4,75654E-29	Not classified
VSAL_I2298	polar flagellar assembly protein FliP	-5,52	4,47284E-22	Cell processes
VSAL_II0323	putative lipoprotein	-5,67	5,43708E-24	Cell envelope
VSAL_II0328	putative anti-sigma F factor antagonist	-5,87	3,71096E-17	Not classified
VSAL_I2286	chemotaxis response regulator protein-glutamate methylest	-6,01	3,61014E-25	Cell processes
VSAL_I2297	polar flagellar assembly protein FliR	-6,08	5,57166E-20	Cell processes
VSAL_I2291	flagellar biosynthesis protein FlhG (flagellar number regulat	-6,15	4,97336E-45	Regulation
VSAL_I2290	RNA polymerase sigma factor for flagellar regulon FliA	-6,16	2,48173E-47	Regulation
VSAL_I2289	chemotaxis protein CheY	-6,37	2,90879E-34	Cell processes
VSAL_I2287	chemotaxis protein CheA	-6,49	1,88629E-36	Cell processes
VSAL_II0322	putative membrane protein	-6,52	7,9386E-33	Cell envelope
VSAL_II0321	putative glycosyl transferase	-6,54	2,37884E-32	Cell envelope
VSAL_I2285	putative chromosome segregation protein	-6,58	9,26224E-43	Cell processes
VSAL_II0320	putative membrane associated signaling protein	-6,69	6,19324E-24	Regulation
VSAL_I1995	phospholipase A1 precursor	-6,74	2,90171E-36	Central intermediary metabolism
VSAL_II0054	hypothetical protein	-6,99	2,77451E-41	Unknown function
VSAL_II2048s	srna	-7,12	4,12774E-21	sRNA
VSAL_II0327	putative nucleotidyl transferase	-7,20	6,7398E-27	Central intermediary metabolism

VSAL_I2288	chemotaxis protein CheZ	-7,47	1,67901E-46	Cell processes
VSAL_II0959	probable flavin reductase LuxG	-8,21	1,43361E-22	Energy metabolism, carbon
VSAL_I2296	polar flagellar assembly protein FliR	-8,23	4,51317E-24	Cell processes
VSAL_I1857	hypothetical protein	-8,47	2,43041E-25	Unknown function
VSAL_I2292	flagellar biosynthesis protein FlhF	-8,48	1,4371E-57	Cell processes
VSAL_I2293	polar flagellar assembly protein FlhA	-8,52	2,11368E-37	Cell processes
VSAL_II0647	hypothetical protein (pseudogene)	-8,90	4,34776E-57	Unknown function
VSAL_II0330	hypothetical protein	-9,42	3,87667E-19	Unknown function
VSAL_I2303	polar flagellar hook-length control protein FliK	-9,44	4,46386E-34	Cell processes
VSAL_I2771	sodium-type polar flagellar protein MotX	-9,87	9,44239E-36	Cell processes
VSAL_II0785	putative exported protein	-10,22	7,31127E-21	Cell envelope
VSAL_II1022	methyl-accepting chemotaxis protein	-11,00	1,82382E-20	Cell processes
VSAL_II0960	long-chain-fatty-acid ligase LuxE	-11,51	8,98905E-28	Regulation
VSAL_I1427	hypothetical protein	-11,55	1,44302E-47	Unknown function
VSAL_II0963	acyl transferase LuxD	-11,57	2,17005E-35	Regulation
VSAL_I2332	flagellar L-ring protein 1 precursor (basal body L-ring protein	-12,21	8,45236E-50	Cell processes
VSAL_II0528	hemolysin secretion protein	-13,42	6,00022E-41	Extrachromosomal /foreign DNA
VSAL_I2328	flagellar hook-associated protein type 3 FlgL	-14,50	6,28532E-43	Cell processes
VSAL_I0937	sodium-driven polar flagellar protein MotB	-15,65	4,83562E-36	Cell processes
VSAL_I2345	putative exported protein	-15,79	3,73537E-33	Cell envelope
VSAL_I2443	putative exported protein	-15,88	2,7362E-80	Cell envelope
VSAL_I2331	flagellar P-ring protein 2 precursor (basal body P-ring protein	-15,93	1,99398E-65	Cell processes
VSAL_I2517	hypothetical protein	-16,85	2,84E-64	Cell processes
VSAL_I2333	flagellar basal-body rod protein FlgG (distal rod protein)	-17,88	1,18175E-58	Cell processes
VSAL_I1951	methyl-accepting chemotaxis protein	-18,18	9,80181E-43	Cell processes
VSAL_II0962	alkanal monooxygenase alpha chain LuxA (bacterial luciferas	-22,32	1,26805E-50	Regulation
VSAL_I2193	methyl-accepting chemotaxis protein	-23,01	1,0873E-45	Cell processes
VSAL_I2444	accessory colonization factor precursor AcfA	-23,51	3,69342E-80	Extrachromosomal /foreign DNA
VSAL_I4140s	srna	-23,74	2,42348E-24	sRNA
VSAL_I0936	sodium-driven polar flagellar protein MotA	-25,09	2,89795E-62	Cell processes
VSAL_I2330	peptidoglycan hydrolase FlgJ	-26,03	1,00342E-54	Cell processes
VSAL_II0961	alkanal monooxygenase beta chain LuxB (bacterial luciferase	-26,11	2,83704E-40	Regulation

VSAL_I2306	polar flagellar assembly protein FliH	-29,57	9,59646E-53	Cell processes
VSAL_I0799	methyl-accepting chemotaxis protein	-30,21	1,9116E-107	Cell processes
VSAL_I2334	flagellar basal-body rod protein FlgF	-33,78	8,14041E-53	Cell processes
VSAL_II0821	putative exported protein	-35,76	7,71066E-54	Cell envelope
VSAL_I2329	hypothetical protein	-45,67	1,3585E-100	Cell processes
VSAL_I2335	flagellar hook protein FlgE	-46,70	7,69854E-91	Cell processes
VSAL_I2336	flagellar basal-body rod protein FlgD	-50,03	1,0142E-118	Cell processes
VSAL_II0964	acyl-CoA reductase LuxC	-51,44	2,46298E-63	Regulation
VSAL_II0957	autoinducer synthesis protein LuxI	-76,65	1,1309E-303	Regulation
VSAL_I2337	flagellar basal-body rod protein FlgC	-123,52	2,9977E-142	Cell processes
VSAL_I2338	flagellar basal-body rod protein FlgB	-161,94	3,111E-147	Cell processes
VSAL_I0014	transposase	-288,93	0,03649322	Extrachromosomal /foreign DNA
VSAL_II0829	transposase	-361,71	0,029665943	Extrachromosomal /foreign DNA
VSAL_I2325	flagellin subunit B	-474,98	2,78595E-54	Cell processes
VSAL_I2319	hypothetical protein	-530,27	6,51909E-15	Cell processes
VSAL_I2310	sigma-54 dependent response regulator	-551,61	2,44338E-08	Regulation
VSAL_I2311	histidine kinase	-732,39	1,02509E-28	Regulation
VSAL_I2326	putative exported protein	-856,26	1,09187E-15	Cell envelope
VSAL_II0454	transposase	-992,34	1,83226E-15	Extrachromosomal /foreign DNA
VSAL_I2313	polar flagellar protein FliS (polar flagellar protein FlaJ)	-1055,08	5,03591E-23	Cell processes
VSAL_I2309	flagellar hook-basal body complex protein FliE	-1095,51	3,19942E-17	Cell processes
VSAL_I2327	hypothetical protein	-1125,34	5,98509E-07	Cell processes
VSAL_I2317	hypothetical protein	-1129,07	4,39919E-06	Cell processes
VSAL_I2314	polar flagellar protein FlaI	-1720,25	4,70719E-19	Cell processes
VSAL_I2315	polar flagellar hook-associated protein 2 (HAP2) (flagellar ca	-2303,85	4,97205E-28	Cell processes
VSAL_I4139s	srna	-2506,87	7,96896E-29	sRNA
VSAL_I2316	polar flagellar protein FlaG (pseudogene)	-2577,98	6,9979E-21	Cell processes
VSAL_I2308	polar flagellar M-ring protein FliF (pseudogene)	-3050,22	3,85043E-30	Cell processes
VSAL_I2318	hypothetical protein	-3661,38	3,39516E-82	Cell processes
VSAL_I2307	polar flagellar motor switch protein FliG	-4806,71	1,53729E-24	Cell processes
VSAL_I2312	sigma 54 dependent transcription regulator	-12952,86	2,78303E-30	Regulation

Additional file 7: Table S5. The differentially expressed genes of *ΔainS* mutant compared to wild type at LCD

VSAL ID	Product	Fold Change	p-value	Functional classes
VSAL_I4113s	srna	2,86	3,34E-08	sRNA
VSAL_II0366	fimbrial protein, Flp/Fap pilin component	2,82	9,19E-06	Cell envelope
VSAL_I1873	UvrABS system protein B (excinuclease ABC subunit B)	2,56	5,91E-17	Macromolecule synthesis, modification
VSAL_I3165s	srna	2,36	0,001647619	sRNA
VSAL_II0128	hypothetical protein, putative phage gene	2,31	0,007186694	Extrachromosomal
VSAL_I1875	phosphorelay protein LuxU	2,23	1,05E-12	Regulation
VSAL_I4073s	srna	2,13	4,88E-05	sRNA
VSAL_II0367	type IV leader peptidase	2,00	0,000249885	Cell envelope
VSAL_I2816	MFS transporter	-2,08	4,38E-05	Transport/binding proteins
VSAL_I2817	hypothetical protein	-2,13	2,65E-06	Unknown function
VSAL_I2717	fimbrial assembly protein PilN	-2,15	0,00492744	Cell envelope
VSAL_II0121	putative exported protein	-2,17	0,056055813	Cell envelope
VSAL_I2831	putative nucleotidyltransferases	-2,17	0,004972996	Not classified
VSAL_I2125	putative membrane protein	-2,24	0,017001579	Cell envelope
VSAL_I2589	ammonium transporter	-2,38	6,89E-09	Transport/binding proteins
VSAL_II0104	putative 6-phosphogluconate dehydrogenase	-2,61	0,000643604	Not classified
VSAL_I2590	nitrogen regulatory protein P-II	-3,00	0,000131905	Regulation
VSAL_I4093s	srna	-6,74	0,039353197	sRNA
VSAL_I4075s	srna	-9,80	0,000174799	sRNA
VSAL_I1158	autoinducer synthase	-20,38	2,61E-17	Regulation

Additional file 8: Table S6. The differentially expressed genes of *ΔainS* mutant compared to wild type at HCD

VSAL ID	Product	Fold Change	p-value	Functional classes
VSAL_II0366	fimbrial protein, Flp/Fap pilin component	4,24	0,001328268	Cell envelope
VSAL_I1875	phosphorelay protein LuxU	2,38	4,69341E-13	Regulation
VSAL_I0859	hypothetical protein	2,26	0,069609831	Unknown function
VSAL_I0860	transcriptional activator MetR	2,23	0,022288361	Regulation
VSAL_I4019s	srna	2,22	3,39333E-05	sRNA
VSAL_II2050s	srna	2,20	9,06771E-05	sRNA
VSAL_I4115s	srna	2,08	0,007553456	sRNA
VSAL_I2349	putative exported protein	2,04	0,000253208	Cell envelope
VSAL_II1002	sodium/proton-dependent alanine carrier protein	-2,02	0,00000255	Transport/binding proteins
VSAL_II0104	putative 6-phosphogluconate dehydrogenase	-2,06	0,003440623	Not classified
VSAL_I1437	putative allophanate hydrolase subunit 1	-2,07	0,000000179	Degradation of small molecules
VSAL_I1517	conserved hypothetical protein	-2,10	0,00000359	Unknown function
VSAL_I4158s	srna	-2,18	0,006693811	sRNA
VSAL_I0972	transposase	-2,30	0,411763513	Extrachromosomal /foreign DNA
VSAL_I1813	sodium/dicarboxylate symporter	-2,40	0,024425236	Transport/binding proteins
VSAL_II0404	conserved hypothetical protein	-2,53	0,088695143	Unknown function
VSAL_I2128	putative exported protein	-3,00	0,020741633	Cell envelope
VSAL_I2356	hypothetical protein	-3,85	0,01509847	Amino acid biosynthesis
VSAL_I0008	putative amino acid ABC transporter, substrate-binding protei	-3,88	0,058806635	Transport/binding proteins
VSAL_I0404	phosphoadenosine phosphosulfate reductase	-5,05	0,028308116	Central intermediary metabolism
VSAL_I0422	ion transporter superfamily protein	-5,89	0,004335758	Transport/binding proteins
VSAL_I0402	sulfite reductase [NADPH] flavoprotein alpha-component	-6,03	0,023538335	Central intermediary metabolism
VSAL_I0423	adenylylsulfate kinase	-6,06	0,004032358	Central intermediary metabolism
VSAL_I0403	sulfite reductase [NADPH] hemoprotein beta-component	-6,91	0,012152786	Central intermediary metabolism
VSAL_I0420	sulfate adenylyltransferase subunit 2	-9,66	0,003264612	Central intermediary metabolism
VSAL_I0421	sulfate adenylyltransferase subunit 1	-10,48	0,001815313	Central intermediary metabolism
VSAL_I1158	autoinducer synthase	-13,72	5,46E-21	Regulation
VSAL_I4075s	srna	-34,66	2,62E-12	sRNA
VSAL_I0014	transposase	-397,71	0,027151653	Extrachromosomal /foreign DNA

Additional file 9

Table S7. **Motility zones of LFI1238, *luxI*$^-$, *ΔainS* and *ΔainSluxI*$^-$, formed on soft agar plates.** Each value represents the average (mm) of biological triplicates ± standard deviation.

Bacterial strains	
LFI1238	26.6 ± 0.57
luxI$^-$	2.0 ± 0.0
ΔainS	30.3 ± 0.57
ΔainSluxI$^-$	31.3 ± 1.15

* The original size of the spotted colony was 2.0 mm.